United States
Environmental Protection
Agency

Municipal Environmental Research
Laboratory
Cincinnati OH 45268

EPA-600/2-78-122
August 1978

Research and Development

EPA

The Swirl Primary Separator

Development and Pilot Demonstration

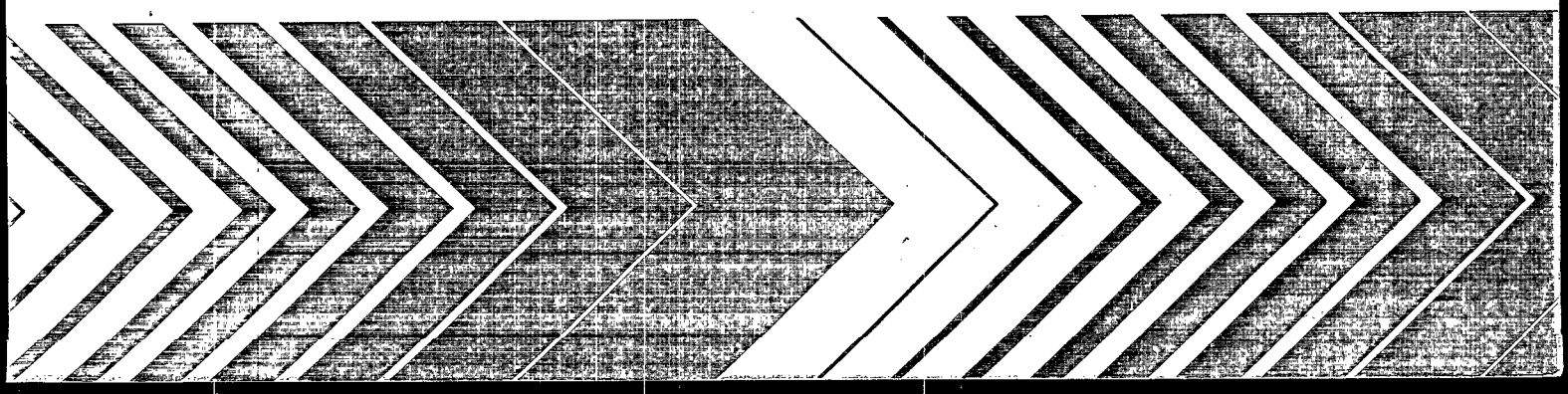

RESEARCH REPORTING SERIES

Research reports of the Office of Research and Development, U.S. Environmental Protection Agency, have been grouped into nine series. These nine broad categories were established to facilitate further development and application of environmental technology. Elimination of traditional grouping was consciously planned to foster technology transfer and a maximum interface in related fields. The nine series are:

1. Environmental Health Effects Research
2. Environmental Protection Technology
3. Ecological Research
4. Environmental Monitoring
5. Socioeconomic Environmental Studies
6. Scientific and Technical Assessment Reports (STAR)
7. Interagency Energy-Environment Research and Development
8. "Special" Reports
9. Miscellaneous Reports

This report has been assigned to the ENVIRONMENTAL PROTECTION TECHNOLOGY series. This series describes research performed to develop and demonstrate instrumentation, equipment, and methodology to repair or prevent environmental degradation from point and non-point sources of pollution. This work provides the new or improved technology required for the control and treatment of pollution sources to meet environmental quality standards.

This document is available to the public through the National Technical Information Service, Springfield, Virginia 22161.

EPA-600/2-78-122
August 1978

THE SWIRL PRIMARY SEPARATOR: DEVELOPMENT AND PILOT DEMONSTRATION

by

Richard H. Sullivan
Morris M. Cohn
James E. Ure
Fred Parkinson
G. Galiana
Ralph R. Boericke
Carl Koch
Paul Zielinski

American Public Works Association
Chicago, Illinois 60637

Contract No. 68-03-0272
Grant No. S-803157

Project Officers

Richard Field
Hugh Masters
Storm and Combined Sewer Section
Wastewater Research Division
Municipal Environmental Research Laboratory (Cincinnati)
Edison, New Jersey 08817

MUNICIPAL ENVIRONMENTAL RESEARCH LABORATORY
OFFICE OF RESEARCH AND DEVELOPMENT
U.S. ENVIRONMENTAL PROTECTION AGENCY
CINCINNATI, OHIO 45268

DISCLAIMER

This report has been reviewed by the Municipal Environmental Research Laboratory, U.S. Environmental Protection Agency, and approved for publication. Approval does not signify that the contents necessarily reflect the views and policies of the U.S. Environmental Protection Agency, nor does mention of trade names or commercial products constitute endorsement or recommendation for use.

FOREWORD

The U.S. Environmental Protection Agency was created because of increasing public and governmental concern about the dangers of pollution to the health and welfare of the American people. Noxious air, foul water, and spoiled land are tragic testimony to the deterioration of our natural environment. The complexity of that environment and the interplay between its components require a concentrated and integrated attack on the problem.

Research and development is that necessary first step in problem solution and it involves defining the problem, measuring its impact, and searching for solutions. The Municipal Environmental Research Laboratory develops new and improved technology and systems for the prevention, treatment, and management of wastewater and solid and hazardous waste pollutant discharges from municipal and community sources, for the preservation and treatment of public drinking water supplies and to minimize the adverse economic, social, health, and aesthetic effects of pollution. This publication is one of the products of that research; a most vital communications link between the researcher and the user community.

The study describes what has been learned from both laboratory and prototype testing of a new type of primary settling device. This device is to be used with urban stormwater runoff and combined sewer overflows, as well as domestic sanitary sewage, to provide primary treatment.

Francis T. Mayo
Director
Municipal Environmental Research
Laboratory

ABSTRACT

A study was conducted to determine if the swirl concentrator principle could be used to provide primary treatment to combined sewer overflows and municipal wastewater. A hydraulic model with synthetic wastewater and a mathematical model were both used to arrive at an optimized configuration and a design basis. The design was then tested under actual wet- and dry-weather flow conditions using a large scale, 1,137 cu m/d (0.3 mgd) pilot constructed in Toronto, Canada. The Toronto pilot evaluations confirmed the accuracy of the design (and associated design curves) developed under the model studies.

The model and pilot studies indicated that the device could achieve 30 to 50 percent settleable solids removal efficiency for flows of less than 22 l/sec (0.5 mgd) at costs comparable to, or less than, conventional treatment units. Overflow rates of two to three times that of conventional units make possible the saving.

Testing of the model and prototype was based upon the need to treat both domestic sanitary sewage and combined sewer overflows. Extensive laboratory work was conducted to determine the settling characteristics of solids to provide laboratory control and provide a correlation between the laboratory and prototype testing programs.

The swirl's height and diameter are equal, providing a relatively deep structure which enhances sludge thickening.

The Toronto pilot evaluations of the prototype unit constructed in Toronto Ontario – 1,137 cu m/d (0.3 mgd) – to determine operating efficiencies confirmed the accuracy of the design and associated curves developed under the model studies.

The report contains thorough descriptions of the hydraulic/mathematical and pilot studies, and most importantly, the detailed design methodology.

This report is in partial fulfillment of U.S. Environmental Protection Agency (EPA) contract 68-03-0272 (for hydraulic and mathematical modeling) jointly sponsored by the American Public Works Association Research Foundation (APWA), and EPA demonstration grant S-803157 (for pilot evaluation) jointly sponsored by APWA and the City of Toronto, Canada. Work was completed in October 1976.

TABLE OF CONTENTS

Page

Forword . . . iii
Abstract . . . iv
Acknowledgements . . . x
Section 1. Conclusions, Recommendations, and Overview of the Studies . . . 1
Section 2. The Study . . . 5
Section 3. Design Guidelines and Construction Costs . . . 23
Section 4. Pilot Treatability Evaluation With Sewage . . . 36
Section 5. Glossary . . . 58
References . . . 58
Appendices
A. Hydraulic Model Study . . . 59
B. Mathematical Model Study . . . 111
References . . . 153
C. Settleability Tests and Hydrualic Characterization of a Pilot (with real sewage) Swirl Separator as a Primary Treatment Facility . . . 154
D. Pilot Test Results . . . 166

FIGURES

Page

1. Isometric: Swirl Primary Separator . . . 3
2. Model Layout . . . 7
3. Swirl Primary Separator: First Layout Tested on Model . . . 9
4. Swirl Primary Separator: Model Layout for Tests 161 to 184 – Modification 10 . . . 10
5. Swirl Primary Separator: Model Layout for Tests 188 to 194 (3 to 9) – Modification 11 . . . 11, 12
6. Gradation Curve for Petrothene Used in Model . . . 14
7. Settling Velocity vs Particle Size for IRA-93 Anion Exchange Resin . . . 15
8. Swirl Primary Separator: Sanitary Sewage in Prototypes Represented by IRA-93 in Model . . . 16
9. Diagram of Swirl Primary Separator Chamber as Represented by Mathematical Model . . . 19
10. Pilot Facility – Metro Toronto . . . 22
11. Predicted Prototype Solids Removal Efficiency for Sanitary Sewage . . . 24, 25
12. Detention Times . . . 26
13a. General Design Dimensions . . . 27
13b. General Design Dimensions . . . 28
14. Swirl Primary Separator . . . 31
15. Conventional Primary Settling Tank . . . 33
16. Cost vs. Diameter, Swirl and Conventional Primary Treatment Units . . . 34
17. Test Layout – Humber Plant – Toronto, Canada 1975 . . . 37
18. Diurnal Flow and Suspended Solids (mg/l) Average of 5 Dry-Weather Days, Humber Plant – Toronto, April 1975 . . . 39
19. Section of Swirl Primary Separator . . . 40
20. Plan of Swirl Primary Separator . . . 41

FIGURES (continued)

21. Dry-Weather Removal of Total Suspended Solids – Toronto, September 1975 46
22. Dry-Weather Removal of Fixed Suspended Solids – Toronto, September 1975 47
23. Dry-Weather Removal of Volatile Suspended Solids – Toronto, September 1975 . . . 48
24. Dry-Weather Removal of Settleable Solids by Volume – Toronto, September 1975 . . 49
25. Dry-Weather Removal of Settleable Solids by Weight – Toronto, September 1975 . . . 50
26. Predicted Versus Actual Solids Removal 54
27. Comparison of Time to Achieve Treatment 55
28. Swirl Primary Separator: Conical Bottom and Low Inlet 60
29. Swirl Primary Separator – Modification 2, (Raised Inlet 61 cm [24 in] Diameter Weir and 71 cm [28 in] Diameter Skirt) 60, 61
30. Swirl Primary Separator: Operating Efficiencies for Modifications 2 and 3 65
31. Swirl Primary Separator: Model Layouts for Tests 20 to 45 – Modification 3 66
32. Prototype Particle Sizes Simulated by Shredded Petrothene 67
33. Swirl Primary Separator: Model Layouts for Tests 27, 28, 34 and 40 – Modifications 3 and 4 68
34. Swirl Primary Separator: Operating Efficiencies for Modifications 3 and 4 69
35. Swirl Primary Separator: Model Layout for Tests 46 to 68 – Modification 5 70
36. Swirl Primary Separator: Operating Efficiencies for Modification 5 71
37. Swirl Primary Separator: Model Layout for Tests 69 to 91 for Modification 6 72
38. Swirl Primary Separator: Operating Efficiencies for Modification 6 73
39. Swirl Primary Separator: Model Layout for Tests 113-136 – Modification 8 75
40. Swirl Primary Separator: Operating Efficiencies for Modification 8 76
41. Swirl Primary Separator: Location of Measuring Points for Velocity Contour Tests 10.98 m (36 ft) Chamber Prototype Scale 1/12 – Modification 6 77
42. Swirl Primary Separator: Tangential Velocity Contours at 0° Position 78
43. Swirl Primary Separator: Tangential Velocity Contours at 90° Position 78
44. Swirl Primary Separator: Tangential Velocity Contours at 180° Position 79
45. Swirl Primary Separator: Tangential Velocity Contours at 270° Position 79
46. Swirl Primary Separator: Model Layout for Tests 92 to 112 – Modification 7 80
47. Swirl Primary Separator: Operating Efficiencies of Closed Bell with Four Orifices – 3.79 cm (1.5 in) θ, 22.9 cm (9 in) High, Skirt 0.61 m (24 in) θ for Modification 7 81
48. Swirl Primary Settler: Location of Measuring Points for Velocity Contour Tests 10.98 m (36 ft) Chamber, Closed Bell with Four Orifices – 0.457 m (1.5 ft) θ, 2.74 m (9 ft) High, Skirt 7.32 m (24 ft) θ Prototype Scale 1/12 – Modification 7 82
49. Swirl Primary Separator: Tangential Velocity Contours at 0° Position 83
50. Swirl Primary Separator: Tangential Velocity Contours at 90° Position 84
51. Swirl Primary Separator: Tangential Velocity Contours at 180° Position 85
52. Swirl Primary Separator: Tangential Velocity Contours at 270° Position 86
53. Swirl Primary Separator: Model Layout for Tests 137 to 160 – Modification 9 88
54. Swirl Primary Separator: Operating Efficiencies for Modification 9 89
55. Swirl Primary Separator: Model Layout for Tests 161 to 184 – Modification 10 . . . 90
56. Swirl Primary Separator: Operating Efficiencies for Modification 10 – Increase of the Skirt Diameter 91
57. Swirl Primary Separator: Operating Efficiencies for Modification 10 – Recovery Rate vs Slot Height 92
58. Modification 10, Petrothene Grains Reaching End of Inlet, and Petrothene Grains Slidin Down Against the Cone Wall Near Inlet 93
59. APWA Swirl Primary Settler: Retention Time vs Discharge With Scale 1/12 94

FIGURES (continued)

60. Swirl Primary Separator: Model Layout for Modification 11 . . . . . 98, 99
61. Swirl Primary Separator: Model Layout for Modification 12 100
62. Swirl Primary Separator: Model Layout With Modification 12 and Inlet Baffle Type 3a 102
63. Swirl Primary Separator: Model Layout with Modification 12 and Inlet Baffle Type 3b 103
64. Swirl Primary Separator: Model Layout with Modification 12 and Inlet Baffle Type 3c 104
65. Swirl Primary Separator: Model Layout with Modification 12 and Inlet Baffle Type 3d 105
66. Swirl Primary Separator: Suggested Recovery Curve for Anion Exchange Resin IRA-93 in Model 149 $\mu > d > 75 \mu$ 106
67. Swirl Primary Separator: Predicted Prototype Solids Recover from Sanitary Sewage 108
68. Recovery Rates on Model as Function of Particle Settling Velocity 109
69. Recovery Rates with Different Particle Settling Velocities for:
    a. 0.91 m (3 ft) Diameter Chamber 110
    b. 1.83 m (6 ft) Diameter Chamber 110
    c. 3.66 m (12 ft) Diameter Chamber 112
    d. 7.33 m (24 ft) Diameter Chamber 112
    e. 10.98 m (36 ft) Diameter Chamber 113
70. Diagram of Laboratory Swirl Chamber Configuration 115
71. Diagram of Swirl Chamber as Represented by Mathematical Model 116
72 Settling Velocity Distribution at 30.5 cm (1 ft) Column Sample Ports 119
73. Settling Velocity Distribution at 61 and 91 cm (2 and 3 ft) Column Sample Ports . . 119
74. Settling Velocity Distribution for all Sample Ports 120
75. Settling Velocity Distribution at Various Column Depths 120
76. Settling Column Data Interpretation: Flocculation vs Nonflocculating Particles . . . 122
77. Streamlines for Initial Lab Configuration with Circular Weir 136
78. Tangential Velocity Contours for Initial Lab Configuration with Circular Weir 137
79. Vertical Velocity Profiles for Initial Lab Configuration with Circular Weir 138
80. Streamlines for Modified Lab Configuration with Radial Gutters and Standpipe Removed 140
81. Tangential Velocity Contours for Modified Lab Configuration with Radial Gutters and Standpipe Removed 141
82. Vertical Velocity Profiles for Modified Lab Configuration with Radial Gutters and Standpipe Removed 142
83. Particle Paths for Initial Lab Configuration with Circular Weir and Particle Settling Velocity of 0.05 cm/sec (0.0016 ft/sec) 143
84. Particle Paths for Modified Lab Configuration with Radial Gutters and Standpipe Removal at Particle Settling Velocity of 0.05 cm/sec (0.0016 ft/sec) 145
85. Particle Paths for Modified Lab Configuration with Radial Gutters and Standpipe Removal at Particle Settling Velocity Equal to Average Upflow Velocity of 0.25 cm/sec (0.0083 ft/sec) 146
86. Particle Paths for Modified Lab Configuration with Radial Gutters and Standpipe Removal at Particle Settling Velocity of 0.3 cm/sec (0.0098 ft/sec) 147
87. Comparison of Smisson 3 m (10 ft) Prototype Data with Theoretical Performance . . 149
88. Correlation of Observed and Theoretical Model Performance 150
89. Settling Velocity Characteristics: Humber Treatment Plant — Storm Flow June 5, 1975 159

FIGURES (continued)

90. Settling Velocity Characteristics: Humber Treatment Plant – Storm Flow June 16, 1975 . . . 159
91. Residence Time Distribution . . . 165
92. Residence Time Distributions . . . 165
93. Fitted Responses . . . 166
94. Fitted Responses . . . 166
95. Fitted Responses . . . 167
96. Fitted Responses . . . 167
97. Percent Dead Volume Versus Flow Swirl Separator . . . 168

TABLES

Page

1. Solids Removal Efficiencies of IRA-93 at Various Discharge Rates . . . 17
2. Comparison of Diameter, Detention Time, and Suspended Solids Removal for Swirl Primary Separator and Detention Time for Conventional Settling for Various Overflow Rates . . . 29
3. Construction Cost of Swirl Primary Separator . . . 32
4. Construction Cost of Conventional Primary Settling Tank . . . 34
5. Comparison of Operation and Maintenance Costs for Primary Treatment Units . . . 35
6. Present Worth, Swirl Separator Primary Treatment Units . . . 35
7. Removal of Total Suspended Solids: Wet-Weather Flow – May 4-July 12, 1975 . . . 37
8. Removal of Total Suspended Solids – June 23-27, 1975 . . . 42
9. Removal of Total Suspended Solids – July 2-8, 1975 . . . 43
10. Removal of Total Suspended Solids: Dry-Weather Flow – May 1-June 10, 1975 . . . 44
11. Summary of Tests – September, 1975 . . . 51
12. Detention Time and Overflow Rate: Primary Tanks – September 1975 and June 1976 52
13. Total Suspended Solids . . . 52
14. Removal of BOD – June 23-July 8, 1975 . . . 55
15. Modifications Tested on the Model . . . 64
16. Successive Modifications of the Model and Recovery Results with Anion Exchange Resin IRA-93 149 $\mu > d > 74\mu$ . . . 95, 96
17. Recovery Rate of IRA-93 at Various Flowrates . . . 101
18. Representation of IRA-93 to Sewage, Based on Scale Factor . . . 107
19. Collision Rates for Various Mechanisms . . . 123
20. Particle Size and Number Density for Various Settling Velocities . . . 126
21. Estimated Collision Rates . . . 128
22. Applicable Boundary Conditions for Particle Continuity Equation . . . 131
23. Particle Settling Velocity Distribution for 100-200 Mesh IRA-93 Resin . . . 148
24. Predicted Removal Efficiency for 100-200 Mesh IRA-93 Resin (0.5 l/sec [0.02 cfs]) . 148
25. Predicted Removal Efficiency for Hypothetical Prototype Unit Using Mathematical Model . . . 153
26. Predicted Removal Efficiency for Hypothetical Prototype Unit Using Laboratory Data . . . 154
27. Model Fitted Parameter Estimates . . . 162
28. The Axial Dispersion Model . . . 163
29. The Equal Tanks-In-Series Model . . . 164
30. Dry-Weather Test Schedule . . . 169
31. Wet-Weather Test Schedule . . . 169
32. Wet Weather Test Data, Swirl Separator – May 4-7, 1975 . . . 170

TABLES (continued)

33. Wet-Weather Test Data, Swirl Separator – May 15-June 12, 1975 171
34. Wet-Weather Test Data, Primary Tanks – May 4-7, 1975 172
35. Heavy Metal Test Data 173
36. Dry-Weather Test Data – Swirl Primary Separator – May 1-11, 1975 174
37. Dry-Weather Test Data – Swirl Primary Separator – May 12-18, 1975 175
38. Dry-Weather Test Data – Swirl Primary Separator – May 30-June 10, 1975 176
39. Dry-Weather Test Data – Swirl Primary Separator – June 16-21, 1976 177
40. Dry-Weather Test Data – Swirl Primary Separator – June 22-25, 1976 177
41. Dry-Weather Test Data – Primary Tanks – May 1-11, 1975 178
42. Dry-Weather Test Data – Primary Tanks – May 12-18, 1975 179
43. Dry-Weather Test Data – Primary Tanks – May 30-June 10, 1975 180
44. Dry-Weather Test Data – Primary Settling Tank – June 16-21, 1976 181
45. Dry-Weather Test Data – Primary Settling Tank – June 22-25, 1976 181
46. Proposed Tests Second Series 182
47. Dry-Weather Test Data – Swirl Primary Separator – June 12-17, 1975 182
48. Dry-Weather Test Data – Primary Tanks – June 23-27, 1975 183
49. Dry-Weather Test Data – Swirl Primary Separator – July 2-8, 1975 184
50. Dry-Weather Test Data – Primary Tanks – July 2-8, 1975 185
51. Proposed Tests Final Series 186
52. Dry-Weather Test Data – September 2, 1975 187
53. Dry-Weather Test Data September 3, 1975 188
54. Dry-Weather Test Data September 4, 1975 189
55. Dry-Weather Test Data September 5, 1975 190
56. Dry-Weather Test Data September 8, 1975 191
57. Dry-Weather Test Data September 9, 1975 192
58. Dry-Weather Test Data September 10, 1975 193
59. Dry-Weather Test Data September 11, 1975 194
60. Dry-Weather Test Data September 12, 1975 195
61. Dry-Weather Test Data September 15, 1975 196
62. Dry-Weather Removal of Settleable Solids By Volume 197
63. Dry-Weather Removal of Settleable Solids By Weight 198
64. Dry-Weather Removal of Total Suspended Solids 199
65. Dry-Weather Removal of Volatile Suspended Solids 200
66. Dry-Weather Removal of Fixed Suspended Solids 201
67. Dry-Weather Removal of Settleable Solids By Volume 202
68. Dry-Weather Removal of Settleable Solids By Weight 203
69. Dry-Weather Removal of Total Suspended Solids 204
70. Dry-Weather Removal of Volatile Suspended Solids 205
71. Dry-Weather Removal of Fixed Suspended Solids 206

EXHIBITS

Page

1. Settling Column Test Methods 158
2. Description of Hydraulic Mixing Models 162, 163, 164

ACKNOWLEDGEMENTS

The American Public Works Association is deeply indebted to the following persons and their organizations for the services they have rendered to the APWA Research Foundation in carrying out this study for the U. S. Environmental Protection Agency.

PROJECT DIRECTOR

Richard H. Sullivan

CONSULTANTS

Morris M. Cohn, P.E.
Paul B. Zielinski, P.E.
Bernard S. Smisson

ALEXANDER POTTER ASSOCIATES, CONSULTING ENGINEERS

Morris H. Klegerman, P.E.
James E. Ure, P.E.

GENERAL ELECTRIC COMPANY

Ralph R. Boericke
Carl Koch

LA SALLE HYDRAULIC LABORATORY, LTD.

F. E. Parkinson
George Galiana

METROPOLITAN TORONTO

Ross L. Clark
Earl Baldock

T. W. BEAK CONSULTANTS

Stephen L. Hodd

AMERICAN PUBLIC WORKS ASSOCIATION STAFF

Ronald H. Ball
Lois V. Borton
Jan A. T. Harvey
John R. Moy
Rose M. Ohlman
Shirley M. Olinger
Cecelia E. Smith
Oleta M. Ward

U. S. ENVIRONMENTAL PROTECTION AGENCY

Richard Field, Chief,
Storm & Combined Sewer Section, (Edison, New Jersey)
Hugh E. Master, Staff Engineer
Storm & Combined Sewer Section (Edison, New Jersey)

SECTION 1
CONCLUSIONS, RECOMMENDATIONS, AND OVERVIEW OF THE STUDIES

CONCLUSIONS

The studies indicate that the swirl flow principle can be a substitute for the function of primary settling. Previously the swirl flow principle was shown to be applicable for the simultaneous flow regulation and rough clarification of combined sewer overflow liquids and for the selective separation of grit in sanitary sewage and admixed sewage and storm runoff.

1. As a result of hydraulic and mathematical model studies, it has been concluded that the swirl separator principle can be utilized to obtain clarification of wastewaters, such as sewage, combined sewer overflows, and stormwater discharges. Such clarification is competitive with conventional settling units for low flow rates and at less than conventional primary settling removal requirements.

2. The swirl separator principle applied to primary separation involves the establishment of long-path circular separation within a cylindrical tank. The opportunity for natural flocculation and the lessened possibility of short circuiting in the chamber appear to improve performance.

3. The absence of moving parts in the swirl separator reduces maintenance and operating costs of the unit.

4. The relatively high overflow rates which may be used with the swirl separator at various levels of suspended solids removal requires less space, thus enhancing its use in wastewater plant expansion and combined sewer overflow and stormwater treatment.

5. Tests covering the settling velocities of sewage and flocculation mechanisms indicate a good relationship between the synthetic solids used in model testing and real sewage.

6. Testing of the pilot unit was conducted under the adverse conditions of wide variations in flowrates of industrial wastes. Thus the fact that the unit performed as well as the existing units indicates that performance may be enhanced under more uniform operating conditions.

7. The cost of constructing a swirl separator for flow of 7.5 l/sec (0.17 mgd) for a suspended solids removal efficiency of 45 percent was less than for a conventional unit, $55,200 to $76,000. However, above this flowrate and removal efficiency, the conventional unit becomes less expensive.

8. With our present knowledge of fine particle scale-up laws, the swirl separator does not appear to be economically competitive for diameters greater than 5.5 m (18 ft). However, model and limited field test results are sufficiently encouraging to suggest construction of a larger experimental unit to provide full scale data for actual sewage.

RECOMMENDATIONS

1. The hydraulic and mathematical model investigations and the prototype tests indicated good removal of sewage solids. The studies, however, may have under-predicted the swirl primary separator efficiencies which can be accomplished. It is recommended that the prototype installation constructed by Metropolitan Toronto be tested at another facility not subject to large variations in industrial waste loads. The potential benefits of low construction cost, applicability of units to augment presently overloaded primary facilities, freedom from mechanical parts or devices to handle sludge residues and ability of the deep conical sludge hopper configuration warrant the expenditure of funds for such an evaluation.

2. Further testing and development of the swirl separator principle should be conducted utilizing mechanical sludge rakes and the modified design basis of Mr. Bernard Smisson.

OVERVIEW OF THE STUDY

The swirl separator can prove to be a highly valuable and innovative tool in the nation's efforts to clean up pollution conditions in its water resources. Previous studies carried out at Bristol, England, but never before duplicated on the American continent, gave indication that the swirl

separator principle could be applied to the separation of liquid and solid phases in wastewaters of various types.

The current studies of the swirl primary separator is, in fact, a "third-generation" investigation of the swirl separator principle. In July 1972, the APWA Research Foundation completed development and evaluation studies of the swirl separator as a combined sewer overflow-regulator facility jointly sponsored by the City of Lancaster, Pennsylvania, and the U.S. Environmental Protection Agency (EPA).[1] The investigations demonstrated the practicability of utilizing the swirl principle for removing settleable and floatable solids from combined sewer overflow and for simultaneously diverting predetermined amounts of so-called foul sewage (concentrated liquid-solids) to downstream wastewater treatment facilities or to holding (storage) chambers.

Encouraged by the results of the swirl separator as a combined sewer overflow regulator/separator[1] device a "second-generation" study was conducted on the development and evaluation of the swirl principle for the selective separation of grit or inorganic solids from wastewater flows.[2] The swirl degritter development was conducted by the American Public Works Association under the sponsorship of the USEPA in 1973.

In 1974 a study of the use of the swirl principle for removal of erosion products from stormwater runoff was conducted.[6]

The present studies of the development of a swirl separator chamber as a primary clarifier of sanitary sewage and combined sewer wastewaters involved the development and evaluation of a hydraulic model at the La Salle Hydraulic Laboratory, La Salle, Quebec, Canada, the verification and validation of hydraulic model findings by mathematical-computer model techniques performed by the General Electric Company, Re-Entry and Environmental Systems Division, at Philadelphia, Pennsylvania, and the evaluation of a prototype unit with santary sewage in Toronto, Ontario.

In addition to the aforementioned model investigations, a supplemental investigation was carried out by Beak Consultants Limited, Rexdale, Ontario, Canada, to determine the settling velocities of combined sewer overflow and stormwater runoff with respect to the application of swirl separator devices as primary separators.[3] These studies were interrelated with the hydraulic and mathematical model investigations because they dictated the nature of the synthetic model-scale solids which were tested and evaluated as representative of actual wastewater solids that would be treated by swirl devices in the field. In conjunction with the prototype field test in Toronto, additional tests of settling characteristics of solids in combined sewer flows and flow patterns within the swirl separator were conducted.

The hydraulic studies covered 12 modifications of a swirl separator chamber originally patterned after the unit previously used in the earlier overflow regulator investigations.[1,2,3] A total series of 194 test runs were carried out, covering determinations of solids settling velocities, flow patterns, solids removal efficiencies, and other pertinent factors. Out of these studies came firm decisions on the most effective size and location of inlet line, shape of bottom cone solids hopper, baffle and overflow weir details, and other internal appurtenances. Figure 1 shows the various parts of the unit. The mathematical model studies were designed to verify all hydraulic patterns and performances.

The studies provided proof of the applicability of the swirl principle to the function of primary clarification of suspended solids-bearing wastewaters. In a short detention period solids are deposited by inertial and gravity action and agglomeration mechanisms. Removal efficiencies matched actual performance of conventional primary settling facilities in shorter periods of time at the Metropolitan Toronto facility. With the design configuration, without chemical additives, the swirl was not found useful above 50 percent suspended solids removal or for flows in excess of 40 l/sec (0.9 mgd) treated to 30 percent solids removal.

The hydraulic model studies were based on synthetic solids made of Amberlite® anion exchange resin IRA-93, which was considered

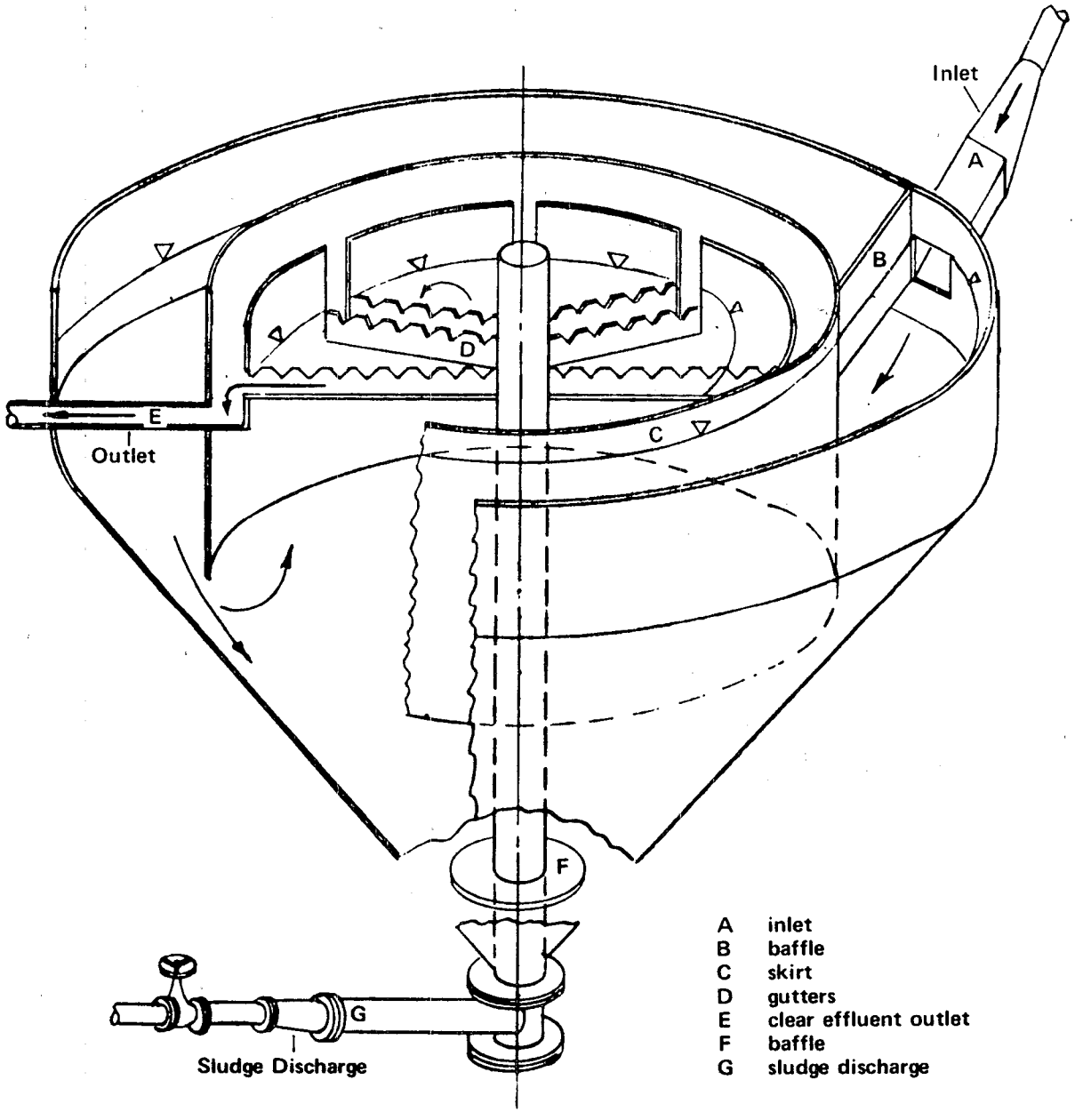

FIGURE 1 ISOMETRIC: SWIRL PRIMARY SEPARATOR

to properly simulate actual solids in sanitary sewage flows.[3] The design criteria are based on Froude Law scale up.

The hydraulic model studies with synthetic solids led to the construction of a 3.7 m- (12 ft) diameter pilot with real sewage for further hydraulic evaluation of swirl flow phenomena, size and geometric configuration of basic chambers and internal structure features, performance in terms of solids removal and the effects of solids coagulation induced by the swirl patterns.

The pilot unit was tested at a design flow of 1,137 m^3/day (0.3 mgd) and at 1,700 m^3/day (0.45 mgd). The results of the tests indicated that the unit performed as effectively, 40 percent suspended solids removal, as conventional basins at the Humber wastewater treatment plant operating at an overflow rate of 81.46 $m^3/day/m^2$ (2,000 gal/day/ft^2) with 1.06 hour detention time. The detention time in the swirl separator was 20.4 minutes and an overflow rate of 108 $m^3/day/m^2$ (2,650 gal/day/ft^2) and 14 minutes with an overflow rate of 162 $m^3/day/m^2$ (3,980 gal/day/ft^2), respectively for the two above mentioned flowrates. However, when the size of the unit is calculated for a full 60 percent suspended solids removal, the size and retention time becomes equal to that of the conventional unit.

General Comments

The hydraulic model design was started in the summer of 1974. At that time the work of Mr. Bernard Smisson was closely evaluated because of his extensive research in the field of secondary motions in flow fields. Mr. Smisson had experimented with both mechanical and nonmechanical configurations. At the time of the study, Mr. Smisson had decided to proceed on the basis of a mechanical scraper to minimize the depth of the unit and improve operating efficiency.

Inasmuch as a primary goal of the current study was to develop a unit for treating combined sewer overflows and urban stormwater runoff, the decision was made to develop a nonmechanical device. With this limiting design feature several major changes exist in the configurations which are different from the current designs being evaluated by Mr. Smisson. Among the major features are the following:

1. **Shape**
   - *This Study* — the height equals diameter with 60° sloped conical bottom
   - *Smisson* — a conventional shaped circular tank
2. **Draw-off clarified flow**
   - *This Study* — conventional gutters with gravity discharge through side of tank
   - *Smisson* — circular weir and central shaft discharge
3. **Draw-off of solids**
   - *This Study* — tests indicate intermittent draw-off best
   - *Smisson* — continuous draw-off and uses mechanical rake
4. **Deflector**
   - *This Study* — found no advantage to inlet baffle or deflector
   - *Smisson* — uses skirt deflector to create distinct zones
5. **Dip plate**
   - *This Study* — found no hindrance to settling from surface interferences, i.e., pipe across outer flow field
   - *Smisson* — does not allow a dip plate or interference in outer flow field

Smisson reports that his configuration is performing better than that found by the APWA under this study.

SECTION 2

THE STUDY

Primary separation of solids is the common denominator of practically all treatment systems whether for sanitary or combined wastewaters plant processes. While present federal laws and the policies of all states require the use of higher degrees of treatment than simple primary clarification, the removal of settleable solids and floatable suspended material from wastewaters by some form of clarification facility is universally practiced. Some secondary treatment systems may forego primary removal of suspended solids prior to their secondary stages, such as in the case of so-called package activated sludge or extended aeration plants, but initial clarification is normally provided in conventional treatment plant design.

The basic conventional methodology of primary clarification usually involves the gravimetric separation of settleable solids, together with floatable materials, in flow-through chambers which provide detention periods and lowered hydraulic velocities that produce deposition and rise of solids and the resultant discharge of a clarified effluent. Decreased flow velocities to provide this gravity clarification phenomenon usually involve relatively large settling chambers and relatively long detention periods.

The swirl separator achieves clarification of solids-laden liquid flows, not by simple gravimetric separation under quiescent settling conditions, but by introducing secondary motion flows. The purpose of this study has been to investigate the application of the swirl separator principle to the process of primary separation of raw wet and dry weather sewage solids and to evolve practical design parameters for prototype installations. The successful achievement of the application of the swirl separator principle for this universal wastewater treatment process could provide relatively speedy, or "flash," solids separation in relatively small chambers without use of mechanical devices for sludge and scum removal, thus providing economy of construction and operation.

HYDRAULIC MODEL STUDY

The hydraulic model studies were carried out by LaSalle Hydraulic Laboratory where the previous investigations of swirl separator for combined sewer overflow regulator purposes and for grit removal by swirl action were undertaken. The experience of this hydraulic laboratory and its knowledge and availability of previous swirl chamber components greatly benefited and expedited the current research work.

The hydraulic model studies, augmented and supported by the mathematical and computer simulation of liquid and particle flowfield conditions were programmed to produce optimum swirl separator chamber dimensions and configurations and structural details of internal appurtenant unit components; to evaluate performance in terms of most effective solids removal efficiencies; and to develop design procedures and parameters that translate the scale model features into full-scale prototype swirl primary separator installations in the field. This section applies to the hydraulic model investigations performed at the LaSalle Hydraulic Laboratory.

In order to initiate the swirl studies, the model chamber previously used as a combined sewer overflow regulator was modified to serve as a primary separator device. Changes were made in the geometrics and internal details of the original unit, including modifications to the chamber depth; floor configuration; inlet shape and location; weir diameter, configuration, and structural details; skirt location, size, and immersion; and slot opening dimension under the skirt.

The first model configuration and all subsequent changes in the main chamber and internal appurtenant units were intended to provide a controlled combination of swirl

flow patterns and gravimetric settling and a bottom hopper shape to expedite the deposition and compaction of deposited sludge solids to a prearranged point of discharge without need for mechanical collectors of any type. An outlet for the hopper sludge was provided in the original model but no routine use of this sludge line was made in the studies. However, intermittent draw-off under flow influence was included in the testing program.

The first model layout was based on various sources of information and experience with units of similar or related intent and design. The general arrangement with a deep skirt for separation of the external and internal sectors of the swirl chamber, as developed by Mr. Smisson in model studies at Bristol, England, was first utilized. The bottom cone of the sludge collecting hopper of the chamber was chosen as a 60° slope for easy movement of sludge to the outlet using gravity force only. Larger inlet line diameter, weir diameter, and skirt diameter than used previously in swirl separator studies of combined sewer overflow regulators [1] and of grit removal facilities[2] were provided.

In order to establish practicable prototype values for the hydraulic model studies the scale of 1 : 12 previously used in regulator overflow and grit separation studies was again utilized. In prototype scale up dimensions, this dictated the use of a 1.22 m (4 ft) square influent sewer, entering a 11 m (36 ft) diameter swirl chamber with overflow weir crest 2.75 m (9 ft) above the upper cylindrical portion of the chamber during the first stage portion of the overall hydraulic model studies. Various changes were subsequently made to improve operational performance but the diameter of the chamber itself was retained throughout.

This size chamber provided a 21 minute detention time in the prototype for a flow rate of 0.31 m^3/sec (11 cfs), corresponding to 0.632 l/sec (0.022 cfs) in the model.

The discharge Q and time to flow relationship can be developed from the continuity equation where Q prototype = L^3 prototype/time prototype or:

$$Q_p = L_p{}^3/t_p \qquad (1)$$

and for the model: $Q_m = L_m{}^3/t_m$.

Combining the continuity equation with the Froude Model Law ($V/\sqrt{Lg}$) leads to the relationship involving the time scale and discharge scale between model and prototype as

$$t_p = \left(\frac{Q_p}{Q_m}\right)^{0.2} t_m \qquad (2)$$

The relation between the discharge Q and the length scale is.

$$\frac{Q_p}{Q_m} = \left(\frac{L_p}{L_m}\right)^{2.5} \qquad (3)$$

To simplify the testing procedure, four model discharge rates were selected to provide workable prototype equivalents, as follows:

0.9m (3 ft) Diameter Model	Detention Time	11 m (36 ft) Diameter Prototype			Detention Time
l/sec	minutes	m^3/sec	cfs	mgd	minutes
0.5	7.67	0.25	8.8	5.7	26
0.632	6.06	0.31	11.0	7.1	21
1.0	3.83	0.50	17.6	11.4	13
1.5	2.56	0.75	26.4	17.1	8.7

Similar calculations for the 3.7 m (12 ft) diameter swirl unit used in pilot scale testing at Toronto are:

Flow Rate			Detention Time	Overflow Rate	
cfs	mgd	m^3/sec	minutes*	gpd/ft^2	m^3/day/m^2
0.232	0.15	0.00657	40	1,326	0.466
0.309	0.2	0.00876	30	1,768	0.621
0.463	0.3	0.013	20	2,650	0.932
0.695	0.45	0.02	13	3,980	1.400

* allows 0.9 m (3 ft) for sludge accumulation

Description of Hydraulic Model

Figure 2 shows the swirl chamber and inlet supply line; a solids hopper and vibrator for introducing test solids into the swirl device via the inlet sewer line; a clear overflow settling basin equipped with a calibrated V-notch weir for gauging discharge flows; a foul outlet connection to the bottom of the swirl chamber, leading to a foul overflow settling tower and recovery screen for recapturing the introduced solids; together with necessary control equipment.

The central unit of the model system was the swirl separation chamber. It consisted of a vertical concrete conical hopper at the bottom with a 60° side slope, topped by a vertical cylinder chamber 91.5 cm (3 ft) in diameter, made of 1.3 cm (0.5 in.) Plexiglas.® In the

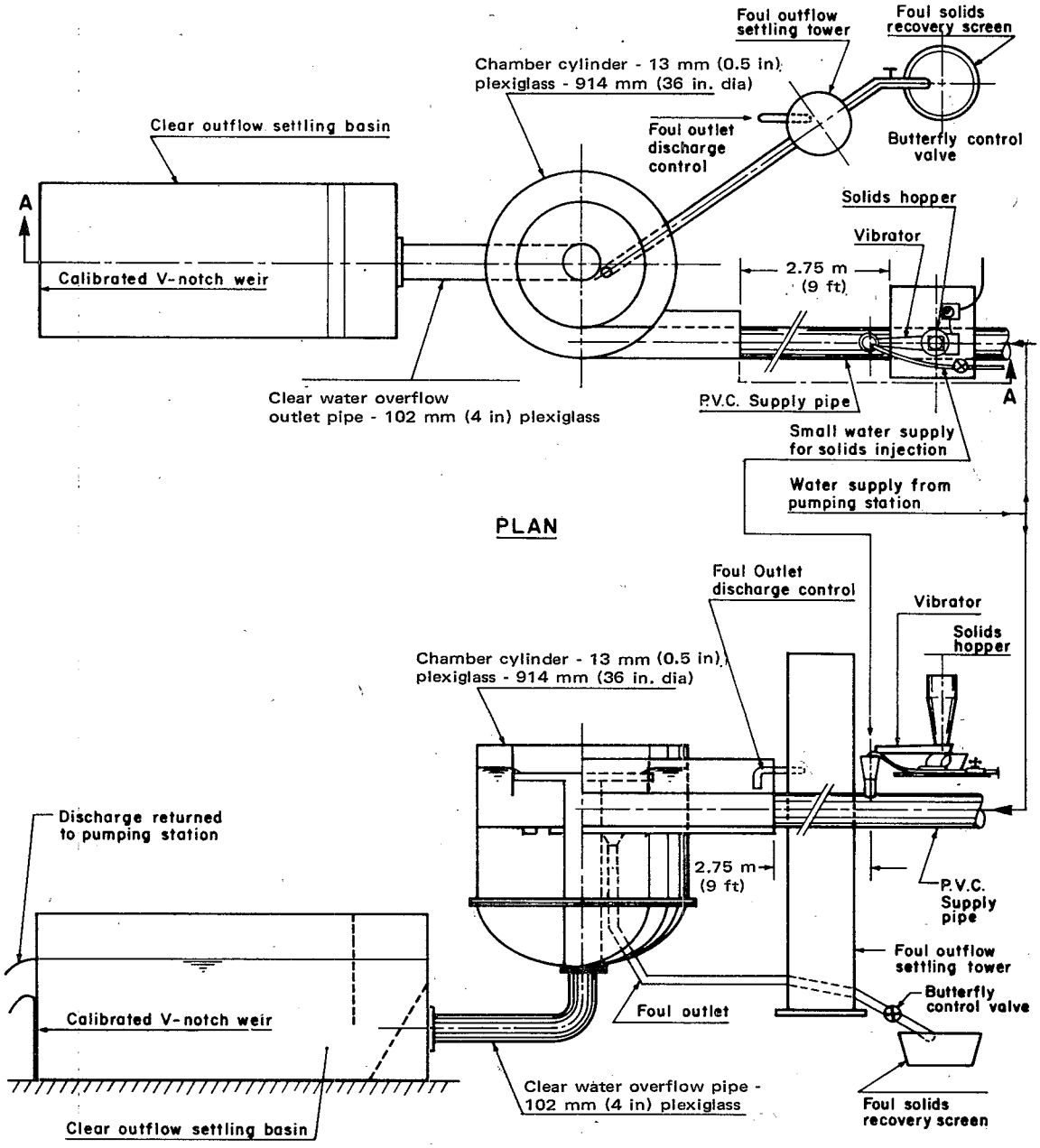

FIGURE 2 MODEL LAYOUT

first phase of the model tests, the bottom cone was adjusted to provide a 10 cm (4 in) wide annular flat bench between the top of the conical hopper and the bottom of the swirl separator cylindrical chamber to serve as a partial chamber floor as shown in Figure 3. For subsequent series of tests, designed to improve the characteristics of the swirl pattern and the solids separation efficiency, the concrete hopper cone was extended upward to the periphery of the chamber wall and the flat bench surface was eliminated, as shown in Figure 4.

A Plexiglas skirt, supported by the chamber wall and concentric to the chamber's vertical axis, divided the chamber into two concentric sectors – inner and outer. The vertical distance from the bottom of the skirt to the bottom of the cylindrical chamber or the top of the conical hopper represented the inter-connecting slot between the two concentric chamber sectors. The slot opening was readily changeable by means of calibrated supporting blocks.

A 15.2 cm (6 in) PVC effluent discharge downshaft installed concentrically around the chamber's vertical axis also provided structural support for the overflow weirs. The height of the weir could be easily changed by adding or removing custom-cut pieces of downshaft.

The vertical downshaft was later removed for subsequent studies to leave the inner chamber unencumbered and the weir was attached to and supported by the skirt. The bottom of the conical hopper was closed and the clear effluent overflowed through a circular gutter fixed around the skirt in the outer chamber, connected to an outside drain with two 2.5 cm (1 in) diameter Tygon® pipes which passed through the chamber wall as shown by Figure 5.

The chamber inflow pipe was 10 cm (4 in.) diameter polyvinyl chloride (PVC) set at a slope of 1/1000. A vibrating solids injection system was placed on the inflow line 2.14 m (9 ft) upstream of the chamber. Water was supplied directly from the constant level tank in one of the laboratory's permanent pumping stations. This supply device was used as long as the recovery of large size grain material injected presented no problem. When smaller grain sizes were used, a closed circuit device was built. PVC pipe was removed and replaced by a 76.2 cm (30 in) long Plexiglas pipe while the solid injection system was reduced to a mere hopper attached on the top of the inlet duct as shown by Figure 5, through which diluted material was introduced into the model at a constant rate.

Outflow from the central pipe, and later from the collecting annular gutter, went to a large settling basin equipped with a calibrated V-notch weir.

A point gauge in a manometer pot read the level in the basin, determining the discharge going over the V-notch weir. This represented the total discharge passing through the separation chamber.

The foregoing descriptions, supplemented by the figures in Appendix A showing the original structural format of the swirl chamber and the subsequent changes involving the elimination of the flat bench at the top of the conical bottom hopper, indicate that variances were made in the model for the purpose of initiating added studies of swirl patterns and performances. These changes were only part of the many structural modifications introduced into the model, and the numerous test runs carried out with each of such physical changes.

In all, twelve modifications were made, involving the shaping of the conical hopper to provide a bench flat floor between it and the cylindrical swirl chamber, and to eliminate this plateau; changes in the elevation of the inlet sewer entering the swirl chamber; shapes of the overflow weir; diameter of the skirt; depth of the skirt; diameter of the weir; use of the overflow weir as a sealed unit, with concentric orifice ports for the upflow of effluent from the bottom chamber to the upper or discharge chamber; variations in slot height under the skirt; elimination of the circular effluent weir and replacement with four radial weirs discharging into the central overflow outlet downdraft pipe; variations in the length of such radial overflow weirs; installation of eight radial effluent weirs with flat-surface crests; conversion of these eight weirs into "saw-tooth" crested weirs; and removal of the central outlet downdraft pipe and discharge of effluent from the collecting

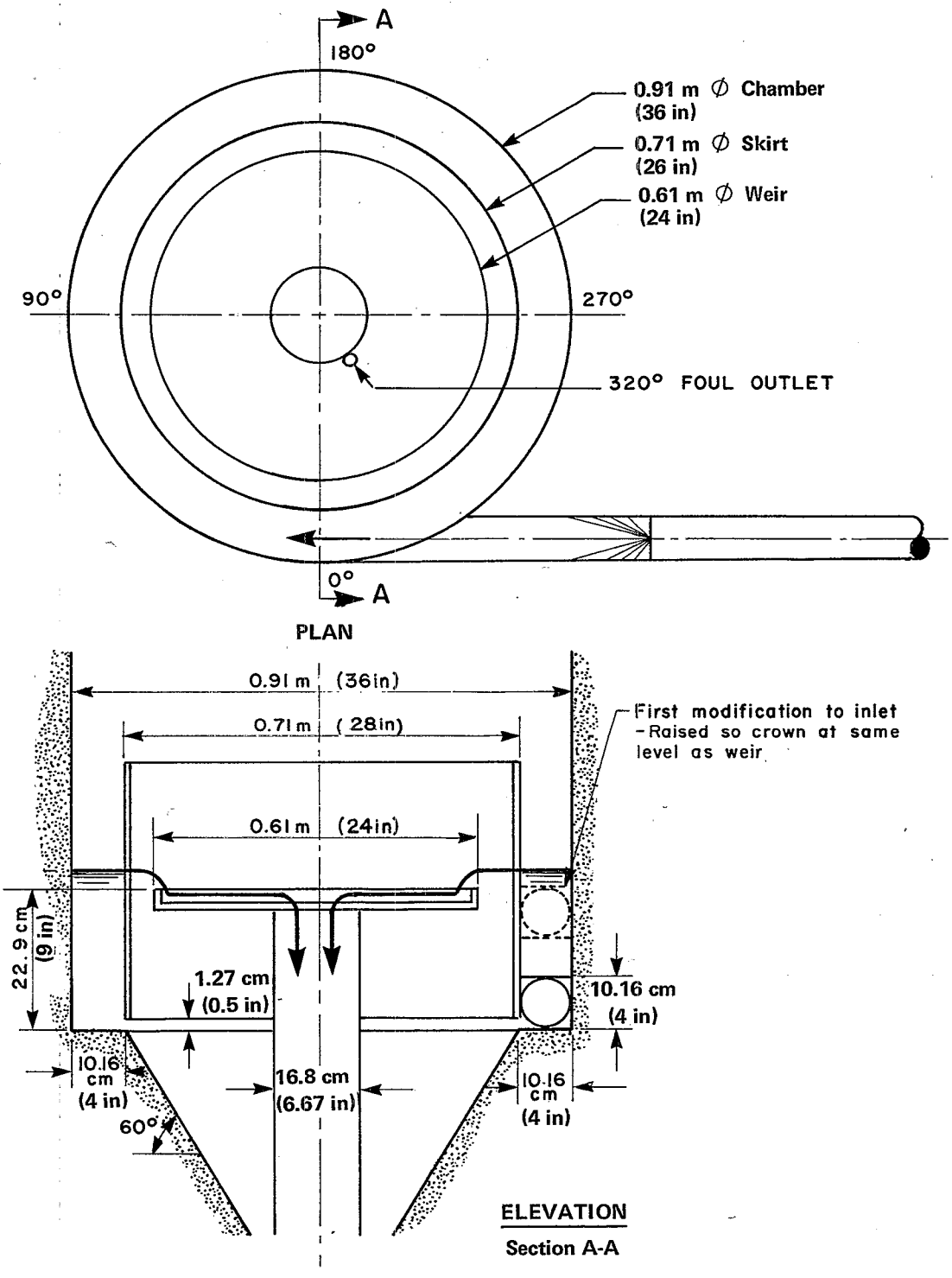

FIGURE 3 SWIRL PRIMARY SEPARATOR
FIRST LAYOUT TESTED ON MODEL

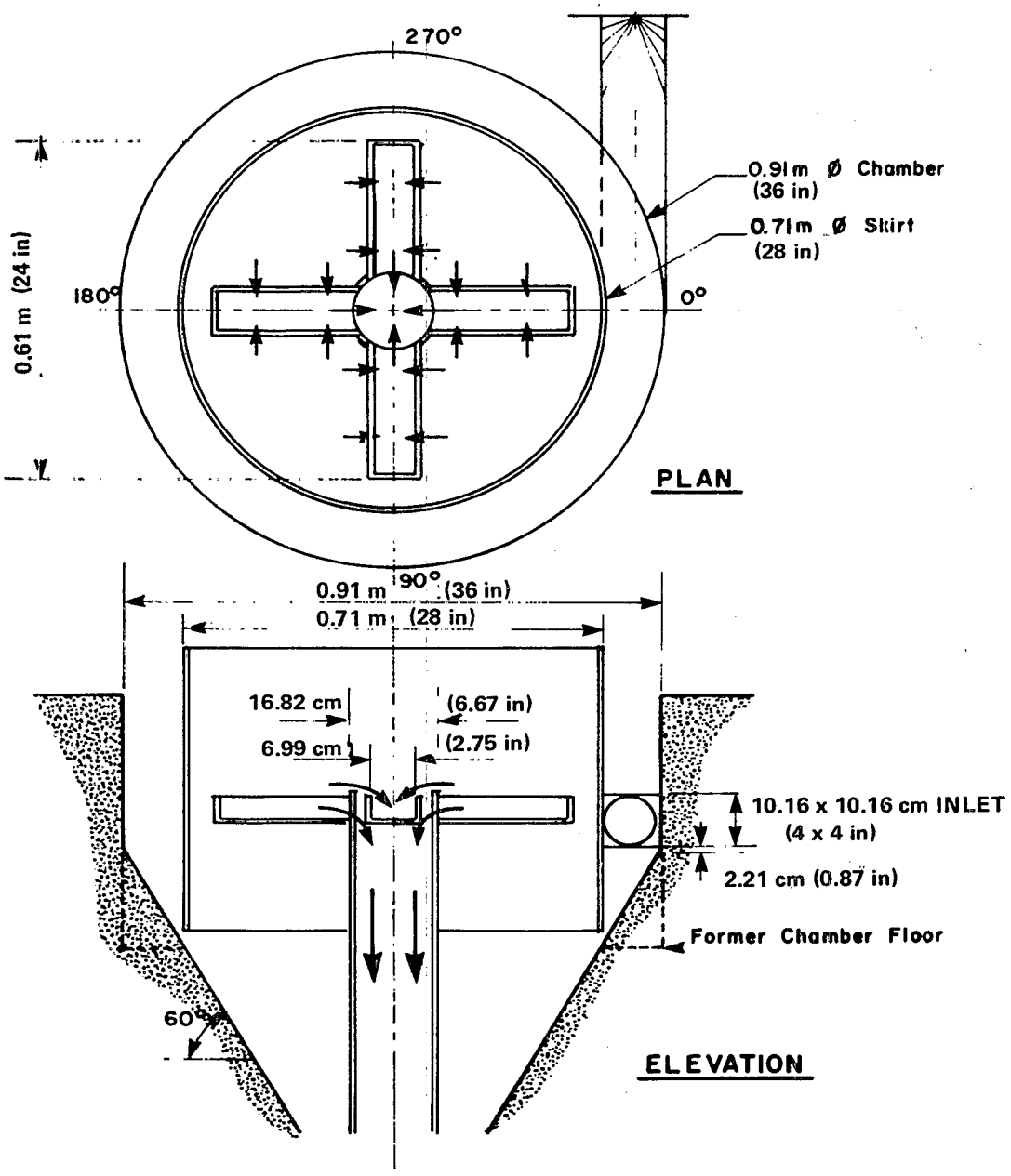

FIGURE 4 SWIRL PRIMARY SEPARATOR
MODEL LAYOUT FOR TESTS 161 to 184 – MODIFICATION 10

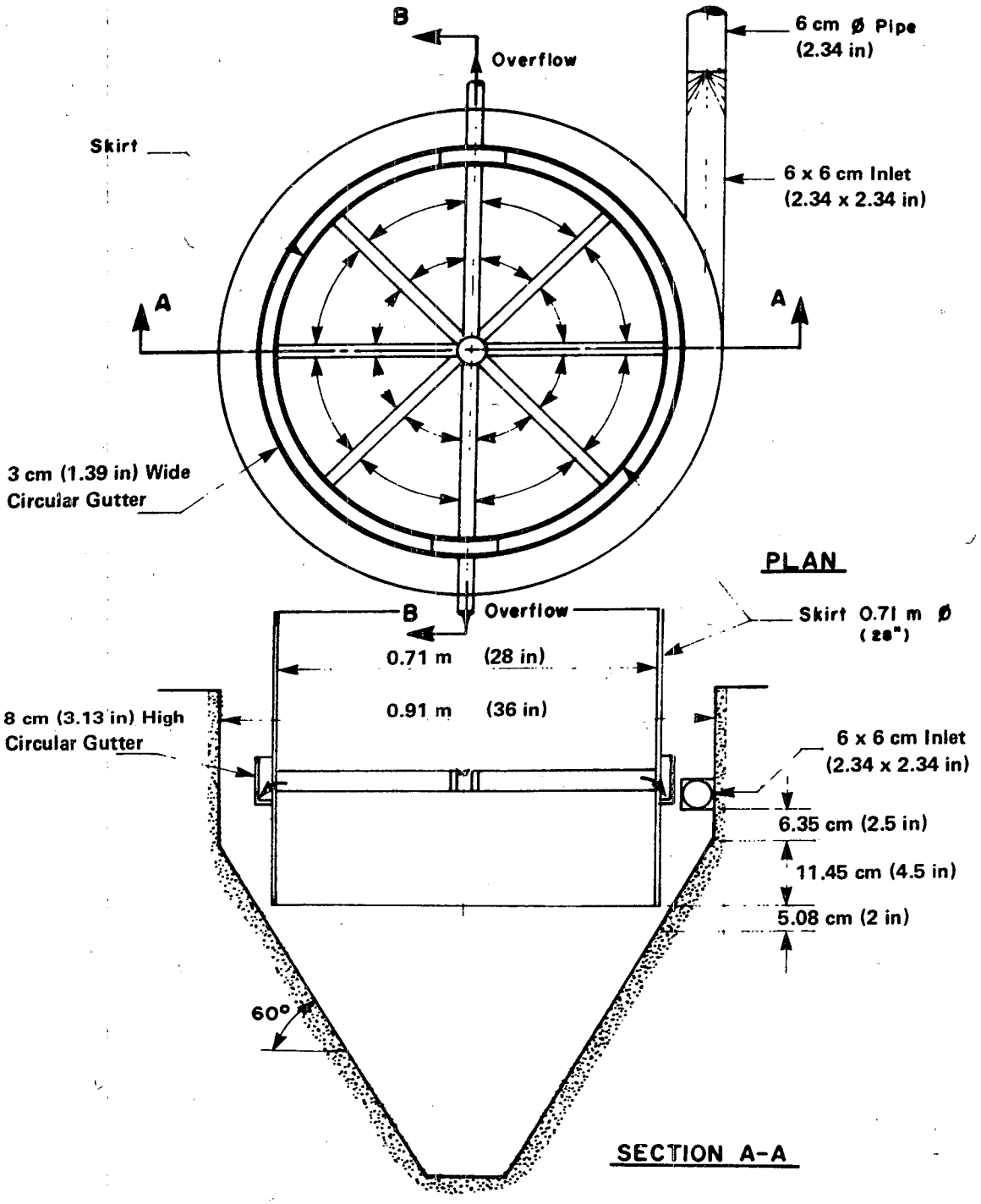

FIGURE 5a SWIRL PRIMARY SEPARATOR
MODEL LAYOUT FOR TESTS 188 to 194 (3 to 9)
MODIFICATION 11

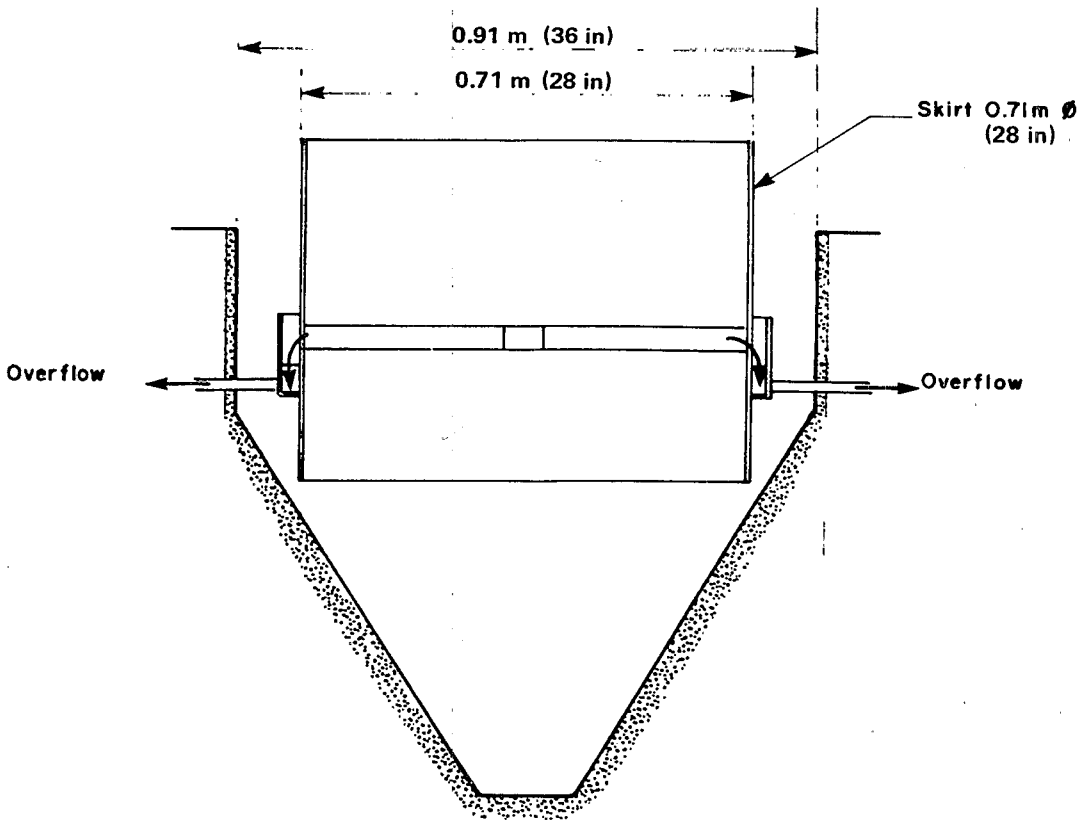

SECTION B-B

FIGURE 5b SWIRL PRIMARY SEPARATOR
MODEL LAYOUT FOR TESTS 188 to 194 (3 to 9)
MODIFICATION 11

weirs via a concentric channel connected by outlet pipes through the swirl chamber wall. Other internal details were involved in the series of model modifications.

Each structural modification was accompanied by a series of runs, all controlled in terms of types of materials added to the flow, rates of flow, removal efficiency studies, tracing of velocity contours and flow patterns; determinations of settling velocities vs. particle size for Petrothene® and IRA-93 anion exchange resin – the two basic materials used to simulate sewage solids of settleable and colloidal characterisitcs; effects of the installation of a baffle deflector at the inlet to the swirl chamber to induce greater secondary flow action. A total of 194 test cycles were involved in all of the structural modifications and the analytical investigations.

Definitive findings on model efficiencies of solids removal from the influent flow depended on the representativeness of the simulated model solids. During the period while the Beak studies[3] were underway to characterize actual sanitary sewage solids components and to develop a synthetic material to represent these material characteristics in model scale, the LaSalle studies were carried out with shredded Petrothene, which was adequate to guide basic determinations of chamber sizes and

geometric internal shapes and dimensions. When the results of the Beak studies became available, a new material – an anion exchange resin designated as IRA-93 manufactured by Rohm and Haas – was utilized in the model studies.

The Petrothene material had been shredded and possessed a gradation curve shown in Figure 6. Settling velocities for this material were plotted vs. particle size, as measured by Beak, and theoretical settling velocities were deduced for material having a specific gravity of 1.01. Subsequently, a family of curves was devised for different specific gravities for the purpose of determining the particle size for each selected specific gravity and ascertaining the comparable settling velocity.

Before the use of the anion exchange resin in the swirl studies was initiated, it was found that relatively uniform solids recoveries of from 95 to 100 percent of Petrothene were being achieved. Thus, the Petrothene did not offer enough range to differentiate between the chamber effectiveness levels covering the modifications to be studied, and it precluded decisions on the swirl geometrics that would produce optimum clarification results.

The use of IRA-93 anion exchange resin provided the flexibility and decision-making characteristics desired in the studies. A nominal specific gravity of 1.04 was given for the new test material and the procedures used for Petrothene in ascertaining settling velocities vs. particle size were reproduced for the more serviceable simulated solids, as shown in Figure 7. The same procedure described earlier for Petrothene was followed in scaling up this curve to different scales to define the settling velocities of particles simulated by the IRA-93. The choice of solids fractions followed the findings of the Beak studies on representative sewage solids characteristics and the recommendation for simulated model particle sizes.

The approach used in determining the actions of various particle sizes was adequate for each such characteristic, but it did not provide information on the distribution of grain sizes in the simulated loading on the swirl model. Subsequent settling column studies by Beak on representative sewage samples at Philadelphia, Pennsylvania, precisely defined the recommended fraction of the crushed IRA-93 material as passing a No. 100 sieve and retained on a No. 200 sieve. A model curve of settling velocities vs. percentages less than or equal to the presence of various particle sizes was evolved for sanitary sewage by the Beak studies and a family of curves covering various particle sizes was developed therefrom, at scales transposed according to Froude's Law. These data permitted calculation of the percentages of sanitary sewage in the differently scaled prototypes that were simulated by the IRA-93 used in the model.

Out of these scalings, Figure 8 was developed. This figure is the key in finding the portions of the prototype sewage simulated by the model material; it was used in the final prediction of prototype recovery rates. While the IRA-93 did not simulate as complete a range of prototype sewage particles as would be desired, it was recognized that sewage composition is highly variable from location to location, and even from time to time in the same system.

Operation of the swirl concentrator as a primary separator facility to replace conventional sedimentation tanks would normally involve a continuous steady state discharge – the design discharge. Since it was the purpose of the model studies to adjust the chamber dimensions and internal appurtenant facilities to the flowrate to be treated, the range of the study was extended to cover the three different flows previously described (0.5, 1.0, 1.5 l/sec). This allowed observations on the behavior of the separation chamber and the variation of the solids recovery rate when conditions of operation were changed. The three flowrates demonstrated the combined influence of the inlet and slot velocities on the solids separation process. The studies covered, in addition, evaluations of the impact of different combinations of weir and skirt dimensions and locations on settling efficiencies.

For each individual test in the overall series, steady-state flow was established and equilibrium attained. One l (17 oz) of wet Petrothene or IRA-93 was injected into the incoming flow over a period of five minutes

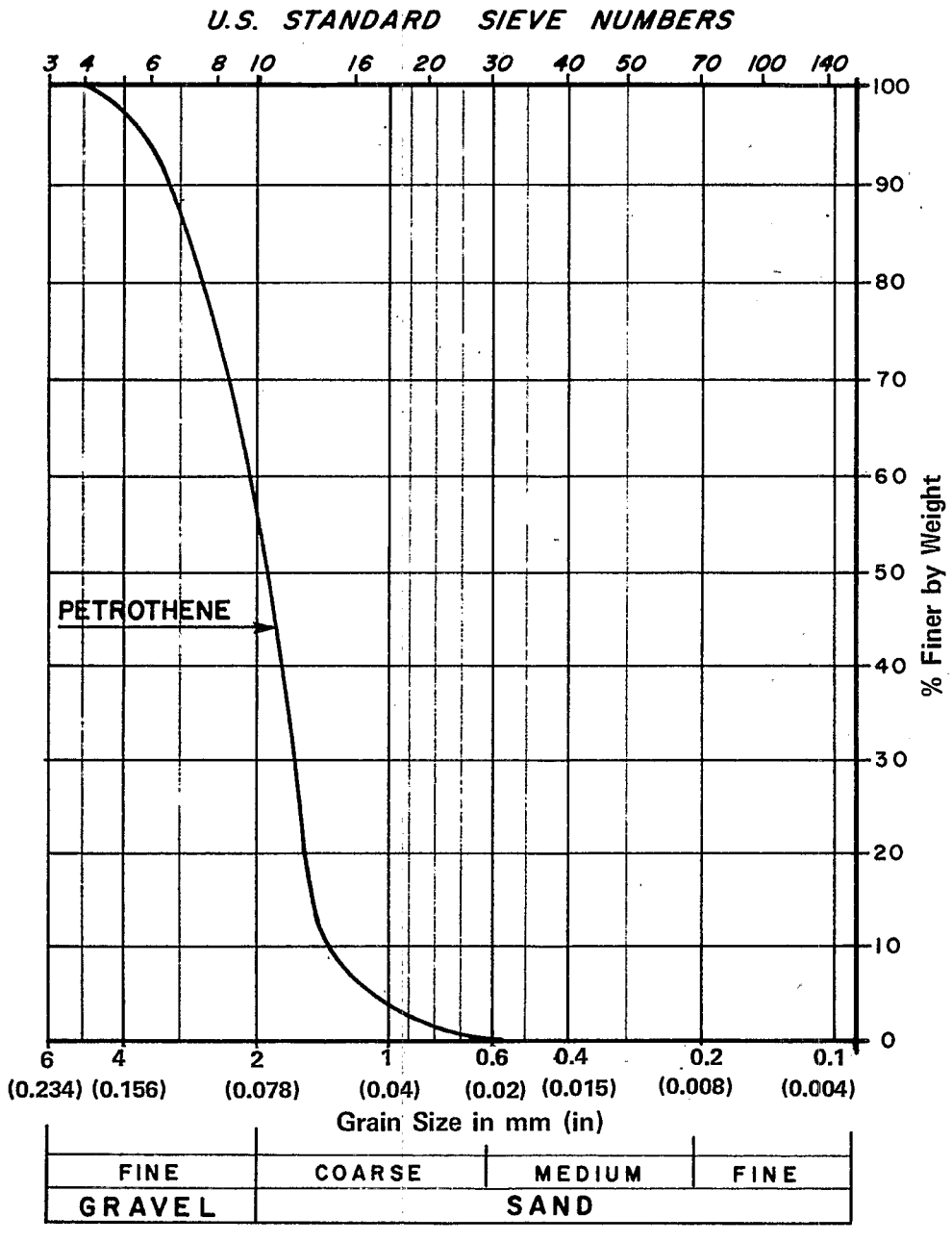

FIGURE 6 GRADATION CURVE FOR PETROTHENE USED IN MODEL

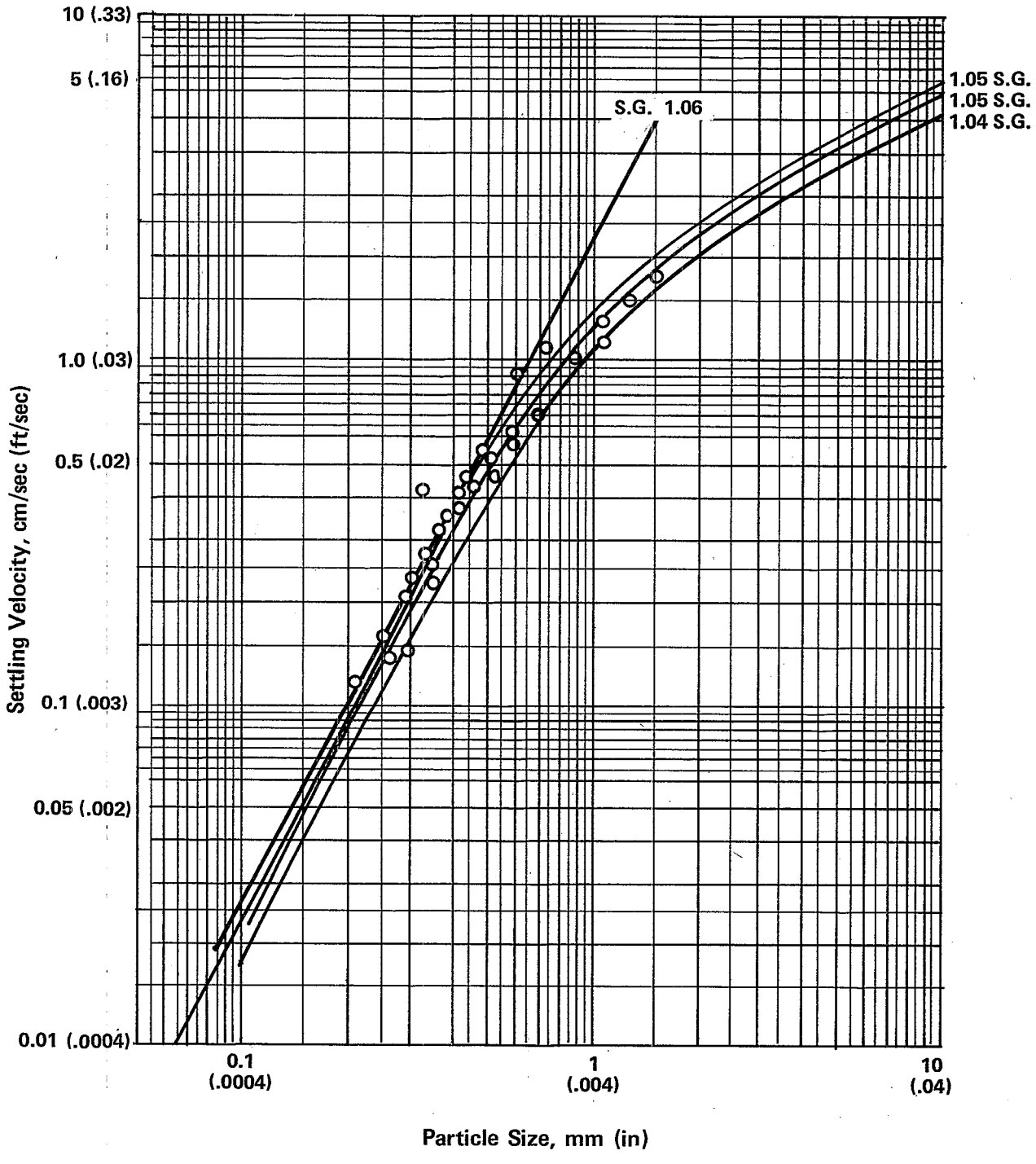

FIGURE 7 SETTLING VELOCITY VS PARTICLE SIZE FOR IRA-93 ANION EXCHANGE RESIN

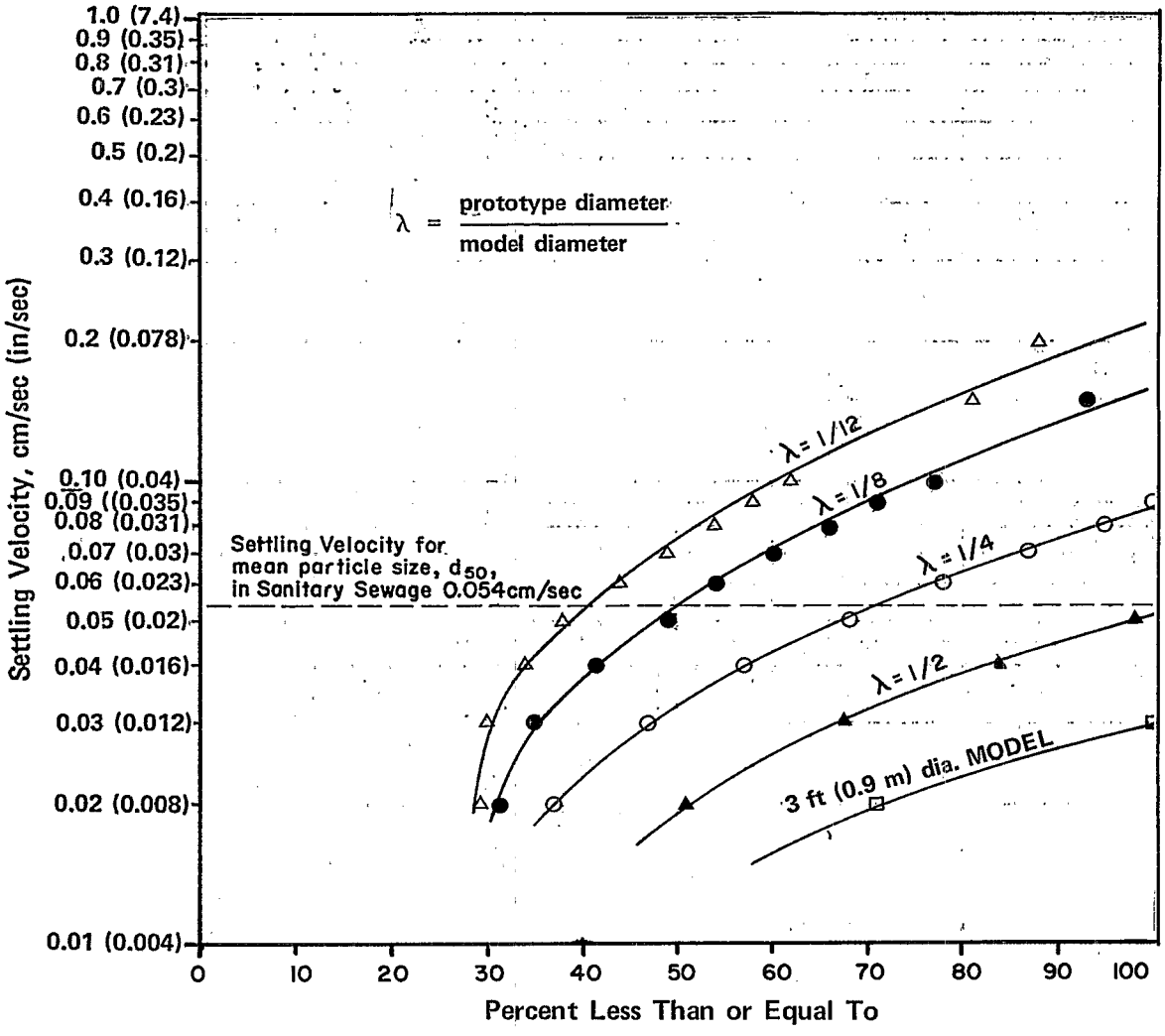

NOTE: IRA-93 used in model had particles $149\mu \geqslant d \geqslant 74\ \mu$

FIGURE 8 SWIRL PRIMARY SEPARATOR
SANITARY SEWAGE IN PROTOTYPES REPRESENTED BY
IRA - 93 IN MODEL

and the model was allowed to run ten minutes after the end of the solids application period. The amounts of the applied solids found in the bottom of the hopper cone and the floating material in the outer sector of the swirl unit were measured separately. The material floating in the settling basin was also measured.

The remaining portion deposited in the settling basin was determined by subtraction, based on the assumption that no material was lost. The swirl solids separation efficiency was taken as the percentage represented by the amount measured on the bottom of the cone as compared to the total found in the cone and on the bottom of the settling basin.

The details of the removal efficiencies achieved with shredded polythene, Petrothene X® and anion exchange resin IRA-93 under varying conditions in the 12 modifications of the swirl chamber outlined above are contained in Appendix A. The findings highlights are listed here:

- Using shredded Petrothene in the model with circular weir, the recovery rate was 84 percent at a rate of 1 l/sec (11.38

mgd) and a 1.2 cm (0.5 in.) slot height. However, with the inlet sewer at the same level as the outer chamber floor, undesirable turbulences were experienced under the weir in both the inner and outer chambers.

- With the crown of the inlet line raised to the level of the weir lip, the recovery rate remained at approximately the same – 78 percent – but it was demonstrated that the turbulence was mainly due to the location of the bottom of the skirt just above the horizontal floor. Recoveries improved as flowrates decreased and detention time increased. Slot height tests were inconclusive. Removal of the skirt resulted in marked reduction of recovery.
- Using ground Petrothene, solids removals paralleled those experienced with shredded Petrothene. High recoveries were produced at 1.0 and 1.5 l/sec (11.38 and 17.07 mgd) rates but they deteriorated when the skirt was removed. At high flows of 1.5 l/sec (17.07 mgd), recovery started at 50 percent but increased progressively as the slot height was increased.
- With a 16.9 cm (6.68 in.) diameter weir, a fairly constant recovery rate of 98 percent was obtained for a flowrate of 0.5 l/sec (5.69 mgd). Recovery rates dropped as the slot height increased and very low performance was recorded for higher slot openings.
- Using anion exchange resin IRA-93 as representative of the fine-grain recovery that would simulate in the model the actual sewage conditions to be encountered in a prototype installation, recovery efficiencies were determined for the successive modifications of the model. Because of changed flow patterns and other factors induced by these changes, solids recoveries ranged from 91 to 81 percent at rates of 0.1 l/sec (1.14 mgd); from 65.3 to 44 percent at rates of 0.3 l/sec (3.42 mgd); from 52 to 23 percent for flows at 0.5 l/sec (5.69 mgd); from 68.8 to 23 percent for flows at 0.75 l/sec (8.54 mgd); and from 33.7 to 27.5 percent at rates of 1.0 l/sec (11.38 mgd).

The predicted solids recovery performances in prototype units, based on the final use of IRA-93 anion exchange resin was in a sense, the culmination of all the studies. The corresponding solids removal efficiencies for the five model flowrates used in the various tests are tabulated in Table 1.

The median settling velocity for sanitary sewage solids was selected as 0.054 cm/sec (0.00177 ft/sec); this was assumed to be the representative point for all sewage to be handled in any prototype. Curves were deduced that would enable a designer to determine removal efficiencies for a given sewage flow as a function of the diameter of the main chamber.

MATHEMATICAL MODEL STUDY

The purpose of the mathematical model study of the swirl primary separator was to validate and verify the findings of the hydraulic model investigation. The applicability of the swirl flow patterns for the purpose of separating solids and liquid phases had been explored previously[1] and verified as a feasible, workable hydraulic principle for use in combined sewer overflow-regulator conditions and for selective removal of

TABLE 1
SOLIDS REMOVAL EFFICIENCIES OF IRA-93 AT VARIOUS DISCHARGE RATES

Model Discharge:					
l/sec	0.1	0.3	0.5	0.75	1.0
cfs	0.0035	0.0106	0.0176	0.0264	0.0352
Recovery Rate:					
Percent	91	58	41	31	27

inorganic grit from organic, lighter solids materials in sanitary and combined sewage.

The approach to mathematical modeling followed the procedures used in the previous study of combined sewer overflow regulation. The flows within the chamber were assumed to be axisymmetric about the vertical axis. The chamber was then overlaid with a computational grid and the flowfield velocities were computed at each grid point by solving the liquid continuity equation and equations of motions. An eddy viscosity condition was utilized to represent the turbulent shear stress. Plots of streamlines and velocity profiles were prepared to portray the liquid flowfield as predicted by the mathematical model.

Particle paths were calculated by superimposing particle settling velocities on the liquid flowfield. The studies demonstrated that a simplified solution could be used to predict a theoretical upper limit on solids removal efficiencies in the swirl chamber. Good agreement was found between the theoretical upper limit of solids recovery and actual removal efficiencies observed in the hydraulic model studies.

The mathematical computer study, substantiated by the hydraulic model findings, provided data upon which to base predicted solids removal efficiencies for prototype installations of swirl settling facilities. The mathematical model work emphasized the importance of exact information on sewage solids settling properties before definitive chamber design can be undertaken.

In mathematical evaluation of the flowfield, a simplified configuration of the swirl settler unit was utilized, as shown in Figure 9. The region between the skirt and the outer wall of the chamber was not included in the mathematical model because most of the particle settling occurs in the main body of the chamber. This simplified the specification of the boundary conditions for the mathematical-computer studies. The liquid flow was assumed to axisymmetric, and the flowfield was assumed to be identical at every radial cross section and independent of the angular position.

The assumption of axisymmetry is appropriate because the flow enters the main portion of the chamber at all points along the circumference of the skirt. As a consequence, the mathematical representation of the liquid flowfield was very close to the actual conditions in the hydraulic model. The eddy-viscosity mixing-length constant and the skin friction coefficient were assumed to be equal to the values obtained in the previous mathematical model studies for combined sewer overflow swirl treatment. A closer agreement between the velocity flowfield predicted by the mathematical model and the hydraulic model could be obtained by refining these values but particle removal efficiencies would be relatively unchanged.

Actual prediction of solids removal efficiencies in any prototype unit, based on mathematical model computations, would require firm information on the properties of actual sewage and the simulated sewage solids used in the hydraulic model. This information was provided by the Beak test program on column settling characteristics. These column test data have been utilized to determine a frequency distribution of the particle settling velocities which can be used to compare settling properties of different materials. Three types of material were considered in the hydraulic and mathematical model studies: Shredded Petrothene, IRA-93 anion exchange resin, and so-called Arizona Road Dust. The latter material simulates the fines and colloidal material in actual sewage but was too costly and unavailable in adequate quantities for extended laboratory studies.

The mathematical model studies examined the phenomena of solids settling in swirl chamber conditions, covering single-settling velocity distribution without any flocculation reactions; hindered settlement in which solids impinge upon each other and thus inhibit simple gravity subsidence; and flocculation or agglomeration mechanisms which result in the coalescence of solids and enhancement of settling characteristics. The agglomeration mechanisms involve the forces of gravity, shear flow, turbulent acceleration, turbulent entrainment, and Brownian motion.

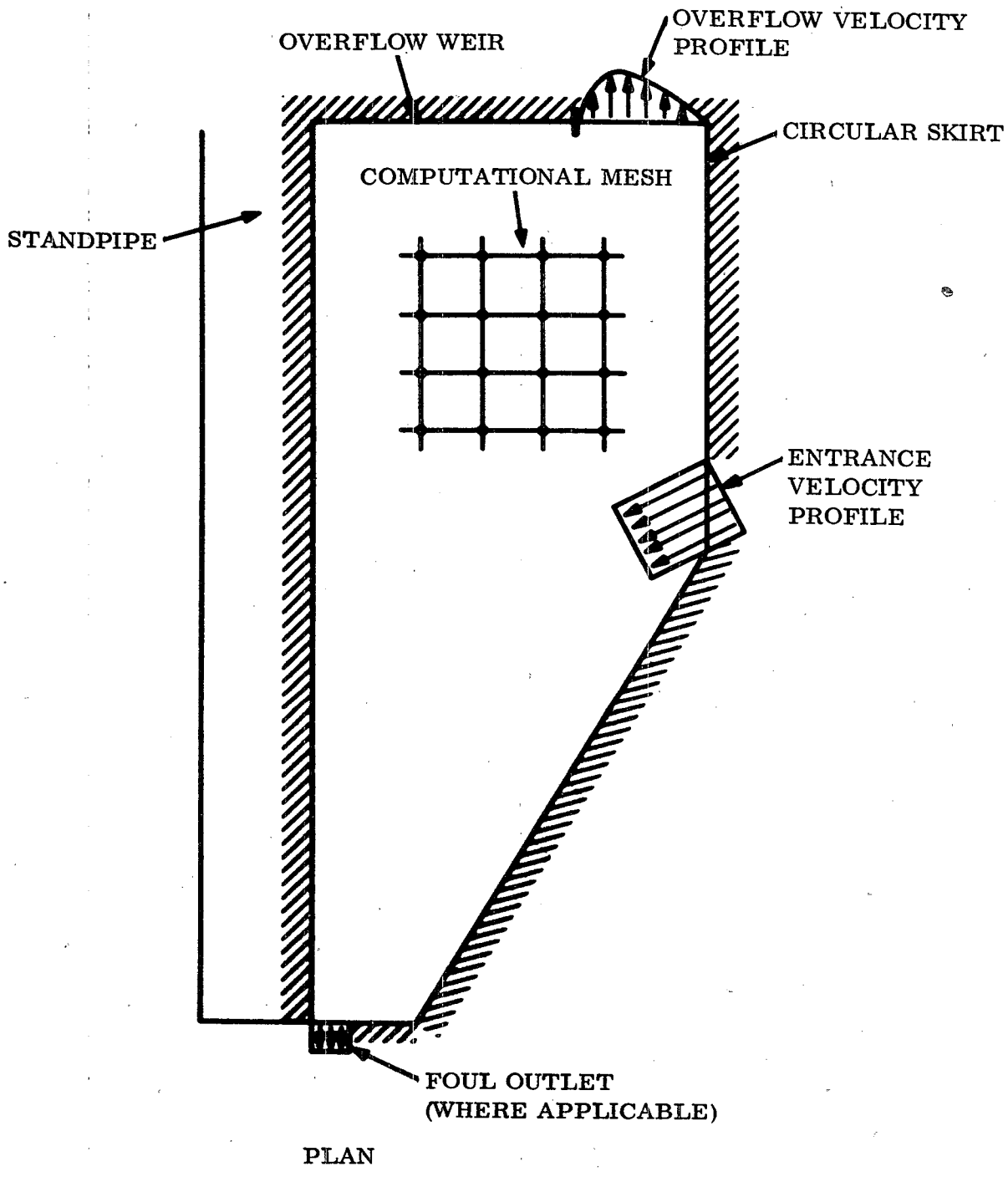

FIGURE 9 DIAGRAM OF SWIRL PRIMARY SEPARATOR CHAMBER AS REPRESENTED BY MATHEMATICAL MODEL

From settling column tests carried out by Beak Consultants, it was concluded that test solids settle as discrete particles while actual sewage can exhibit flocculation properties even at low concentrations. The mathematical model studies involved detailed analyses of the kinetics of flocculation. It was found that the degree of flocculation or agglomeration is dependent on particle collisions and estimates were made of the number of collisions which result from the mechanisms of gravity action, shear action, turbulent acceleration, turbulent entrainment, and Brownian motion. The turbulent entrainment mechanism was found to be the most important in the outer annulus section of the swirl separator where most of the inlet energy is dissipated.

It was found numerically impractical to carry out exact mathematical modeling of the flocculation effects on particle settling rates. Therefore, to accommodate the flocculation phenomenon in actual sewage a settling velocity distribution was assumed, indicative of sewage after flocculation in the inlet sewer and outer annulus of the swirl chamber. This condition will produce a settling velocity distribution equivalent to that obtained by the gravity mechanism in the Beak settling column test procedures. This was deemed to be a conservative assumption.

The full report on the mathematical model studies is included as Appendix B. It describes in detail the intricate methodologies utilized in developing calculations of particle flow, in terms of particle paths; boundary conditions; numerical methods; scaling techniques of the liquid flowfield; and scaling of the particle flows. In order to maintain similar liquid flows in different size swirl separation facilities it is necessary to use Froude scaling, relating liquid flow velocities by the square root of the scale factor and flowrates by the 5/2 power of the scale factor. A simplified equation was evolved for obtaining a first estimate of removal efficiency for a particle having a specified settling velocity, given the size and design flowrate of any prototype unit. A more accurate estimate of the removal efficiency can be obtained by scaling back the prototype flowrate and particle settling velocity to the laboratory model.

The mathematical model of the liquid flowfield was varied concurrently with the various modifications made in the hydraulic laboratory model to achieve improved solids removal efficiencies. Quantitative comparisons showed close concurrence between hydraulic and mathematical findings. Tangential velocity contours and streamlines for modified laboratory configurations were mathematically plotted. Removal efficiencies were projected mathematically for what was assumed to be the most typical for the materials used in the hydraulic model tests. The mathematical model predicted a 33.2 percent removal as the maximum limit on swirl chamber performance at a 0.5 l/sec (5.69 mgd) flow for IRA-93 resin having a size range from 100 (0.149 mm or 0.00049 in.) to 100 mesh (0.074 mm or 0.00024 in.). The actual IRA-93 resin solids removal observed in the hydraulic model was in the general range of 50 percent.

Initially four possible explanations were offered for this apparent discrepancy: swelling of resin material on contact with water, with consequent variations in settling velocity; electrostatic attractions of particles to the chamber walls or to other particles; failure of particles to completely disperse as single particles; and stratification of solids in the region under the skirt, producing higher concentrations along particle paths and improvement in settling. Subsequent investigations ruled out the first three phenomena but the stratification of solids material under the skirt was observed in the hydraulic model.

Appendix B also describes the effect of scaling on chamber performance and the influence of geometric variables on the efficiency of solids removal. The complexity of the data required to use the mathematical model makes it generally impractical to use for general design. The appendix describing the model has been included to assist future research work and to provide the theoretical basis for what was observed in the hydraulic laboratory.

THE PILOT STUDY

In August, 1974, the Department of Public Works (DPW) of Metropolitan Toronto constructed a 3.7 m (12 ft) diameter pilot unit. The unit followed the recommended design with two exceptions: a mechanical scum rake and the use of a slender central support column. The unit was fabricated of steel and installed by DPW employees at the Humber Wastewater Treatment Plant.

The Humber plant treats combined sewer flow from a large industrial district. The plant has experienced severe overloading problems and during the period of the testing, a major plant expansion was being undertaken. The total flow to the plant averages about 227,400 m^3/day (60 mgd) and can more than double during precipitation events.

Flow to the swirl concentrator was pumped from the influent flume to the primary tanks through a Parshall flume. Flow was varied to follow the rate of flow to the plant in the May-July tests but was kept constant in all subsequent tests.

Figure 10 contains photographs of the facility.

The influent flume leads to six primary tanks. Each primary tank is 10.4 m (34 ft) wide and 72.7 m (237 ft) long, with average depth of 3.2 m (10.6 ft). Total volume of the primary tanks is 14,540 m^3 (513,400 ft^3). Total surface area is 449 m^2 (4,833.2 ft^2).

The details of the swirl separator are as follows: diameter is 3.7 m (12 ft); distance from overflow weir to bottom of straight sides is 0.53 m (1.75 ft); the 60-degree cone-shaped bottom is 2.9 m (9.5 ft) deep. The surface area of the tank is 10.5 m^2 (113 ft^2). The volume of the tank below the weir elevation is 16.3 m^3 (577 ft^3). If the bottom 1.2 m (4 ft) of the cone, with volume of 0.9 m^3 (32 ft^3), is designated as sludge storage then the net volume of the cone is 15.9 m^3 (560 ft^3). Prior to testing of the unit, detailed testing was conducted to characterize the flow and the flow rate. Beak Consultants Ltd., conducted tests to determine the settling rate characteristic of the solids and compared the results to the IRA-93 particles used in the hydraulic model study. Beak also studied the flow characteristics within the swirl unit and concluded that plug flow conditions prevailed.

Initial tests were conducted from April 29 to June 12 with disappointing results. Analyses of the data indicated that sludge was not being drawn off at frequent enough intervals.

A second series of tests was conducted at the design capacity of 1,137 m^3/day (0.3 mgd) and 1,700 m^3/day (0.45 mgd) from June 23 to July 8. This corresponds to overflow rates of 108 m^3/day m^2 (2,650 gal/day/ft^2) and 162 m^3/day/m^2 (3,980 gal/day/ft^2), and detention times of 20 minutes and 13 minutes, respectively.

The tests were run during week days for four hours a day. Tests were started at 11:00 a.m. in order to allow a minimum of three hours after wasted activated sludge had been returned to the system. Samples were taken each one-half hour and hourly composited samples were prepared for analysis. Both settleable and suspended solids were determined.

A final series of tests were run from September 2 to 15 with slightly revised procedures.

The results of the test program are presented in Section 4, Test of a Pilot Unit, and the Beak study results are contained in Section 8, Appendix C.

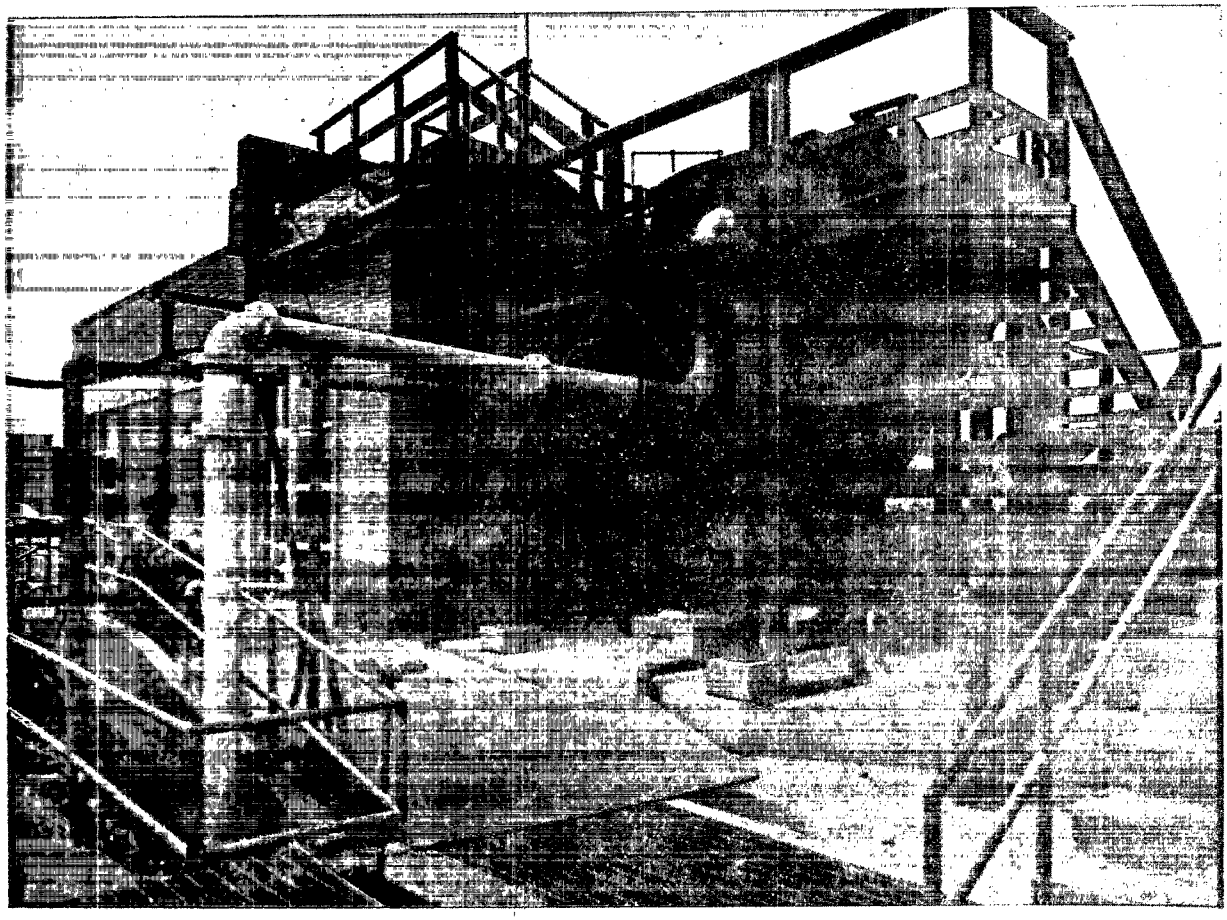

FIGURE 10 PILOT FACILITY – METRO TORONTO

Sludge Drawoff
Collection and Valve

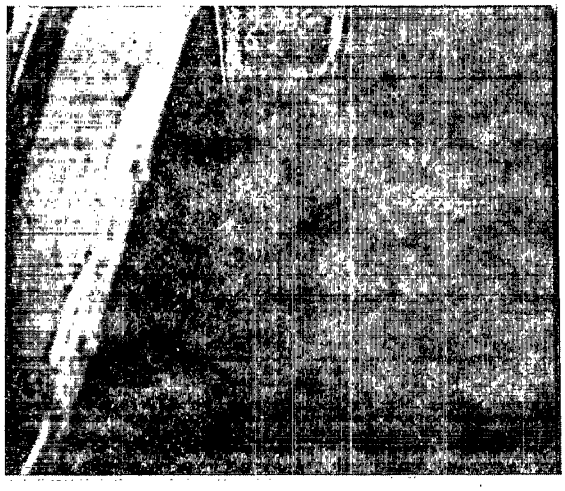

Interior View of Internal
Support for Wires

SECTION 3

DESIGN GUIDELINES AND CONSTRUCTION COSTS

Conventional primary sedimentation tanks are generally designed on the basis of overflow rate and, to a lesser extent, on detention time. The term "overflow rate" or "surface settling velocity" is the unit volume of flow per unit of time divided by the unit of tank area. In U.S. customary units this is expressed as gallons per day per square foot (gal/day/ft^2) and in metric units may be expressed as cubic meters per day per square meter (m^3/day/m^2). The American Society of Civil Engineers (ASCE) Manual of Engineering Practice Number 36[4] lists data on various primary settling tanks which indicate removal of suspended solids ranging from 20 to 80 percent. Figure 6 of that publication indicates the relation between removal of suspended solids and overflow rate. Many tanks fall in the range of 60 to 70 percent removal of suspended solids. If we accept 60 percent removal of suspended solids as a desirable objective then Figure 6 indicates the necessary overflow rate is 36.67 m^3/day/m^2 (900 gal/day/ft^2). The ASCE manual's curve in this range of suspended solids removal has been verified by more analyses of field data by Smith.[5] Detention time is no longer considered as the only factor in design of primary settling tanks. However, the use of tanks with liquid depths of 2.13 to 3.66 m (7 to 12 ft) combined with accepted overflow rates will result in nominal detention times of 1 to 2 hours. For instance, the use of a 3.05 m (10 ft) liquid depth with an overflow rate of 36.67 m^3/day/m^2 (900 gal/day/ft^2) will result in a detention time of 2 hours.

The equation developed by Smith[5] from the analyses of field data can be used to estimate the removal efficiency (percent) of suspended solids, η as a function of overflow rate (OVFRA) in gpd/ft^2 as follows:

$$\eta = 0.82e^{-OVFRA/2,780}$$

For OVFRA = 36,668 l/d/m^2 (900 gpd/ft^2), η = 59.3 percent. This value is in reasonable agreement with the 60 percent removal estimated by the use of the ASCE figure for a 36,668 l/d/m^2 (900 gpd/ft^2) overflow rate.

The swirl separator was not found suitable for use where 60 percent removal of suspended solids is the desired objective due to the size and resulting cost of the unit compared to conventional units. It appears that after the heavier, more easily handled solids are removed from the flow field, only quiescent settling will accomplish the balance of the solids removal. From the tests which were conducted, the low efficiency of solids removal and long detention times make large units impractical with the present design. Table 2 gives the flow and detention times for several size units as taken from Figures 11 and 12. The table indicates that the swirl separator has less detention time than conventional settling tanks over a small range of flows. At a diameter of 5.5 m (18 ft) the detention time necessary to achieve 40 to 50 percent suspended solids removal is approximately that of conventional units.

The design of the swirl separator is based neither on overflow rate nor detention time, but on the results of model tests. However, these two parameters are useful in comparing the size of the swirl separator with a conventional tank.

DESIGN PROCEDURE

Figures 11, 12, and 13 are used for design.

As indicated, the swirl separator cannot economically achieve conventional suspended solids removal of 60 percent. Therefore, the following design example is based upon 45 percent suspended solids removal, which is near the upper level of its efficiency for sanitary flow. Settling characteristics of combined sewer overflow solids are usually better than for sanitary sewage.

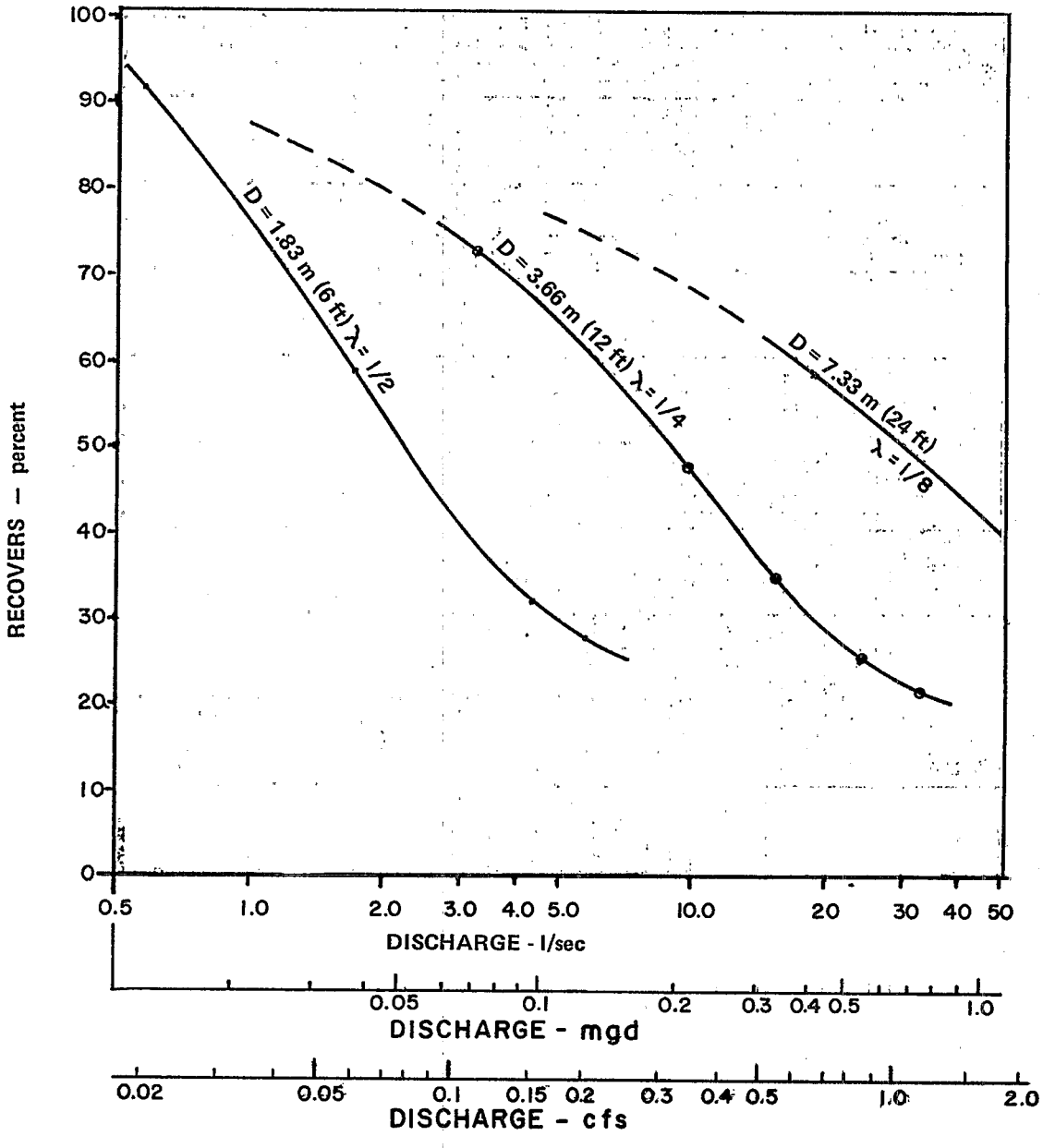

FIGURE 11a PREDICTED PROTOTYPE SOLIDS REMOVAL EFFICIENCY FOR SANITARY SEWAGE

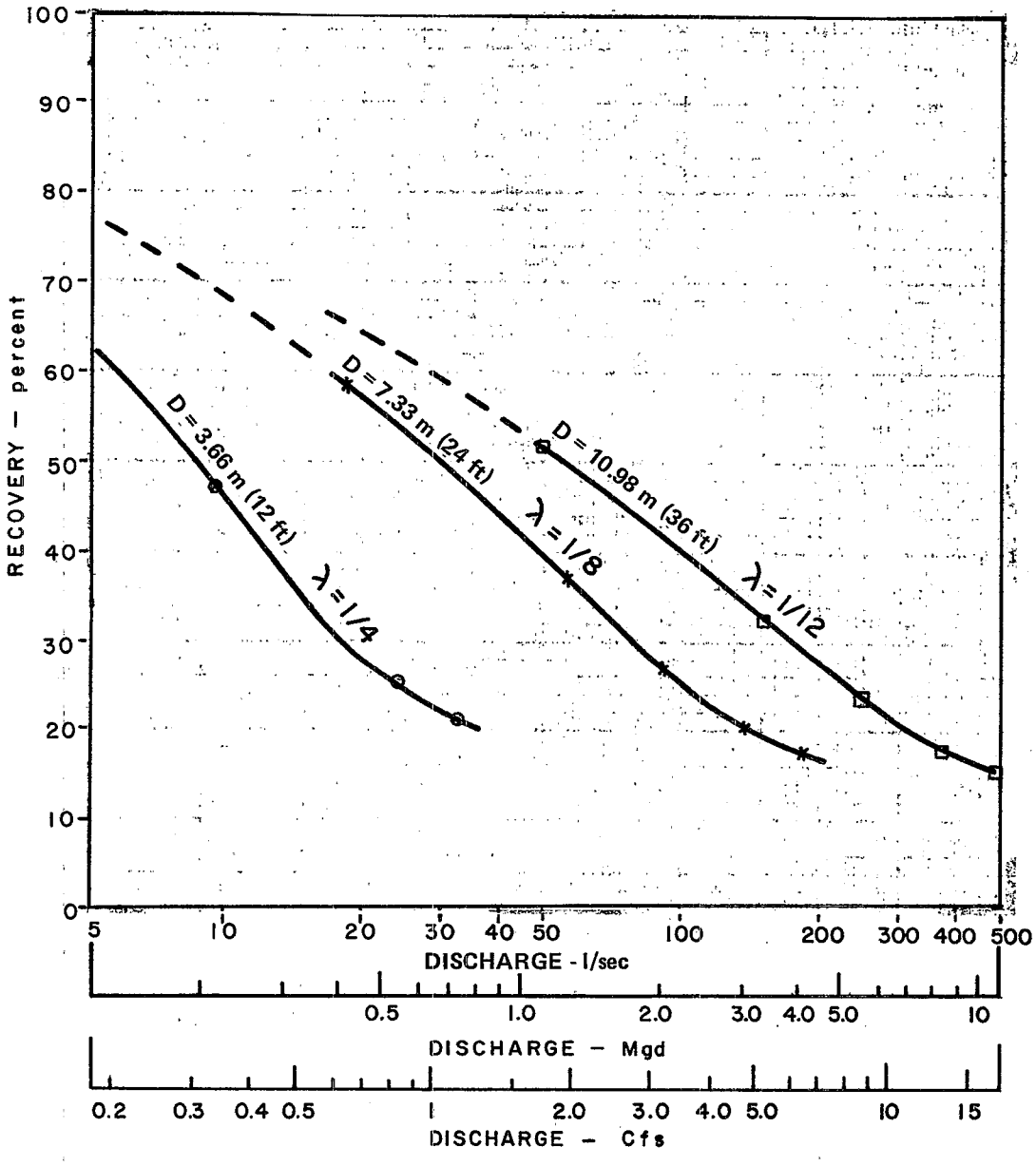

FIGURE 11b PREDICTED PROTOTYPE SOLIDS REMOVAL EFFICIENCY FOR SANITARY SEWAGE

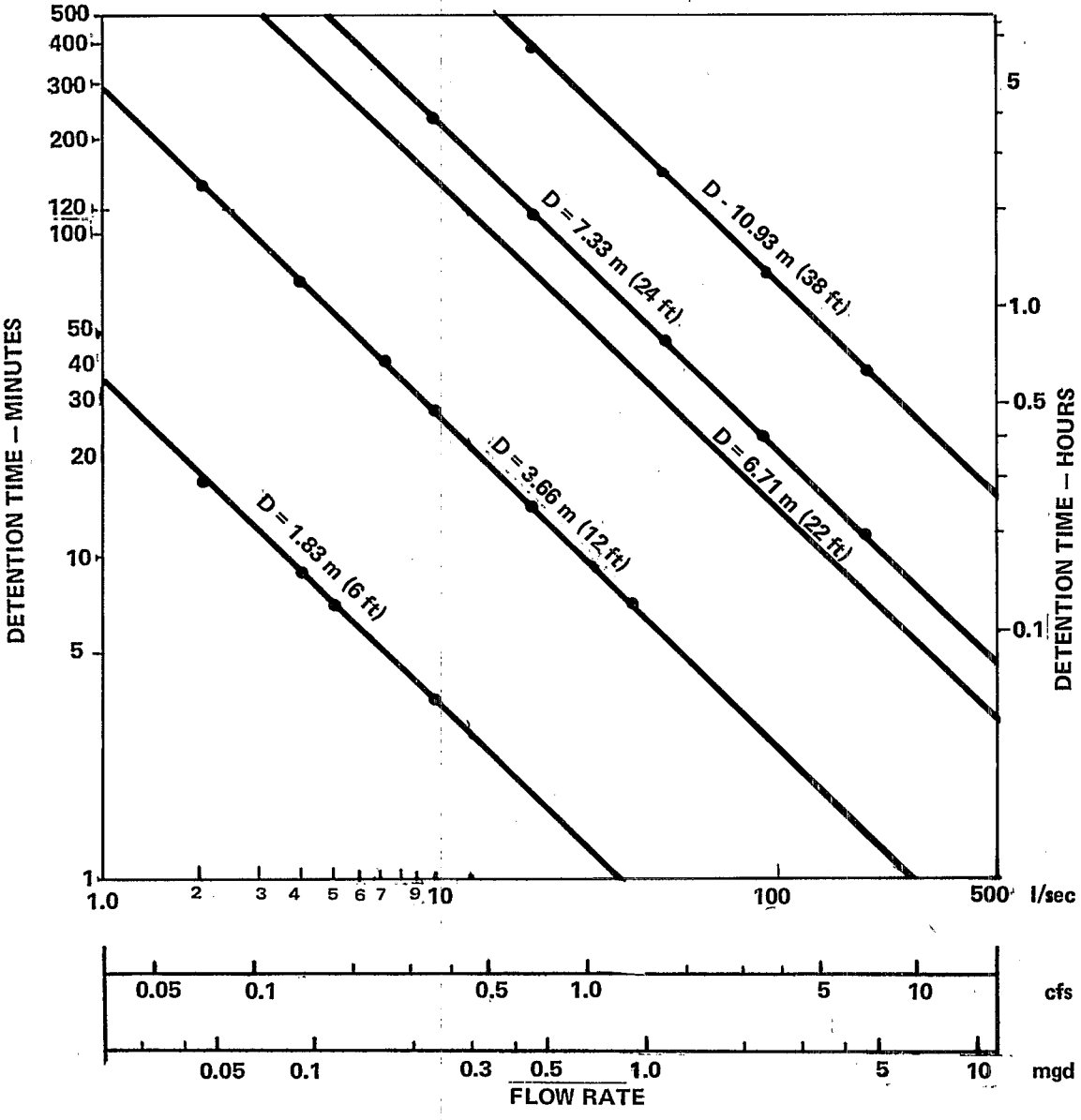

FIGURE 12 DETENTION TIMES

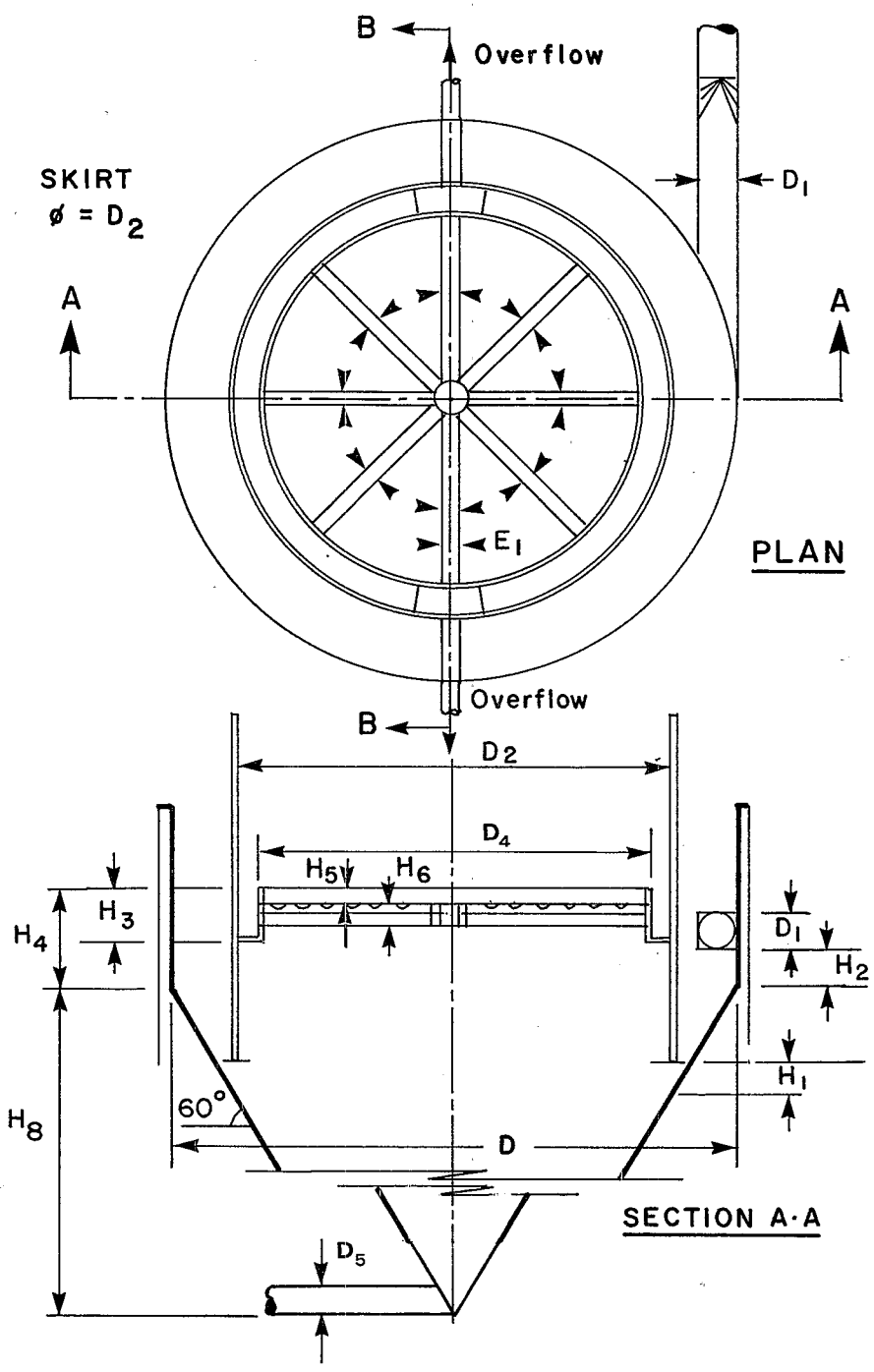

FIGURE 13a GENERAL DESIGN DIMENSIONS

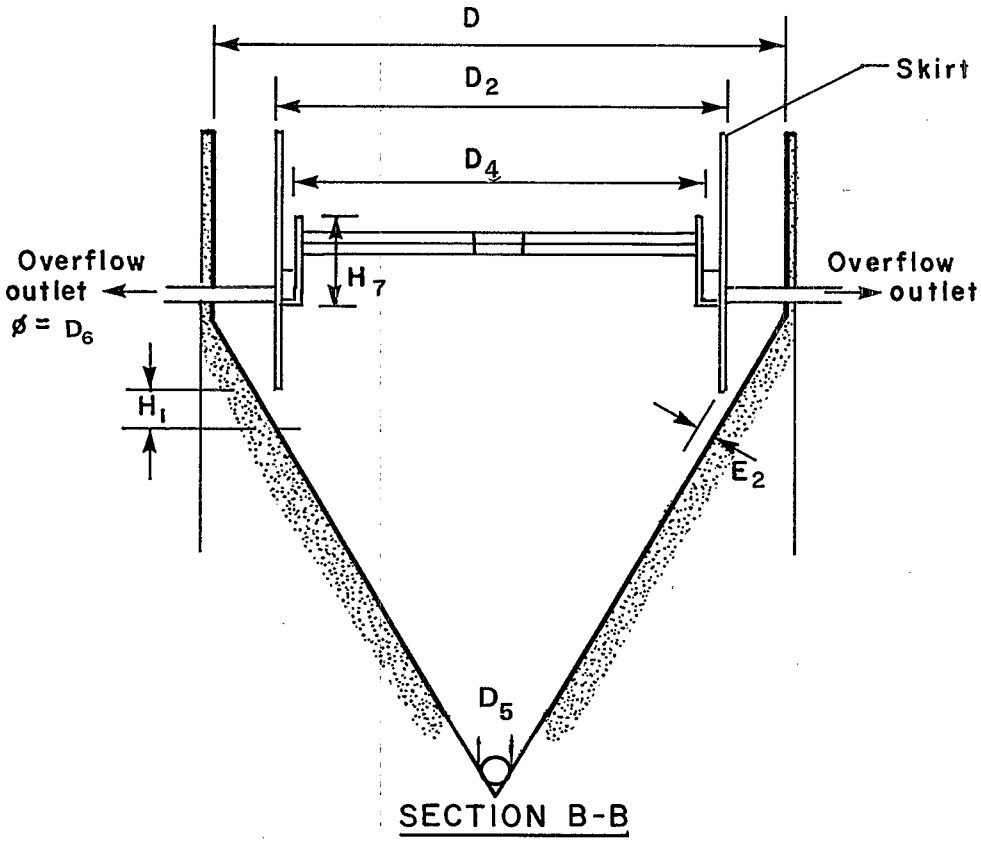

D = Diameter of Chamber (from Figure)

D_1	= 0.066 D	INLET	H_2	= 0.07 D	INVERT ELEV.
D_2	= 0.67 D	SKIRT	H_3	= 0.125 D	CIRCULAR GUTTER HEIGHT
D_4	= 0.58 D	GUTTER			
D_5	= 0.056 D	SLUDGE DRAW OFF	H_4	= 0.2 D	CIRCULAR GUTTER TOP ELEV.
D_6	= 0.042 D	OUTLET	H_5	= 0.04 D	GUTTER TOP ABOVE WEIR LIP
E_1	= 0.028 D	WEIR GUTTER WIDTH	H_6	= 0.04 D	WEIR GUTTER DEPTH
E_2	= 0.028 D	SLOT WIDTH	H_7	= 0.19 D	GUTTER DEPTH AT OUTLET
H_1	= 0.056 D	SLOT HEIGHT	H_8	= 0.8 D	CONE HEIGHT

Note: Elevations are referred to Top of Cone.

FIGURE 13b GENERAL DESIGN DIMENSIONS

Normal practice is to provide a minimum of two plant units of each type in a plant. Thus the initial construction phase would include at least two primary settling tanks.

From Table 2 it is obvious that if the detention time is to be less than that of a conventional unit, the diameter will be less than 5.5 m (18 ft). Thus, for 40 percent suspended solids removal, the maximum flow would be 10 l/sec (0.22 mgd). Since in conventional practice two tanks are used, the maximum plant design capacity would be 20 l/sec (0.44 mgd) or less.

The design of a swirl primary separator follows:

1. Plant design average daily flow is 15 l/sec (0.34 mgd)
2. Removal efficiency of suspended solids desired is 45 percent
3. Use two swirl primary separators. Design flowrate per unit is 7.5 l/sec (0.17 mgd). Peak flowrate is 11.2 l/sec (0.26 mgd).
4. Enter Figure 11a or 11b with design flowrate. For 45 percent efficiency, select η = 3.7 m (12 ft). Surface area is 10.5 m^2 (113 ft^2). Overflow rate is 61,295 l/day/m^2 (1,505 gal/day/ft^2).
5. Enter Figure 12 with design flowrate of 7.5 l/sec (0.17 mgd) and D of 3.7 m (12 ft). Detention time is 37 minutes.

Note: For conventional settling units, the detention time would be 51 to 63 minutes.

6. Enter Figure 11a with peak flow of 11.2 l/sec (0.26 mgd) and D of 3.7 m (12 ft). Read recovery is 38 percent.
7. Enter Figure 12 with peak flow of 11.2 l/sec (0.26 mgd) and D of 3.7 m (12 ft). Read detention time is 25 minutes.
8. Determine dimensions of structure from Figure 13, as follows:

D = 3.7 m (12 ft) inside diameter of tank
D_1 = 0.24 m (0.8 ft) inlet (side of square)
D_2 = 2.4 m (8 ft) skirt diameter
D_4 = 2.1 m (7 ft) gutter diameter

From the values given for D_2 and D_4 the circular gutter width is 0.3 m (1 ft). D_4 does not appear to be a critical dimension insofar as the tank performance is concerned and therefore we assume the gutter width could

TABLE 2
COMPARISON OF DIAMETER, DETENTION TIME, AND SUSPENDED SOLIDS REMOVAL FOR SWIRL PRIMARY SEPARATOR AND DETENTION TIME FOR CONVENTIONAL SETTLING FOR VARIOUS OVERFLOW RATES

		Swirl % S.S. Removal											
		30			40			50			60		
Diameter		Flow		Detention Time	Flow		Detention Time	Flow		Detention Time	Flow		Detention Time
m	(ft)	l/sec	(mgd)	(min)	l/sec	(mgd)	(min)	l/sec	(mgd)	(min)	l/sec	(mgd)	(min)
1.8	6	4.5	0.1	8	2.8	0.06	13	2	0.05	18	1.6	0.04	24
3.6	12	15	0.34	19	9.8	0.22	30	6.5	0.15	45			
5.5	18	27	0.60	30	15	0.33	54	10	0.22	75			
6.1	20	28	0.62	35									

CONVENTIONAL SETTLING TANKS

% S.S. Removal	Overflow Rate		Detention Time (min)
	l/day/m^2	gal/day/ft^2	(10 ft depth or over)
60	36,653	900	120
50	57,017	1,400	77
40	51,453	2,000	54
30	114,034	2,800	38

Table 2 (continued)

OVERFLOW RATE COMPARISON FOR SWIRL SEPARATOR

Flow		Overflow Rate	
l/sec	mgd	l/day/m^2	gal/day/ft^2
Diameter 1.8 m (6 ft)			
4.5	0.1	144,170	3,540
2.8	0.06	86,340	2,120
2	0.05	72,085	1,770
1.6	0.04	57,625	1,415
Diameter 3.6 m (12ft)			
15	0.34	122,585	3,010
9.8	0.22	79,415	1,950
6.5	0.15	54,165	1,330
Diameter 5.5 m (18 ft)			
27	0.6	96,110	2,360
15	0.33	52,945	1,300
10	0.22	35,230	865
Diameter 6.1 m (20 ft)			
28	0.62	80,435	1,975

be changed if greater width is necessary to carry off the weir discharge.

D_5 is not a critical dimension. Suggest D_5 = 0.2 m (0.67 ft).

D_6 is not a critical dimension and designer may select size depending on hydraulics. Suggest D_6 = 0.2 m (0.67 ft).

H_1 = 0.2 m (0.67 ft) slot height.

H_2 = 0.25 m (0.84 ft) vertical distance from invert to junction of tank slope and tank side.

H_3 = 0.45 m (1.5 ft) height of circular gutter.

H_4 = 0.73 m (2.4 ft) vertical distance from top of circular gutter to junction of tank slope and tank side.

H_5 = 0.15 m (0.48 ft) vertical distance from circular gutter top to overflow weir.

H_6 = 0.15 m (0.48 ft) depth of weir gutter. Designer should check to make sure this depth is adequate.

H_7 = 0.69 m (2.28 ft) vertical distance from gutter top to invert of outlet pipe.

H_8= 2.92 m (9.6 ft) depth of chamber with sloping sides. The horizontal dimensions of sludge hopper bottoms are usually no larger than 0.61 m (2.0 ft). If the bottom is given this width then H_8 will be reduced by 0.53 m (1.73 ft). Hence H_8 = 2.4 m (7.9 ft).

E_1 = 0.1 m (0.33 ft) weir gutter width.

E_2 = 0.1 m (0.33 ft) slot width at right angles to slope.

The size of the resultant structure for an average design flow of 7.5 l/sec (0.17 mgd) is shown in Figure 14.

The design and size of the overflow weirs and effluent gutters should be based on principles used in conventional primary tanks and should be revised from the values derived from Figure 13 as required.

CONSTRUCTION COSTS

A conventional round tank designed to handle the same flow and at the same suspended removal efficiency 7.5 l/sec (0.17 mgd), 45 percent suspended solids, would have essentially the same diameter, but less depth.

Cost estimates of the swirl primary separator were made for two purposes: 1) to indicate the probable construction cost of the facility; and 2) to compare its costs with that of a conventional primary settling tank designed for the same efficiency.

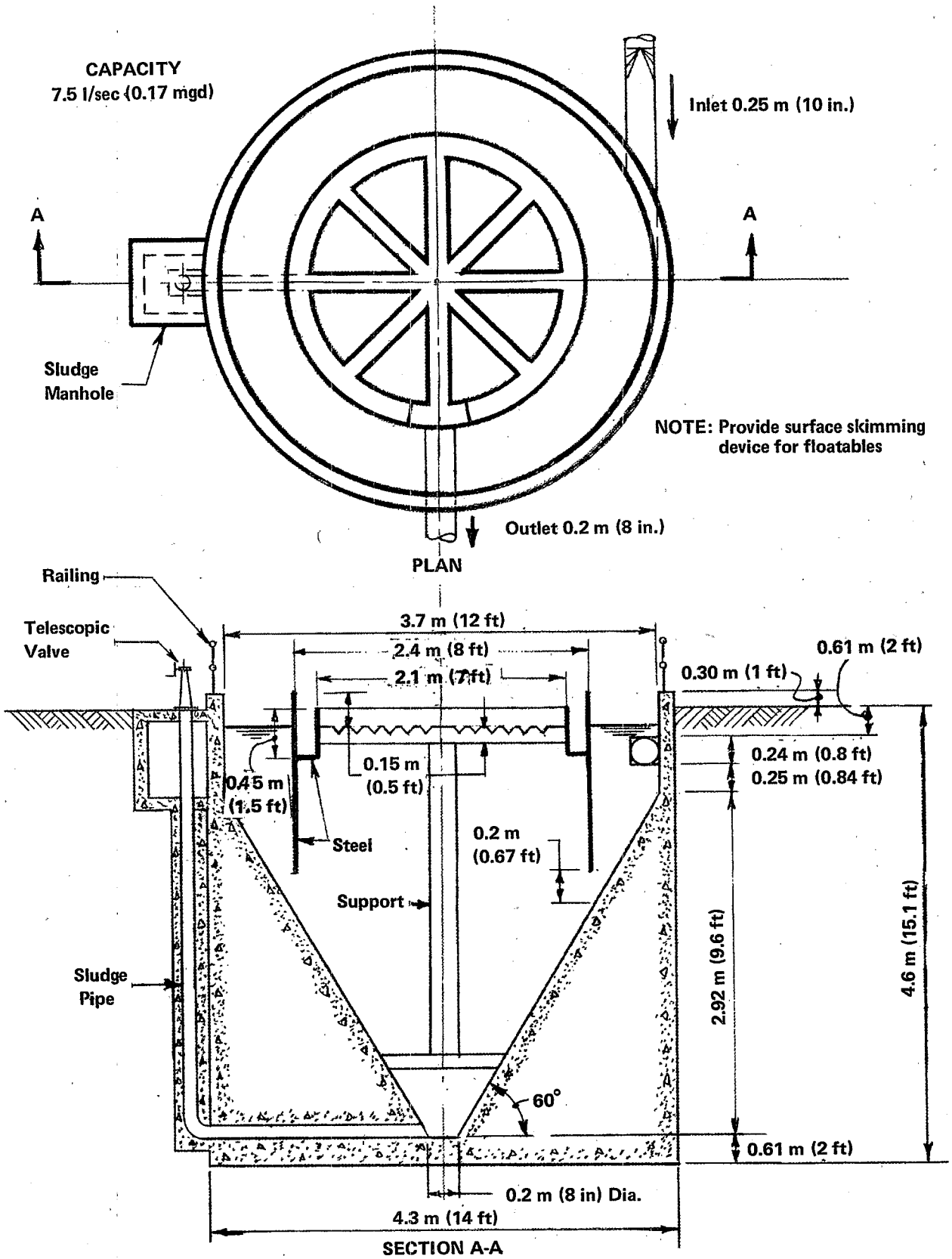

FIGURE 14 SWIRL PRIMARY SEPARATOR

The cost estimates are considered to be reasonable engineer's estimates. However, during periods of economic inflation, it is not unusual for contractors' bids to materially exceed engineers' estimates.

Cost Basis

The costs are based on the following:

a. Engineering News Record Construction Cost Index average for U.S. is 2,100.

b. Unit prices as follows:

Steel Sheet Piling (for temporary use during construction)	$86/m^2	$ 8/ft^2
Excavation	$16/m^3	$ 12/yd^3
Reinforced concrete (swirl)	$195/m^3	$150/yd^3
Reinforced concrete (conventional	$326/m^3	$250/yd^3

Note: The concrete for the swirl unit will require less reinforcing steel, thus a lower cost.

c. Contingency and engineering costs 25 percent of the foregoing items.

The estimated quantities of materials are based on the dimensions shown in Figures 14 and 15.

The swirl separator dimensions are derived in the previous section. It is assumed that the ground surface is 0.6 m (2 ft) above the crown of the inlet pipe and the top of tank is 0.3 m (1 ft) above ground surface. Since the top of overflow weir is 0.2 m (0.7 ft) above crown of inlet pipe, this provides 0.7 m (2.3 ft) of freeboard above the weir.

The conventional primary settling tank dimensions are inside diameter of 3.6 m (12 ft) and side water depth of 2.44 m (8 ft). These dimensions provide an overflow rate of 61,260 l/day/m^2 (1,500 gal/day/ft^2) and a detention time of 57 minutes. The tank is set to provide a freeboard of 0.7 m (2.3 ft) with top of wall 0.3 m (1 ft) above ground surface.

The following assumptions are made for both structures:

a. Excavation is all in earth. The unit price includes cost of backfilling.

b. Temporary steel sheet piling is required 0.61 m (2 ft) outside exterior walls of structure.

c. Equipment cost for conventional settling tank includes cost of rake-type sludge collector with fixed bridge and center drive, scum collector, weir plates, telescopic valve, and electrical work.

d. Miscellaneous costs for swirl separator includes cost of skirt, weirs, gutters, telescopic valve, center support for weir gutters, piping, and railing around tank.

e. Miscellaneous costs for conventional settling tank includes piping within limits of structure, gratings, and railing around periphery of tank.

Cost of Swirl Separator as a Primary Separator

The estimated construction cost of a swirl separator with a capacity of 7.5 l/sec (0.17 mgd) is $55,250. The breakdown of this cost is shown in Table 3.

TABLE 3
CONSTRUCTION COST OF SWIRL PRIMARY SEPARATOR

Capacity 7.5 l/sec (0.17 mgd)

Item	Quantity	Amount
Sheet Piling	128 m^2 (1,380 ft^2)	$ 11,000
Excavation	340m^3 (440 yd^3)	5,450
Reinforced Concrete	125 m^3 (160 yd^3)	18,750
Miscellaneous Costs	Job	9,000
Subtotal		$ 44,200
Contingent & Engineering Costs	25%+	11,050
	Total	$ 55,250

Cost of Conventional Primary Settling Tank

The estimated construction costs of a conventional primary settling tank with a capacity of 7.5 l/sec (0.17 mgd), based on the dimensions shown in Table 4, is $75,940. The breakdown of this cost is also shown in Table 4.

As the capacity of the swirl unit increases, there is a rapid increase in cost as compared to the cost of conventional units, due mostly to the increased excavation sheeting and amount of reinforced concrete. Similar construction calculations were made for comparable units having a capacity of

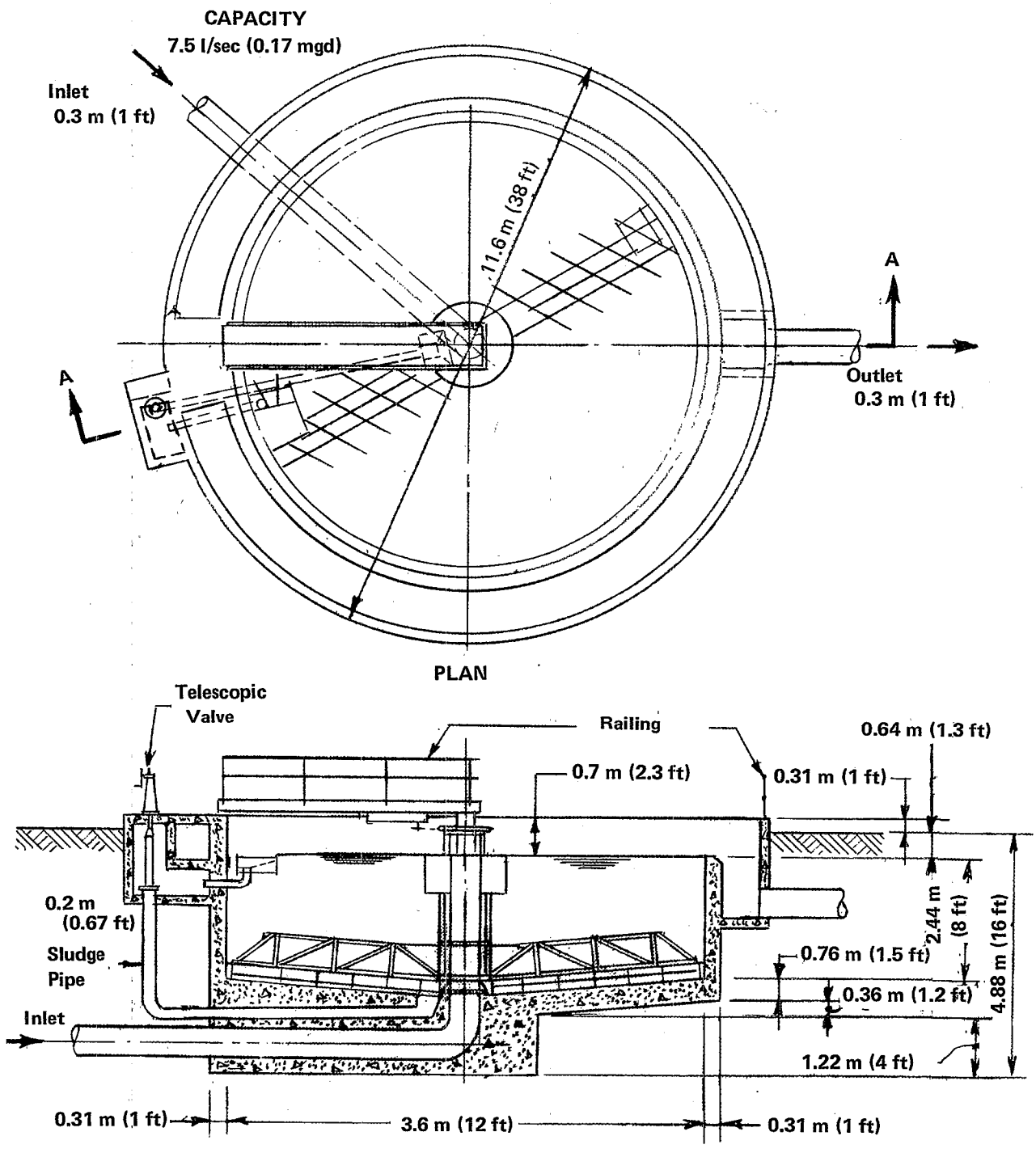

NOTE: Drawing not to scale

FIGURE 15 CONVENTIONAL PRIMARY SETTLING TANK

TABLE 4
CONSTRUCTION COST
OF CONVENTIONAL
PRIMARY SETTLING TANK
Capacity 7.5 l/sec (0.17 mgd)

Item		
Sheet Piling	.96 m^2 (1,050 ft^2)	$ 8,230
Excavation	345 m^2 (450 yd^3)	5,520
Reinforced Concrete	40 m^3 (51 yd^3)	10,000
Equipment	Job	35,000
Miscellaneous	Job	2,000
Subtotal		$60,750
Contingent & Engineering Costs	25%+	15,190
	Total	$75,940

21.9 l/sec (0.5 mgd) with a suspended solids efficiency of 65 percent. The construction cost of the swirl unit was estimated to be $55,250 and the conventional unit $75,940. Figure 16 is a plot of the cost comparisons made.

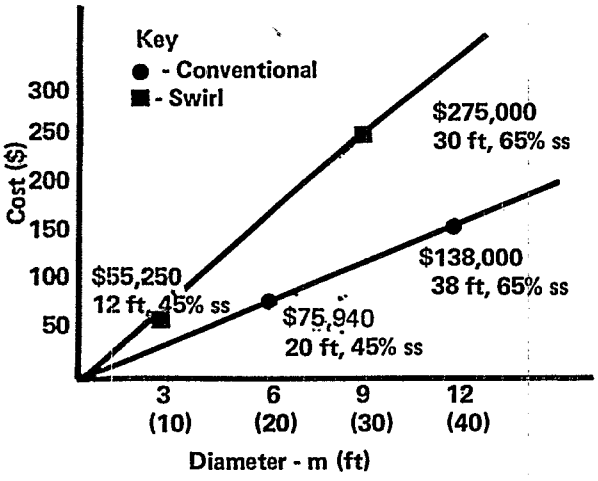

FIGURE 16 COST VS DIAMETER, SWIRL AND CONVENTIONAL PRIMARY TREATMENT UNITS

Operating and maintenance costs for a 43.8 l/sec (1 mgd) unit, the smallest size for which USEPA data is available, can be estimated as shown in Table 5.

Comparison of Costs

From the foregoing it is seen that the construction cost of the swirl separator will be $55,250 compared to $75,940 for a conventional settling tank. Annual O & M costs may be $3,000 less with the swirl unit. The surface area required for units of this low volume does not appear to warrant a comparison of land cost savings.

This comparison assumes that the two structures will produce equal results in removal of suspended solids in raw sewage. The sizing of the conventional primary settling tank is based on standard design criteria. The sizing of the swirl primary separator is based on model results in the laboratory using IRA-93 resin as representative of suspended solids in raw sewage.

Cost comparison of large size units do not appear warranted at this time. A different configuration is obviously needed for large units to avoid the adverse construction costs of such a deep structure. A flat bottom with scrapers as suggested by Smisson, sacrificing the principal of no moving parts appears reasonable.

PRESENT WORTH

The present worth of the swirl separator units is shown in Table 6. The present worth is based on a life of 20 years and an interest rate of 6-1/8 percent. Hence the present worth of the operation and maintenance costs for a 20-year period is 11.35 times the annual cost.

For the unit with capacity of 7.5 l/sec (0.17 mgd) at 45 percent ss removal the present worth of the conventional unit is $117,500 and the swirl separator is $62,500. Thus the present worth of the conventional unit is 88 percent greater than that of the swirl separator.

For the unit with capacity of 21.9 l/sec (0.5 mgd) and 60 percent ss removal the present worth of the conventional unit is $179,500 compared to $282,200 for the swirl separator. Thus the present worth of the conventional unit is 57 percent less than that of the swirl separator.

TABLE 5
COMPARISON OF OPERATION AND MAINTENANCE COSTS FOR PRIMARY TREATMENT UNITS

	Conventional	Swirl
1. Labor: Operation, 1 hr/day @ $7/hr	$1,820	—
Maintenance, 0.54 hr/day @ $7/hr	910	$455
2. Materials and Supplies:		
$300/yr x 325/150.6 (Ratio 1975/1971 EPA Cost Index)	650	—
3. Power: 2 pumps @ ½ hp, 1hr/day $0.03/kwh	100	100
4. Annual Maintenance @ 3% of capital cost		
Primary tank sludge collections	100	
Raw sludge plunger pumps	80	80
Total Annual O&M	$3,660	$635

TABLE 6
PRESENT WORTH SWIRL SEPARATOR PRIMARY TREATMENT UNITS

	Conventional Tank	Swirl Separator
Capacity 7.5 l/sec (0.17 mgd) (45% ss removal)		
Construction Cost	$75,940	$55,250
Operation and Maintenance Cost	41,540	7,200
Cost Total Present Worth	$117,480	$62,450
Capacity 269 l/sec (0.5 mgd) 60% ss removal		
Construction Cost	$138,000	$275,000
Operation and Maintenance Cost	41,540	7,200
Cost Total Present Worth	$179,540	$282,200

SECTION 4

PILOT TREATABILITY EVALUATIONS WITH SEWAGE

The opportunity to investigate the swirl separation phenomenon in the field was made available by the installation of a pilot unit at the Humber Wastewater Treatment Plant of the Municipality of Metropolitan Toronto, Canada.

The findings described in this section are based on conditions at the Toronto installation and the comparison between the swirl pilot performance and that of the conventional settling tanks in use at the plant. While specific conclusions have been drawn as a result of the swirl pilot study they must be characterized as applying *only* to these conditions. No single field investigation of a previously unevaluated treatment method — whether it demonstrated highly favorable or unfavorable performance — can be taken as the final proof of applicability. Further investigations, under different conditions and for different applications and purposes, would be desirable.

The Humber Wastewater Treatment Plant has six rectangular-shaped primary settling tanks, each with a width of 10.36 m (34 ft), a length of 72.24 m (237 ft), and average depth of 3.24 m (10.62 ft). The six tanks have total surface area of 449 m^2 (48,350 ft^2) and a volume of 14,540 m^3 (513,400 ft^3). The plant, during the period of the 1975 tests, was operating far in excess of design capacity. Plant additions were under construction to add treatment and sludge handling facilities.

Pilot Test Results

The swirl separator was installed initially near the grit removal chamber in September 1974. Several preliminary test runs were made at this location on sewage pumped out of the effluent end of the grit chamber.

These tests indicated removal of total suspended solids ranging from 0 percent to 64.7 percent for various flows. No data were available on test procedures for this preliminary tryout run.

Following these preliminary test runs, the swirl unit was moved to the influent end of the primary settling tanks and installed as shown in Figure 17. The initial evaluation was made with two test runs, each of seven days duration, with average flows of 13.1 l/sec (0.30 mgd) and 19.7 l/sec (0.45 mgd), respectively, in the swirl separator. The overflow rates for these flows would be 0.932 and 1.4 $m^3/day/m^2$ (2,650 and 3,980 gal/day/ft^2) with corresponding detention times of 20 and 13 minutes. The flow in the swirl was varied in accordance with the diurnal flow to the plant.

In order to gain information concerning conditions during periods of stormflow, the swirl separator testing was modified during actual storm periods.

If rainfall occurred during the tests and the plant flow exceeded the diurnal flow by 788 l/sec (18 mgd) the swirl was operated at a constant rate of 18.8 l/sec (0.43 mgd). The detailed test schedule for dry-weather periods is shown in Table 30, and the tests for wet-weather periods in Table 31 of Appendix D. Limited tests for heavy metals on influent and effluent samples to the primary tank during dry-weather flow periods were also conducted to allow an evaluation of treatability. These tests were scheduled on a weekly basis.

The first series of tests was carried out between April 29th and June 12, 1975. There were eight separate storm events in this period. The results for the swirl separator with a flow of 18.8 l/sec (0.43 mgd) are given in Tables 32 and 33. Tables 34 and 35 show the comparable results for the primary settling tanks, including the test results for heavy metals. The heavy metal testing indicates considerable concentrations of the metals in the sludge with greater uniformity of concentration in the sludge than in the effluent.

For the eight storm events, the removal of total suspended solids in the swirl separator ranged from zero to 34.4 percent, with an average of 10.4 percent. The removals for the primary tanks ranged from zero to 79.7 percent, with an average of 32.8 percent. These results are shown in Table 7.

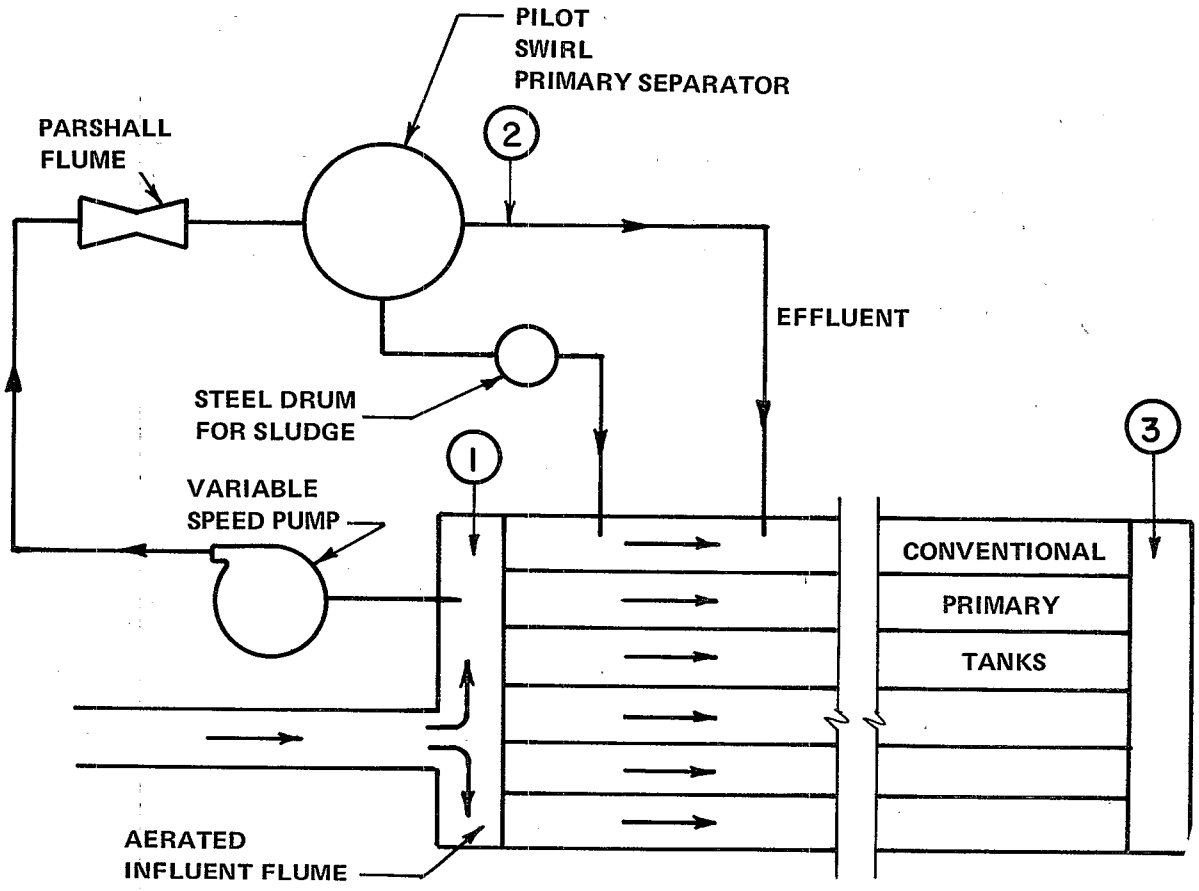

1 INFLUENT GRAB SAMPLE
2 SWIRL EFFLUENT GRAB SAMPLE
3 PRIMARY SETTLING TANK GRAB SAMPLE

FIGURE 17 TEST LAYOUT – HUMBER PLANT – TORONTO, CANADA 1975

TABLE 7
REMOVAL OF TOTAL SUSPENDED SOLIDS – WET-WEATHER FLOW, MAY 4–JULY 12, 1975

	Percent Removal	
Date	Swirl Concentrator	Primary Tanks
Average Flow	18.8 l/sec (0.43 mgd)[1,2]	5,688 l/sec (130 mgd)[3]
May 4	0	0
May 5	0	37.5
May 6	0	19.0
May 7	17.7	79.7
May 15	34.4	70.4
May 31	4.0	0
June 4-5	0	10.2
June 12	27.1	45.6
Total	83.2	262.4
Average	10.4	32.8

[1]Constant Flow, overflow rate: 155 m^3/day/m^2 (3,805 gal/day/ft^2); detention time: 14 minutes.

[2]Sludge drawoff interval – 4 hours.

[3]Average for days during which storm occurred, overflow rate: 110 m^3/day/m^2 (2,688 gal/day/ft^2); detention time: 42 minutes.

The diurnal flow of the Humber Plant, based on hourly measurements taken in April 1975, is shown in Figure 18. The total flow to the primary tanks is shown with and without waste activated sludge for the period.

Waste activated sludge is normally pumped to the primary tank influent only during the night hours but some waste activated sludge may return to the primary tanks by gravity during the daytime hours. Figure 18 also shows the variation in total suspended solids and volatile suspended solids. The concentration of total and volatile suspended solids is highest between the hours of 2:00 a.m. and 8:00 a.m. when flow is lowest due to the return of waste activated sludge to the plant influent. The variation in suspended solids during the daytime hours may be due to discharge of industrial wastes which enter the metropolitan sewers. It is recognized that unpredictable slugs of such wastes may affect the plant influent at any time of any day.

The return of waste activated sludge to the primary tanks will be discontinued in the future by modification in design and operation. To avoid the presence of waste activated sludge in the influent and its effect on effluent quality to the greatest extent possible during the study, the final tests on the swirl unit and on the plant primary tanks during runs in September 1975 were conducted from 1100 hours (11:00 a.m.) to 1500 hours (3:00 p.m.). During this period the total plant flow, based on Figure 18 data, is fairly constant and decreases only about five percent.

Based on the developmental work at the LaSalle Hydraulic Laboratory it was decided to use a swirl separator with a diameter of 3.66 m (12 ft) for parallel tests with the Humber Plant conventional primary tanks. Based on data given in Figure 13b, the dimensions selected for the swirl separator are shown in Figure 19 and 20.

The Toronto pilot unit was constructed with a mechanized skimmer for scum collection in the outer ring instead of using a scum pipe as recommended by the hydraulic laboratory and as shown in Figure 19 and 20. A washing spray was provided to convey the scum out of the swirl chamber. The chamber was sized for a minimum flow of 7.88 l/sec (0.18 mgd) and a design flow of 16.2 l/sec (0.37 mgd). However, in the final tests the flows were 13.1 l/sec (0.3 mgd) and 19.7 l/sec (0.45 mgd). The surface area of the swirl concentrator is 10.49 m^2 (113 ft^2). The total volume below the weir elevation is 16.34 m^3 (577 ft^3). When the bottom of the cone is filled 0.91 m (3 ft) deep with settled solids, the liquid volume is reduced to 15.86 m^3 (560 ft^3). Thus the average volume is 16.1 m^3 (568.5 ft^3) and at a flow rate of 13.1 l/sec (0.3 mgd) the detention time is 20.4 minutes. A variable speed suction pump was installed in the aerated influent flume to the primary tanks for the purpose of providing the swirl unit with the same raw wastewater as was being handled by the plant tanks. The flow was lifted about 3.6 m (12 ft) and conveyed through a Parshall flume to the swirl separator. The swirl effluent was returned to the primary tanks. Sludge was withdrawn from the swirl separator by gravity into a 0.18 m^3 (50 gal) steel drum and, after measurement and sampling, was discharged into the primary tanks. A line diagram of the layout is shown in Figure 17. The sampling points to compare performance of the swirl chamber and the plant primary tanks are shown.

Series of Tests

Relatively poor performance of the swirl separator during early test periods was observed. It was thought that the causes of the poor performance were the return of waste activated sludge during the night hours and infrequent sludge drawoff. The sludge removed from the swirl separator at four-hour intervals had a solids content of about 4.5 percent. This is similar to the solids content of the sludge removed from the conventional tank. The separator sludge volume was only about 12 percent of the sludge volume removed from the primary tanks based upon flow.

It was concluded that the swirl separator hopper lacked the storage volume to permit withdrawals at four-hour intervals and that the relatively large volume occupied by sludge in the upper cylindrical portion of the swirl unit was consequently carried out by the dynamic swirling flow in the effluent

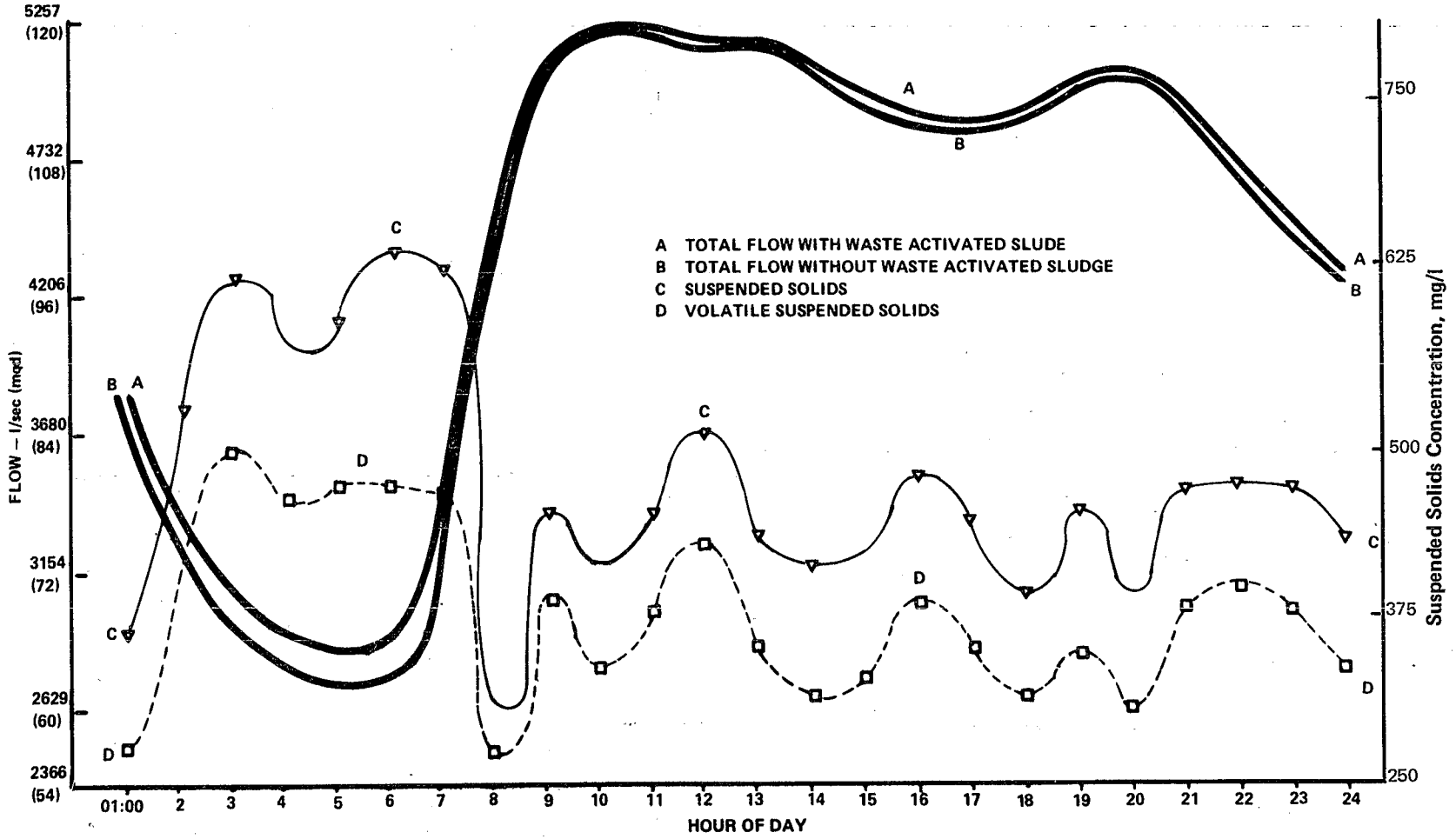

FIGURE 18 DIURNAL FLOW AND SUSPENDED SOLIDS (mg/l). AVERAGE OF 5 DRY-WEATHER DAYS HUMBER PLANT – TORONTO, APRIL 1975

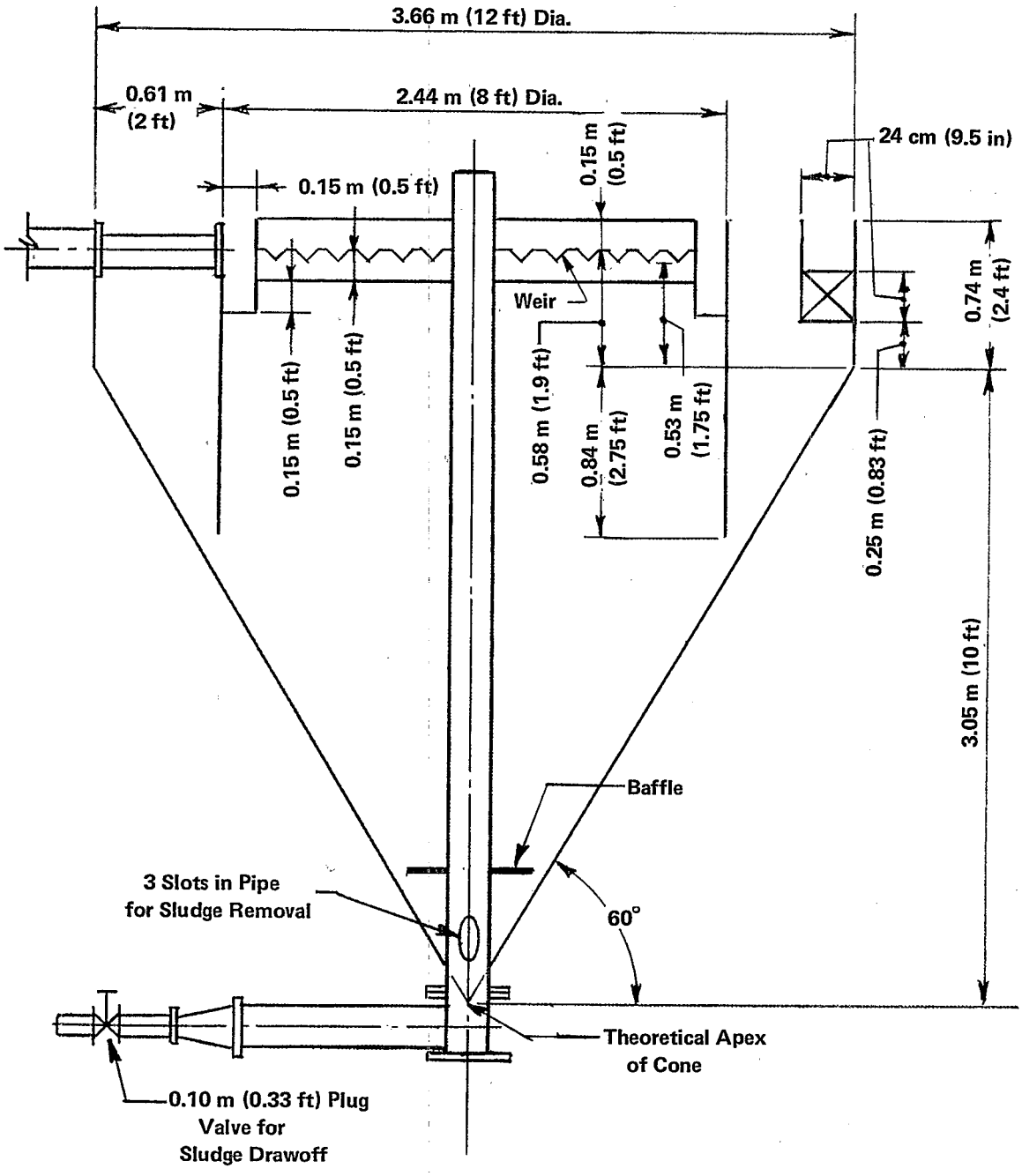

SECTION A-A

FIGURE 19 SECTION OF SWIRL PRIMARY SEPARATOR

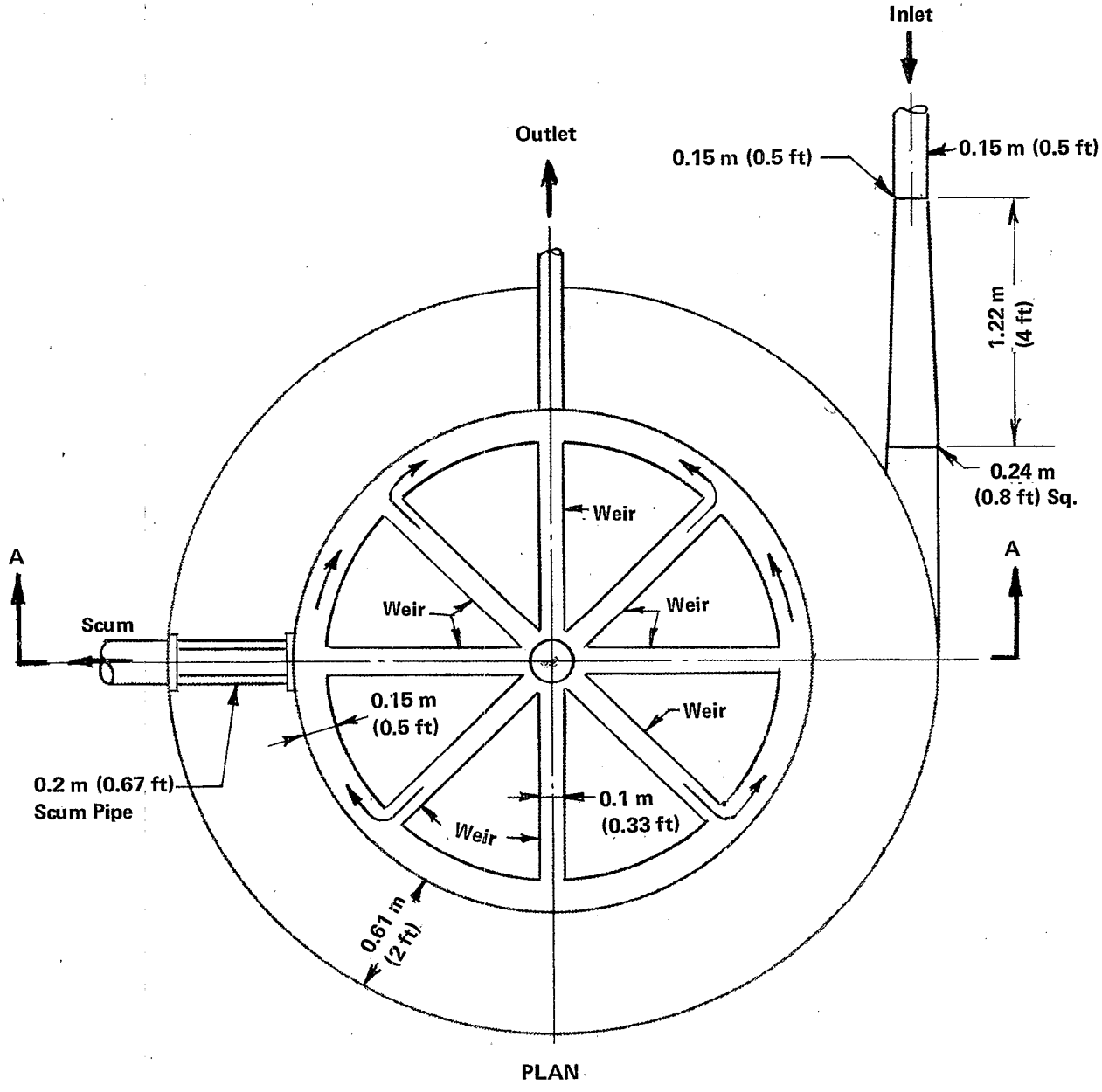

FIGURE 20 PLAN OF SWIRL PRIMARY SEPARATOR

discharge. Therefore, it was decided to limit the tests to four hours during the peak daytime hours when it was assumed that there was little or no return of waste activated sludge, and to reduce the number of tests as shown in Table 46 of Appendix D. To improve sludge withdrawal from the swirl separator a horizontal disc was installed as a baffle immediately above the sludge opening in the vertical riser pipe.

The second series of tests (June 23 to 27, 1975) were run with an average flow of 13.1 l/sec (0.30 mgd); and from July 2 to 8, 1975, with an average flow of 19.7 l/sec (0.45 mgd). These flowrates were varied to agree with the diurnal flow to the plant. The results of these tests are given in Tables 47,48,49. and 50 of Appendix D and all results are for dry weather conditions. With an average flow of 13.1 l/sec (0.30 mgd) to the swirl separator, and hourly removal of sludge, the removal of total suspended solids ranged from 9.8 to 49.5 percent, with an average of 36.6 percent. The removals in the primary tanks ranged from 14.1 to 57.3 percent, with an average of 43.8 percent. Thus, the removal in the primary tanks was about 20 percent greater than the removal in the swirl. These results are shown in Table 8.

During the second series of tests, the average flow to the swirl separator was increased to 19.7 l/sec (0.45 mgd), and sludge withdrawal was increased to half-hour intervals to prevent excessive build-up in the swirl hopper. The removal of total suspended solids in the swirl separator ranged from 2.8 to 27.2 percent with an average of 17.7 percent. In the primary tanks the removals ranged from 0 to 50 percent with an average of 16.6 percent. These results are shown in

TABLE 8
REMOVAL OF TOTAL SUSPENDED SOLIDS, JUNE 23-27, 1975 (DRY-WEATHER)

Date	Average Influent Concentration (mg/l)	PERCENT REMOVAL Swirl Separator[1,2]	Primary Settling Tanks[3]
Average Flow		13.1 l/sec (0.3 mgd)	4,239 l/sec (96.9 mgd)
June 23	380	49.5	42.1
24	525	36.8	57.3
25	488	48.4	42.6
26	904	38.5	62.8
27	368	9.8	14.1
Average		36.6	43.8

ADDITION OF WASTE ACTIVATED SLUDGE

Date	Time Pumping Ceased	Duration of Pumping (Hrs)
June 23	9:00	9
24	8:00	8
25	10:00	10
26	9:30	9.5
27	9:30	9.5

[1] Overflow rate: 108 m^3/day/m^2 (2,650 gal/day/ft^2); detention time: 20 min.
[2] Sludge drawoff at 1 hr intervals
[3] Overflow rate: 81.8 m^3/day/m^2 (2,004 gal/day/ft^2); detention time: 57.1 min.

Table 9. These removals were less than 50 percent of those obtained in the initial second series tests at the lower flow of 13.1 l/sec (0.3 mgd). Therefore, it was decided to carry out additional tests using slightly revised procedures which were conducted in September 1975.

The detailed data for the dry-weather tests made from May 1 to June 10 are given in Tables 36, 37 and 38 for the swirl separator, and for the primary settling tanks in Tables 41, 42 and 43, Appendix D. With a flow of 13.1 l/sec (0.30 mgd) in the swirl separator the removal of total suspended solids ranged from zero to 50.3 percent, with an average of 23.5 percent for the 14 days. When the flow through the swirl separator was increased to 19.7 l/sec (0.45 mgd), the removal ranged from zero to 16.9 percent, with an average of 7.2 percent for the seven days. By comparison, the removals in the primary tanks ranged from 48.8 to 88.3 percent with an average of 68.8 percent for the first period of 14 days. For the second period of seven days, the removals in the primary tanks ranged from 30.4 to 83.8 percent with an average of 62.1 percent. These results are shown in Table 10.

The sampling and analytical program for the third and fourth series of tests is shown in Table 51 of Appendix D. These tests are similar to the previous series except that analyses were limited to determination of solids and were taken hourly on a composite of two samples rather than once in four hours on a composite of four samples. The flowrates to the swirl concentrator were kept constant during the four-hour test period because the variation in plant flow in that period was only 10 percent. Tests for BOD and COD were

TABLE 9
REMOVAL OF TOTAL SUSPENDED SOLIDS, JULY 2-8, 1975 (DRY-WEATHER)

Date	Average Influent Concentration (mg/l)	PERCENT REMOVED: Swirl Separator[1,2]	PERCENT REMOVED: Primary Settling Tanks[3]
Average Flow		19.7 l/sec (0.45 mgd)	4,244 l/sec (97.0 mgd)
July 2	464	25.8	17.2
3	436	2.8	0
4	512	16.4	15.6
7	500	27.2	0
8	440	16.4	50
Average		17.7	16.6

ADDITION OF WASTE ACTIVATED SLUDGE

Date	Time Pumping Ceased	Duration of Pumping (Hrs)
July 2	11:00	11
3	9:00	9
4	9:00	9
7	9:00	9
8	9:00	9

[1] Overflow rate: 162 m^3/day/m^2 (3,980 gal/day/ft^2); detention time: 14 min.

[2] Sludge drawoff at 0.5 hr intervals

[3] Overflow rate: 82 m^3/day/m^2 (2,005 gal/day/ft^2); detention time 42.6 min.

TABLE 10
REMOVAL OF TOTAL SUSPENDED SOLIDS – DRY WEATHER FLOW, May 1 – June 10, 1975

Date	Average Influent Concentration (mg/l)	Swirl Separator	Primary Settling Tanks
Average Flow		**13.1 l/sec (0.3 mgd)**	**4,012 l/sec (91.7 mgd)**
May 1	576	32.6	66.5
2	412	13.6	55.7
3	432	12.0	85.3
8	456	21.0	74.2
9	460	21.7	58.5
10	512	10.1	77.9
11	476	0.0	67.7
30	660	30.9	62.3
June 2	620	25.2	48.8
4	668	50.3	65.9
7	632	44.3	88.2
8	572	20.3	88.3
9	712	37.6	60.8
10	472	9.3	63.7
Average		23.5	68.8
Average Flow		**19.7 l/sec (0.45 mgd)**	**3,924 l/sec (89.7 mgd)**
May 12	444	8.1	52.0
13	428	0.0	30.4
14	476	7.6	56.5
15	604	9.3	65.4
16	476	8.4	68.5
17	428	0.0	83.8
18	568	16.9	78.2
Average		7.2	62.1

Flow	Swirl Separator 13.1 l/sec (0.3 mgd)	Swirl Separator 19.7 l/sec (0.45 mgd)	Primary Settling Tanks 4,012 l/sec (91.7 mgd)	Primary Settling Tanks 3,924 l/sec (89.7 mgd)
Overflow Rate				
$m^3/day/m^2$	108	162	79.2	73.7
$(gal/day/ft^2)$	(2,650)	(3,980)	(1,896)	(1,855)
Detention Time (min)	20.4	14	60.3	61.7

deleted. Sludge was removed from the swirl separator at one-half hour intervals. Effluent samples were collected at time intervals after the influent samples, more or less equivalent to the detention time in the unit. Effluent samples from the primary tanks were taken one hour after the influent samples, to conform with the theoretical detention time of the units.

The data for the tests made from September 2 to 15, 1975, are given in Tables

52 to 61 in Appendix D. Data for tests made from June 16 to 25, 1976, are given in Tables 39, 40, 44 and 45 of Appendix D.

The April 1976 tests were conducted to determine solids removal efficiencies at 6.6 l/sec (0.15 mgd) and 8.7 l/sec (0.2 mgd). The overflow rates were thus 54.1 $m^3/day/m^2$ (1,376 $gal/day/ft^2$) and 72 $m^3/day/m^2$ (1,766 $gal/day/ft^2$).

The percent removal of the various solids parameters for the September 1975 tests are shown in Tables 62 to71 in Appendix D. The removals are shown for each hourly test, and averaged for each day and for the five days' run at each flow. The data show that on some days there was considerable variation in the percent removal for the hourly tests. This may have been due to three factors: (1) Grab samples were used for sampling. Tests were made on composites of two grab samples taken one-half hour apart. Grab samples of raw sewage may vary considerably in solids content. More consistent results may have been obtained if automatic samplers had been used to provide a composite over a four-hour period with samples taken at intervals of a few minutes. (2) The actual detention times may have differed from the theoretical detention times since the flow in both the swirl separator and the primary tanks may have been subject to "short circuiting." The actual detention time may have been as much as 50 percent of the theoretical detention time. For this reason the effluent samples may not have reflected the true change in the influent samples. (3) There were industrial wastes in the raw influent flow. Further, the discharge of industrial wastes into the sewer system tributary to the Humber plant may have caused temporary but abrupt changes in the percent of solids in the plant influent or the settling velocities of the industrial discharged solids.

The foregoing reasons may account for the erratic results obtained in the hourly tests. Therefore, it is considered appropriate to disregard the hourly results and use the averages of the daily tests and the average of the five-day test runs. These results are shown graphically in Figures 21 through 25.

During the five-day test period, with a flow of 13.1 l/sec (0.3 mgd) and an overflow rate of 108 $m^3/day/m^2$ (2,650 $gal/day/ft^2$) and a detention time of 20.4 minutes in the swirl separator, the removal percentages of all five of the tests were greater in the swirl separator than in the primary tank. The removal of total suspended solids for all five days was 43.1 percent for the swirl separator compared to 41.9 percent for the primary tanks.

With a flow of 19.7 l/sec (0.45 mgd) and an overflow rate of 155 $m^3/day/m^2$ (3,805 $gal/day/ft^2$) and a detention time of 14 minutes through the swirl separator, it outperformed the primary tank in removal of settleable solids – 47.7 percent for the former versus 36.3 percent for the latter. In terms of suspended solids, the swirl chamber removed 25.3 percent versus 36.0 percent for the primary tank.

The average of the five four-hour test runs is shown in Table 11.

EVALUATION OF SOLIDS TESTS

The Recommended Standards for Sewage Works by the Great Lakes–Upper Mississippi River Board of State Sanitary Engineers (commonly referred to as the 10-State Standards) contain criteria for design of primary settling tanks for use in secondary treatment plants. These stipulate depths of not less than 2.13 m (7 ft) but no mention is made of criteria for removal of settleable or suspended solids. A curve is given for BOD removals based on surface settling rate – i.e., overflow rate. The percent BOD removal ranges from 22 percent at overflow rate of 81.46 $m^3/day/m^2$, (2,000 $gal/day/ft^2$), to 32 percent at 36.66 $m^3/day/m^2$ (900 $gal/day/ft^2$), and to 37 percent at 16.29 $m^3/day/m^2$ (400 $gal/day/ft^2$).

The ASCE Manual of Engineering Practice No. 36[4] is more specific. This manual states that the object of settling tanks is to remove settleable solids and to reduce the suspended solids content of the sewage. It states that both displacement time (detention time) and surface area should be considered in design and that detention periods of 60 to 120 minutes should, in theory remove 50 to 70 percent of the influent suspended solids. Figure 6 of ASCE Manual No. 36[4] indicates the relationship between overflow rate and

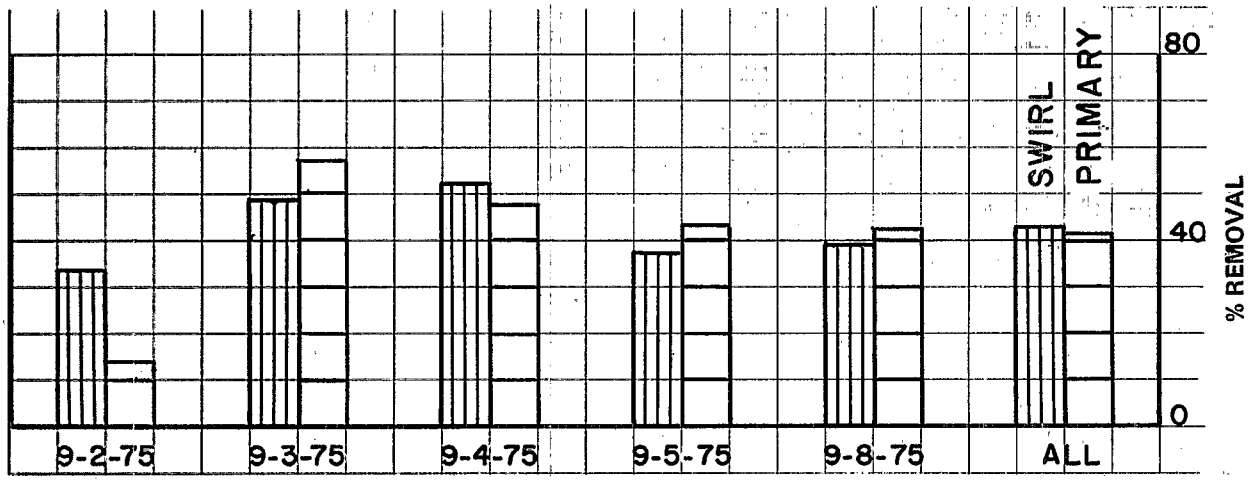

Swirl 13.1 l/sec (0.3 mgd) Overflow rate — 108 m^3/day/m^2 (2,650 gal/day/ft^2)
Primary 4,121 l/sec(94.2 mgd) Overflow rate — 79.42 m^3/day/m^2 (1,950 gal/day/ft^2)

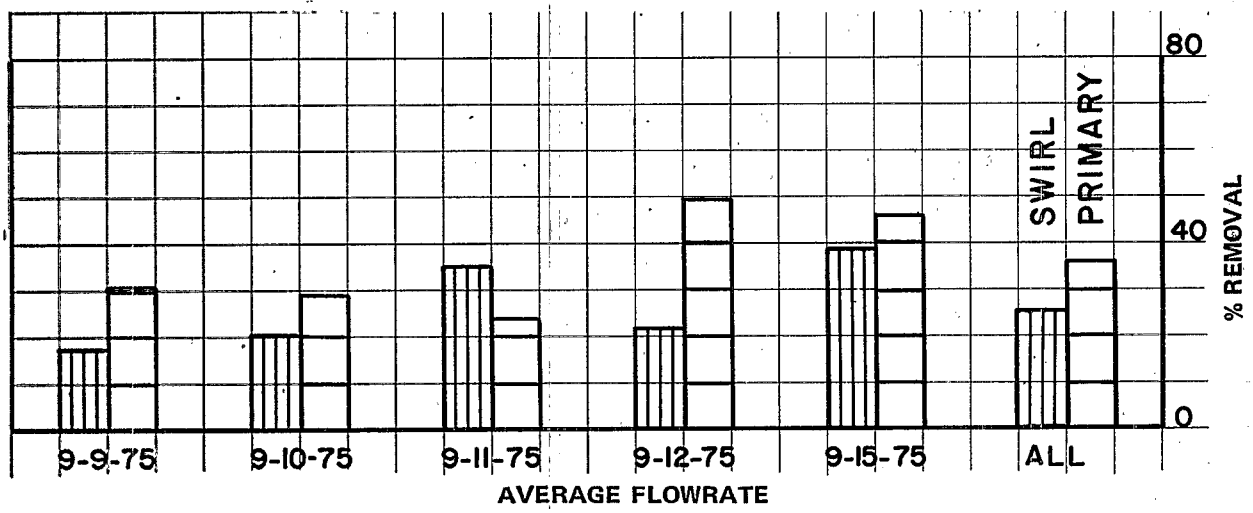

Swirl 19 .74/sec (0.45 mgd) Overflow rate — 108 m^3/day/m^2 (2.650 gal/day/ft^2)
Primary 4,340 l/sec(99.2 mgd) Overflow rate — 83.5 m^3/day/m^2 (2,050 gal/day/ft^2)

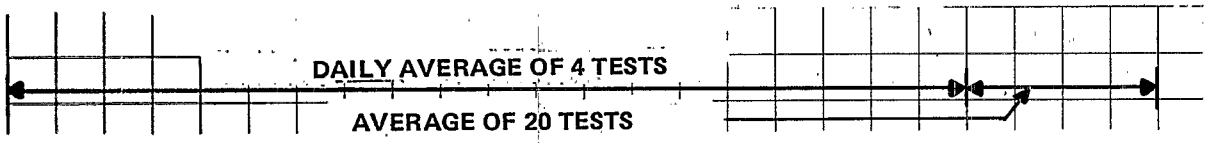

FIGURE 21 DRY-WEATHER REMOVAL OF TOTAL SUSPENDED SOLIDS
TORONTO, September 1975

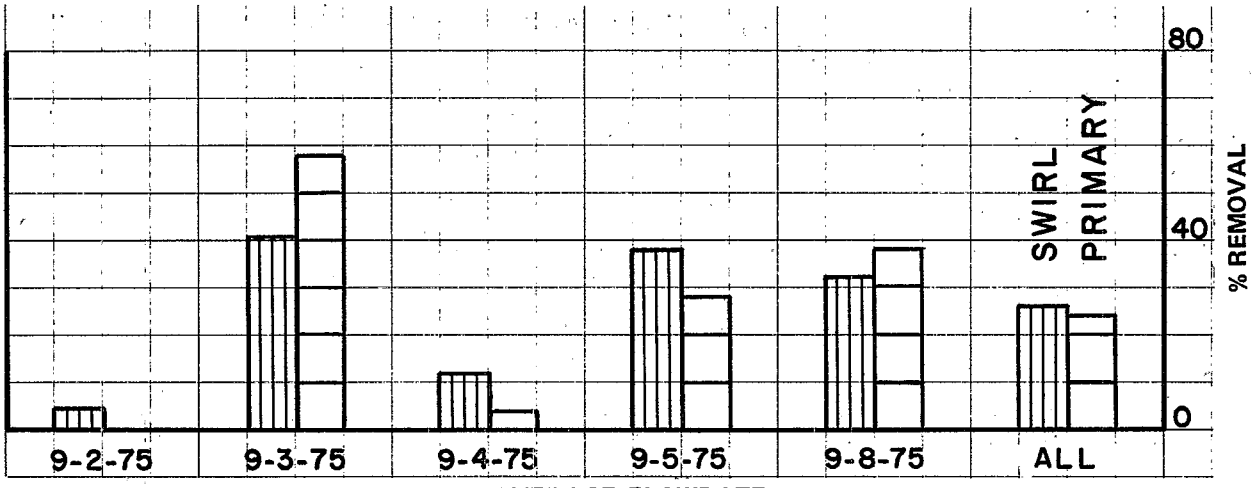

Swirl 13.1 l/sec (0.3 mgd) Overflow rate — 108 m^3/day/m^2 (2,650 gal/day/ft^2)
Primary 4,121 l/sec(94.2 mgd) Overflow rate — 79.42 m^3/day/m^2 (1,950 gal/day/ft^2)

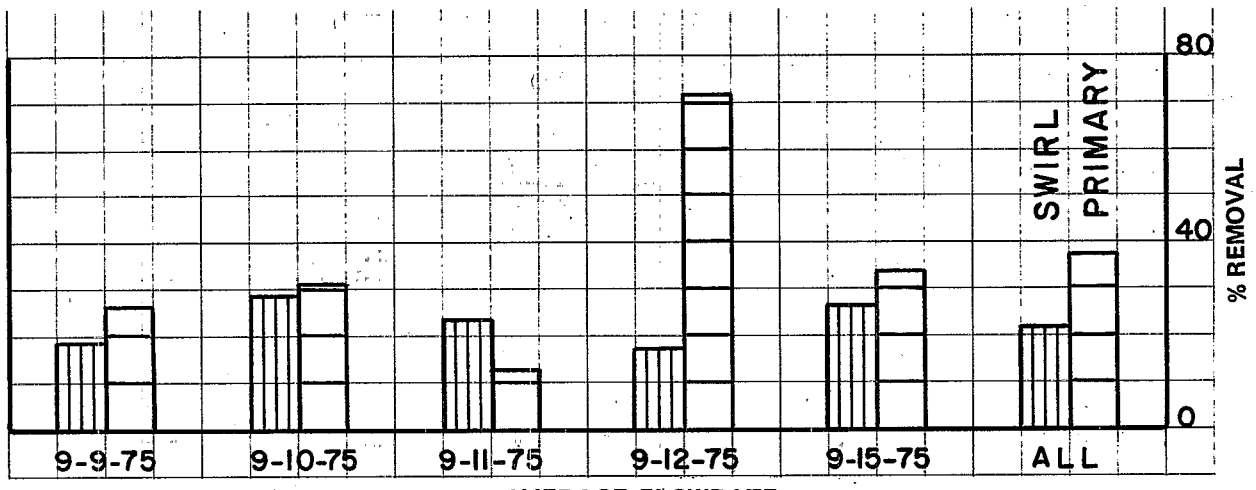

Swirl 19.7 l/sec (0.45 mgd) Overflow rate — 108 m^3/day/m^2 (2,650 gal/day/ft^2)
Primary 4,340 l/sec(99.2 mgd) Overflow rate — 83.5 m^3/day/m^2 (2,050 gal/day/ft^2)

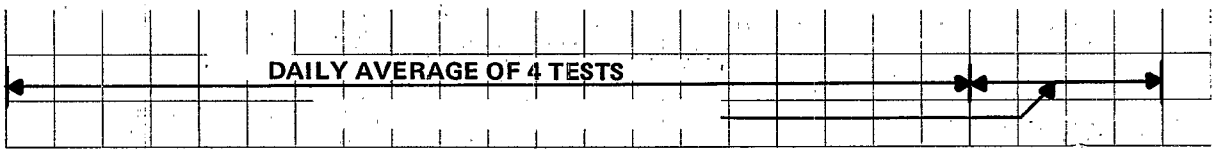

FIGURE 22 DRY-WEATHER REMOVAL OF FIXED SUSPENDED SOLIDS — TORONTO, September 1975

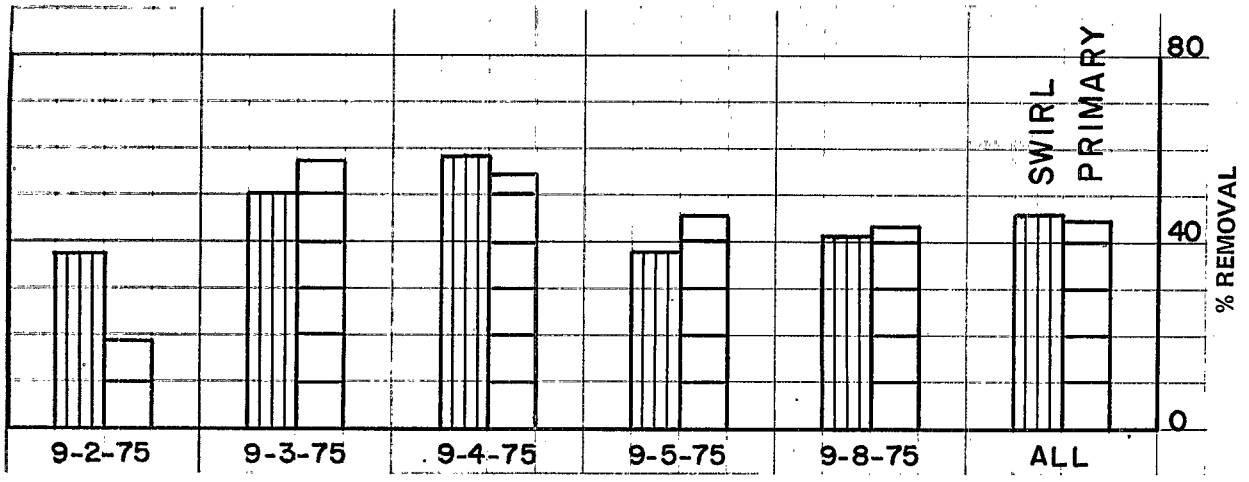

Swirl 13.1 l/sec (0.3 mgd) Overflow rate — 108 $m^3/day/m^2$ (2,650 gal/day/ft^2)
Primary 4,121 l/sec(94.2 mgd) Overflow rate — 79.42 $m^3/day/m^2$ (1,950 gal/day/ft^2)

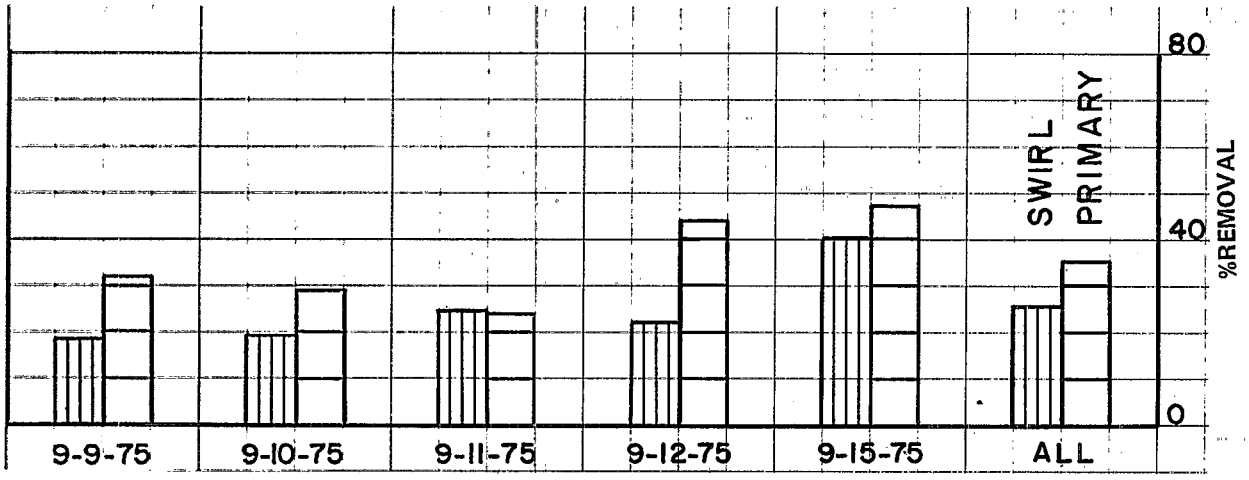

Swirl 19.7 l/sec (0.45 mgd) Overflow rate — 108 $m^3/day/m^2$ (2,650 gal/day/ft^2)
Primary 4,340 l/sec(99.2 mgd) Overflow rate — 83.5 $m^3/day/m^2$ (2,050 gal/day/ft^2)

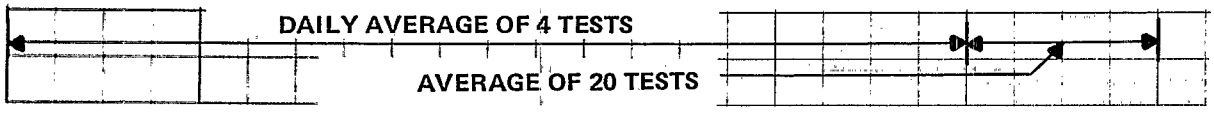

FIGURE 23 DRY-WEATHER REMOVAL OF VOLATILE SUSPENDED SOLIDS TORONTO, September 1975

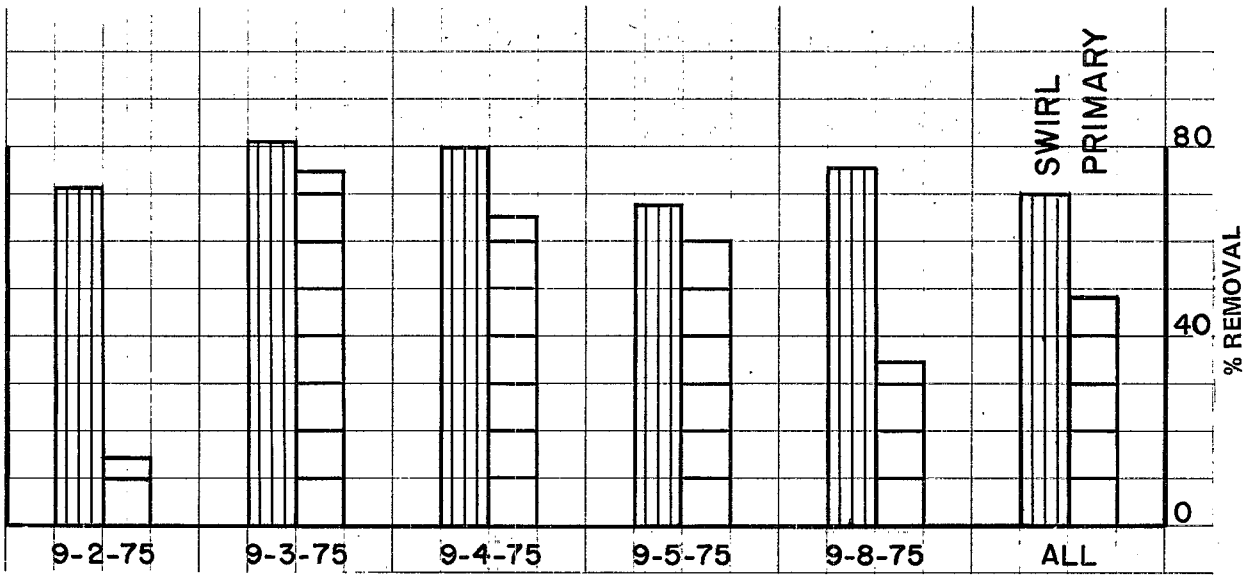

Swirl 13.1 l/sec (0.3 mgd) Overflow rate — 108 $m^3/day/m^2$ (2,650 gal/day/ft^2)
Primary 4,121 l/sec(94.2 mgd) Overflow rate — 79.42 $m^3/day/m^2$ (1,950 gal/day/ft^2)

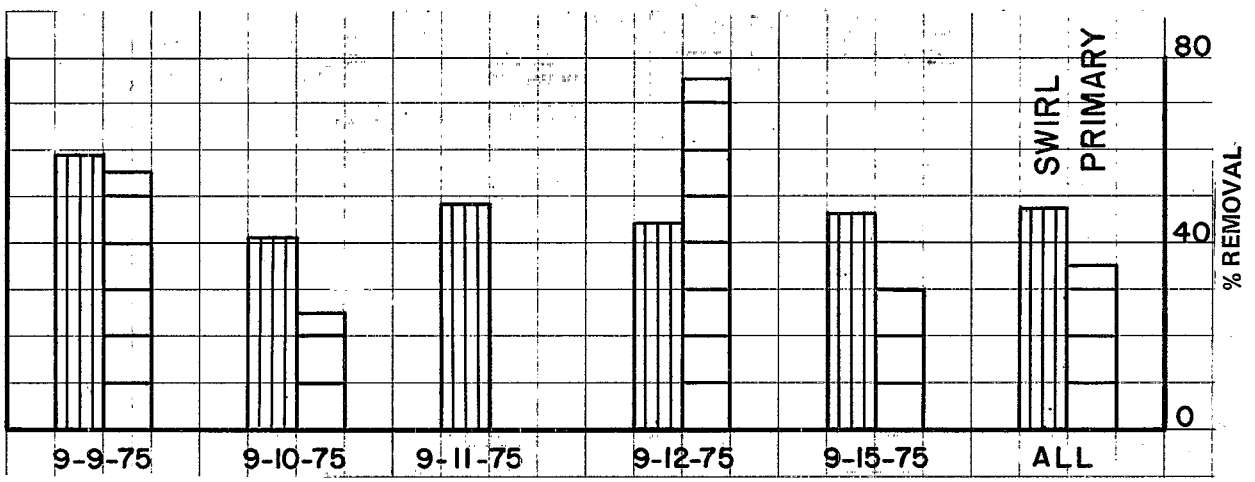

Swirl 19.7 l/sec (0.45 mgd) Overflow rate — 108 $m^3/day/m^2$ (2,650 gal/day/ft^2)
Primary 4,340 l/sec(99.2 mgd) Overflow rate — 83.5 $m^3/day/m^2$ (2,050 gal/day/ft^2)

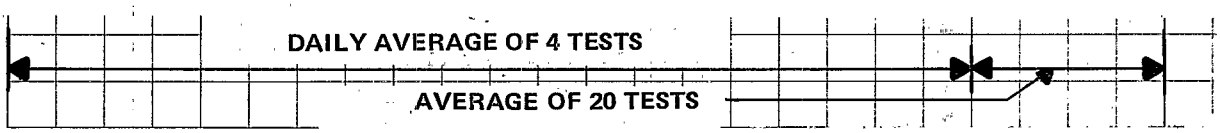

FIGURE 24 DRY-WEATHER REMOVAL OF SETTLEABLE SOLIDS BY VOLUME
TORONTO, September 1975

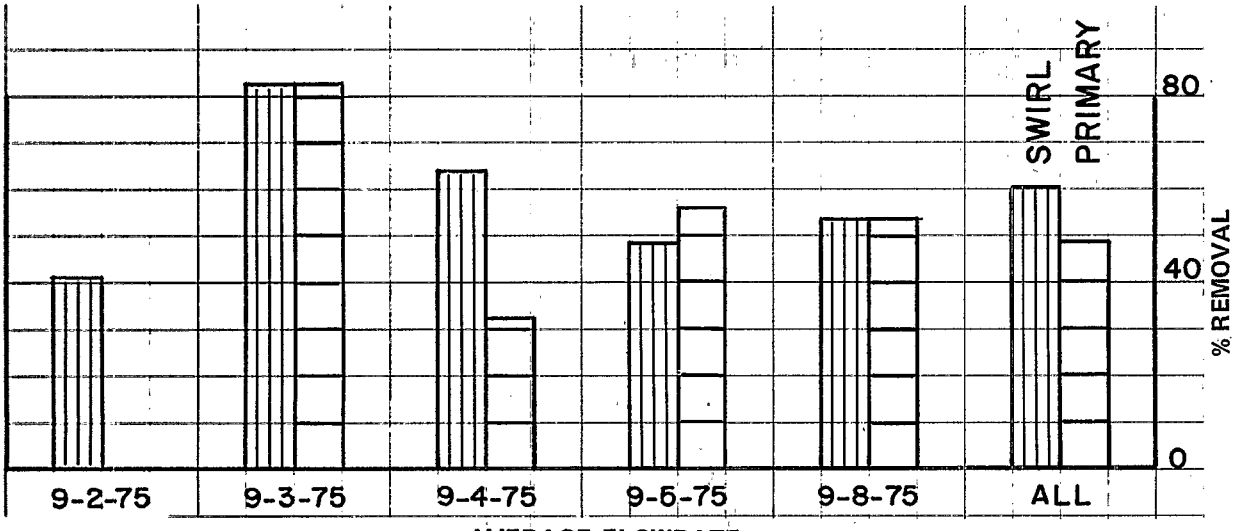

AVERAGE FLOWRATE

Swirl 13.1 l/sec (0.3 mgd) Overflow rate — 108 m^3/day/m^2 (2,650 gal/day/ft^2)

Primary 4,121 l/sec(94.2 mgd) Overflow rate — 79.42 m^3/day/m^2 (1,950 gal/day/ft^2)

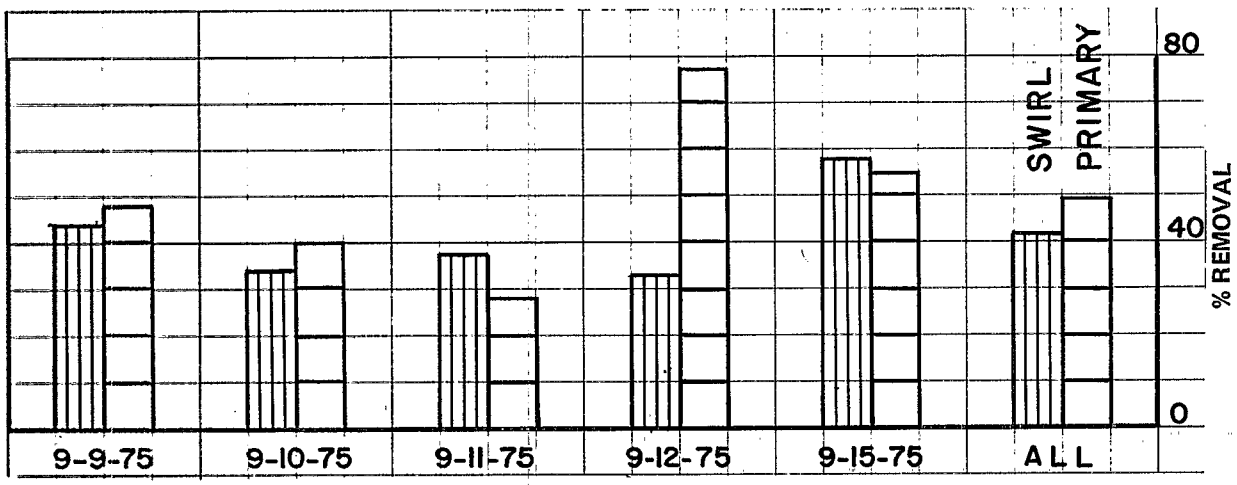

AVERAGE FLOWRATE

Swirl 19.7 l/sec (0.45 mgd) Overflow rate — 108 m^3/day/m^2 (2,650 gal/day/ft^2)

Primary 4,340 l/sec(99.2 mgd) Overflow rate — 83.5 m^3/day/m^2 (2,050 gal/day/ft^2)

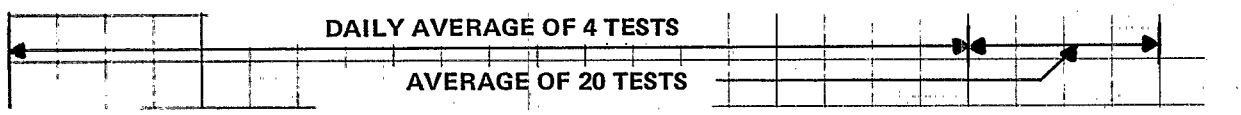

FIGURE 25 DRY-WEATHER REMOVAL OF SETTLEABLE SOLIDS BY WEIGHT
TORONTO, September 1975

TABLE 11
SUMMARY OF TESTS – SEPTEMBER, 1975 (DRY-WEATHER)

Swirl Flow		PERCENT REMOVAL (all samples) Swirl	Primary	(only samples where positive removal) Swirl	Primary
0.3	Settleable solids, ml/l	75.2	49.1	75.2	49.1
0.3	Settleable solids mg/l	60.4	48.8	67.3	55.3
0.3	Total suspended solids, mg/l	43.1	41.9	43.1	46.3
0.3	Volatile suspended solids, mg/l	45.8	44.8	45.8	47.2
0.3	Fixed suspended solids, mg/l	26.5	24.2	38.3	45.4
0.45	Settleable solids, ml/l	47.7	36.3	47.7	43.4
0.45	Settleable solids mg/l	42.0	49.7	43.7	49.7
0.45	Total suspended solids, mg/l	25.3	36.0	25.3	36.0
0.45	Volatile suspended solids, mg/l	25.9	35.8	25.9	35.8
0.45	Fixed suspended solids, mg/l	22.0	37.1	29.8	57.4

Swirl Constant Flow l/sec	mgd	Primary Average Flow l/sec	mgd
13.1	0.3	4,121	94.2
19.7	0.45	4,340	99.2

Note: Each result is average of five four-hour tests

suspended solids removal, based on actual plant results. The median line on this graph is an indication of expected performance although actual plant results vary widely from this line. Based on the foregoing criteria, a primary settling tank with an overflow rate of 36.66 $m^3/day/m^2$ (900 $gal/day/ft^2$) would remove 60 percent of suspended solids. Such a tank, with an average depth of 3.05 m (10 ft) would have a detention time of two hours. Work by Smith[5] confirms these general guidelines.

The detention times and overflow rates for the 10 four-hour tests made in September 1975 are shown in Table 12. During the first five tests, the average detention time was 0.93 hour and the overflow rate was 83.50 $m^3/day/m^2$ (2,050 $gal/day/ft^2$). The average removal of suspended solids was 36.0 percent compared to 40 percent indicated in Figure 6 of ASCE Manual No. 36[4]. Thus, it can be concluded that the primary tanks were removing on the average a reasonable amount of suspended solids, especially if it is assumed that some flow of waste activated sludge continued to circulate through the primary tanks throughout the day hours while the tests were underway.

Additional tests were conducted on the primary treatment units in June of 1976, and these data are shown at the bottom of Table 13. These results are more varied than those taken in the September 1975 tests, regardless of the fact that the detention times and overflow rates are similar.

The pilot swirl separator, as constructed at the Humber Plant, is shown in Figures 19 and 20. The gross volume below the weir elevation is 16.28 m^3 (575 ft^3). During the September 1975 series of tests, sludge was withdrawn at one-half hour intervals. The maximum sludge volume collected during the four-hour test run was 3.54 m^3 (935 gal). With seven drawoffs, the average amount stored in each half hour period between pumping periods was 0.44 m^3 (67 gal). This volume of sludge would occupy about 0.62 m (2 ft) of depth in the bottom hopper and would reduce the volume available for sewage to 16.03 m^3 (566 ft^3). Using this volume, the detention time for a flow of 13.1 l/sec (0.3 mgd) would be 20.4 minutes; for a flow of

TABLE 12
DETENTION TIME AND OVERFLOW RATE – PRIMARY TANKS, SEPTEMBER 1975 AND JUNE 1976 (DRY-WEATHER)

Date	Flow l/sec	Flow m^3/sec	Flow mgd	Detention Time Hours	Overflow Rate $m^3/day/m^2$	Overflow Rate $gal/day/ft^2$	Percent Removal Suspended Solids
1975							
9-2	4,218	4.22	96.4	0.99	0.678	1,930	14.0
9-3	4,139	4.14	94.6	0.97	0.689	1,960	57.5
9-4	4,169	4.17	95.3	0.97	0.692	1,970	48.2
9-5	3,373	4.05	92.5	1.00	0.671	1,910	43.2
9-8	3,369	4.04	92.4	1.00	0.671	1,910	42.7
Average			94.2	0.98		1,940	41.9
Maximum Deviation				2%		2%	
9-9	3,491	4.19	95.7	0.96	0.696	1,980	30.9
9-10	3,426	4.11	93.9	0.98	0.682	1,940	29.6
9-11	3,964	4.76	108.7	0.85	0.787	2,240	22.9
9-12	3,933	4.73	107.9	0.85	0.783	2,230	49.8
9-15	3,281	394	90.0	1.02	0.653	1,860	46.0
Average			99.2	0.93		2,050	36.0
Maximum Deviation				10%		10%	
1976							
6-16	4,350	4.35	99.4	0.93	0.722	2,055	66.0
6-17	4,150	4.15	94.7	0.97	0.688	1,957	75.0
6-18	4,170	4.17	95.3	0.97	0.692	1,970	0
6-19	3,870	3.87	88.4	1.04	0.642	1,827	61.0
6-22	4,060	4.06	92.6	0.99	0.673	1,914	3.0
6-23	4,170	4.17	95.2	0.97	0.692	1,968	15.0
6-24	4,200	4.20	96.0	0.96	0.698	1,984	6.0
6-25	4,490	4.49	102.5	0.90	0.745	2,119	72.0

TABLE 13
TOTAL SUSPENDED SOLIDS REMOVAL (DRY-WEATHER)

	Influent Concentration (mg/l)	% Removal in Swirl Separator	Flow in Primary l/sec	Flow in Primary mgd	% Removal in Primary
Swirl Primary Flow: 8.7 l/sec (0.2 mgd)					
June 16, 1976	133	62	4,354	99.4	66
June 17, 1976	164	48	4,148	94.7	75
June 18, 1976	162	63	4,174	95.3	0
June 21, 1976	175	72	3,872	88.4	61
Average – 61.25					
Swirl Primary Flow: 6.8 l/sec (0.15 mgd)					
June 22, 1976	187	72	4,056	92.6	3
June 23, 1976	169	72	4,170	95.2	15
June 24, 1976	138	72	4,205	96.0	6
June 25, 1976	158	67	4,490	102.5	72
Average – 70.75					

Swirl 0.15 mgd corresponds to 1,326 gpd/ft^2 (54.1) $m^3/day/m^2$ – 40 minute detention time
Swirl 0.2 mgd corresponds to 1,768 gpd/ft^2 (72.2) $m^3/day/m^2$ – 30 minute detention time

19.7 l/sec (0.45 mgd) it would be 13.6 minutes. These calculations are based upon the volume available for the liquid. In reality, much of the cone hopper volume is not used as flow-through space. If only the volume of the cylindrical portion of the swirl were considered, its volume would be 9.8 m^3 (349 ft^3) resulting in a detention time of 12.4 minutes at a flow of 13.1 l/sec (0.3 mgd) and 8.3 minutes at a flow of 19.7 l/sec (0.45 mgd). Thus the real detention time is between these values. For economic comparison with conventional primary settling tanks, the most adverse condition was chosen.

The surface area of the swirl separator is 10.5 m^2 (113.1 ft^2). With a flow of 13.1 l/sec (0.3 mgd) the overflow rate is 107.9 $m^3/day/m^2$ (2,650 $gal/day/ft^2$), and with a flowrate of 19.7 l/sec (0.45 mgd) the overflow rate is 162.1 $m^3/day/m^2$ (3,980 $gal/day/ft^2$). In Table 64 the removal of total suspended solids in the swirl separator with a flow of 13.1 l/sec (0.3 mgd) is 43.1 percent compared to 41.9 percent in the primary tanks. Therefore, the performance of the swirl separator with a flow of 13.1 l/sec (0.3 mgd) and an overflow rate of 108.3 $m^3/day/m^2$ (2,650 $gal/day/ft^2$) may be considered to be equivalent to the primary tank with an overflow rate of 81.46 $m^3/day/m^2$ (2,000 $gal/day/ft^2$) and a one-hour detention time.

In Table 69 the removal of total suspended solids in the swirl separator with a flow of 19.7 l/sec (0.45 mgd) is 25.3 percent. This percent removal is below design standards and hence it is concluded that the swirl separator of the size used was not suitable for this high rate of flow.

Additional tests conducted on the swirl pilot unit during June 1976 at the lower flow rates of 6.57 l/sec (0.15 mgd) and 8.76 l/sec (0.2 mgd) yielded total suspended solids removals in the swirl unit which were significantly better than those discussed earlier. The averages for the two tests are 61.25 and 70.75 percent respectively for the two flowrates. The calculated test data are shown in Table 13 and the actual data are presented in Tables 39,49,44 and 45 in Appendix D. All test procedures were similar to those used in the September, 1975, tests. The increased detention times resulted in significant improvement in removal efficiencies.

One of the purposes of these tests was to confirm the laboratory results obtained at the LaSalle Hydraulic Laboratory where synthetic sewage solids were used. The resultant design curves were given in Figure 11.

The results obtained in the Toronto tests for a swirl separator with a diameter of 3.66 m (12 ft) are compared in Figure 26 with the results predicted from the laboratory model tests. Thus with a flow of 13.1 l/sec (0.30 mgd) the laboratory predicted 37 percent removal, versus 43.1 percent obtained at Toronto. For a flow of 19.7 l/sec (0.45 mgd) the laboratory predicted a removal of 28 percent, versus 25.3 percent obtained at Toronto. The two results obtained in the field do not vary enough from the laboratory findings to cause any change in the curves developed from the LaSalle model study. Thus, it can be concluded that the field work has confirmed the laboratory work, based on the tests to date.

Figure 27 compares the time to achieve treatment for the swirl primary and the conventional unit at Toronto. The high initial efficiency of the 3.7 m (12 ft) unit is evident.

For the June 1976 tests, the 6.57 l/sec (0.15 mgd) flow shows a predicted removal efficiency of 57 percent in Figure 11a, while the 8.76 l/sec (0.2 mgd) flow shows a predicted removal efficiency of 48 percent. In both cases, the actual removals exceeded the predicted performance.

EVALUATION OF BOD TESTS

The Recommended Standards for Sewage Works by the Great Lakes-Upper Mississippi River Board of State Sanitary Engineers (10-States Standards) includes a figure relating BOD removals to overflow rates in primary settling tanks. It also states: "However, BOD removals for sewage containing appreciable quantities of industrial wastes should be determined by laboratory tests and consideration of the quantity and characteristics of the waste."

In the second series of tests conducted for four-hour periods from June 23 to July 8,

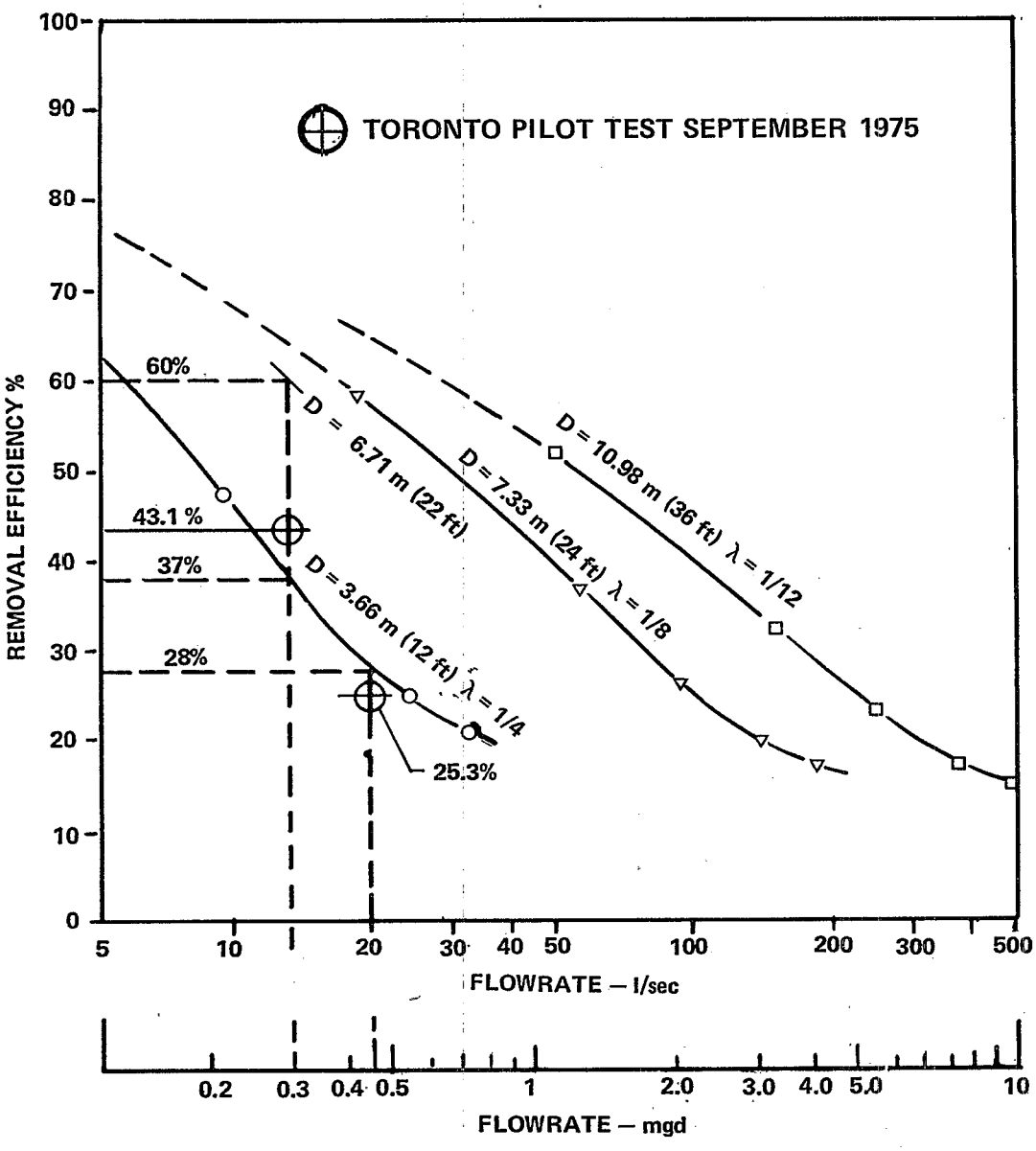

FIGURE 26 PREDICTED VERSUS ACTUAL SUSPENDED SOLIDS REMOVAL

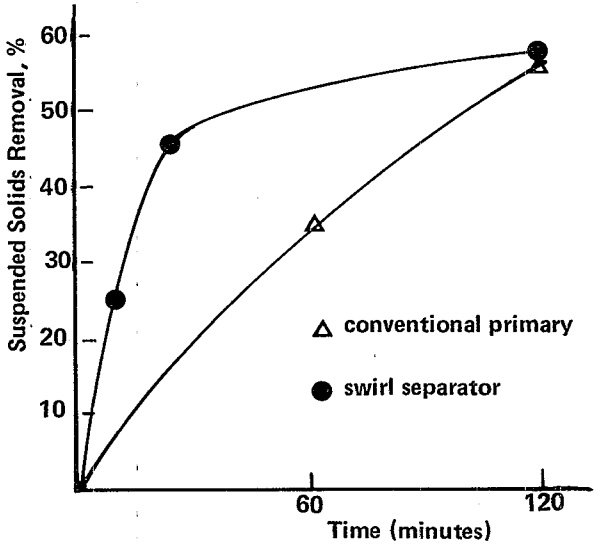

FIGURE 27 COMPARISON OF TIME TO ACHIEVE TREATMENT

BOD_5 tests were carried out; the results are shown in Tables 47, 48, 49 and 50. The percent removal of BOD_5 derived from these tests is shown in Table 14. During the test period, the average percent removal in the primary tanks was 13.1 percent. For the overflow rate of 81.46 $m^3/day/m^2$ (2,000 $gal/day/ft^2$) in the primary tank the 10-States Standards indicates a removal of 22 percent. Hence, the removal was about 60 percent of the anticipated amount. The removal percentage for the swirl separator with a flow of 13.1 l/sec (0.3 mgd) and an overflow rate of 108 $m^3/day/m^2$ (2,650 $gal/day/ft^2$) was slightly less than for the primary tank.

In the tests made from July 2nd to 8th, the removal percent in the primary tanks was 5.2 percent, versus 22 percent shown in the 10-States Standards. Thus, the removal was about 24 percent of expectation. Again, the

TABLE 14
REMOVAL OF BOD_5–
JUNE 23-JULY 8, 1975

Date 1975	Influent (mg/l)	Effluent (mg/l)		% Removal	
		Swirl	Primary	Swirl	Primary
6-23	284	248	251	12.6	11.6
6-24	301	278	227	7.6	24.6
6-25	300	247	277	17.6	7.7
6-26	382	361	343	5.5	10.2
6-27	339	289	295	14.7	13.0
Average	321	285	279	11.2	13.1

Data for above

Flow: Swirl Separator = 13.1 l/sec (0.3 mgd)
Primary Tanks = 4,245 l/sec (96.9 mgd)

Overflow Rate:

Swirl = 108 m^3 / day/m^2 (2,650 gal/day/ft^2)
Primary Tanks = 81.46 m^3 /day/m^2 (2,000 gal/day/ft^2)

7-2	332	326	321	1.8	3.3
7-3	296	295	290	0.0	2.0
7-4	361	309	314	14.4	13.0
7-7	307	307	332	0.0	0.0
7-8	347	343	302	1.1	13.0
Average	329	316	312	4.0	5.2

Data for above

Flow: Swirl Separator = 19.7 l/sec (0.45 mgd)
Primary tanks = 4,254 l/sec (97.1 mgd)

Overflow Rate:

Swirl = 155 m^3/day/m^2 (3,805 gal/day/ft^2)
Primary Tanks = 81.87 m^3/day/m^2 (2,010 gal/day/ft^2)

removal in the swirl separator with a flow of 19.7 l/sec (0.45 mgd) was slightly less than that in the primary tanks – 4.0 versus 5.2 percent. Basically, the function of primary clarification is removal of suspended and settleable solids rather than BOD.

SETTLEABILITY OF COMBINED SEWAGE FLOW SOLIDS

A report was prepared by Beak Consultants Ltd. on the settling velocity characteristics of Toronto wastewater solids in storm flow periods and on the hydraulic character of the swirl separator and the primary settling tanks. This report is contained as an Appendix C to this report.

Samples were collected of the sewage influent to the plant during two storm events. Samples were collected from the influent channel to the primary tanks during the rising, peaking, and falling phases of the storm flows. Settling column tests performed on these samples indicated that the settling characteristics of the combined sewage solids were similar to the Amberlite IRA-93 anion exchange resin used to simulate sewage solids in the previous laboratory work by LaSalle.

The settling column tests also showed increased settleability of the solids during the storm event. Thus, in the first storm, for a constant overflow rate of 173 $m^3/day/m^2$ (4,240 $gal/day/ft^2$), the predicted solids removals were 74, 76, and 81 percent for rising, peaking, and falling storm conditions, respectively. In the second storm event for the same overflow rate, the predicted solids removals were 60, 80, and 83 percent for rising, peaking, and falling storm conditions, respectively. The actual removal of total suspended solids during the first storm was zero percent in the swirl separator and 10.2 percent in the primary tanks. The overflow rate in the swirl separator was 155 $m^3/day/m^2$ (3,800 $gal/day/ft^2$). The average overflow rate for the day in the primary tanks was 59 $m^3/day/m^2$ (1,449 $gal/day/ft^2$) but during the storm period it was as high as 105.4 $m^3/day/m^2$ (2,575 $gal/day/ft^2$).

In the second storm event no records were provided for solids removals in the swirl separator and the primary tanks.

Tracer studies, using fluorescent dye, were conducted on the swirl and the primary tanks to determine the character of the hydraulic flow. The results of the tracer study showed that the hydrodynamics of the swirl separator lie more towards the plug flow regime of mixing than they do in the primary clarifiers. The apparent decrease in active volume and shift towards plug flow which occurs as the flow increases in the swirl separator would indicate that the quiescent cone of fluid along the axis of the swirl may increase with increasing flow.

Removal efficiency decreases as the mixing regime shifts from plug flow to well-mixed conditions. The results of the tracer study would predict that the swirl, being closer to plug flow in all cases tested, would accomplish the same removal as the primary clarifiers but at a significantly higher upflow velocity or surface overflow rate.

INTERPRETATION AND OTHER APPLICATIONS

The statement was previously made that the results should be interpreted as specifically relating to the flow conditions, wastewater character, and treatment plant operating procedures indigenous to the demonstration installation. This statement was intended to limit the findings of this single investigative application to *this* application only, and to avoid the hazard of extrapolating these findings to represent what a similar swirl separator might accomplish under other test circumstances.

With this disclaimer, it is possible to interpret the performance of the swirl unit at the Humber plant, *vis-a-vis* the treatment efficiencies of the primary settling tanks at this location. Recognition must be made of the possible deleterious effect of "hang-over" waste activated sludge in the influent on the performance of the swirl unit which would, necessarily, be relatively incapable of retaining light, semi-colloidal solids under the flow pattern conditions in such a settling device. In addition, the unpredictable presence of industrial wastes of some types could have had an adverse effect on clarification under swirl flow conditions.

Further, indeterminate phenomena may have failed to be disclosed because of grab sampling and compositing practices during the test runs. These, and other factors, have been referred to in the preceding portions of this pilot report.

However, the following interpretations of the study data are valid for the Toronto pilot installations:

- The Toronto swirl pilot, in general, confirmed the basic findings of the LaSalle Laboratory research study, as described in Appendix C. Some phases of performance were better than anticipated; others were less effective.
- The Toronto swirl unit, thus, demonstrated the ability of this type of hydraulic flow to achieve removals of wastewater solids under both dry-weather and wet-weather flow conditions.
- The Toronto swirl separator offered no advantages over the primary settling tanks at the treatment plant, based on standard design criteria, in terms of solids removal. For small treatment facilities if 60 percent suspended solids removal was not required, the swirl might be cost effective.
- With heavy solids which are a characteristic of wet-weather flow conditions, the efficiency of solids removal is improved as compared to dry-weather flow conditions.
- The Toronto swirl separator, due to the nature of the wastewater flow, achieved lower BOD removals than the conventional primary settling tanks, and less removal efficiency than would normally be expected. Later tests performed at lower flow rates yielded total suspended solids removals which exceeded predicted performance.
- The basic advantage of the swirl clarification principle is that it requires no mechanical devices or equipment for the removal of settled solids from the retention hopper. This advantage is achieved by providing greater depth than required by so-called conventional mechanical primary settling tanks, thus, imposing additional cost and construction problems for the former type of primary facility.

As stated, a swirl pilot unit under operational conditions other than those imposed at the Toronto plant may show primary settling efficiencies that offer advantages over regular clarification facilities, but this can be demonstrated only by other test installations. Such further applications should be encouraged to avoid the drawing of overall conclusions that are based on only *one* installation at Toronto. Further investigations must be proposed and made with full recognition of the comparative performances described in this report.

The absence of mechanical solids removal devices in the swirl separator may make it particularly applicable and advantageous in some locations and for some purposes where clarification is carried out at other than treatment plant sites that are adequately manned by operation personnel. Such an application could be one at a combined sewer overflow location upstream of the treatment plant or adjacent to an automatic pumping station.

The handling of sludge from the swirl hopper would require periodic removal of this material to some type of storage and disposal facility. In addition, scum removal equipment will be needed. Both the scum and sludge withdrawal problems are common to all types of primary treatment units.

SECTION 5

GLOSSARY

Long-Flow Pattern – The path of the swirl flow pattern through the swirl separator, induced by proper baffling which causes the liquid to traverse the circular chamber more than once and prevents the incoming flow from being diverted or short-circuited directly to the overflow weir, thereby inducing the solids to discharge into the foul sewer channel and outlet.

Settling Velocity – Downward velocity of a particle in sewage.

Settleable Solids – That portion of the solids contained in the wastewater flow into a swirl chamber which will subside and be collected in the chamber due to gravity and other liquid-solids kinetic conditions induced by the controlled swirl flow pattern. (Note: Not all suspended solids are settleable solids, such as colloidal or other finely dispersed solids.)

Suspended Solids – 1) The quantity of material deposited when a quantity of water, sewage, or other liquid is filtered through an asbestos mat in a Gooch Crucible or a 0.35 m-0.45 m millipore fiberglas filter.[6] 2) Solids that either float on the surface of, or are in suspension, on water, wastewater, or other liquids, and which are largely removable by laboratory filtering.

REGISTERED TRADEMARKS

Plexiglas
Amberlite
Tygon
Petrothene
Petrothene X
Polythene

REFERENCES

1. American Public Works Association – *The Swirl Concentrator as a Combined Sewer Overflow Regulator Facility;* EPA Report No. EPA-R2-72-008, NTIS No. PB 214 134, September, 1972.

2. Sullivan, R.H., et al – *The Swirl Concentrator as a Grit Separator Device,* EPA Report No. EPA-670/2-74-026; NTIS No. PB-233 964. June, 1974.

3. Dalrymple, R.J., et al – *Physical and Settling Characteristics of Particulates in Storm and Sanitary Wastewaters* – EPA Report No. EPA-670/2-75-011, NTIS No. PB-242 001, April, 1975.

4. Society of Civil Engineers – *Sewage Treatment Plant Design; Manual No. 36,* ASCE-WPCF, New York, 1959.

5. Smith, R. – *Preliminary Design of Simulation of Conventional Wastewater Renovation Systems Using the Digital Computer* – U.S. Department of the Interior, FWPCA, 1968.

6. *Standard Method for the Examination of Water and Wastewater* – American Water Works Association, Water Pollution Control Federation, American Public Health Association, 14th edition, 1975. p. 94.

APPENDIX A

HYDRAULIC MODEL STUDY

Previous studies of the swirl concentrator principle have investigated its application as a combined sewer overflow regulator and as a grit chamber. Hydraulic model research resulted in the development of swirl chamber configurations and dimensions that will produce effective solids-liquid separations and design criteria for prototype installations were evolved. The present study was undertaken to determine the application of the swirl chamber principle to the primary clarification of wastewater flows.

The same model used in the previous studies was retained and modified to meet the new criteria of primary clarification facilities. These criteria involved differences in solids content and characteristics, and reduced flows, with slower, gentler rotation in the chamber. Changes in solids content of influent flows involved the use of lighter and finer solids material in the model to simulate actual conditions in field prototype installations.

Utilization of such finer material introduced the need for laboratory measuring techniques not available through the LaSalle Hydraulic Laboratory staff, so model test monitoring analyses were performed by Beak Consultants, Ltd.*

Principle and Scope of the Study

The principle used in the primary settling structure is a controlled combination of solids settling, rotational velocity, flow equalization of spill of clarified liquid over the overflow weir, and the slope and shape of the chamber floor in order to produce the best possible removal of the solids.

Although a foul outlet was provided during fabrication of the hydraulic models, no regular use of it was made to test its collecting efficiency. Intermittent draw-off during flow was assumed to be the means of removing the settled solids, or sludge, in actual prototype units.

The basic layout was evolved from several different sources: Mr. Smisson's general arrangement with deep skirt; 60 degree bottom chamber cone from the experience of Sogreah Hydraulic Laboratory, Grenoble, France; larger diameter inlet, weir and skirt diameters from LaSalle's previous experience. The initial layout is shown in Figures 2 and 28.

In order to establish practical prototype values for the study, the same scale of 1:12 already used for the earlier studies, was retained. This means the model would be operating with a 1.22 m (4 ft) square sewer coming into a 10.98 m (36 ft) diameter chamber during the first stage of the study. Later, the square sewer was reduced to 0.72 m (2.36 ft), while the chamber remained unchanged.

The size chamber, with the weir crest 2.75 m (9 ft) above the chamber floor, would give 21 minutes of retention to 0.31 m^3/sec (11 cfs), corresponding to 0.632 lit/sec (0.022 cfs) on the model.

To simplify the testing, three model discharges were selected whose prototype equivalents would be as follows:

Model		Prototype	
l/sec	m^3/sec	cfs	mgd
0.5	0.25	8.8	5.7
1.0	0.50	17.6	11.4
1.5	0.75	26.4	17.1

MODEL DESCRIPTION

The central feature of the model was the separation chamber itself, which took the form of a vertical concrete cone with 60 degree side slope, topped concentrically by a vertical cylinder 91.5 cm (36 in) diameter made of 13 mm (0.5 in) Plexiglas®. In the first stage of the tests, the height of the cone was adjusted so as to leave between the top of the cone and the cylinder a 10 cm (4 in) wide annular flat bench called the chamber floor, as shown in Figure 3. Later, for subsequent series of tests, the concrete cone was extended

* See Section 11, page 6.

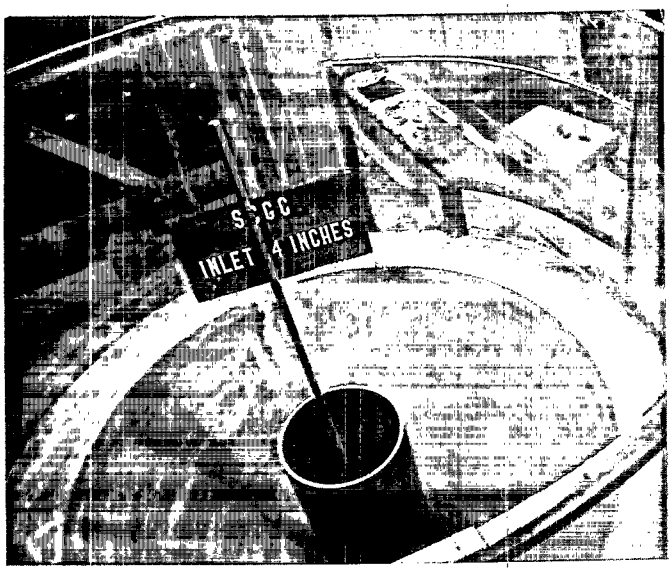

Empty Chamber Showing Conical Bottom and Low Inlet – Invert Level with Outside Floor
Original Layout

FIGURE 28 SWIRL PRIMARY SEPARATOR
(CONICAL BOTTOM AND LOW INLET)

A.
Raised Inlet – Crown 22.86 cm (9 in) Above Outside Floor
Modification 2

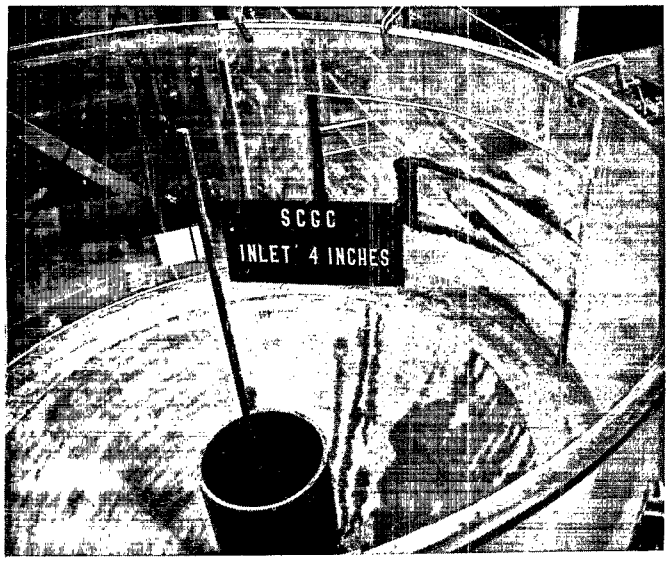

FIGURE 29 SWIRL PRIMARY SEPARATOR, MODIFICATION 2,
(RAISED INLET 61 cm [24 in] DIAMETER WEIR AND 71 cm [28 in] DIAMETER SKIRT)

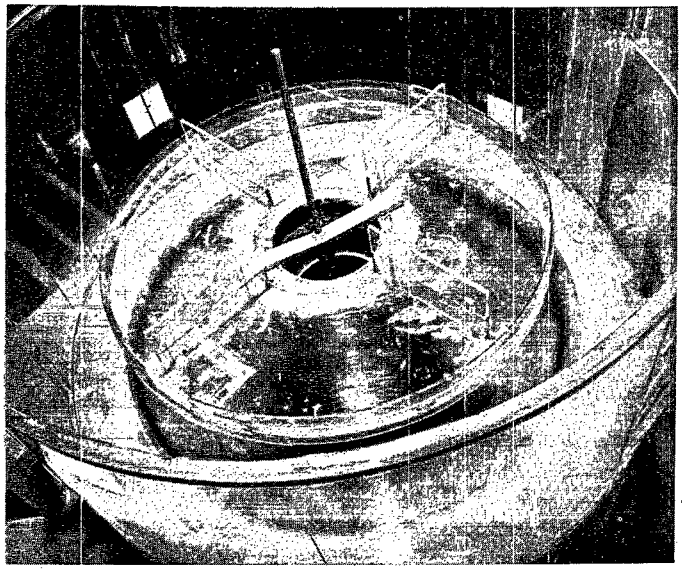

B.
Conical Bottom and Raised Inlet with 61 cm (24 in) Diameter Weir Inlet Crown Level with Weir Lip Modification 2

C.
Conical Bottom and Raised Inlet Chamber with 61 cm (24 in) Diameter Weir and 71 cm (28 in) Diameter Skirt Modification 2

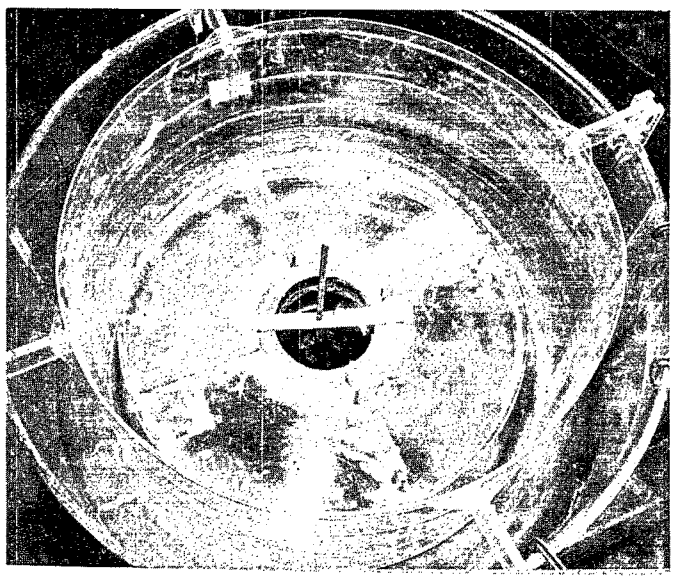

FIGURE 29 SWIRL PRIMARY SEPARATOR, MODIFICATION 2, (RAISED INLET 61 cm [24 in] DIAMETER WEIR AND 71 cm [28 in] DIAMETER SKIRT)

upward to the periphery of the chamber wall so as to eliminate the horizontal bench floor.

A Plexiglas skirt, supported by the chamber wall and concentric to the cone axis, divided the chamber into two parts; the inner and outer chambers. The vertical distance from the bottom of the skirt to the surface of the cone determined the slot height below the skirt. The distance could be changed at will by means of calibrated supporting blocks.

In the center of the cone, an embedded PVC pipe, 15.2 cm (6 in) inside diameter, provided the support for the circular weir and the outlet to evacuate the clear overflow spilling over the weir. The level of the weir could be raised or lowered at will by adding or removing custom-cut pieces of the supporting pipe.

The overflow pipe was later removed to leave the inner chamber unencumbered and the weir was attached to the chamber skirt. The bottom of the cone was closed and the clear overflow was evacuated by means of a circular gutter fixed around the skirt in the outer chamber connecting with two 2.5 cm (1 in) diameter Tygon® hoses passing through the chamber wall.

Inflow to the chamber was supplied through a polyvinyl chloride (PVC) pipe 10 cm (4 in) diameter set at a slope of 1/1,000. A vibrating solids injection system was placed on this supply line 2.14 m (9 ft) upstream of the chamber. Water supply to the model through the pipe was taken directly from the constant level tank in one of the laboratory's permanent pumping stations. This supply device was used as long as the recovery of the large-size grain material injected presented no problems. When smaller grain sizes were used, a closed circuit device was built. The PVC supply pipe was removed and replaced by a 76.2 cm (30 in) long Plexiglas pipe while the solids injection system was changed to provide just a hopper attached to the top of the inlet duct, by means of which diluted material was introduced into the model at a constant rate.

Overflow from the central pipe, and later from the collecting annular gutter, was delivered to a large settling basin equipped with a calibrated V-notch weir.

A point gauge in a manometer pot read the level in the basin, thus determining the discharge passing over the V-notch weir, and, hence, the total discharge passing through the separation chamber.

Solids Simulation

The swirl settler development tests were being carried out at the same time that Beak Consultants were conducting studies to characterize the suspended solids in actual sanitary sewage, and to identify a suitable material to be used in the laboratory to simulate this material. While Beak's work was underway, first-stage testing was performed, using shredded Petrothene®. This was adequate to guide basic chamber shape choices. When the result of Beak's investigations became available, a new material, an Anion Exchange Resin designated as IRA-93, manufactured by Rohm and Haas, was used as described in Section II.

Testing Procedure

Operation of the swirl concentrator as a primary settler would normally involve a continuously varying discharge, which can be characterized by the average daily flow taken as the design discharge. Since it was the purpose of the model to adjust the chamber dimensions to the discharge to be treated, the range of the study was extended to cover three different flows.

This process allowed observation of the behavior of the separation chamber and the variation of the recovery rate when conditions of operation changed. It has already been mentioned that the selected discharges used for each layout were 0.5 l/sec (0.017 cfs), 1.0 l/sec (0.035 cfs) and 1.5 l/sec (0.053 cfs). These three series of results emphasized the combined influence of the inlet and slot velocities on the settleable separating process. Different combinations of weir and skirt were also tested.

For each individual test, the steady-state discharge was established in the model and equilibrium conditions established. One l (34 oz) of wet Petrothene, sg 1.01, grain size ranging from 1 to 3 mm (0.039 to 0.118 in), was injected into the supply pipe using the same vibrating rate for all tests. The full liter was added over a period of 5 minutes and the model was allowed to run 10 minutes after the end of the injection.

The amount of Petrothene found on the bottom of the cone or floating in the outer chamber was measured separately. The Petrothene floating in the settling basin was also measured. The remaining portion deposited in the settling basin was found by subtraction, assuming no material was lost.

The recovery rate was taken as the percentage represented by the amount measured on the bottom of the cone as compared to the total found in the cone and on the bottom of the settling basin.

SETTLEABLE SOLIDS RECOVERY RESULTS

In discussing settleable solids for the purpose of this section of the report, reference is made to the recovery rates for shredded Polythene® and Petrothene X. As described in Section II, the shredded Polythene and Petrothene X was considered as representing organic materials over the ranges as defined in the discussion. The different steps followed in the model testing are recorded in Table 15.

1. Tests Carried Out With Circular Weir

a) Material Used for Testing: Shredded Polythene: Although the recovery rate was encouraging (84 percent for 1 l/sec and a 1.2 cm [0.5 in] slot height), the first tests carried out with the inlet sewer at the same level as the outside floor in the chamber revealed the existence of undesirable turbulence and under the weir in both the outer and inner chambers.

Subsequent tests performed with the inlet crown raised to the level of the weir lip, 22.9 cm (9 in) above the floor – and with other conditions unchanged, as shown in Figure 29, showed no improvement in the recovery rate (78%), as shown in Figure 30. However, it appeared evident that the turbulence created in the chamber was mainly due to the bottom of the skirt being just above the horizontal floor or bench.

The flow tended to descend outside the skirt, turn under the lip quickly, and roll up inside, creating a degree of turbulence. This turbulence entrained more suspended particles in the effluent passing over the weir.

This led to the use of a smaller diameter skirt which would sit lower in the cone. A 61 cm (24 in) diameter skirt, together with a 50.8 cm (20 in) diameter disc weir, as portrayed in Figure 31, were selected and tested. The whole series of tests and the results are shown in Figure 32. The curves appear and the results are shown in Figure 31, Prototype Particle Sizes Simulated by Shredded Petrothene. The curves appear relatively uniform in that the recoveries improved as the discharge decreased or the retention time increased. On the other hand, slot height tests were inconclusive at this stage of the test program. The smaller diameter skirt, sitting deeper inside the cone, noticeably improved the recovery rate.

Test 27 carried out without a skirt, as shown in Figure 33, showed a sharp drop in the recovery rate (less than 50 percent) and proved that the skirt was an essential part of the separation chamber.

b) Tests Carried Out with Ground Petrothene X: The results of tests 28 and 33, shown in Figure 34, which were repeats of tests 20 to 27, proved the consistency of the results already obtained with shredded Polythene, as shown in Figure 30.

Further tests carried out with 1.0 and 1.5 l/sec (0.035 and 0.053 cfs) discharges showed that the recovery rate remained high for small and intermediate flows, then dropped slightly when the skirt was removed. For the high flow 1.5 l/sec, the recovery rate started in the 50 percent range, but showed a progressive improvement as the slot opening was increased.

Removal of the skirt proved to be less significant in this case, as shown on the right-hand side of Figure 34.

Visual observations of the flow pattern obtained with a 50.8 cm (20 in) diameter weir showed the existence of a central mass of water around the central overflow pipe, under the weir, representing a zone 5 cm (2 in) to 7.65 cm (3 in) wide, which apparently had no flow-through discharge, was not rotating, and in which very few sediment particles could be detected. This observation led to reducing the weir diameter. The extreme case was selected first: that is, the weir was

TABLE 15
MODIFICATIONS TESTED ON THE MODEL

Mod Nbr.	Ref. Figure	Tests Number	Skirt ∅ cm (in)	∅ cm (in)	Height Above Chamber Floor	Inlet Elevation	Recovery Fig. Ref.
Material Used Shredded Polythene (up to Test 27) and Petrothene X 10 x 10 cm (4 x 4 in) Inlet Duct, 10 cm (4 in) flat chamber floor							
1	2		11.0 (28)	61.0 (24)	23.0 (9)	Invert at bottom Elevation	
2	12	1 to 19	71.0 (28)	61.0 (24)	23.0 (9)	Crown at Weir Elev.	13
3	14	20 to 45	61.0 (24)	51.0 (20)	23.0 (9)	Crown at Weir Elev.	13 and 16
4	15	27, 28, 34 and 40	61.0 (24)	51.0 (20)	23.0 (9)	Crown at Weir Elev.	16
5	17	46 to 68	61.0 (24)	17.0 (6.625)	23.0 (9)	Crown at Weir Elev.	18
6	19	69 to 91	61.0 (24)	38.0 (15)	23.0 (9)	Crown at Weir Elev.	20
7	28	92 to 112	61.0 (24)	closed bell	23.0 (9)	Crown at Weir Elev.	29
8	21	113 to 136	61.0 (24)	38.0 (15)	33.0 (13)	Crown 10 cm (4 in) under weir level	22
9	35	137 to 160	61.0 (24)	4 radial gutters	23.0 (9)	Crown at Weir level	36
10 x 10 cm (4 x 4 in) Inlet Duct, Cone Extended to Chamber ∅							
10	37	161 to 184	71.0 (28)	4 radial gutters	12.4 cm (4.875 in) above top of cone	Crown at Weir level	38
Material Used Anion Exchange Resin IRA-93 149 u d 74 u 6 x 6 cm (2.4 x 2.4 in) Inlet Duct, Cone Extended to Chamber ∅							
10	37	185 to 195 (0) (10)	71.0 (28)	4 radial gutters	12.4 cm (4.875 in) above top of cone	Crown at Weir level	39

Note: Test numbers in parentheses refer to second series started with fine material.

TABLE 15 (continued)

Mod Nbr.	Ref. Figure	Tests Number	Skirt Ø cm (in)	Ø cm (in)	Height Above Chamber Floor	Inlet Elevation	Recovery Fig. Ref.
		Central pipe overflow removed 6 x 6 cm (2.4 x 2.4 in) Inlet Duct, Cone Extended to Chamber Ø					
11	41	196 to 204 (11) (19) 232 to 235 (48) (51)	71.0 (28)	8 radial gutters	Weir lip 2 cm (0.78 in) above top of duct	Crown 12.4 cm (4.875 in) above top of cone	47 and 49
12	42	205 to 231 (20) (47) 236 to 243 (52) (59)	61.0 (24)	8 radial gutters	Weir lip 2 cm (0.78 in) above top of duct	Crown 12.4 cm (4.875 in) above top of duct	47 and 49

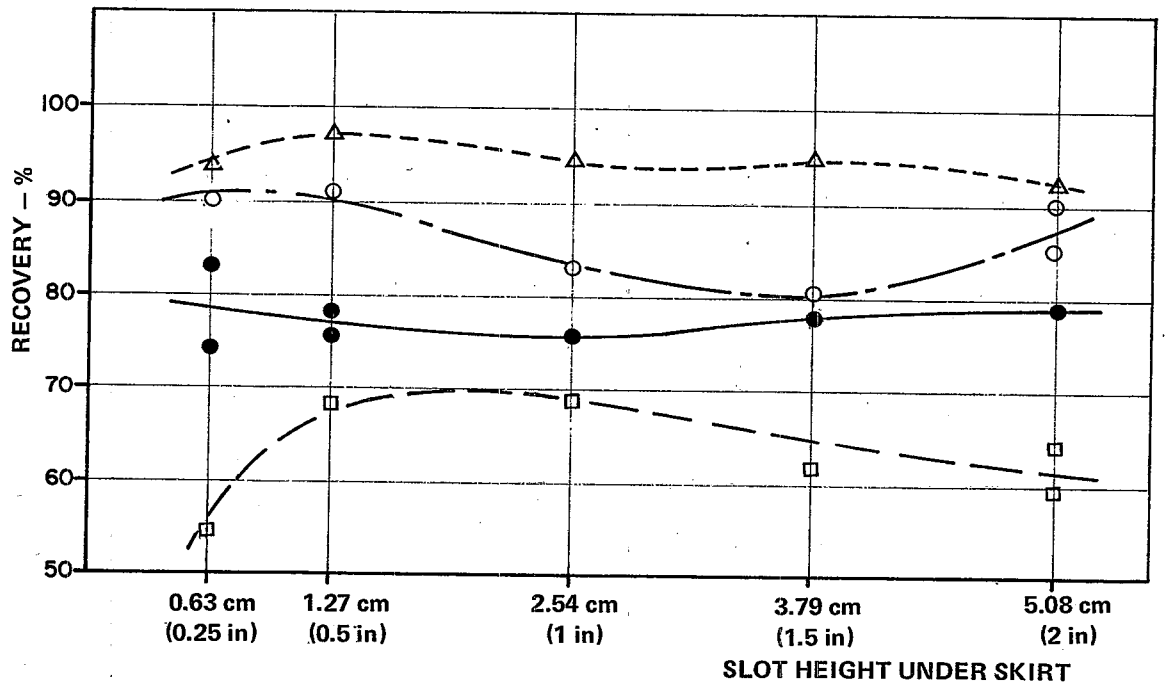

TESTS 5-9 : QM = 1 l/sec (0.035 cfs), SKIRT 0.71 m (28 in) Ø ——●—— ②

TESTS 10-14: QM = 1.5 l/sec (0.052 cfs), SKIRT 0.71 m (28 in) Ø — — □ — — ②

TESTS 15-19: QM = 0.5 l/sec (0.017 cfs), SKIRT 0.71 m (28 in) Ø ——-—○—-— ②

TESTS 20-27: QM = 0.5 l/sec (0.017 cfs), SKIRT 0.61 m (24 in) Ø ------△------ ③

MOD

MATERIAL USED: shredded polythene – nominal SG 1.01
– grain sizes 1-3 mm (0.039-0.118 in)
irregular shapes

FIGURE 30 SWIRL PRIMARY SEPARATOR
OPERATING EFFICIENCIES FOR MODIFICATION 2 AND 3

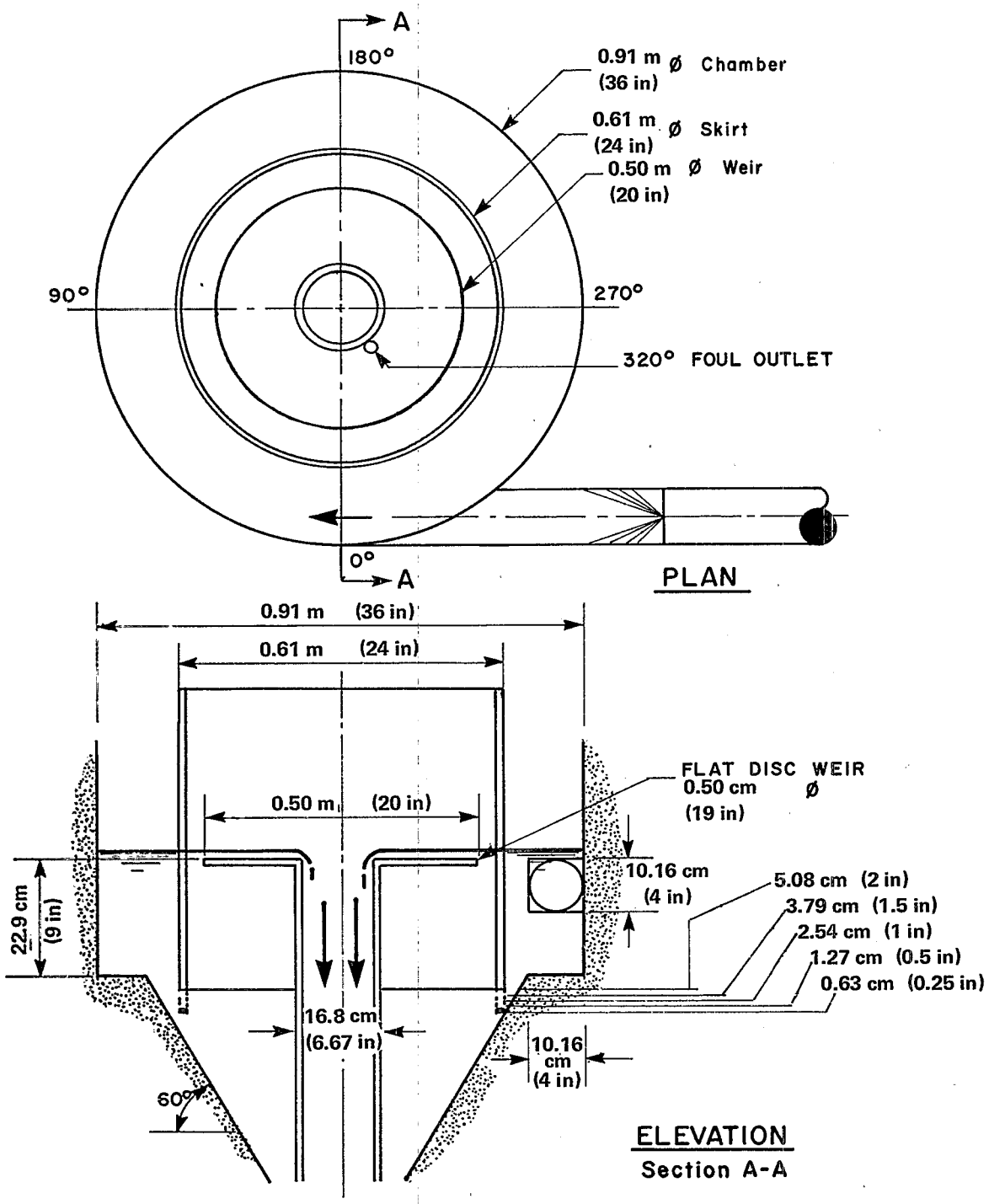

FIGURE 31 SWIRL PRIMARY SEPARATOR
MODEL LAYOUTS FOR TESTS 20 TO 45
MODIFICATION 3

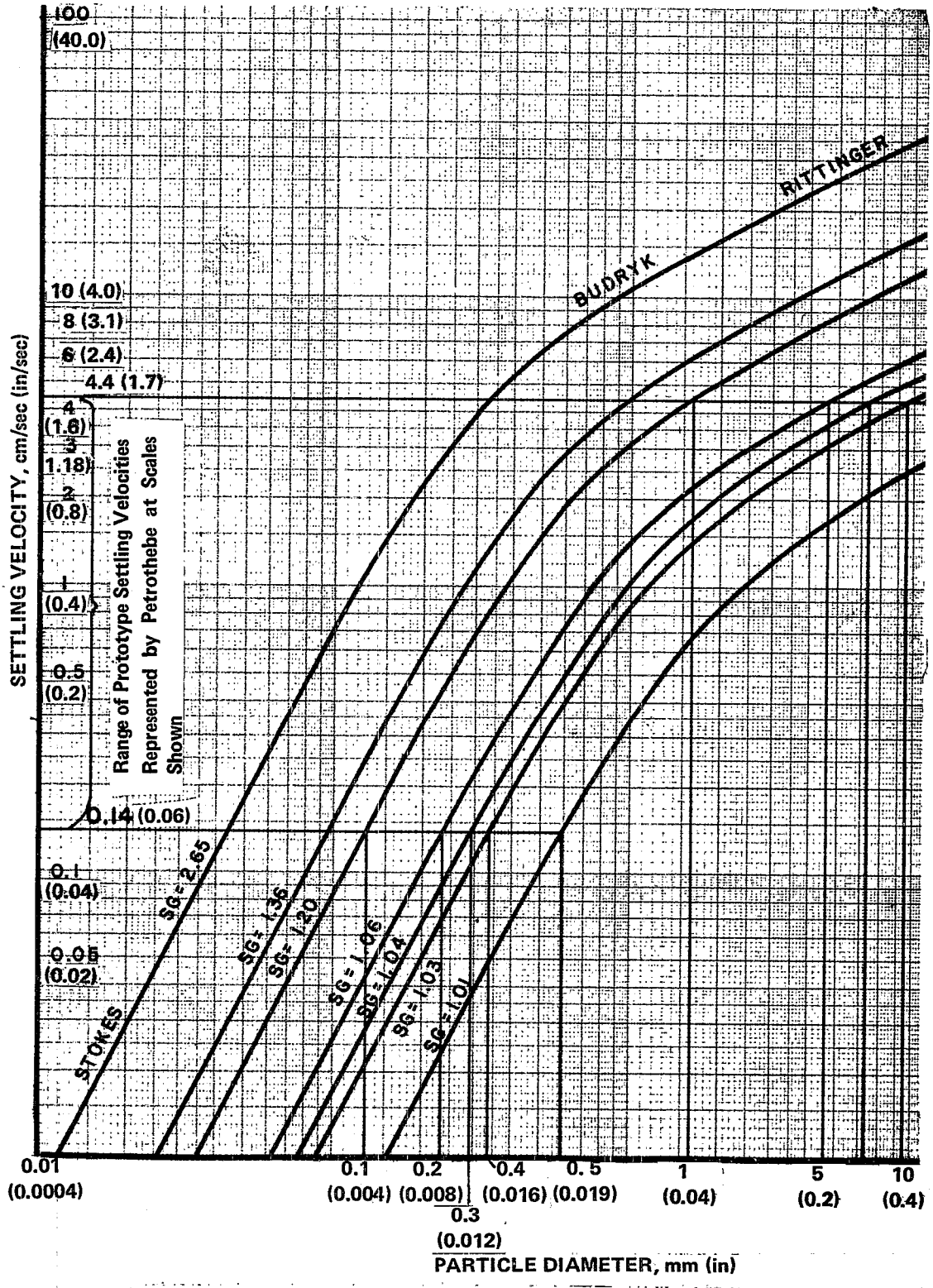

FIGURE 32 PROTOTYPE PARTICLE SIZES SIMULATED BY SHREDDED PETROTHENE

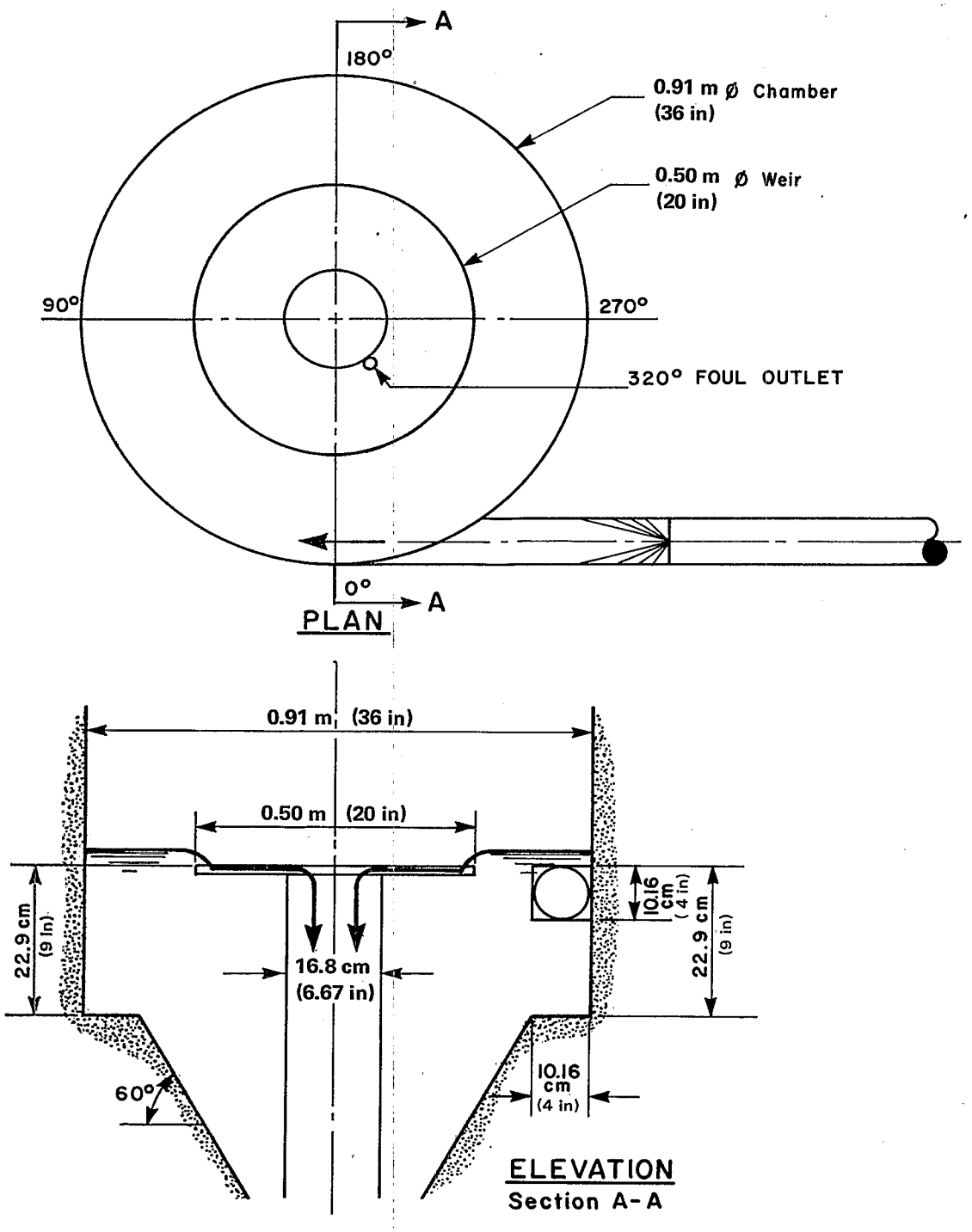

FIGURE 33 SWIRL PRIMARY SEPARATOR
MODEL LAYOUTS FOR TESTS 27, 28, 34, AND 40
MODIFICATION 3 AND 4

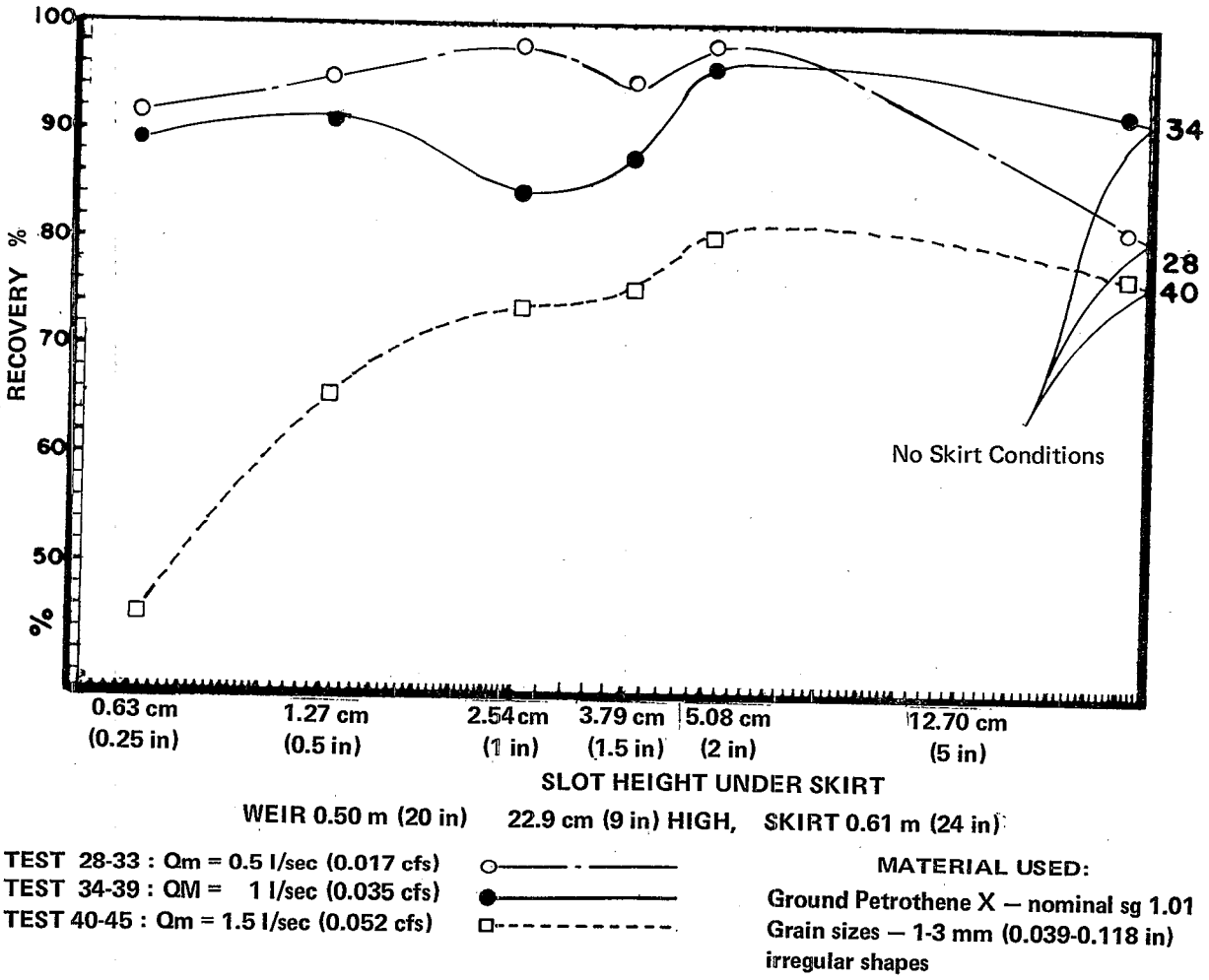

FIGURE 34 SWIRL PRIMARY SEPARATOR OPERATING EFFICIENCIES FOR MODIFICATION 3 AND 4

completely removed, leaving just the central pipe opening, 16.8 cm (6.63 in) in diameter, as shown in Figure 35. Furthermore, in order to pinpoint the recovery fall-off point, a 12.7 cm (5 in) slot height was added to the five already used.

Results obtained with the 16.8 cm (6.63 in) diameter weir showed a fairly constant 98 percent recovery rate for the 0.5 l/sec (0.15 gal/sec) flow. Greater discharges provided less successful recoveries. The recovery rate decreased as the slot height increased, achieving very low values for higher openings, as shown in Figure 36.

Observations showed that this reduced recovery was caused by a rising helical flow generated inside the conical chamber around the central overflow pipe. As the flow increased, the current stirred up sludge sediment which had already deposited on the bottom after sliding down the conical hopper wall. The bottom deposit was caught by the ascending current and carried up to the weir lip and discharged with the overflow.

An intermediate solution was then tested, using a 38.1 cm (15 in) diameter weir disc as portrayed in Figure 37. No helical flow pattern was observed. As shown in Figure 38, no

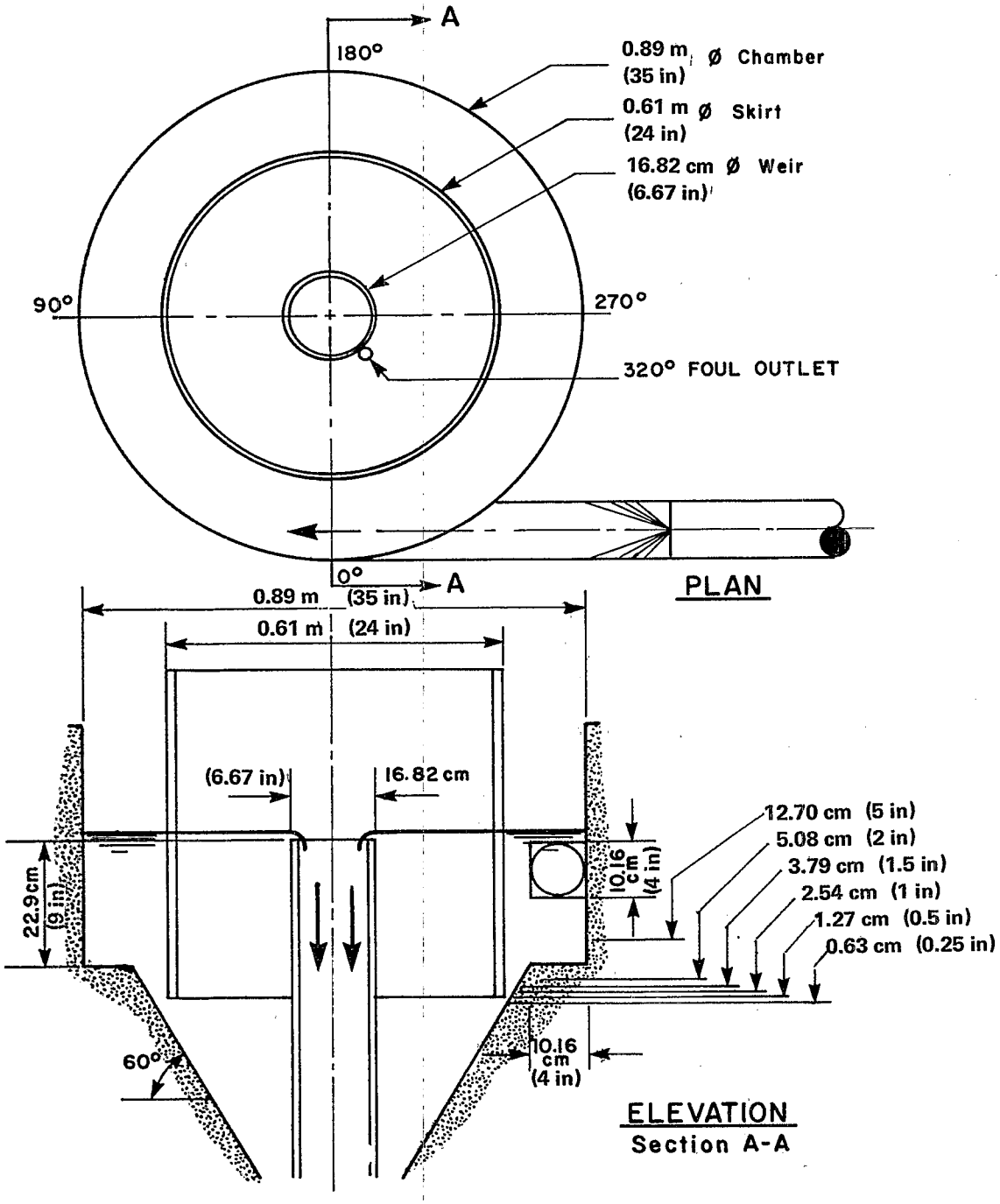

FIGURE 35 SWIRL PRIMARY SEPARATOR
MODEL LAYOUT FOR TESTS 46 TO 68
MODIFICATION 5

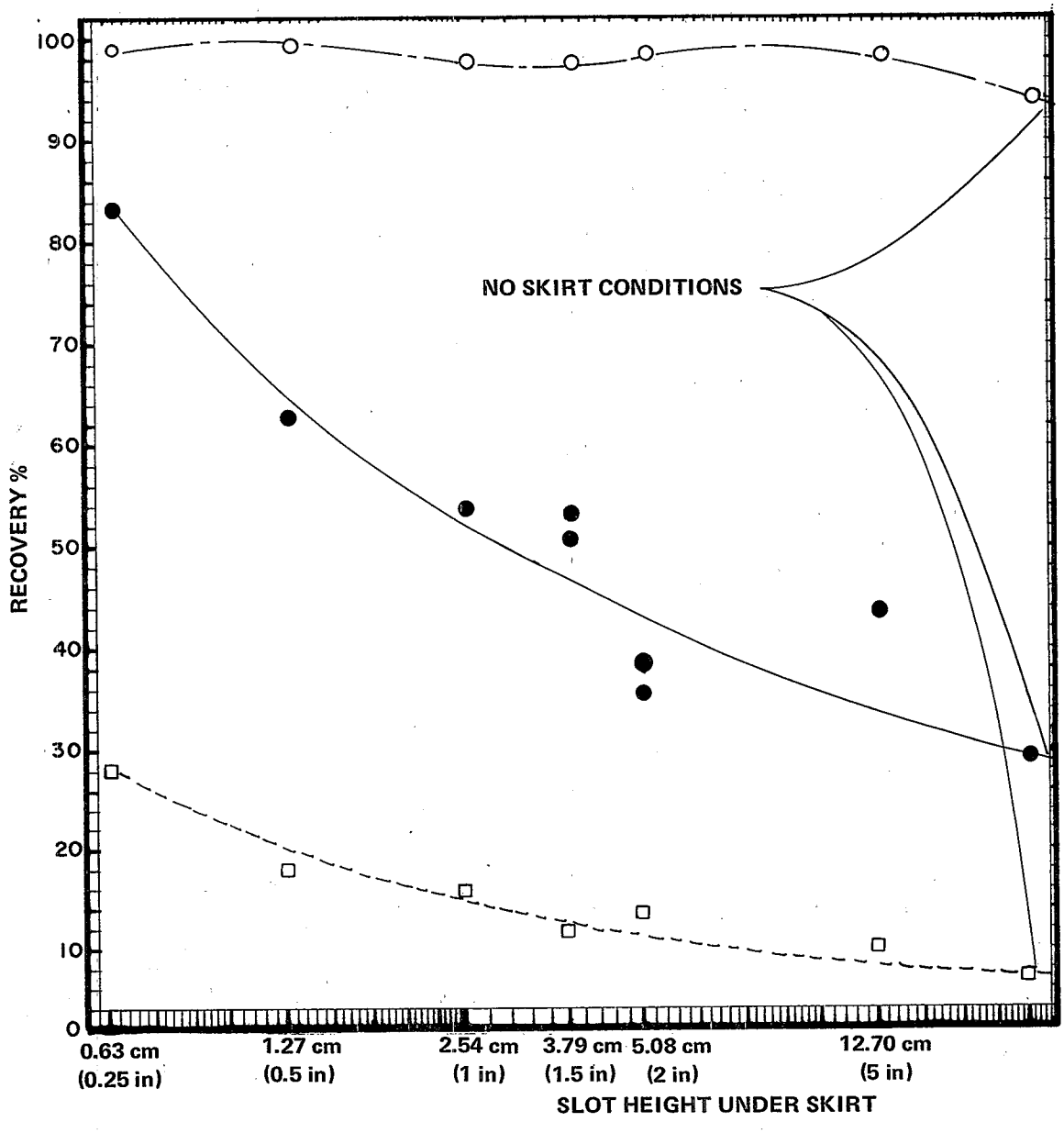

FIGURE 36 SWIRL PRIMARY SEPARATOR
OPERATING EFFICIENCIES FOR MODIFICATION 5

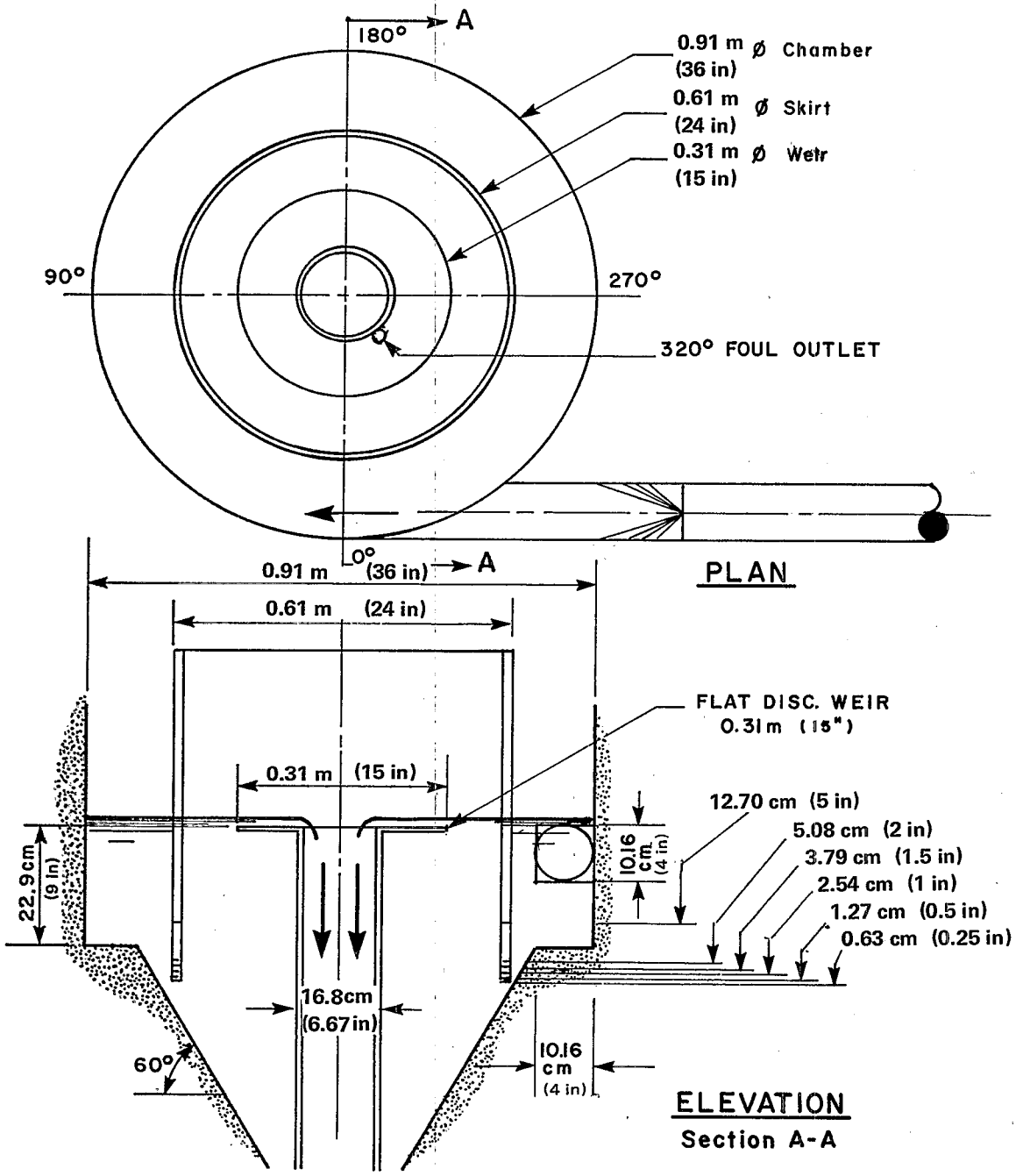

FIGURE 37 SWIRL PRIMARY SEPARATOR
MODEL LAYOUT FOR TESTS 69 TO 91
MODIFICATION 6

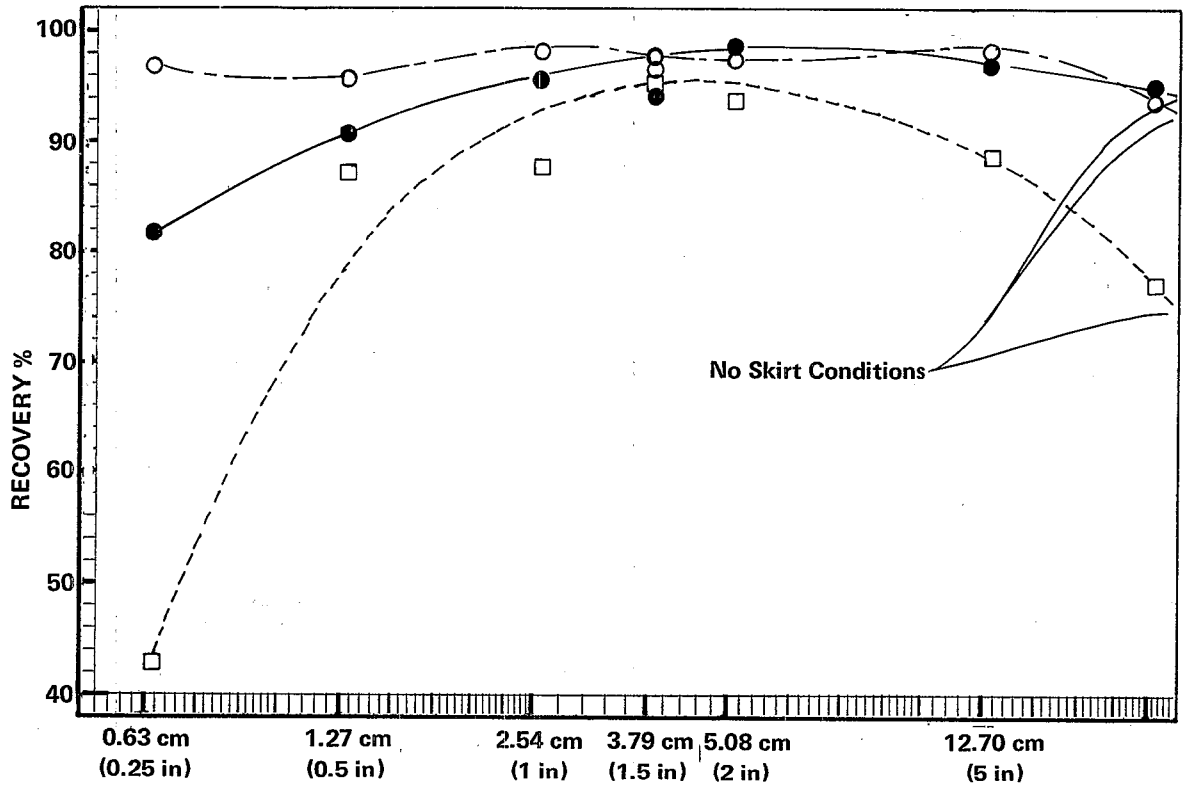

FLAT DISK WEIR 0.31 m (15 in) 22.9 cm (9 in) HIGH, SKIRT 0.61 m (24 in)

TESTS 69-76 : QM = 0.5 l/sec (0.017 cfs)
TESTS 77-84 : QM = 1.0 l/sec (0.035 cfs)
TESTS 85-91 : Qm = 1.5 l/sec (0.052 cfs)

MATERIAL USED: Ground Petrothene X — nominal sg 1.01
Grain sizes 1-3 mm (0.039-0.118 in)
irregular shapes

FIGURE 38 SWIRL PRIMARY SEPARATOR
OPERATING EFFICIENCIES FOR MODIFICATION 6

change in the recovery curve occurred for the small discharge of 0.5 l/sec (0.0187 cfs). However, the two other curves showed a very interesting phenomenon, with the slot between 3.7 and 5.4 cm (1.5 and 2 in). High recovery rates were not less than 94 percent for the three discharges, then dropped off with greater or smaller slots.

c) Recovery Rate Versus Height of Weir Above the Chamber Floor: In order to pinpoint the influence of weir height above the chamber floor, results were determined for the 38.1 cm (15 in) weir disc. At 23 cm (9 in) above the floor, as shown in Figure 38, the recovery curves diverged for the three discharges considered except in the slot range 3.7 to 5.4 cm (1.5 to 2 in) where recovery rates were not less than 94 percent.

Raising the weir lip to 33 cm (13 in) from the floor, as shown in Figure 39, resulted in flattening the recovery curves and brought them closer to the 0.5 l/sec (0.0187 cfs) flow efficiency which stayed constant at 98 percent, as shown in Figure 40. Hence, for slots of 5 to 12.7 cm (2 to 5 in) high, recovery rates were not less than 97 percent. Recovery dropped off for greater or smaller slots.

d) Flow Velocities Inside the Chamber: A series of measurements was carried out with the 38.1 cm (15 in.) weir disc, with configuration as shown in Figure 29. Flow velocity was taken inside the chamber by means of a midget current meter successively set up at positions shown on Figure 41. Measurements were made with a model flow discharge of 1 l/sec (0.035 cfs), a 2.5 cm (1 in) slot, and a 61 cm (24 in) skirt.

Results plotted are the horizontal tangential component of the flow velocity. Direction of flow is assumed going into the paper. Interpolation between measured positions yielded the velocity contours shown on Figures 42 through 45.

e) 38 cm (15 in) Weir Disk:

At 0° position, close to the sewer inlet outside the skirt, flow velocity ranged from 25.9 cm/sec (0.85 ft/sec) at the bottom, to 36.6 cm/sec (1.2 ft/sec) at the surface. As the flow progressed to the different positions, it showed a slight decrease of the surface velocity accompanied by a slight increase at the bottom.

Momentum inside the skirt progressively lessened from the slot inlet to the free surface. Under the weir itself, velocity contours were featured by flow patterns simulating rotating concentric cylinders whose velocity increased with the distance from the central downdraft pipe.

2. Tests Carried Out with Closed Bell and Four Orifices

In order to avoid concentration of flow in the area extending between the weir lip and skirt, a new weir was tested consisting of a closed bell with four orifices of 3.8 cm (1.5 in) diameter, as shown in Figure 46 for Tests 92 to112. Results obtained are presented in Figure 47. They showed a fairly constant recovery rate for the three discharges considered over the 5 cm to 33 cm (2 to 13 in) slot height range. Recovery efficiency for the largest discharge of 1.5 l/sec (0.053 cfs) proved to be only two percent below the intermediate and low flow performances.

a) Flow Velocity Inside the Closed Bell Chamber with Four Orifices 3.8 cm (1.5 in): Flow velocities were taken inside the chamber at positions shown in Figure 48. Flow contour patterns are shown in Figures 49 to 52. The same phenomenon as described above occurred in the chamber outside the skirt although it was less pronounced. Within the skirt, high velocities concentrated under the orifices with a marked tendency to increase the rotating effect 24.4 cm/sec (0.8 ft/sec) at 180 degrees. The same concentric layers with increasing velocity outward from the central downdraft pipe existed, with maximum velocities present under the orifices.

Since the closed bell with orifices improved the recovery rate, and flattened the curves at the highest values, it was expected that better results could be achieved if the orifices were placed so as to produce a better radial flow distribution. That was to be the next step in the study approach, but a radial weir gutter was suggested during discussions in a team meeting as more likely to provide better upward flow distribution inside the skirt. If successful, the new device would avoid both an undesirable concentration of flow on the one hand, and helical ascending currents on the other. It would, however,

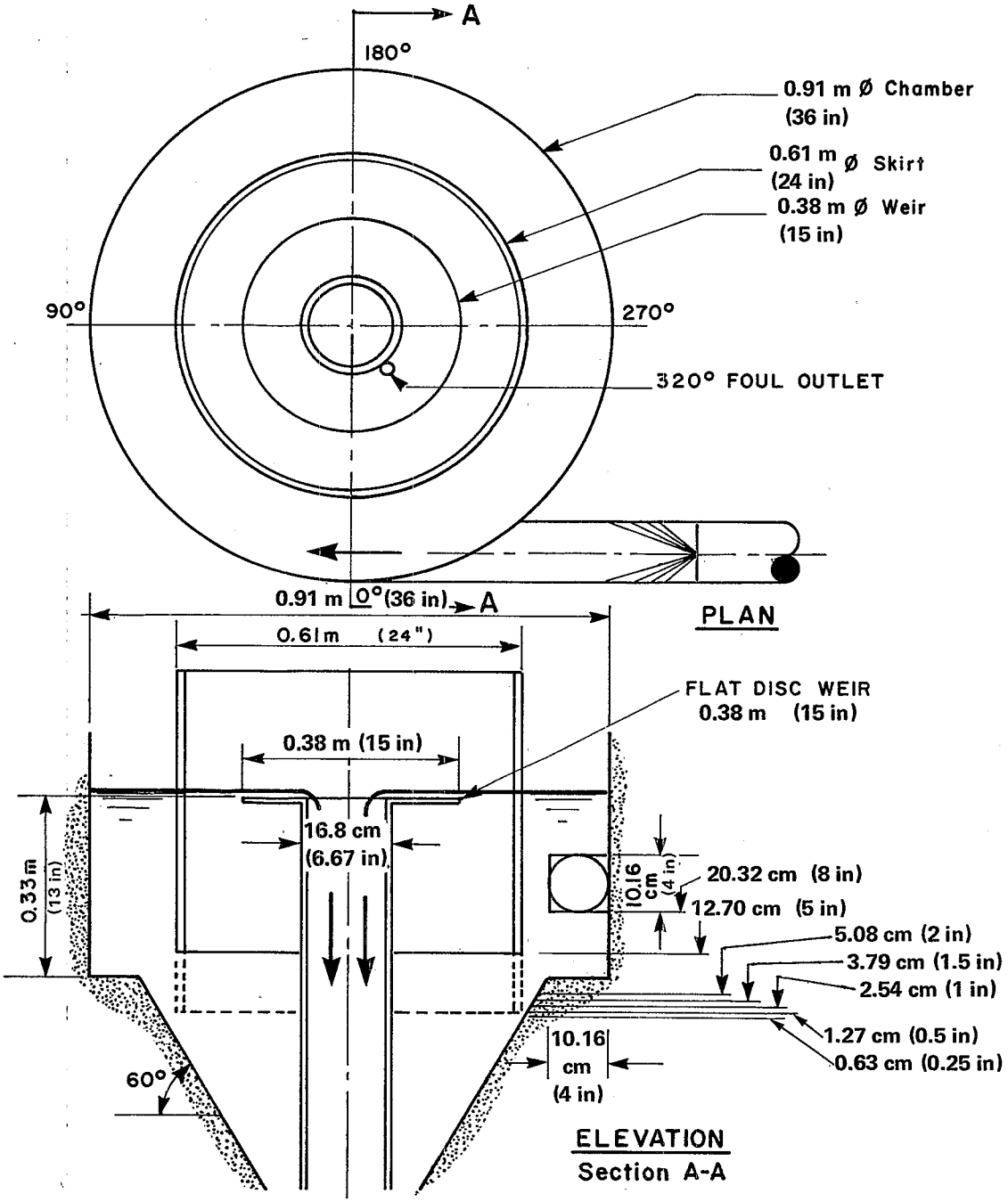

FIGURE 39 SWIRL PRIMARY SEPARATOR
MODEL LAYOUT FOR TESTS 113 TO 136
MODIFICATION 8

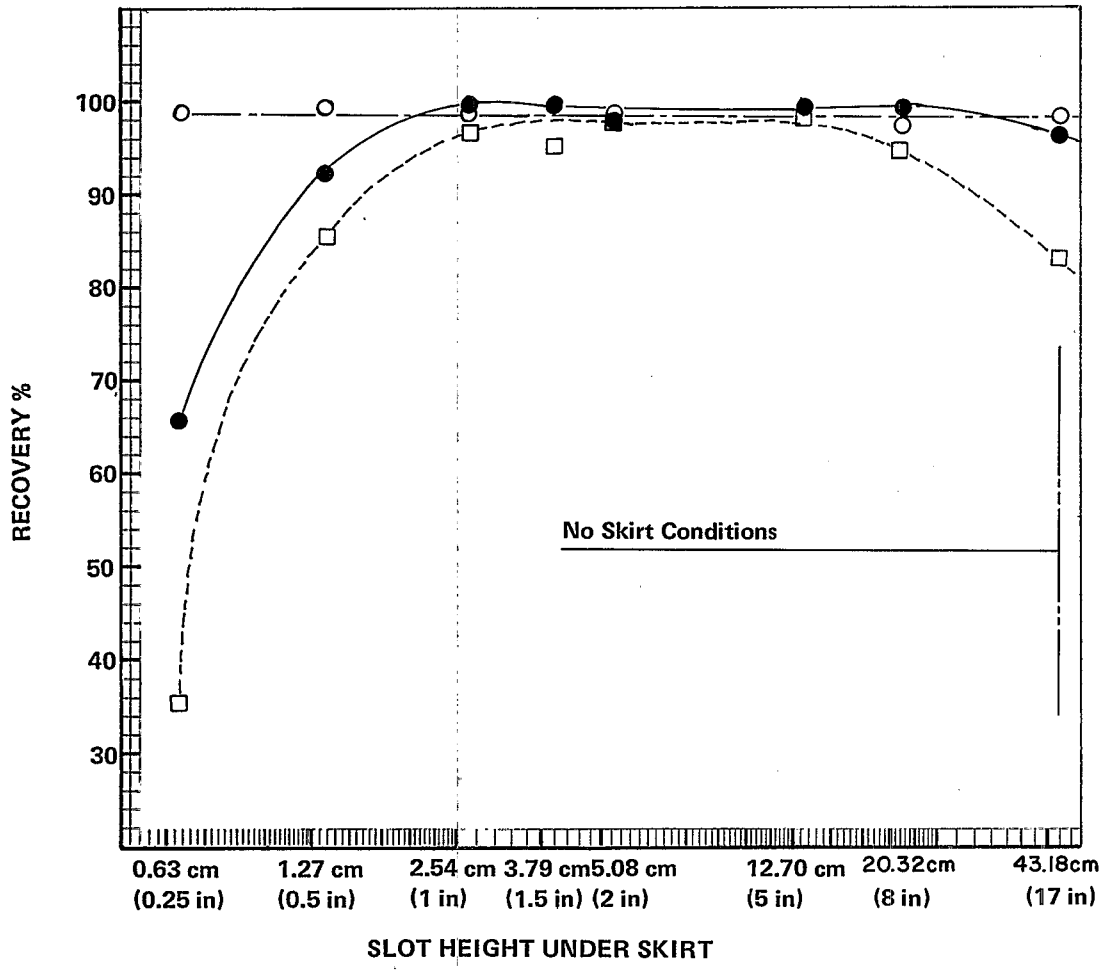

FLAT DISC WEIR 0.38 m (15 in) 0.33 m (13 in) HIGH, SKIRT 0.61 m (24 in)

TESTS 113-119, 135 : QM = 0.5 l/sec (0.017 cfs) ○ ——— · ———
TESTS 120-126, 136 : QM = 1.0 l/sec (0.035 cfs) ● ———————
TESTS 127-134 : Qm = 1.5 l/sec (0.052 cfs) □ - - - - - - - - - - - -

MATERIAL USED: Ground Petrothene X — nominal sg 1.01
Grain sizes — 1-3 mm (0.039-0.118 in)
irregular shapes

FIGURE 40 SWIRL PRIMARY SEPARATOR
OPERATING EFFICIENCIES FOR MODIFICATION 8

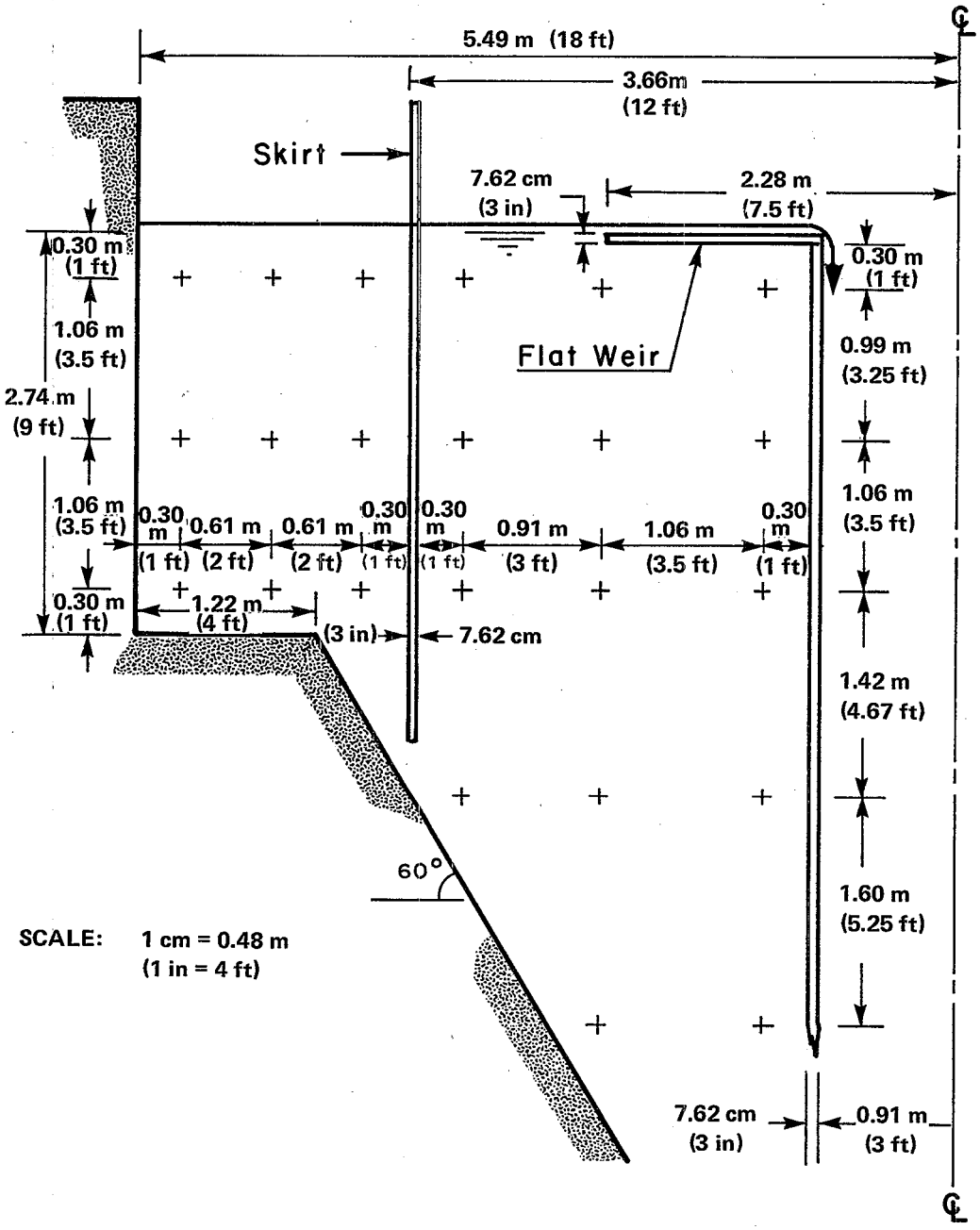

FIGURE 41 SWIRL PRIMARY SEPARATOR LOCATION OF LOCATION OF MEASURING POINTS FOR VELOCITY CONTOUR TESTS 10.98 m (36 ft) CHAMBER PROTOTYPE SCALE 1/12 MODIFICATION 6

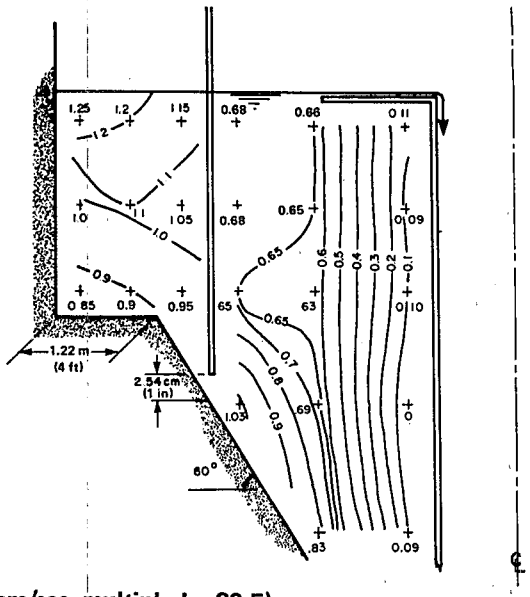

NOTE: Velocities in ft/sec (to get cm/sec, multiply by 30.5)

FIGURE 42 SWIRL PRIMARY SEPARATOR
TANGENTIAL VELOCITY CONTOURS AT 0° POSITION
10.98 m (36 ft) CHAMBER
DISCHARGE = 0.49 m^3/sec (17.6 cfs)
PROTOTYPE SCALE 1/12
MODIFICATION 6

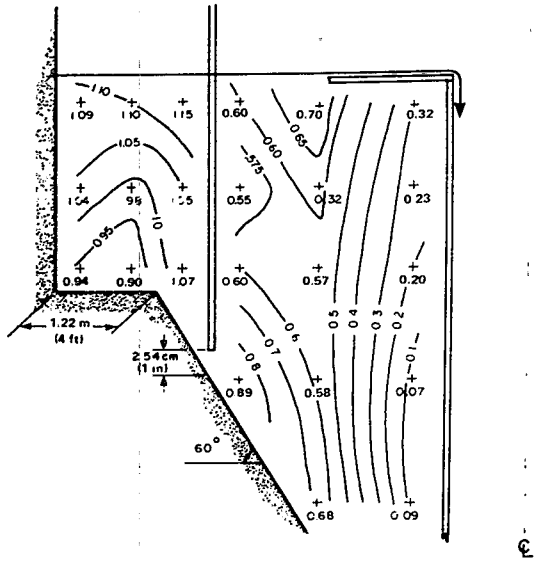

NOTE: Velocities in ft/sec (to get cm/sec, multiply by 30.5)

FIGURE 43 SWIRL PRIMARY SEPARATOR
TANGENTIAL VELOCITY CONTOURS AT 90° POSITION
10.98 m (36 ft) CHAMBER
DISCHARGE = 0.49 m^3/sec (17.6 cfs)
PROTOTYPE SCALE 1/12
MODIFICATION 6

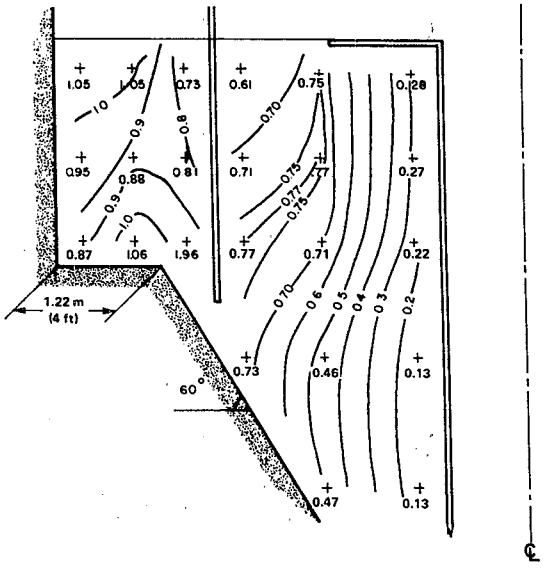

NOTE: Velocities in ft/sec (to get cm/sec, multiply by 30.5)

FIGURE 44 SWIRL PRIMARY SEPARATOR
TANGENTIAL VELOCITY CONTOURS AT 180° POSITION
10.98 m (36 ft) CHAMBER
DISCHARGE - 0.49 m^3/sec (17.6 cfs)
PROTOTYPE SCALE 1/12
MODIFICATION 6

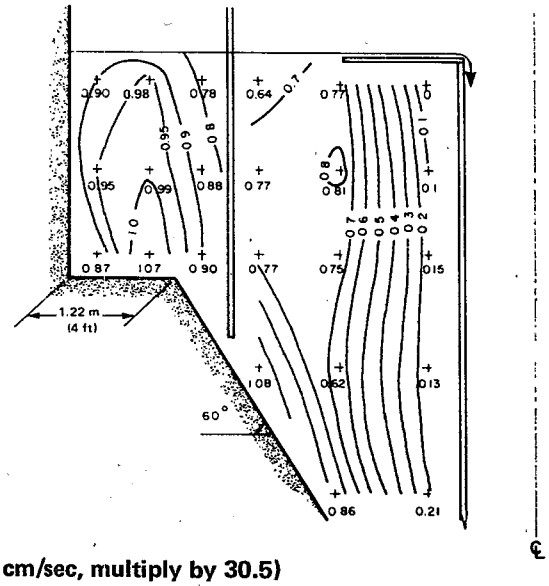

NOTE: Velocities in ft/sec (to get cm/sec, multiply by 30.5)

FIGURE 45 SWIRL PRIMARY SEPARATOR
TANGENTIAL VELOCITY CONTOURS AT 270° POSITION
10.98 m (36 ft) CHAMBER
DISCHARGE = 0.49 m^3/sec (17.6 cfs)
PROTOTYPE SCALE 1/12
MODIFICATION 6

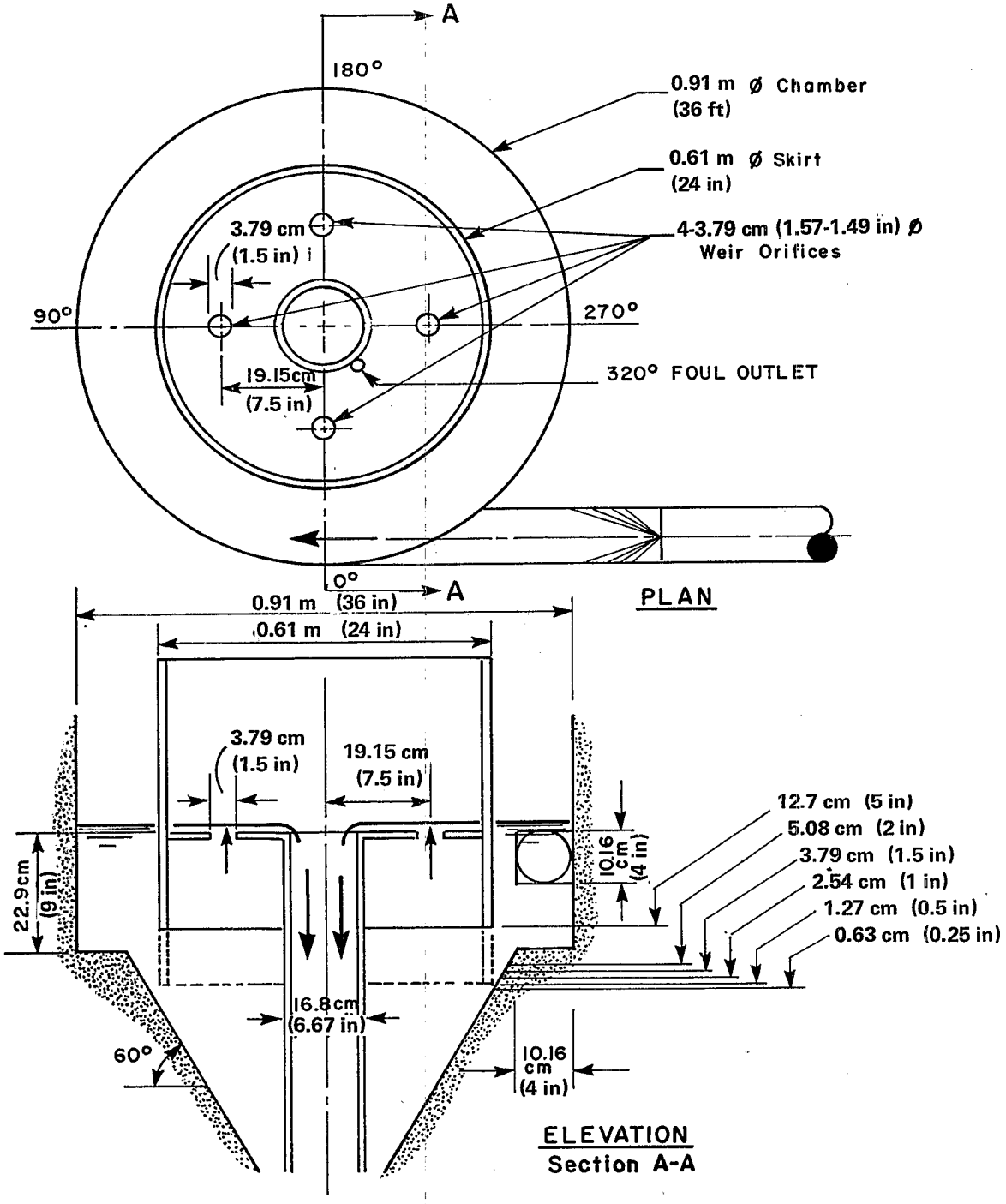

FIGURE 46 SWIRL PRIMARY SEPARATOR
MODEL LAYOUT FOR TESTS 92 TO 112
MODIFICATION 7

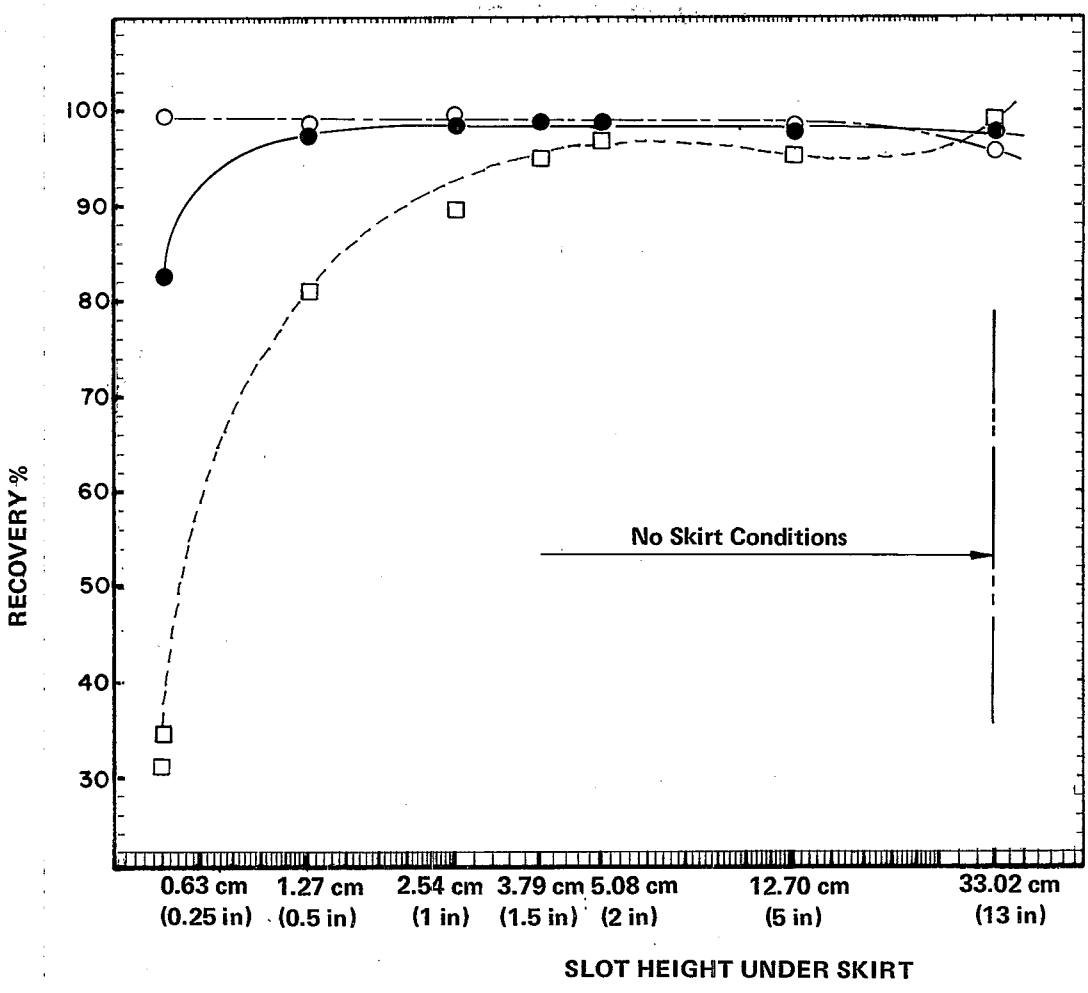

TESTS 92-98 : Qm = 0.15 l/sec (0.005 cfs) ○——·——
TESTS 99-105 : Qm = 1.0 l/sec (0.035 cfs) ●————
TESTS 106-112 : Qm = 1.5 l/sec (0.052 cfs) □----------

FIGURE 47 SWIRL PRIMARY SEPARATOR
OPERATING EFFICIENCIES OF CLOSED BELL
WITH FOUR ORIFICES – 3.79 cm (1.5 in) ∅,
22.9 cm (9 in) HIGH, SKIRT 0.61 m (24 in) ∅
FOR MODIFICATION 7

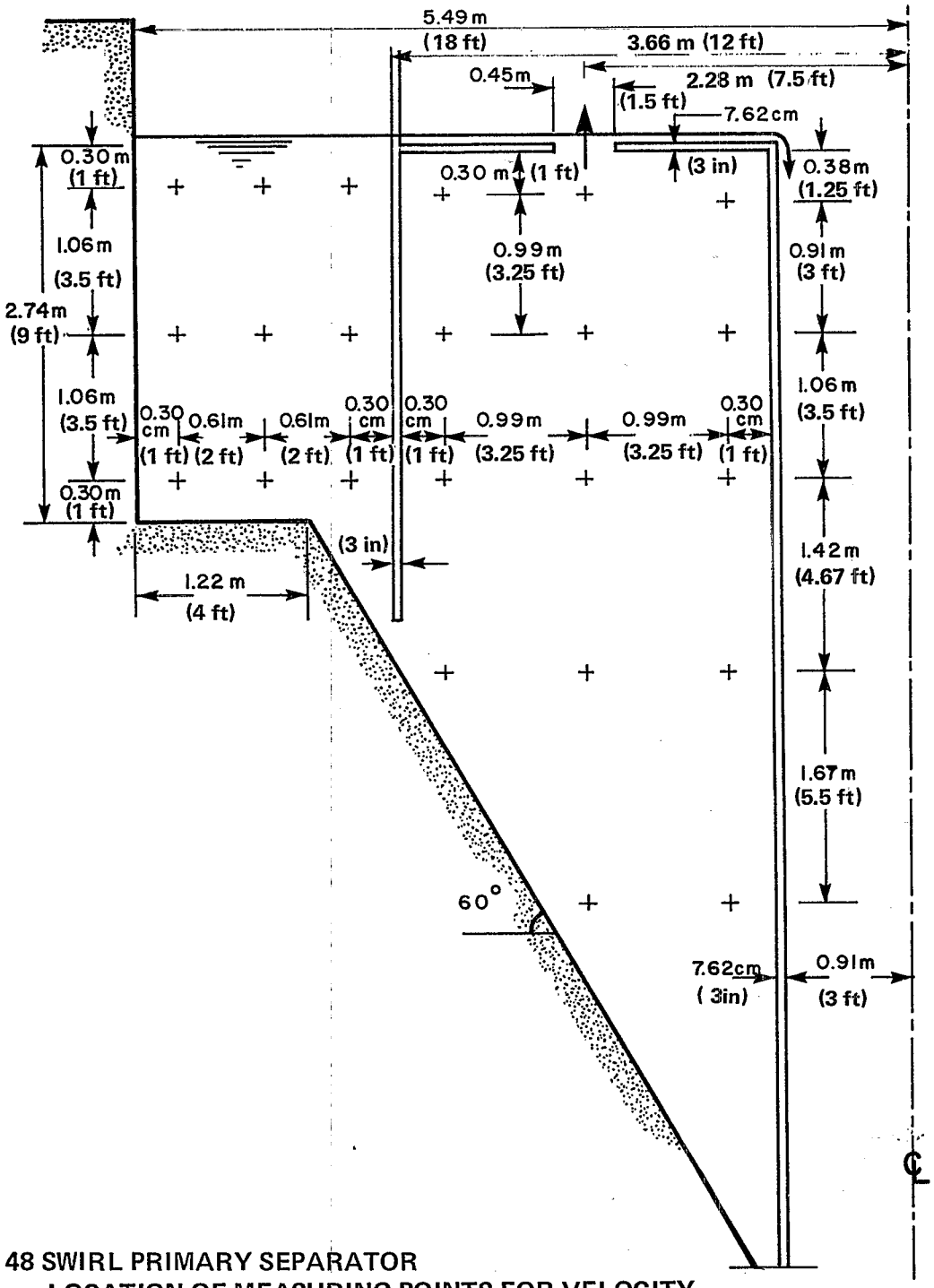

FIGURE 48 SWIRL PRIMARY SEPARATOR
LOCATION OF MEASURING POINTS FOR VELOCITY
CONTOUR TESTS 10.98 m (36 ft) CHAMBER
CLOSED BELL WITH FOUR ORIFICES – 0.457 m (1.5 ft) Ø,
2.74 m (9 ft) HIGH, SKIRT 7.32 m (24 ft) Ø
PROTOTYPE SCALE 1/12
MODIFICATION 7

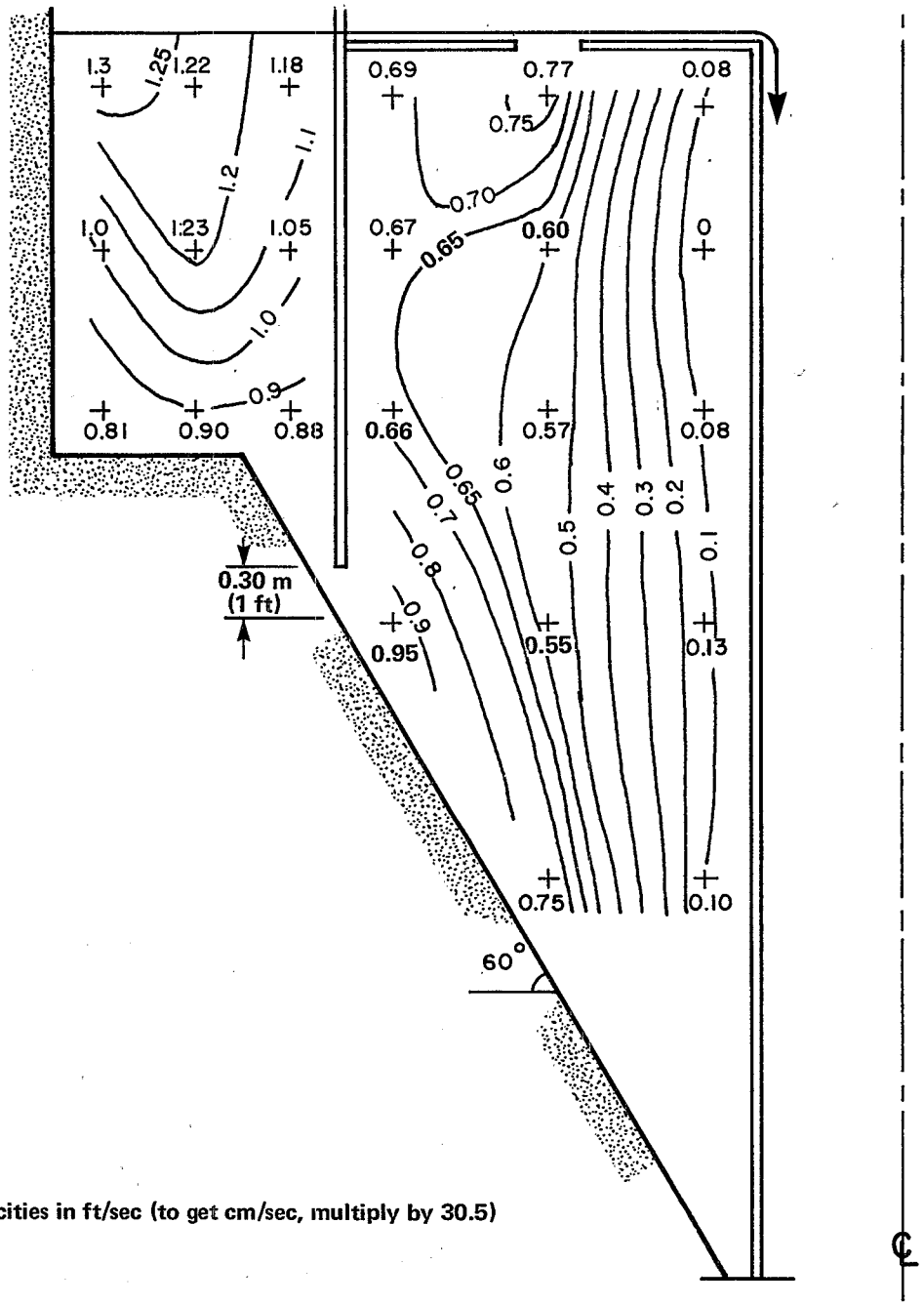

NOTE: Velocities in ft/sec (to get cm/sec, multiply by 30.5)

FIGURE 49 SWIRL PRIMARY SEPARATOR
TANGENTIAL VELOCITY CONTOURS AT 0° POSITION
10.98 m (36 ft) CHAMBER
DISCHARGE = 0.49 m^3/sec (17.6 cfs)
PROTOTYPE SCALE 1/12
MODIFICATION 7

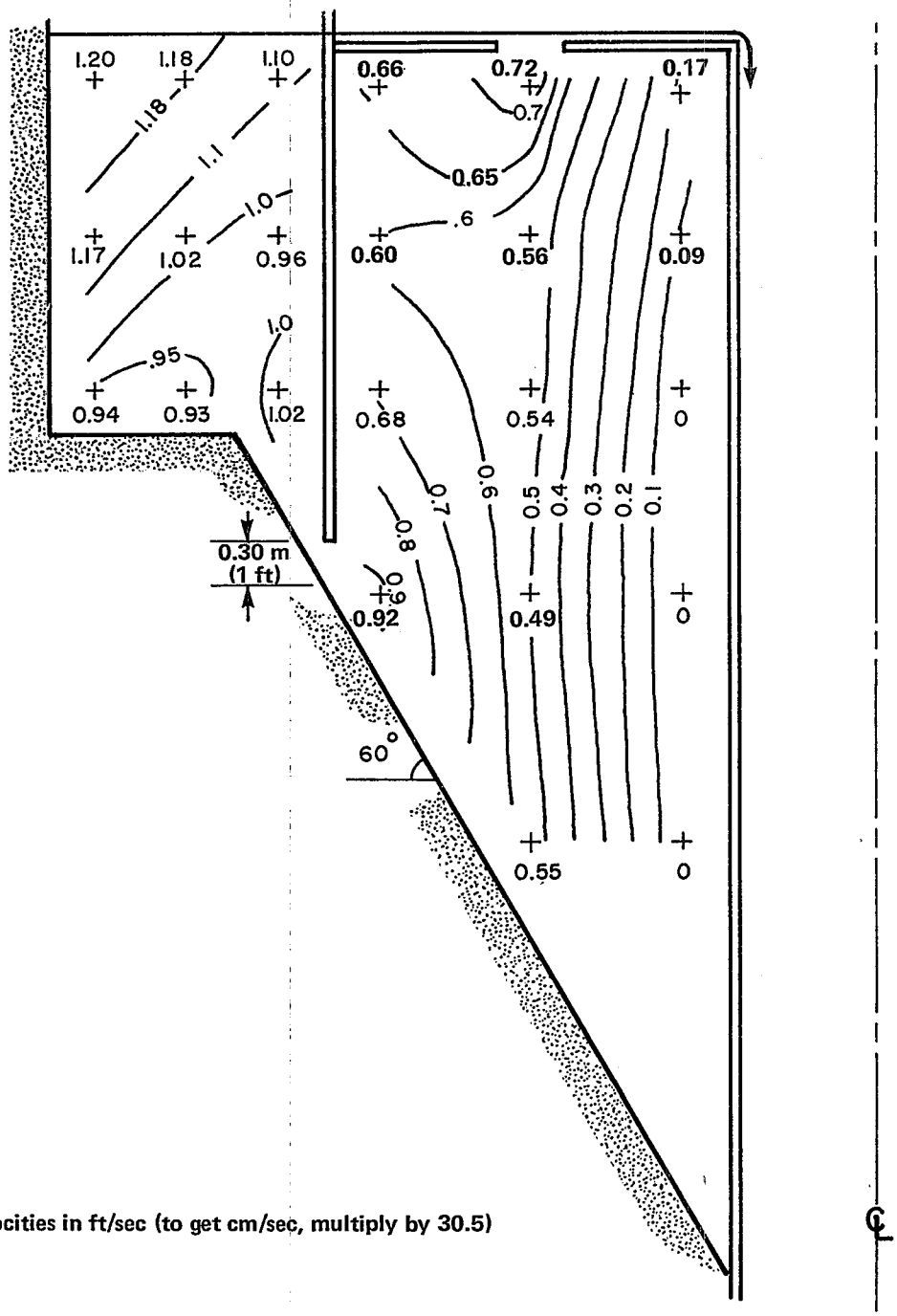

NOTE: Velocities in ft/sec (to get cm/sec, multiply by 30.5)

FIGURE 50 SWIRL PRIMARY SEPARATOR
TANGENTIAL VELOCITY CONTOURS AT 90° POSITION
10.98 m (36 ft) CHAMBER
DISCHARGE = 0.49 m^3/sec (17.6 cfs)
PROTOTYPE SCALE 1/12
MODIFICATION 7

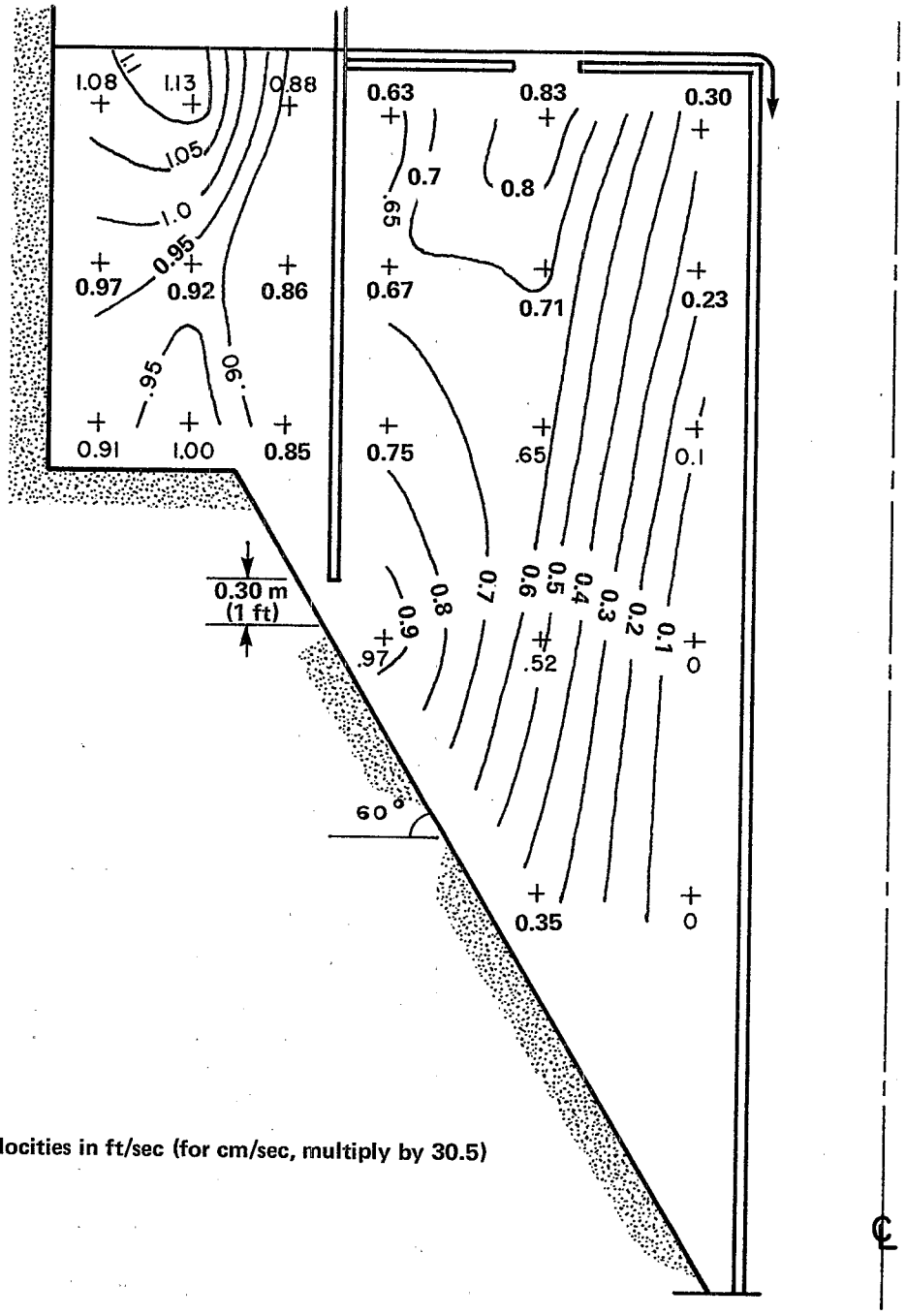

NOTE: Velocities in ft/sec (for cm/sec, multiply by 30.5)

FIGURE 51 SWIRL PRIMARY SEPARATOR
TANGENTIAL VELOCITY CONTOURS AT 180° POSITION
10.98 m (36 ft) CHAMBER
DISCHARGE = 0.49 m^3/sec (17.6 cfs)
PROTOTYPE SCALE 1/12
MODIFICATION 7

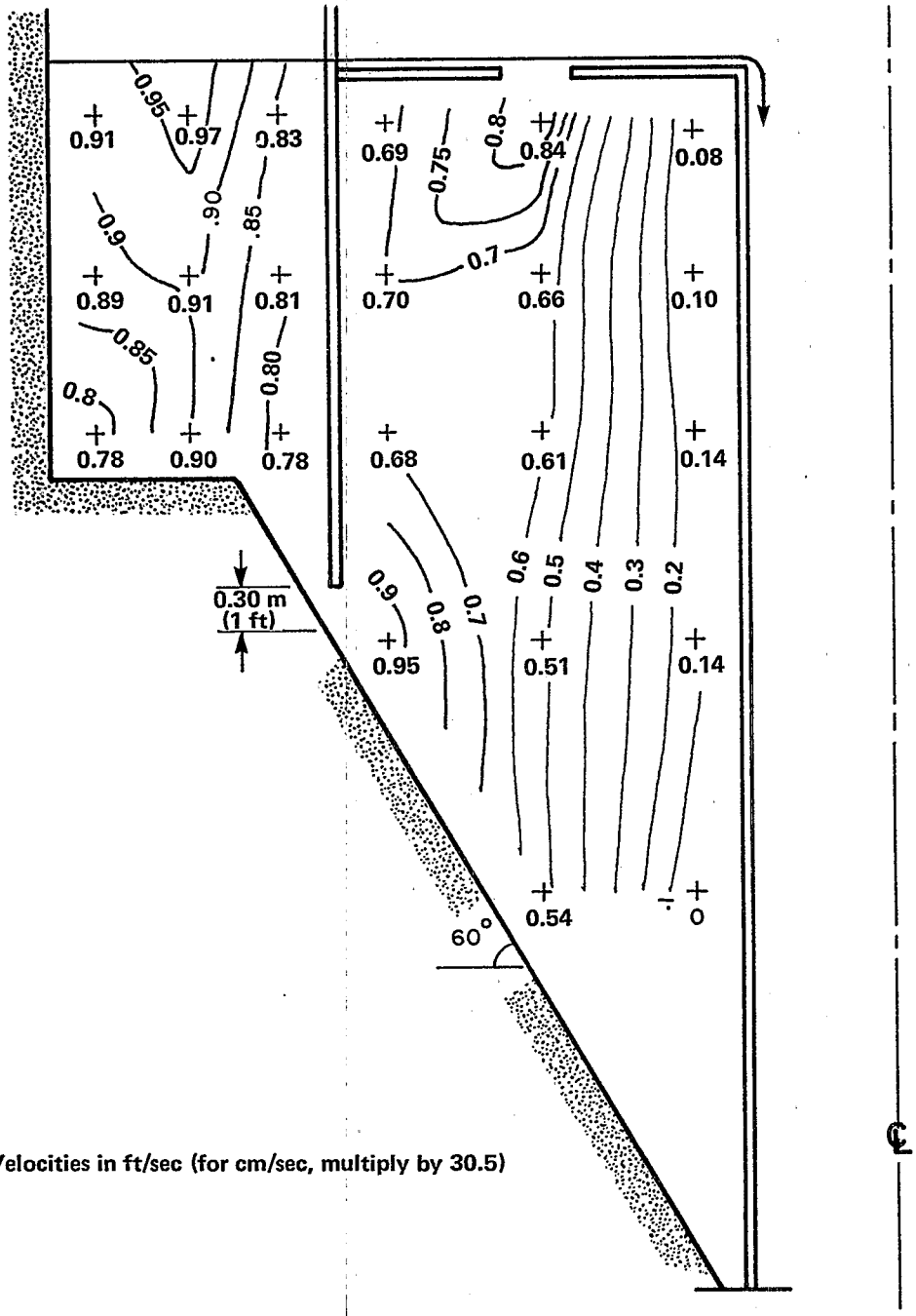

NOTE: Velocities in ft/sec (for cm/sec, multiply by 30.5)

FIGURE 52 SWIRL PRIMARY SEPARATOR
TANGENTIAL VELOCITY CONTOURS AT 270° POSITION
10.98 m (36 ft) CHAMBER
DISCHARGE = 0.49 m^3/sec (17.6 cfs)
PROTOTYPE SCALE 1/12
MODIFICATION 7

introduce obstacles into the free motion flow at least at the surface.

Tests Carried Out with Radial Weir Gutters

a) Flat Chamber Floor 10 cm (4 in) Wide with Four Weir Gutters: Gutters were 7 cm wide by 5 cm high (2.75 in by 2 in), inside dimension. They extended radially 29.2 cm (11.5 in) from the center line of the chamber. The gutter crests were set horizontally 23 cm (9 in) above the chamber floor, as depicted in Figure 53.

b) Recovery Rate Vs Slot Height: Figure 54 presents the results of the study of recovery rates vs slot height. Results were disappointing, considering previous recovery rates obtained with the closed bell and 4 orifices 3.8 cm (1.5 in) diameter. The curves converged at the 5 cm (2 in) slot where the recovery rate was 98 percent for the 0.5 and 1.0 l/sec (0.0187 and 0.0375 cfs) discharges, and 95 percent for the 1.5-l/sec (0.0562 cfs) discharge. The efficiency dropped off for greater or smaller slots.

c) Conical Bottom Extended up to Chamber Wall: The 10 cm (4 in) flat chamber floor utilized in the studies up to test 160 delayed the fall of particles into the conical bottom zone as they entered the chamber. The model showed that Petrothene grains described an angular trajectory of about 90 degrees, after leaving the inlet duct before crossing the edge of the flat floor. This phenomenon produced a substantial concentration of grains in the 90 degree to 270 degree area, which hampered the free falling motion of grains. This was particularly true for small slot heights.

In addition to this, some deposits formed on the flat chamber floor, about 45 degrees from the inlet when small discharges 0.5 l/sec (0.0187 cfs) were tested. To avoid these difficulties the flat portion of the chamber floor was eliminated and the conical section was extended up to meet the full chamber diameter. The inlet bottom was then set 2.2 cm (0.875 in) above the cone top, as shown in Figure 55.

To remain consistent with the previous test approach, the crests of the four gutter weirs were set at the same elevation as the inlet top, as shown in Figure 53.

d) Increase of the Skirt Diameter: By taking advantage of the new chamber floor, a larger skirt could be built in order to increase the size of the internal chamber. Subsequent tests were performed with a 71 cm (28 in) diameter skirt, thus reducing the width of the external channel to 10 cm (4 in).

The slot height was measured as usual with respect to the level of cone corresponding to 71 cm (28 in) diameter, as shown in Figure 56.

e) Recovery Rate Vs Slot Height: These new conditions gave fairly good results, since flattening of the recovery curves was greatly improved. As shown in Figure 57, the efficiency corresponding to small (0.5 l/sec [0.0187 cfs]) and intermediate (1 l/sec [0.0375 cfs]) discharges reached to the 99 percent level for the whole range of slot heights, including no-skirt conditions. The recovery rate for high discharge (1.5 l/sec [0.0562 cfs]) dropped for slot heights under 2.5 cm (1 in), then remained constant at the 98 percent level up to the 20.3 cm (8 in) slot height. Removing the skirt caused a drop of two percent, bringing the efficiency rate down to 96 percent. Figure 58 shows the conditions involved.

FINE GRAIN RECOVERY TEST PROCEDURE

Anion Exchange Resin IRA-93 with grain size $149\mu \geq d \geq 74\mu$ (passing No. 100 sieve and retained on No. 200) was used to represent settleable solids. An improved measuring procedure was developed with the assistance of Beak Consultants, Ltd., for the subsequent tests.

The principle involved in this phase of the model study was to treat the same amount of water (1,800 l [478 gal]) with a constant influent concentration of 38 ppm, at different discharges and to analyze samples of the overflow liquor.

Selected discharges were, respectively, 0.1, 0.3, 0.5, 0.75 and 1 l/sec (0.0035, 0.010, 0.018, 0.026, and 0.035 cfs). Constant solids concentration was obtained by injecting 3 cc of material at equally spaced intervals of time depending upon the discharges. 100-cc samples of overflow and pump inlet were regularly taken so as to provide two composite samples. Sampling operations began after four retention times had elapsed, as depicted in Figure 59, and made at the

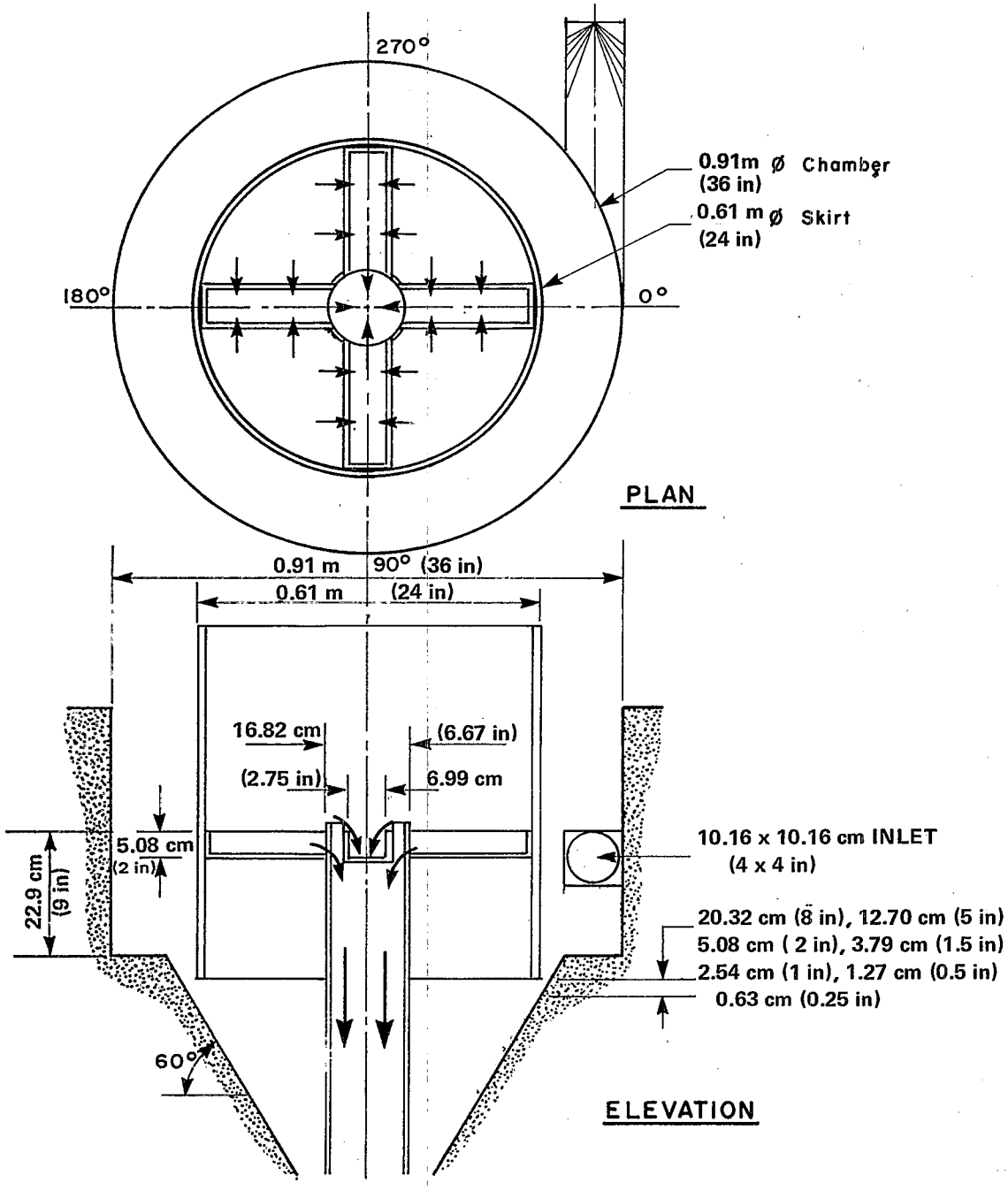

FIGURE 53 SWIRL PRIMARY SEPARATOR
MODEL LAYOUT FOR TESTS 137 TO 160
MODIFICATION 9

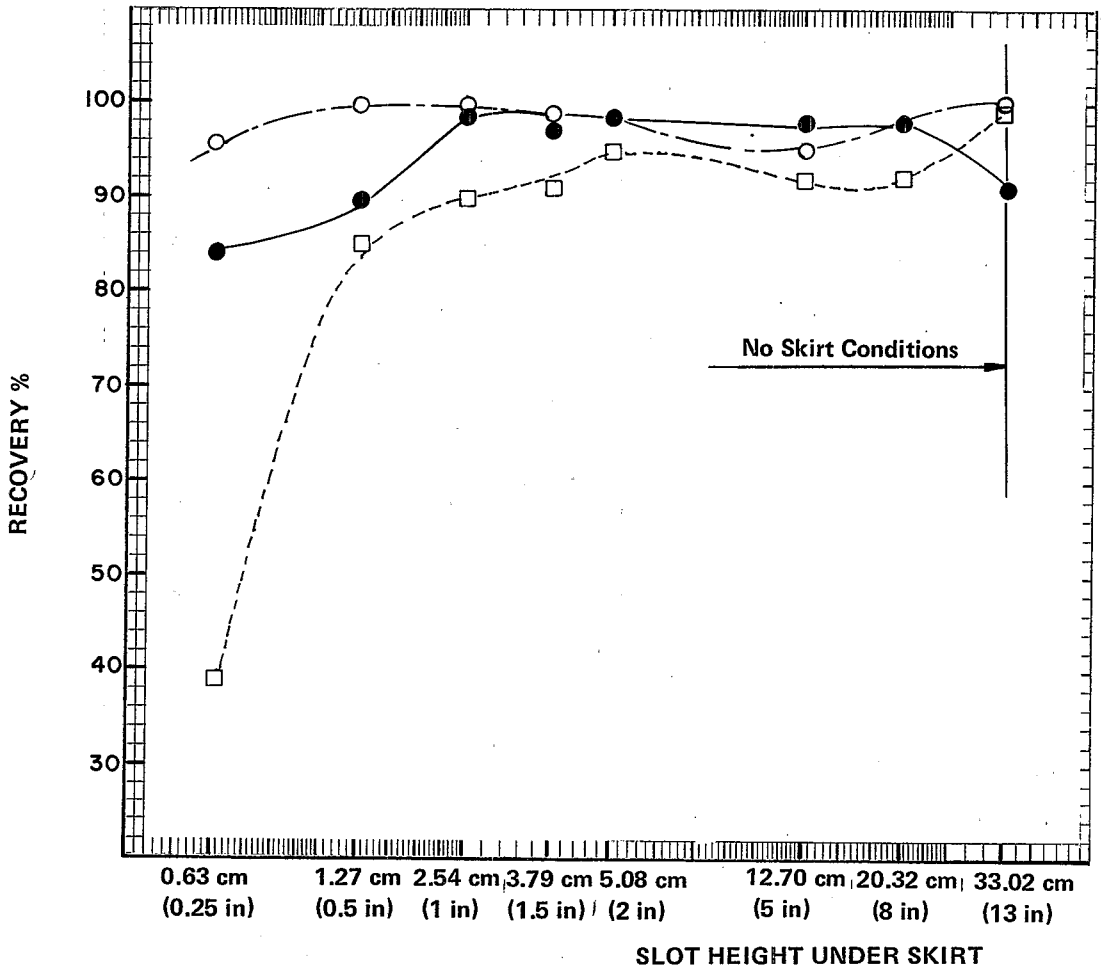

4 RADIAL GUTTER WEIRS 7.62 cm (3 in) x 5.08 cm (2 in) – 22.9 cm (9 in) HIGH
SKIRT 0.61 cm (24 in)

TESTS 137-144 : Qm = 0.5 l/sec (0.017 cfs) ○ ——— - ———
TESTS 145-152 : Qm = 1.0 l/sec (0.035 cfs) ● ———————
TESTS 153-160 : Qm = 1.5 l/sec (0.052 cfs) □ - - - - - - - - - -

MATERIAL USED: Ground Petrothene X – nominal sg 1.01
Grain sizes – 1-3 mm irregular shapes

FIGURE 54 SWIRL PRIMARY SEPARATOR
OPERATING EFFICIENCIES FOR MODIFICATION 9

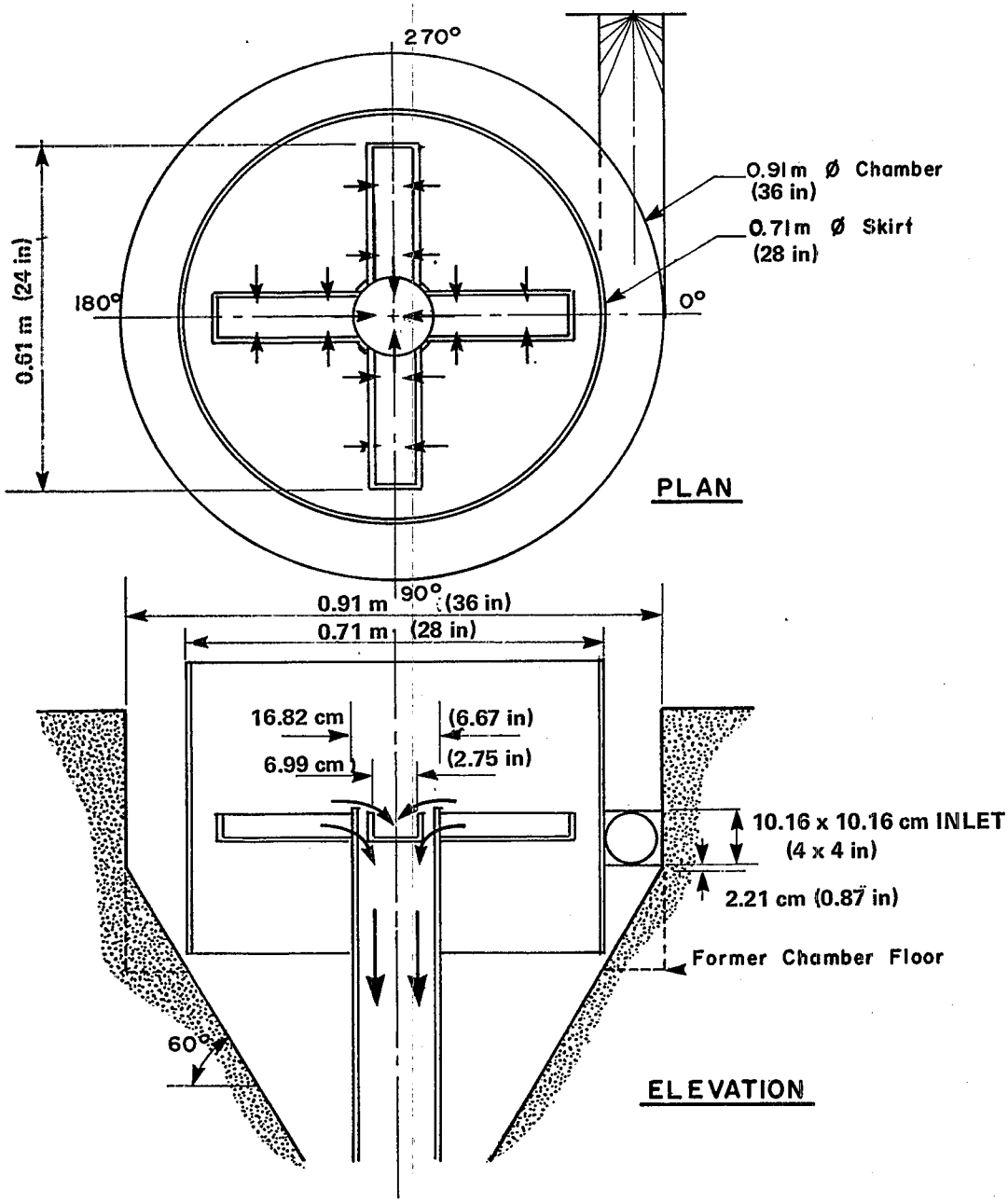

FIGURE 55 SWIRL PRIMARY SEPARATOR
MODEL LAYOUT FOR TESTS 161 TO 184
MODIFICATION 10

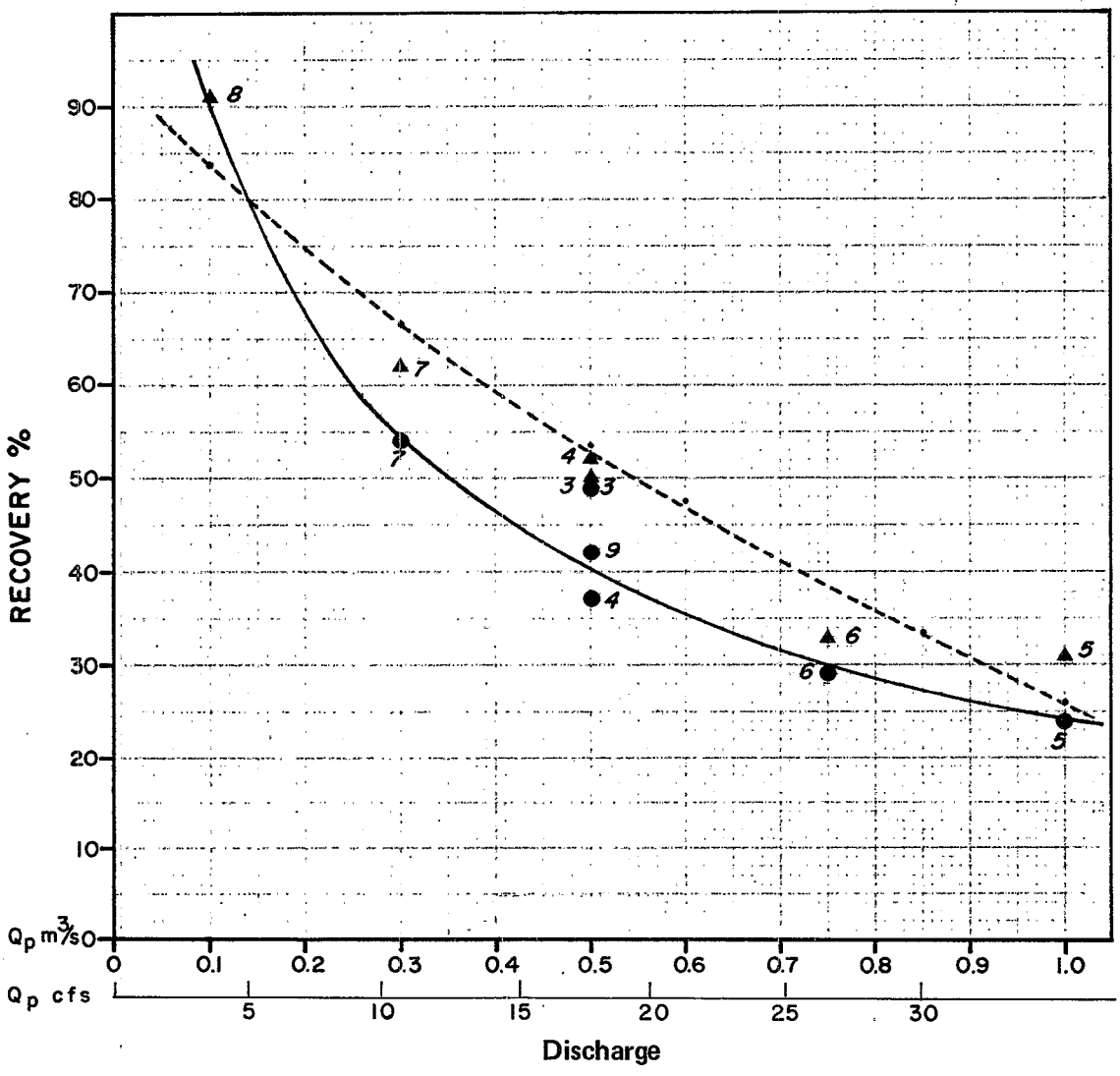

FOR MODEL CONDITIONS SEE FIGURE 37
SLOT HEIGHT 5.08 cm (2 in)
Material Used : Anion Exchange Resin IRA-93
Grain Size : $149\mu > d > 74\mu$

●——● Results obtained by volumetric measurements of recovered material

▲----▲ Results obtained by sample analysis done by Beak

FIGURE 56 SWIRL PRIMARY SEPARATOR
OPERATING EFFICIENCIES FOR MODIFICATION 10
Increase of Skirt Diameter

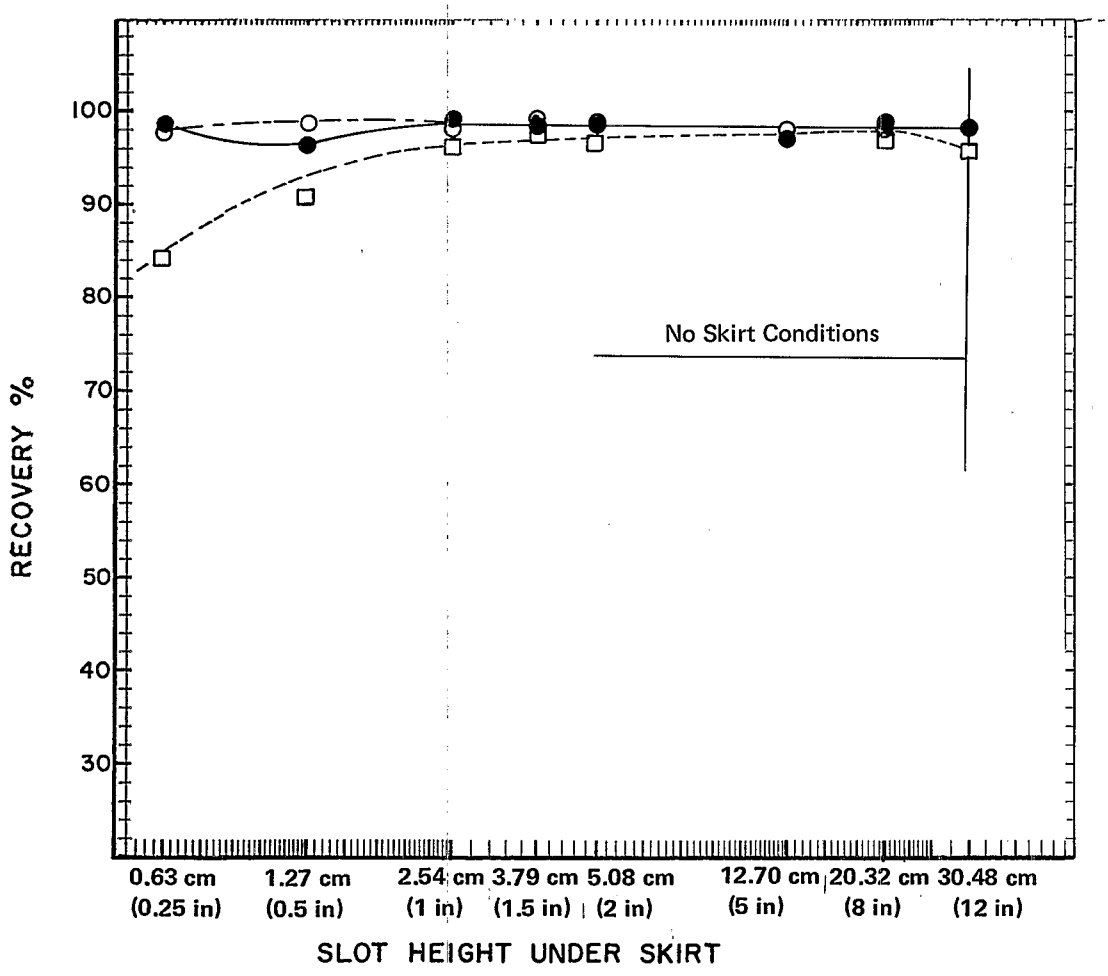

4 RADIAL GUTTER WEIRS 7.62 cm (3 in) x 5.08 cm (2 in) LIP AT TOP OF INLET — SKIRT 0.71 m (28 in) ∅ (SEE FIGURE)

TESTS 161-168 : Qm = 0.5 l/sec (0.017 cfs)
TESTS 169-176 : Qm = 1.0 l/sec (0.035 cfs)
TESTS 177-184 : Qm = 1.5 l/sec (0.052 cfs)

MATERIAL USED: Ground Petrothene X — nominal sg 1.01
Grain sizes — 1-3 mm (0.039-0.118 in)
irregular shapes

FIGURE 57 SWIRL PRIMARY SEPARATOR
OPERATING EFFICIENCIES FOR MODIFICATION 10
Recovery Rate versus Slot Height

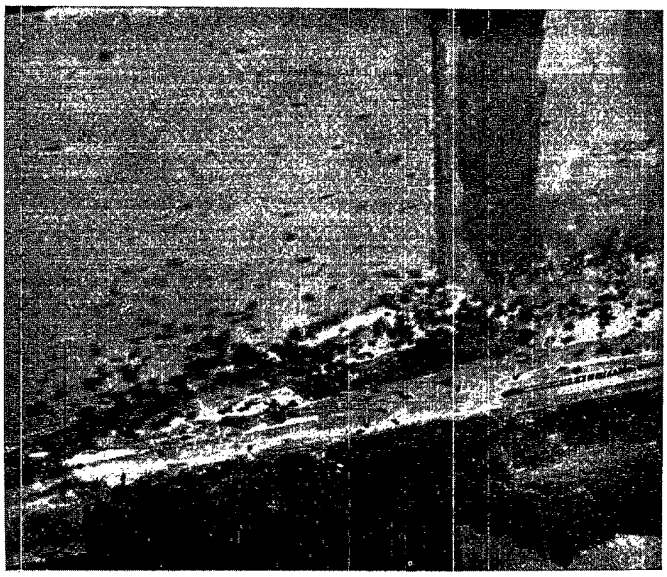

Petrothene grains reaching end of 10 x 10 cm (4 x 4 in) inlet Modification 10

Petrothene grains sliding down against the cone wall near inlet Modification 10

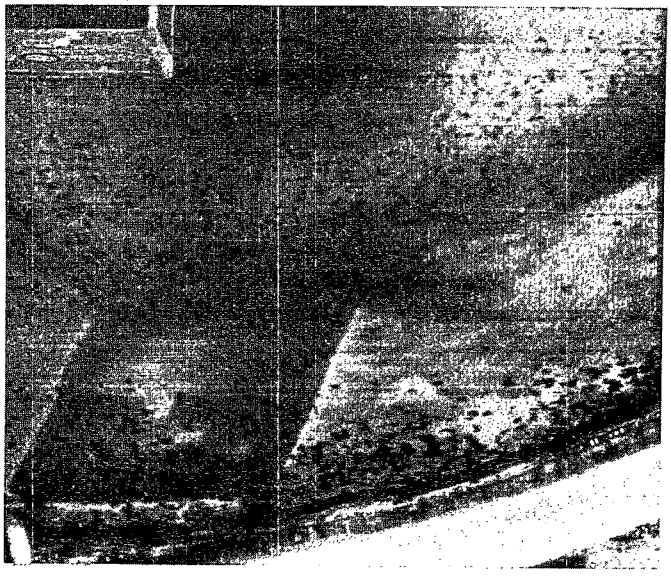

FIGURE 58 MODIFICATION 10, PETROTHENE GRAINS REACHING END OF INLET, AND PETROTHENE GRAINS SLIDING DOWN AGAINST THE CONE WALL NEAR INLET

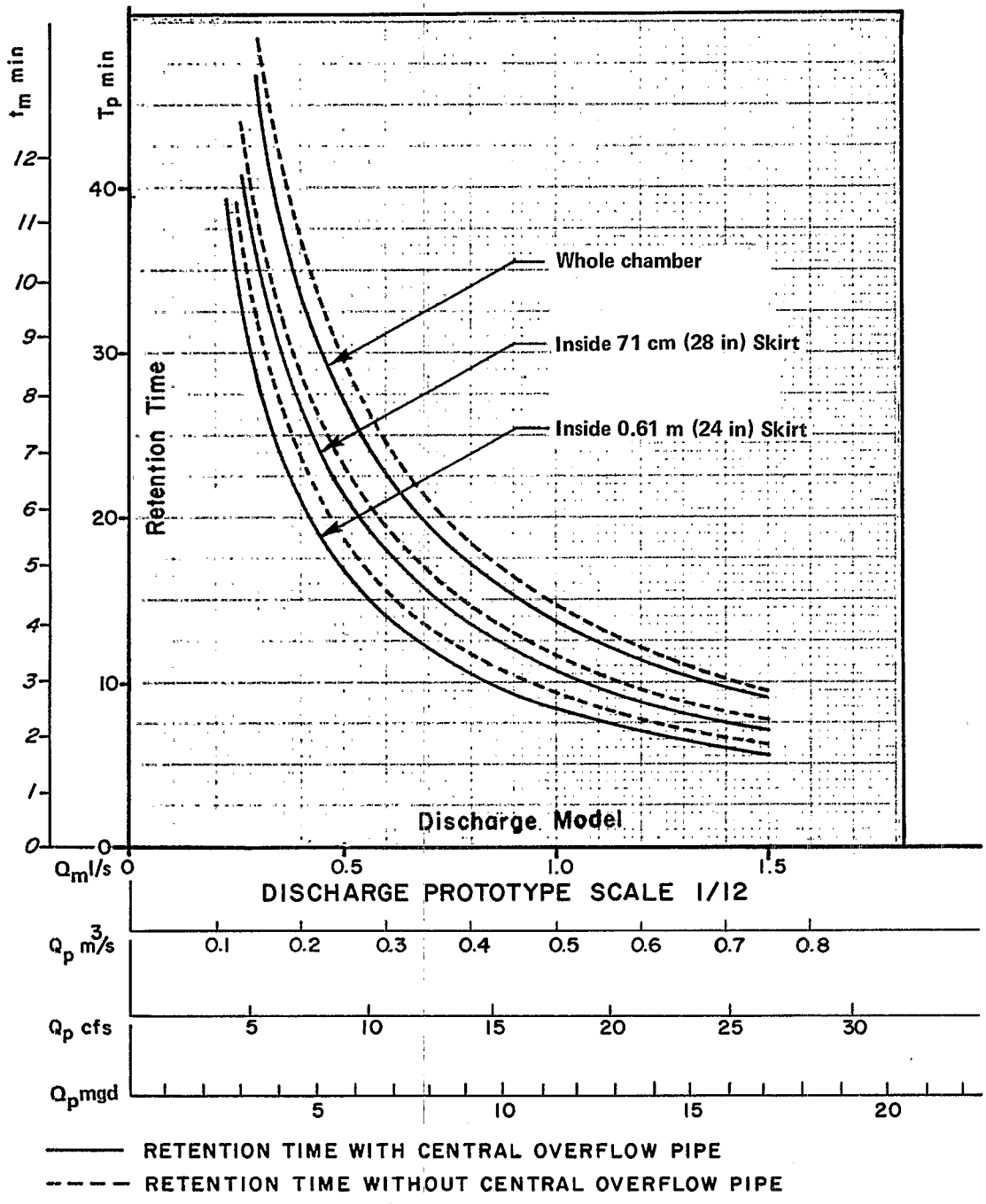

FIGURE 59 SWIRL PRIMARY SEPARATOR
RETENTION TIME Vs DISCHARGE WITH SCALE 1/12

rate of one 100-cc sample every two injections.

The model was left running without injection for one more retention time, then stopped. In addition to collecting samples which were sent to Beak for concentration analyses, volumetric measurements of the material respectively deposited in the chamber and overflow tank were also carried out. The volumetric measurements proved to be too time-consuming and they were later discontinued.

A new test numbering series was started for studies with the fine material. Test 1 in the new series corresponded to Test 185 in the old series. Both numbers are given in the resume in Table 15, whereas only the new series is referred to in Table 16.

Original Model Conditions

The first series of tests with fine material was carried out with the layout shown on Figure 55. This configuration provided the following details:

- The conical section extended up to the chamber diameter, eliminating the flat floor.
- Four radial weir gutters, 7 cm (2.75 in) wide by 5 cm (2 in) high – inside dimensions – extended radially 29.2 cm (11.5 in) from the chamber axis.
- The weir lip was located at inlet crown elevation.
- The skirt was 71.1 cm (28 in) in diameter.
- The central overflow cylinder had an outside diameter of 16.8 cm (6.87 in).

To provide uniform comparable results, the slot height under the skirt for this series of tests was set at 5.1 cm (2 in), the value which gave the best recovery rate for Petrothene with discharges ranging from 0.5 to 1.5 l/sec (0.98 to 0.0525 cfs) as shown in Figure 54.

The results of this second series of tests are recorded in Table 16.

Fine Grain Recovery Results and Comments

As shown on Figure 56 , the recovery of fine settleable solids dropped progressively with increasing discharge rates. Such results were expected since the time allowed for a

TABLE 16
SUCCESSIVE MODIFICATIONS OF THE MODEL AND RECOVERY RESULTS WITH ANION EXCHANGE RESIN IRA 93 $149\mu > d > 74\mu$

Stage No. Mod. Skirt Inlet Size	Other Model Features	Discharge Q_m l/s and Q_p mgd				
		Q_m 0.1 Q_p 1.14	0.3 3.42	0.5 5.69	0.75 8.54	1.0 11.38
1 Mod. 10 71.1 cm (28 in) 10 x 10 cm (4 x 4 in) Inlet	4 radial wiers Central column No deflector	91 (8)	62 (7)	52 (4) (9)	32 (6)	30 (5)
2 Mod. 11 71.1 cm (28 in) 6 x 6 cm (2.37 x 2.37 in) Inlet	8 radial weirs gutter in outer ch No central column No deflector	96 (51)	52 (48)	40 (15)	31 (49)	27.5 (50)

TABLE 16 (continued)

Stage No. Mod. Skirt Inlet Size	Other Model Features	Discharge Q_m l/s and Q_p mgd Q_m 0.1 0.3 0.5 0.75 1.0 Q_p 1.14 3.42 5.69 8.54 11.38
2a Mod. 11 71.1 cm (28 in) 6 x 6 cm (2.37 x 2.37 in) Inlet.	Same as 2 22.9 cm (9 in) emerging deflector	87 (18) 54 (19) 37 (17)
3 Mod. 12 61 cm (24 in) 6 x 6 cm (2.37 x 2.37 in) Inlet	8 radial weirs gutter in outer ch no central column no deflector	81 (26) 90.5 (58) 64 (21) 65.3 (53) 33 (33) 30 (20) 41 (40) 36 (32) 53 (57) 23 (27) 66.8 (54) 40 (56) 33.7 (55)
3a Mod. 12 61 cm (24 in) 6 x 6 cm (2.37 x 2.37 in) Inlet	Same as 3 22.9 cm (9 in) Emerging def. to bottom of duct	56 (23) 40 (22) 42 (31) 52 (34) 42 (35)
3b Mod. 12 61 cm (24 in) 6 x 6 cm (2.37 x 2.37 in) Inlet	Same as 3 radial deflector Top of duct to top of cone	55 (37) 35 (36) 27 (38)
3c Mod. 12 61 cm (24 in) 6 x 6 cm (2.37 x 2.37 in) Inlet	Same as 3 24.1 cm (9.5 in) long deflector Top of duct to top of cone	49.5 (40) 38 (39) 37.4 (41)
3d Mod. 12 61 cm (24 in) 6 x 6 cm (2.37 x 2.37 in) Inlet	Same as 3 24.1 cm (9.5 in) long deflector Top of duct to bottom of duct	51.6 (44) 43.7 (43) 30.5 (42) (59)
3i Mod. 12 61 cm (24 in) 6 x 6 cm (2.37 x 2.37 in) Inlet	Same as 3 Draw off underflow 5%	44 (24) 23 (25)

Note: Percentage recoveries given in plain typed figures in body of table; i.e. 44.
Test numbers in second series shown in circles; i.e. (24)

particle to settle shortened progressively as the discharge increased, as portrayed in Figure 59.

Efficiency rates determined from volumetric measurements decreased from 91 percent for 0.1 l/sec (0.0035 cfs), to 24 percent for 1 l/sec (0.035 cfs). Recovery values derived by Beak from the sample analyses were slightly higher, as shown by the dotted line in Figure 59.

This can be explained by the difficulties encountered in recovering the finer material for the volumetric measurements. Part of the solids material was lost during each test despite all precautions taken. The loss probably represents the portion of the material finer than No. 200 sieve (74 microns), but which was retained as dust in the sample during the original dry sieving.

The results of the concentration analyses performed by Beak must be accepted as providing the better representation of the recoveries.

MODIFICATION OF THE MODEL FOR FINE RECOVERY – STAGE 2

The next steps taken in the attempt to increase the efficiency of the swirl chamber consisted of:

1) Removing the central cylinder used for overflow evacuation.
2) Increasing the number of radial weir gutters to 8, so as to better distribute the flow inside the chamber.
3) Increasing the inlet velocity to avoid solids deposits in the inlet.

The new structural details of the model are shown in Figure 60. They include:

- 8 Radial Weir Gutters were provided, 4 cm (1.6 in) high by 2 cm (0.8 in) wide with crest at 2 cm (0.8 in) above the inlet crown elevation.
- The inlet was reduced to a 6 x 6 cm (2.35 x 2.35 in) square duct, with top elevation at the same level with respect to the end of cone wall as in previous conditions.
- The skirt was 71 cm (28 in) in diameter.
- The slot height was 5 cm (2 in).
- The overflow was discharged over a circular gutter 8 cm (3.5 in) high by 3 cm (1.2 in) wide fixed around the outside of the skirt and communicating with the overflow tank by two 2.5 cm (1 in) diameter tygon tubes were passing through the chamber wall.

TEST RESULTS AND COMMENTS (MODIFICATION 11) – STAGE 2

Tests carried out under the new conditions with the same material proved to be disappointing. The recovery rate varies unevenly, showing some gain for the small discharge of 0.1 l/sec (0.0035 cfs) but a loss under all other operating conditions.

This was probably due to the velocity increase which occurred in the outer chamber, resulting from the simultaneous reduction of the inlet duct cross section and of the outer chamber volume due to the presence of the circular gutter for collecting the overflow.

A similar test run with the 0.5 l/sec (0.018 cfs) discharge, and Arizona Road Dust with grain size $20\mu \geqslant d \geqslant 10\mu$ and SG = 2.65, showed a relatively minor decline of the recovery rate – 36 percent instead of the previous 40 percent obtained with IRA-93 Anion Exchange Resin.

Additional tests carried out with a 22.86 cm (9 in) long deflector at the inlet end (Stage 2a) did not prove to be conclusive in the improvement of the recovery rate.

MODIFICATION 12 – (STAGE 3)

In order to decrease the velocity prevailing in the outer chamber, the skirt diameter was reduced to 61 cm (24 in), giving a ratio D_2/D (skirt to chamber diameter) equal to 2/3. The radial cross section of the outer chamber was, thus, increased by about 50 percent, as shown in Figure 61.

Results obtained when tests were repeated did not always yield the same values. Plotted points were widely scattered, especially for the 0.5 l/sec (0.18 cfs) dischcarge. In this zone, the repeated values ranged from 30 to 50 percent. Conversely, at the 0.3 l/sec

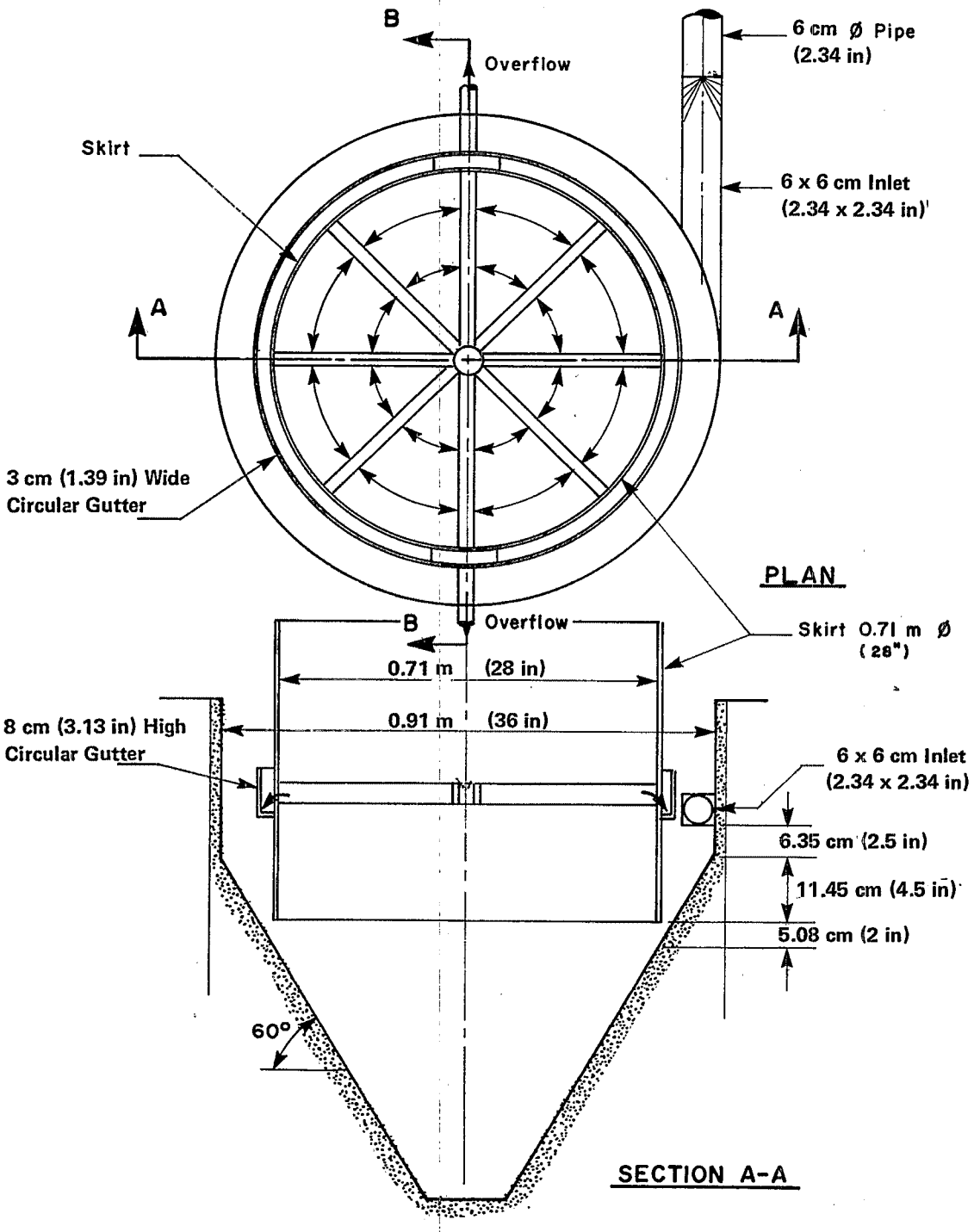

FIGURE 60 SWIRL PRIMARY SEPARATOR MODEL LAYOUT FOR MODIFICATION II

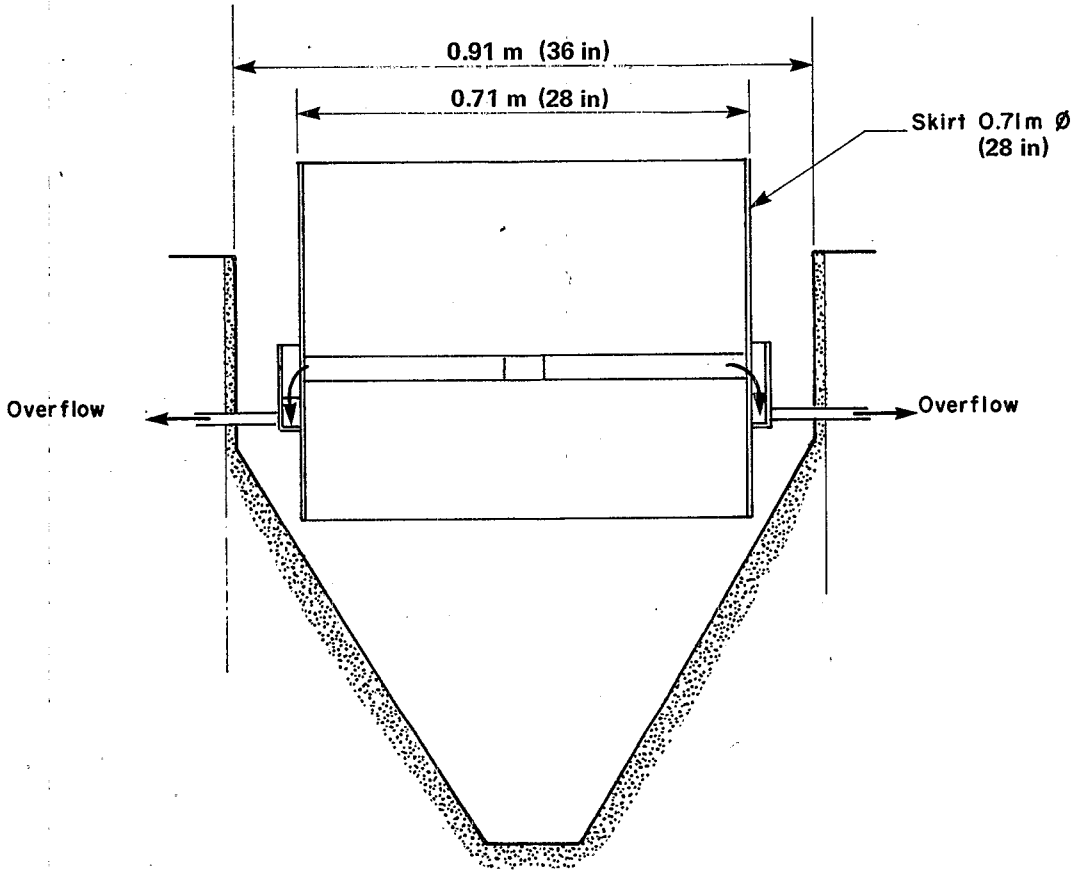

SECTION B-B

FIGURE 60 SWIRL PRIMARY SEPARATOR
MODEL LAYOUT FOR MODIFICATION II

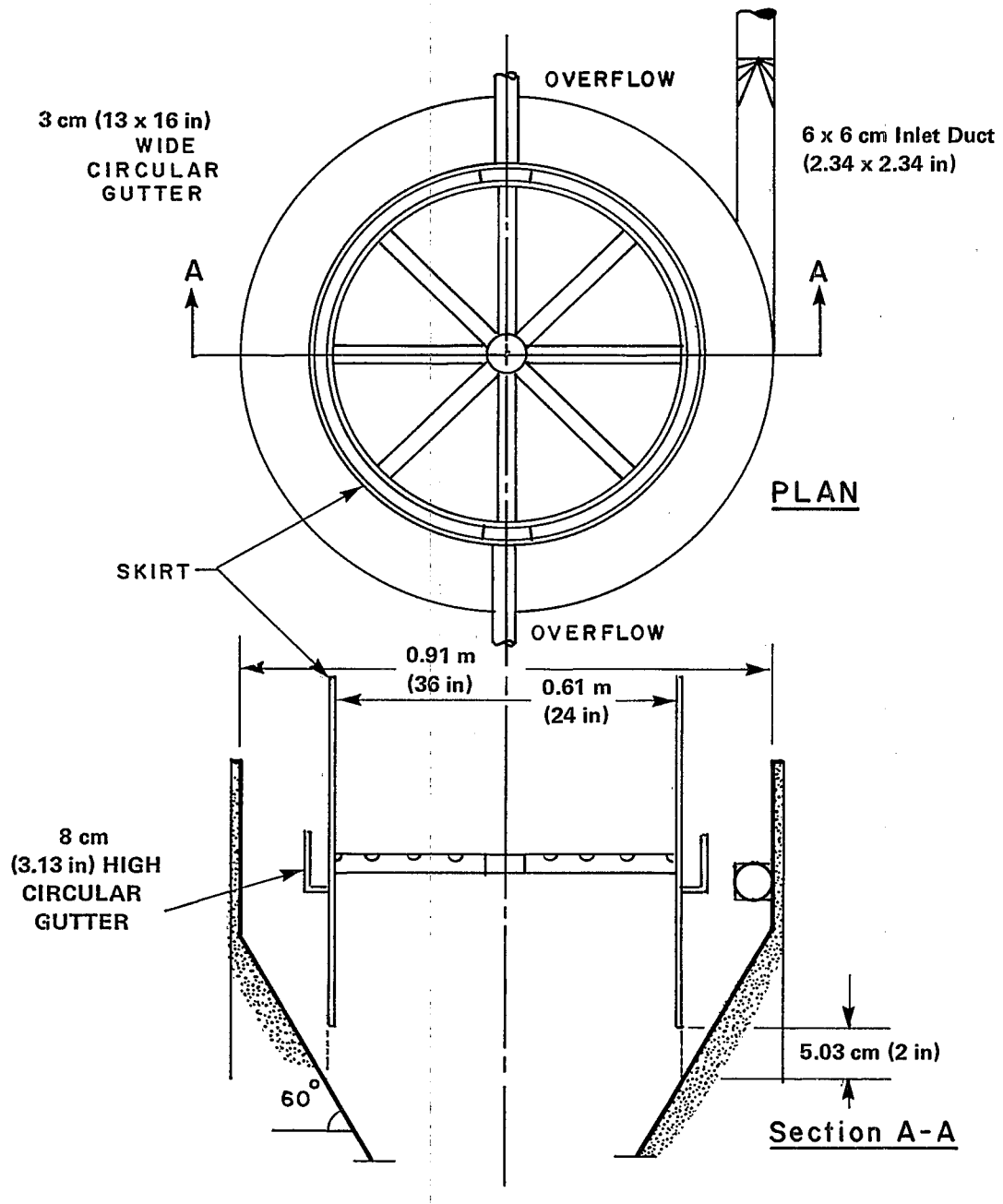

FIGURE 61 SWIRL PRIMARY SEPARATOR
MODEL LAYOUT FOR MODIFICATION 12

(0.011 cfs) level, results showed a relative consistency at 65 percent.

In an attempt to improve the recovery rates by slowing down the flow velocity in the outer chamber, various baffles were tested at the inlet. The first baffle tested was set in between the outside chamber wall and the circular collector gutter on the skirt, as shown in Figure 62. As listed in Table 16, this produced a slight improvement in recoveries. However, it was found that having the baffle emerge from the water, stopping the surface flow, also impeded the floatables movement, leaving them randomly scattered around the outer chamber.

A submerged baffle, as shown in Figure 63, was tried next. This radial arrangement decreased the recoveries for all discharges. A layout with the same cross section as 3b, but with the baffle tangential to the skirt was next tested, as shown in Figure 64. This provided an improvement, but still did not perform the recovery achieved with Baffle 3a.

Finally, the configuration shown in Figure 65 was tested. Results from these tests were inconclusive, showing slightly less recovery for 0.3 l/sec (0.011 cfs) and slightly more for 0.5 l/sec (0.018 cfs) than for baffle 3a. However, since baffle 3d combined fairly satisfactory recoveries and the advantage of leaving the surface uninterrupted, it is the recommended form.

INFLUENCE OF CONTINUOUS UNDERFLOW DRAW-OFF

Only two tests were carried out with a continuous discharge of deposited slurry being drawn off through the foul outlet. These tests were performed with total inflow discharges of 0.3 and 0.5 l/sec (0.011 and 0.018 cfs), respectively. In each case, 5 percent of the inflow volume was withdrawn through the foul outlet. The model layout used was that for Modification 12, without any baffles, as shown in Figure 61.

The results, as outlined in Table 16, for Tests 24 and 25, showed a distinct drop in recoveries when compared with the tests achieved without any foul draw-off. Observations on the model indicated that the discharge going to the foul outlet catalyzed increased velocities in the lower regions of the conical bottom. These, in turn, were sufficient to resuspend particles which had been settled out along the floor higher up in the cone. Once in suspension for the second time, a greater portion of the particles was intrained upward and carried over the gutter weirs with the chamber overflow liquid.

Comments

Analysis of the recovery values for the various layouts tested in the fine grain materials series given in Table 16 shows considerable random scatter. Some of this was obviously due to experimental error, but the time was not available to carry out repeat tests in many cases.

It was necessary, therefore, to decide subjectively on the recovery curve which best described the structure's operation in the laboratory. The one selected is shown on Figure 66. This curve was developed graphically as representing the best mean of the data points for the tests performed with baffles. In fact, the test results were not decisive enough to allow an absolute selection of the best baffle configuration. However, from observations on the model it appeared that the Type 3d layout presented certain advantages, so this one is recommended for prototype testing.

PREDICTED PROTOTYPE SOLIDS RECOVERY

As discussed in the preceding section of this report, recovery curve evolved for the IRA-93 in the model studies is as shown in Figure 66. For the five model discharges used in the tests, the corresponding recovery rates are given in Table 17.

TABLE 17
RECOVERY RATE OF IRA-93 AT VARIOUS FLOWRATES

Model Discharge:					
l/sec	0.1	0.3	0.5	0.75	1.0
cfs	0.0035	0.0106	0.0176	0.0264	0.0352
Recovery Rate:					
%	91	58	41	31	27

In order to transpose this model curve to prototype, reference was then made to Figure

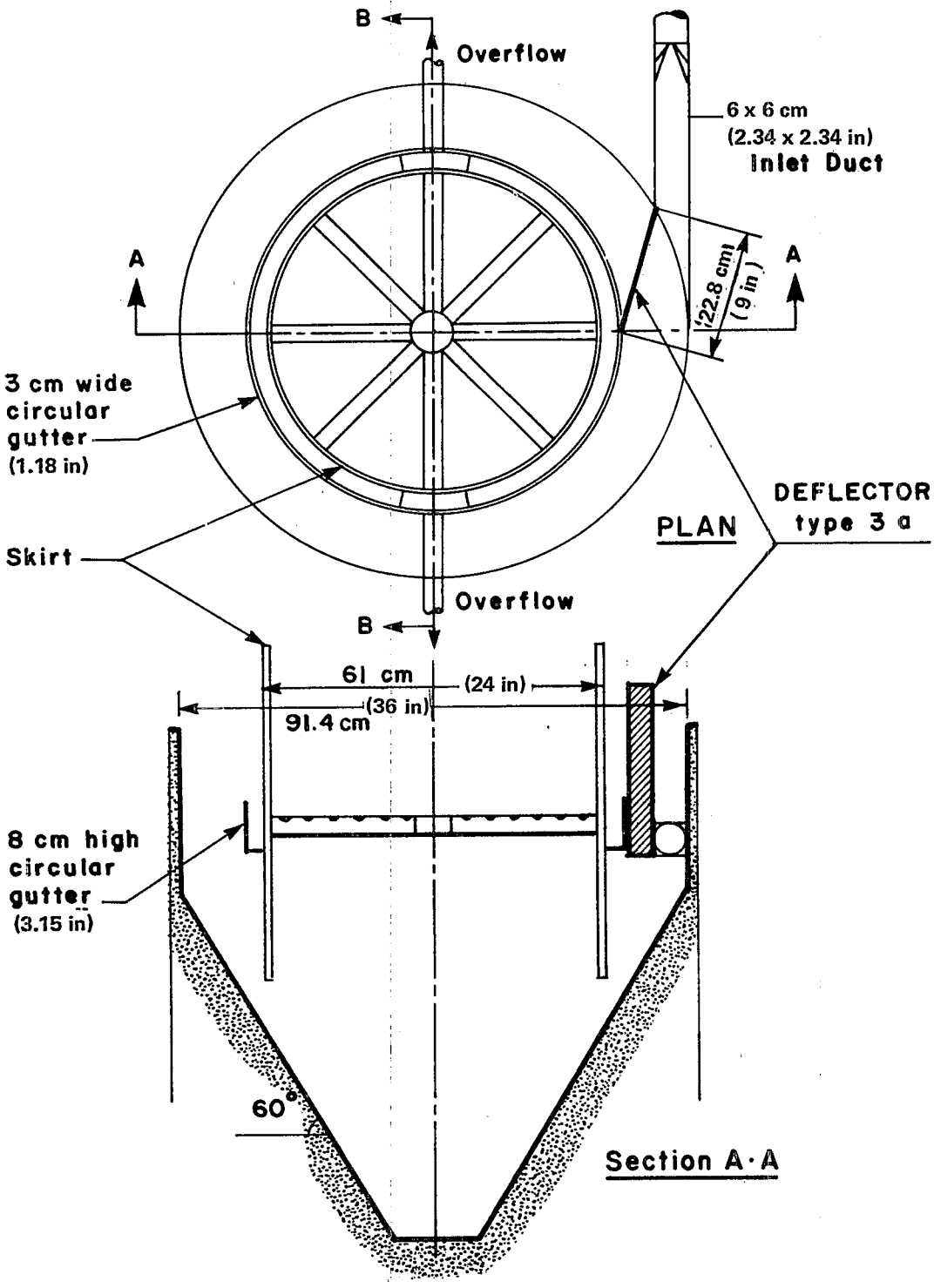

FIGURE 62 SWIRL PRIMARY SEPARATOR
MODEL LAYOUT WITH MODIFICATION 12 AND INLET
BAFFLE TYPE 3a

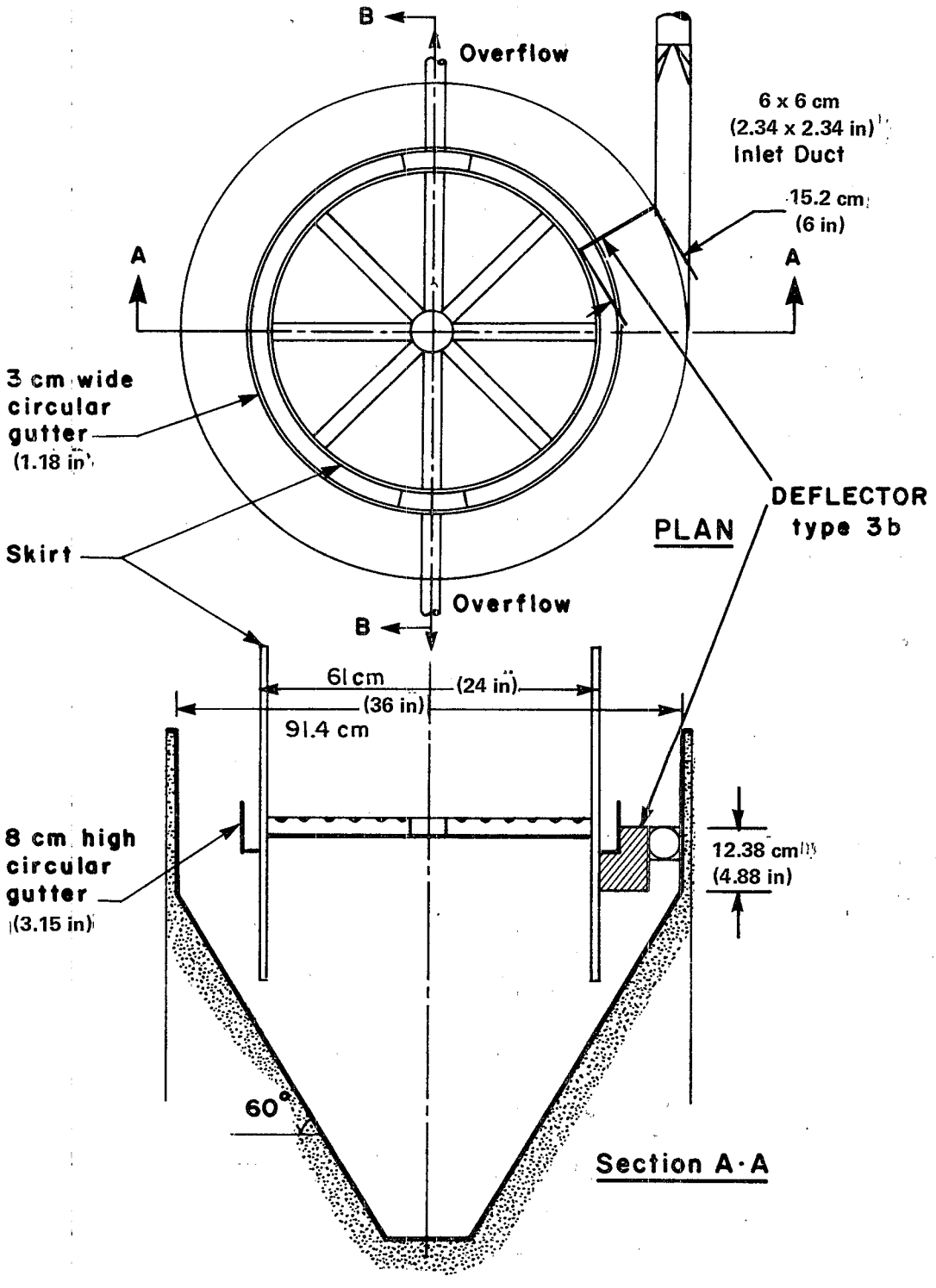

FIGURE 63 SWIRL PRIMARY SEPARATOR
MODEL LAYOUT WITH MODIFICATION 12 AND INLET
BAFFLE TYPE 3b

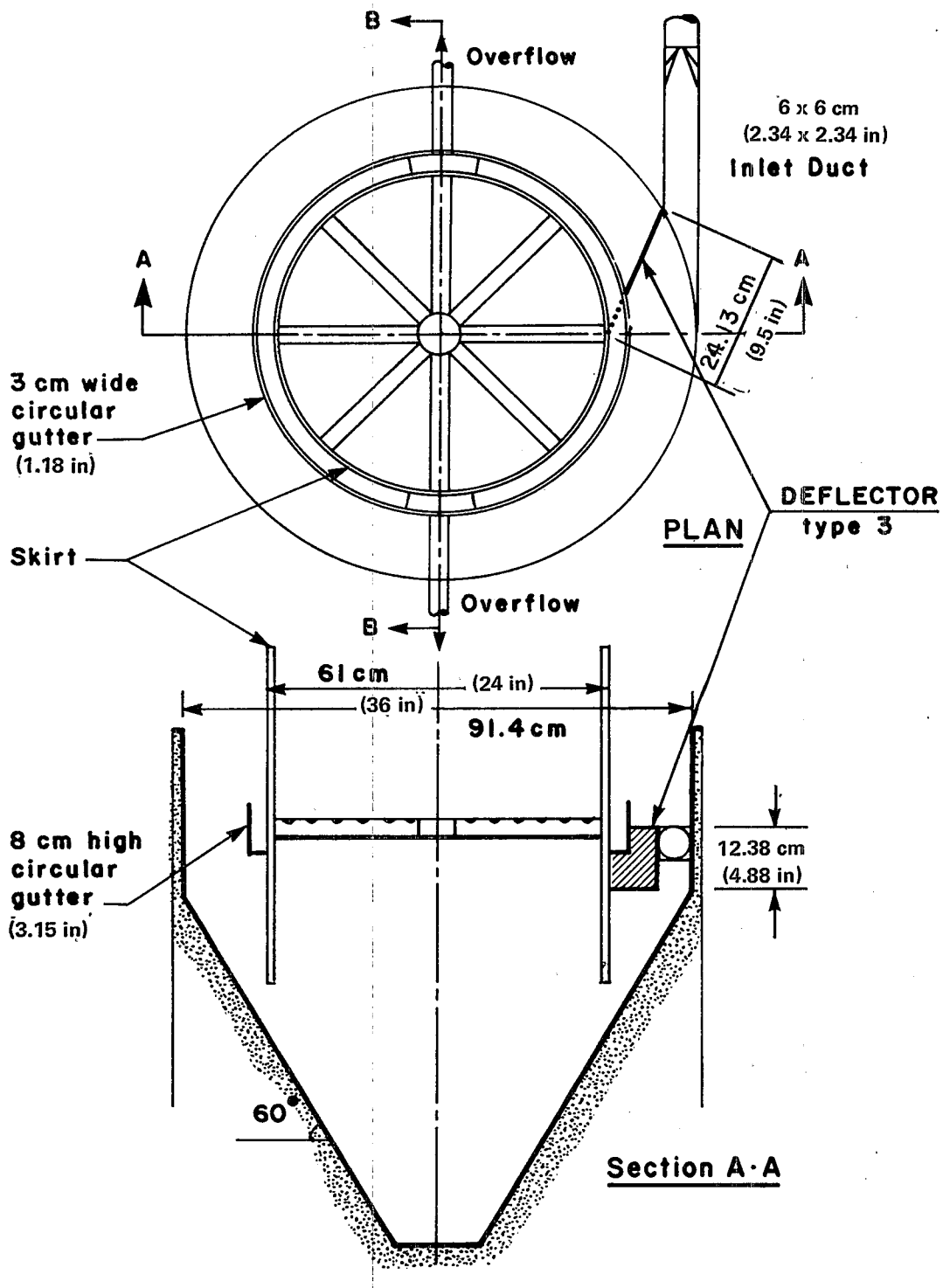

FIGURE 64 SWIRL PRIMARY SEPARATOR
MODEL LAYOUT WITH MODIFICATION 12 AND INLET
BAFFLE TYPE 3c

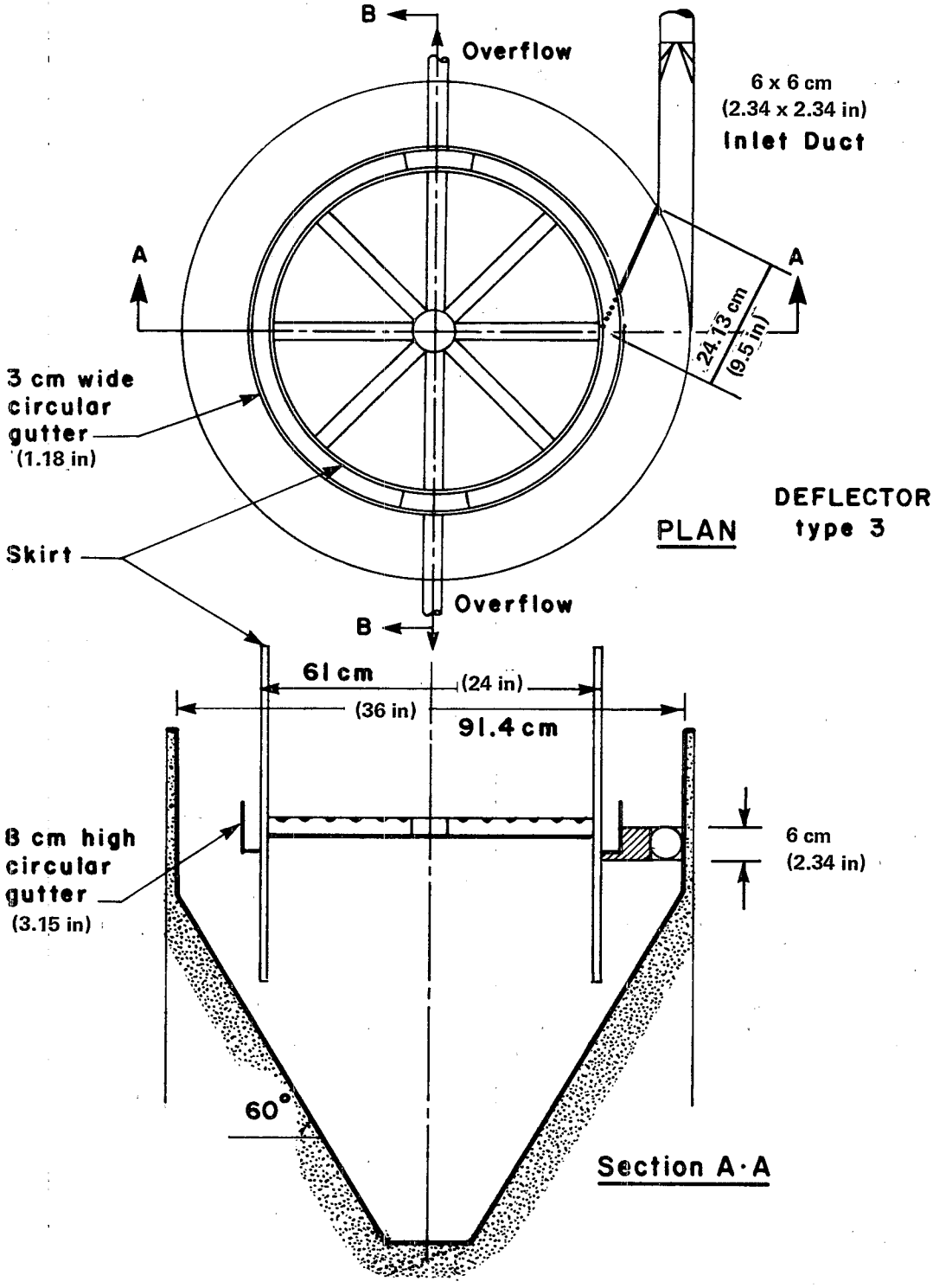

FIGURE 65 SWIRL PRIMARY SEPARATOR
MODEL LAYOUT WITH MODIFICATION 12 AND INLET
BAFFLE TYPE 3d

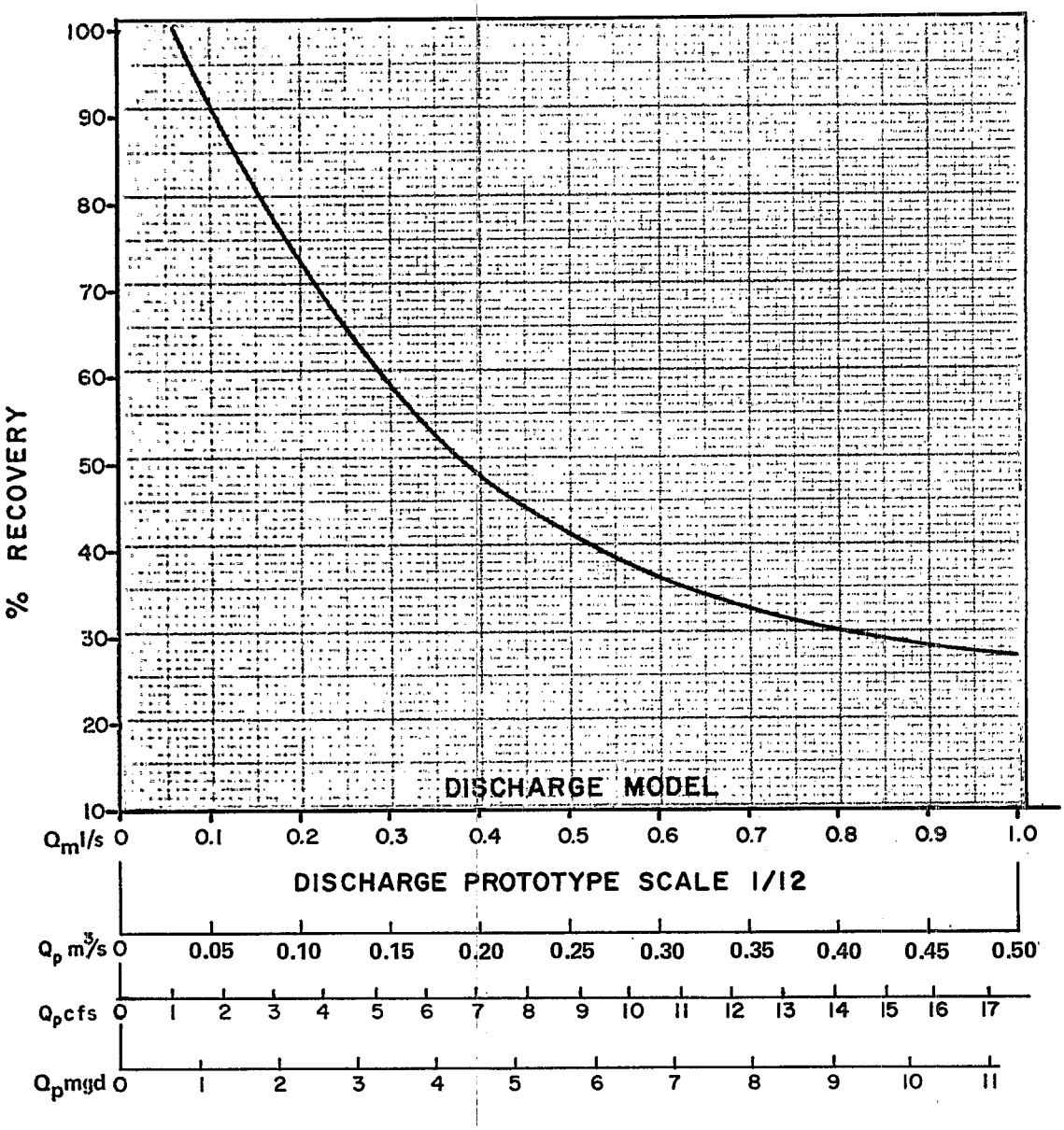

FIGURE 66 SWIRL PRIMARY SEPARATOR
SUGGESTED RECOVERY CURVE FOR ANION
EXCHANGE RESIN IRA-93 IN MODEL
$149\mu > d > 75\mu$

36, which charted the portions of prototype sewage represented by the IRA-93 in the model. Values were selected from the recommended curve, Figure 36, for each of the scales being considered, as shown in Table 18.

TABLE 18
REPRESENTATION OF IRA-93 TO SEWAGE, BASED ON SCALE FACTOR

SCALE	1:12	1:8	1:4	1:2	Model
Percent Represented	56	64	79	100	100
Prototype Chamber (m)	10.98	7.33	3.66	1.83	0.915
Diameter (ft)	36	24	12	6	3

Finally, each "Percent Represented" value from Table 18 was multiplied by the "Recovery Rates" from Table 16, and plotted in Figure 67 as a function of the appropriate scaled-up discharge, and chamber diameter.

It is therefore possible to use a given discharge in Figure 67, to determine what solids recovery from sanitary sewage could be obtained with various sized chambers. It must be remembered that these recovery rates were based on the sewage samples as defined by the settling velocity distribution curve in Figure 35.

Since it is possible that other uses of the swirl concentrator as a primary settler may be considered, it was necessary to express the recovery rates for a range of different particle settling velocities. The first step in determining this was to refer to tests carried out for the 0.5 l/sec (0.018 cfs) case on the model using materials covering a range of settling velocities. The data for these tests are shown in Figure 68.

Next, the model recovery curve in Figure 66 was re-drawn as the bold line on semi-logarithmic paper in Figure 69a. This curve corresponds to the IRA-93 with particle sizes $74\mu \leqslant d \leqslant 149\mu$. The point indicated as a star is for the 0.5 l/sec (0.018 cfs) discharge for this material. Vertically above this point, in circles, were plotted even settling velocities at their corresponding recovery rates taken from Figure 68.

The final step is based on the rationale that, although these other particle settling velocity materials were tested only for one discharge, it is assumed that they would have the same form of recovery rate curve as the IRA-93, $74\mu \leqslant d \leqslant 149\mu$ over the range of discharges for which it was tested. Following this approach, the curve of the bold line on Figure 69a was re-drawn to form a family of curves, each one passing through the control point on the 0.5 l/sec (0.018 cfs) line.

With these curves established for the model a straightforward application of the Froude Law transposed the original bold line to Figures 69b, c, d, and e for the larger prototypes. The same procedure was followed in laying out the different settling velocity control points above the working point scaled-up from the 0.5 l/sec (0.018 cfs), and then drawing the family of parallel recovery rate curves.

After the ranges of discharges of normal operation for the different sized chambers had been determined, computations were carried out to ascertain the corresponding retention times. The approach followed was to consider the whole volume of the chamber, both inside and outside the skirt, up to the radial gutter crest level. The results of this work are presented in Figure 12.

The design procedure is given in Section III.

Conclusions

1. With an inlet pipe to chamber diameter ratio of 0.11, the solids recovery in the chamber was relatively high. However, the velocities in the inlet were so low that solids deposition would certainly occur there.
2. The inlet was reduced to a ratio of 0.07, meaning that prototype velocities in the inlet would be in the range of 30.5 cm/sec (1 ft/sec), thus eliminating the possibility of serious deposition. The chamber recovery rate dropped slightly.
3. Tests with the inlet below the water level in the chamber gave poor recoveries. Later testing with the inlet crown at the same level as the overflow weirs proved that this was the best setting.
4. The flat floor around the outside perimeter of the chamber was eliminated

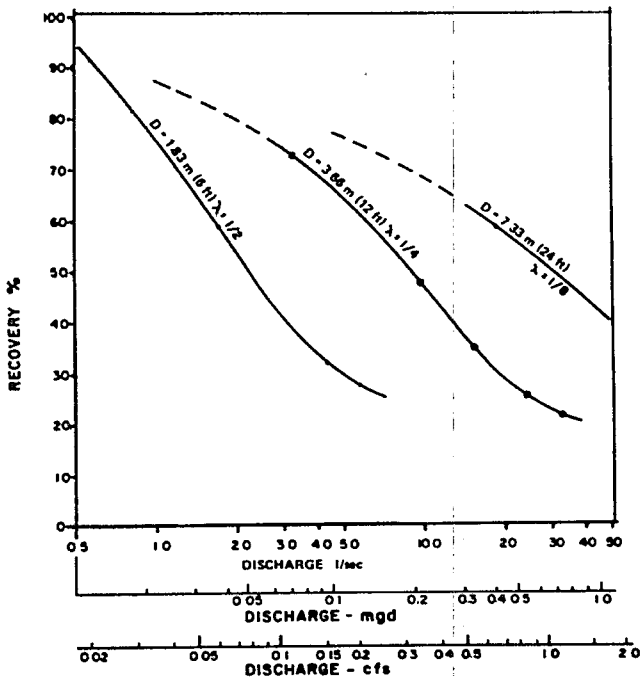

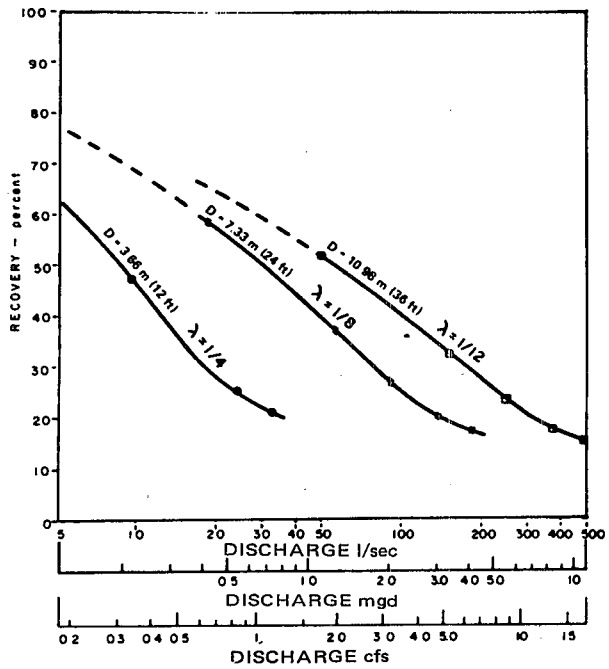

FIGURE 67 SWIRL PRIMARY SEPARATOR PREDICTED PROTOTYPE SOLIDS RECOVERY FROM SANITARY SEWAGE

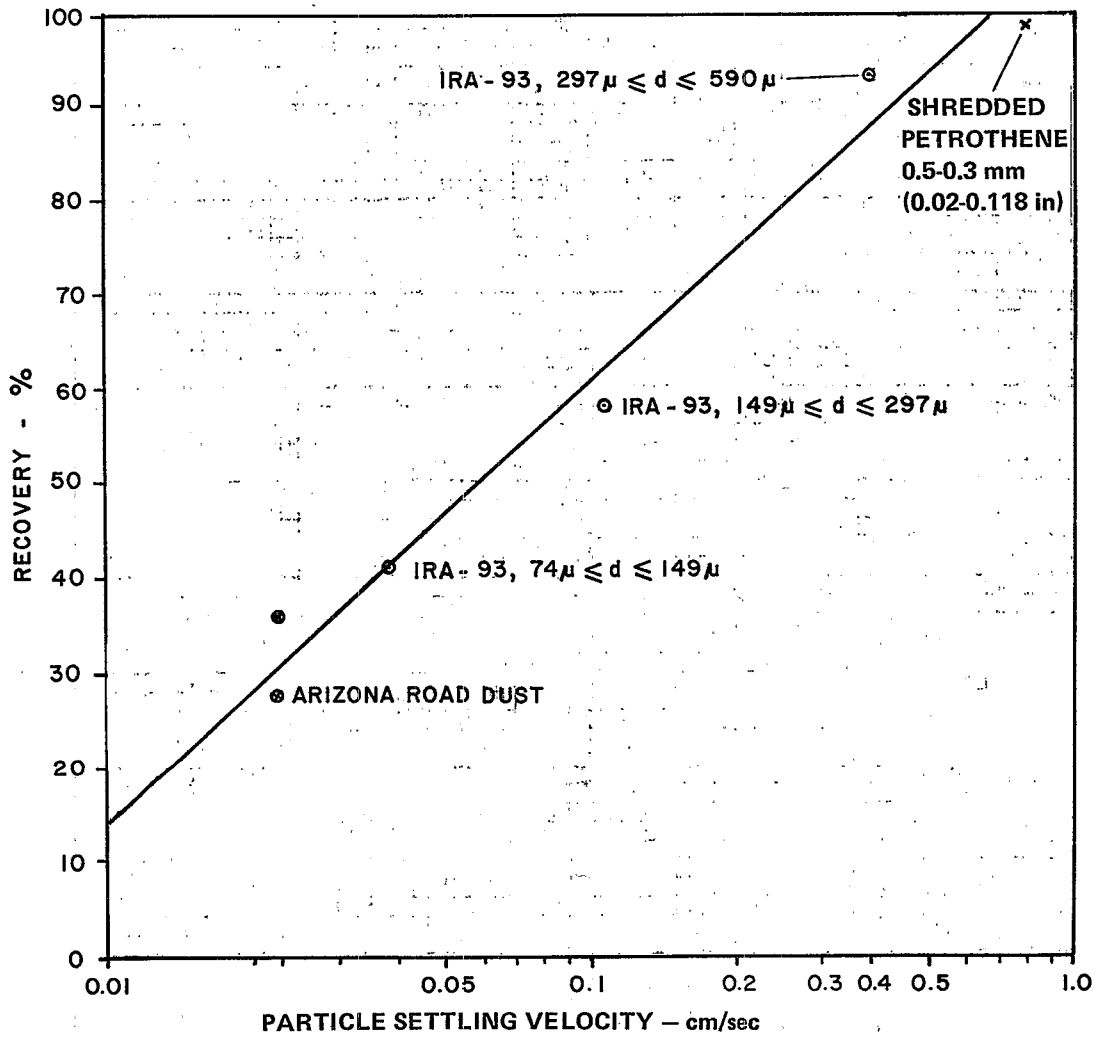

NOTE: Tests with different materials done for discharge
0.5 l/s (0.02 cfs)

FIGURE 68 RECOVERY RATES ON MODEL AS FUNCTION OF PARTICLE SETTLING VELOCITY

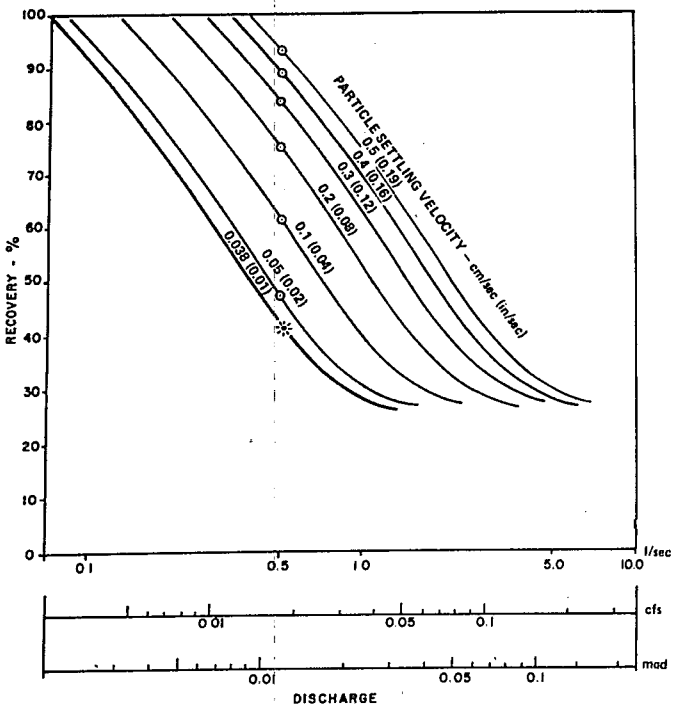

FIGURE 69a RECOVERY RATES FOR 0.91 m (3 ft) DIAMETER CHAMBER WITH DIFFERENT PARTICLE SETTLING VELOCITIES

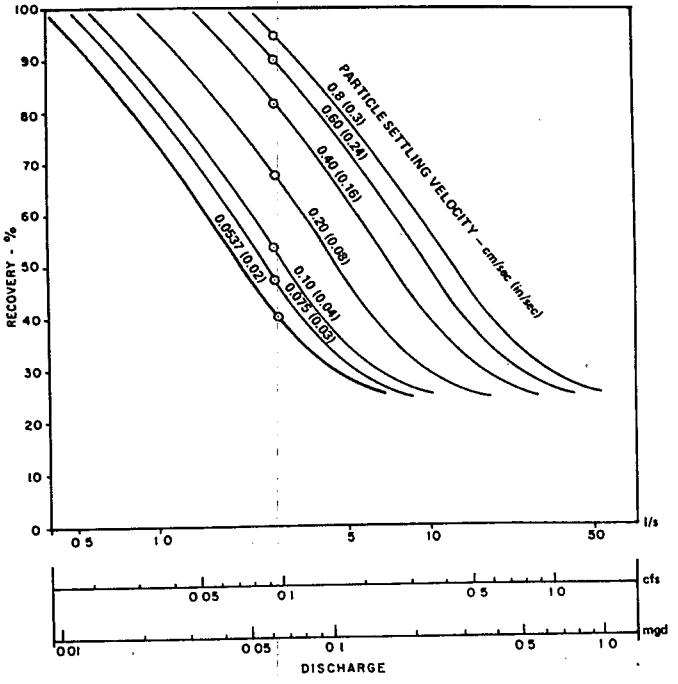

FIGURE 69b RECOVERY RATES FOR 1.83m (6 ft) DIAMETER CHAMBER WITH DIFFERENT PARTICLE SETTLING VELOCITIES

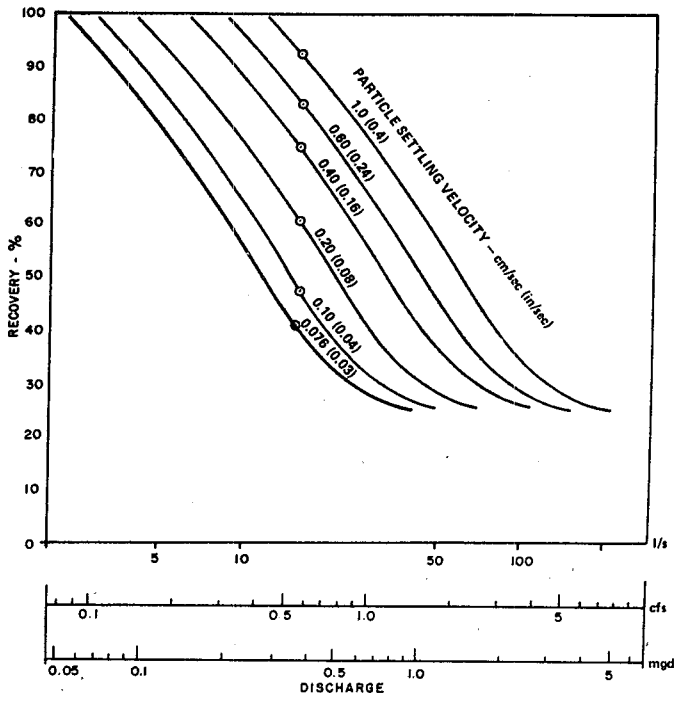

FIGURE 69c RECOVERY RATES FOR 3.66m (12 ft) DIAMETER CHAMBER WITH DIFFERENT PARTICLE SETTLING VELOCITIES

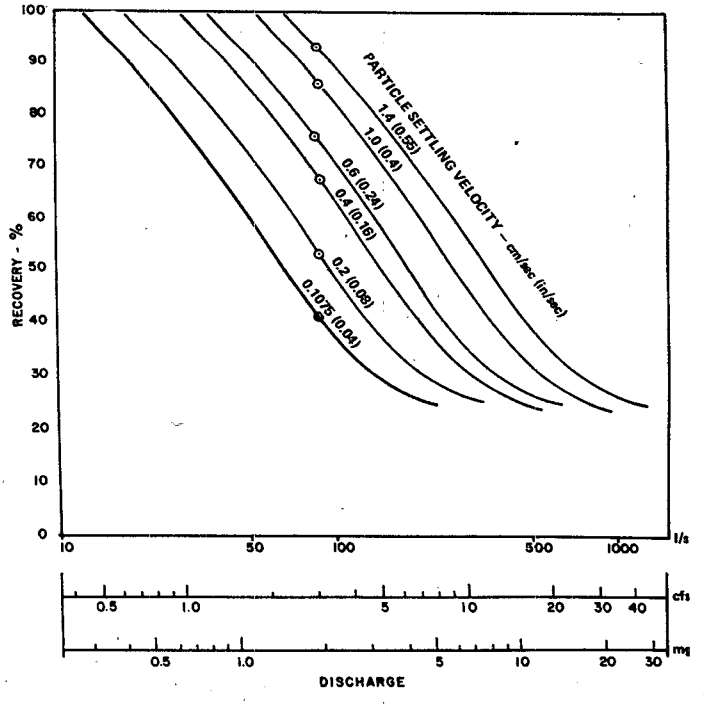

FIGURE 69d RECOVERY RATES FOR 7.33m (24 ft) DIAMETER CHAMBER WITH DIFFERENT PARTICLE SETTLING VELOCITIES

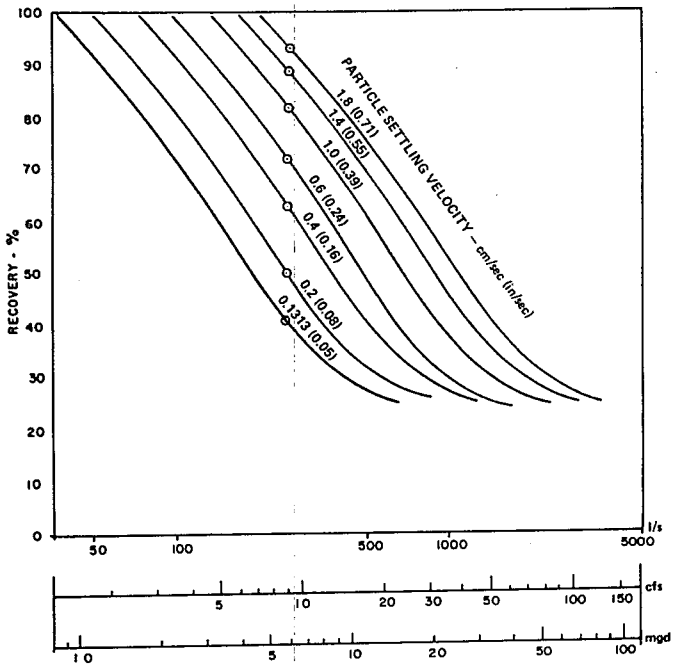

FIGURE 69e RECOVERY RATES FOR 10.98m (36 ft) DIAMETER CHAMBER WITH DIFFERENT PARTICLE SETTLING VELOCITIES

on two grounds; first, it caused a flow disturbance as the flow went over the edge down into the cone section of the chamber; and second, deposits formed on it and remained entrained there.

5. The 60 degree conical floor angle, continuing up to the chamber perimeter diameter provided the best geometrical pattern.
6. A skirt-chamber diameter ratio of 2:3 was found to be the most efficient. This arrangement left a sufficiently large annular chamber to allow first-stage sedimentation for the flow.
7. The skirt was lowered until the slot between its lower edge and the conical floor was 0.08D. At this position, the slot entrance to the inner chamber was sufficiently far enough below the inlet to eliminate any inflow disturbance.
8. Circular overflow weirs inside the skirt were eliminated, because they left a large dead water zone around the central downpipe under the weirs.
9. Closing the top of the skirt to form a closed bell with orifices in the top for clear overflow showed some promise, but this pattern involved problems with dead water zones at the center under the bell.
10. Radial overflow gutters proved to be the most efficient arrangements to create upflow over the whole cross section of the inner chamber.
11. Tests carried out with fine grain material were difficult and time-consuming, and the results were indeterminate.
12. Analysis of these data presented a good indication of the structure's general capabilities at the model scale. However, it was not possible to obtain specific detailed measurements to make a selection among the various forms of inlet baffles that were tested.
13. Construction of the first prototype unit should make provision for testing different baffle arrangements.
14. A first design procedure was developed, based on the "typical" sewage used in this project.
15. A second design procedure was then developed for use over a range of prototype particle settling velocities.

APPENDIX B

MATHEMATICAL MODEL STUDY

INTRODUCTION

Previous studies have shown that a swirl concentrator can be an effective device for the separation of grit and solids from stormwater flows.[1] The objective of this study was to evaluate whether these same principles could be applied to the primary clarification of sewage and combined sewer discharges. The role of the General Electric Company toward the fulfillment of this objective was to develop a mathematical model of the particle and liquid flowfields.

The general geometry of the swirl concentrator is shown in Figure 70, Laboratory Swirl Concentrator Configuration. The inflow enters the device tangentially in an annular region between the circular skirt and outer wall. The flow is then directed below the skirt and into the central region. The liquid then flows upward and leaves the chamber at the top. Although Figure 70 illustrates a circular overflow weir, this weir was later replaced with radial gutters. The central standpipe was also removed and replaced with a discharge structure external to the device.

The approach to the mathematical modeling of the swirl concentrator closely follows the techniques used in previous studies of secondary motion flow devices. The flows within the chamber are assumed to be axisymmetric about the vertical axis. The chamber is then overlaid with a computation grid and the liquid flow velocities are computed at each grid point by solving the liquid continuity equation and equations of motion. An eddy viscosity was utilized to represent the turbulent shear stress. Plots of streamlines and velocity profiles have been prepared to depict the liquid flowfield as predicted by the mathematical model.

Particle paths have been calculated by superimposing particle settling velocities on the liquid flowfield. Under certain assumptions, it was demonstrated that a simplified solution could be used to predict a theoretical upper limit on the removal efficiencies. Good agreement was observed between the theoretical upper limit and actual removal efficiencies observed by LaSalle Hydraulic Laboratory in its hydraulic model studies.

A design example is presented, illustrating how both the mathematical model and laboratory data can be used to predict removal efficiencies for a prototype chamber. Attention is called to the need for good characterization of the sewage settling properties for proper chamber design.

LIQUID FLOW CALCULATIONS

Equations of Motion

The ultimate configuration of the primary swirl concentrator was derived from meetings of the project team and from test data obtained by LaSalle Hydraulic Laboratory. Figure 70 depicts the geometry of the physical laboratory model utilizing a circular overflow weir and a central standpipe outlet arrangement. Certain assumptions were required in order to reduce the configuration to a form amenable to mathematical modeling. Figure 71 illustrates the simplified configuration used in the mathematical model. It is pointed out that the region over which the mathematical model has been applied does not include the annular region between the skirt and outer wall. This region was disregarded since most particle settling will occur in the main body of the chamber. It also greatly simplified the specification of the boundary conditions for the mathematical model.

The basic assumptions and methods used in developing the mathematical model are essentially the same as those used in the previous study of swirl chambers as applied to stormwater overflows.[2] The liquid flow has been assumed to be axisymmetric. This implies that the flowfield is identical at every radial cross section and independent of the angular position. This allows the use of only two independent variables (r, the radial

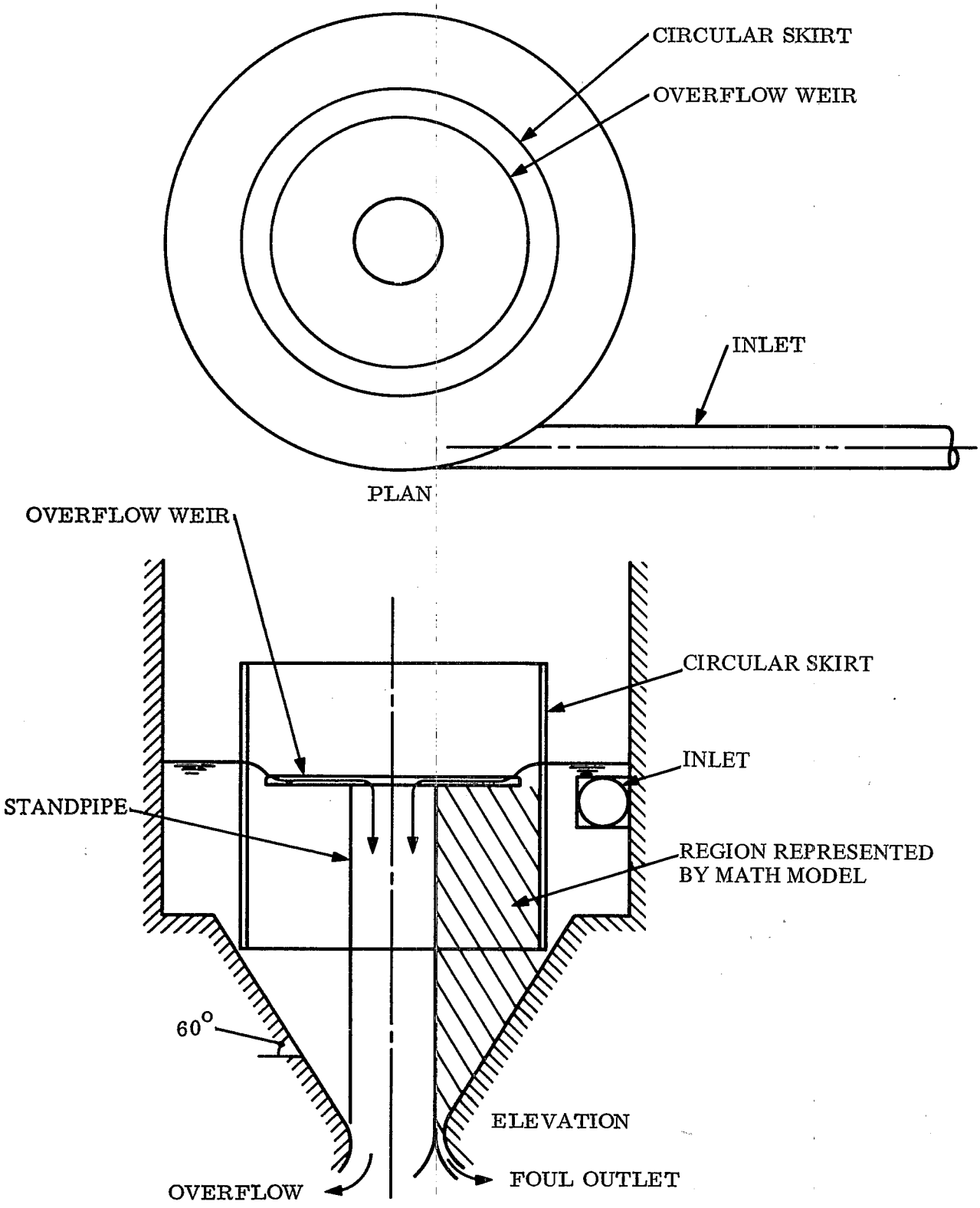

FIGURE 70 DIAGRAM OF LABORATORY SWIRL CHAMBER CONFIGURATION

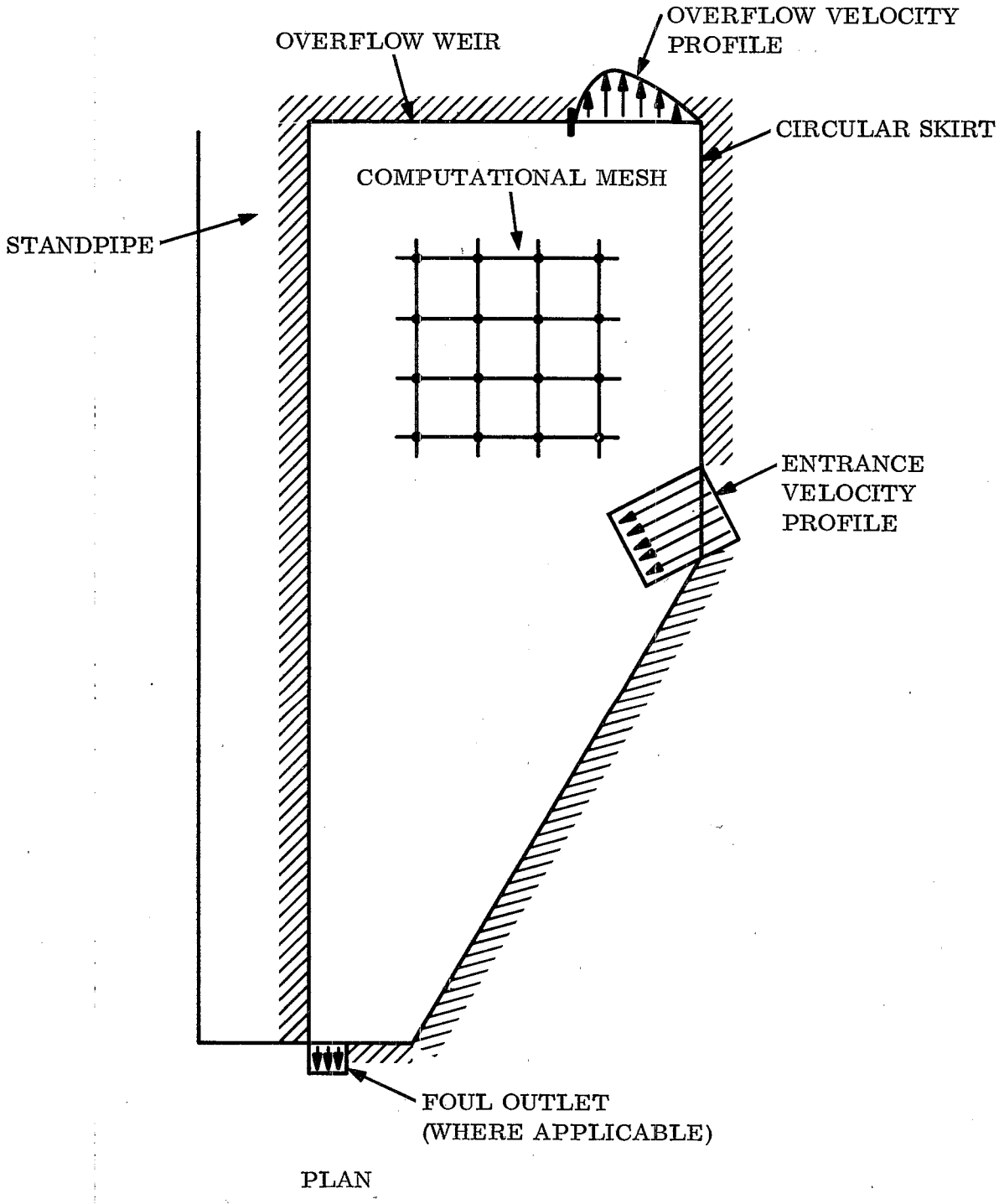

FIGURE 71 DIAGRAM OF SWIRL CHAMBER AS REPRESENTED BY MATHEMATICAL MODEL

position; and z, the depth) to completely define the flowfield. In addition, the liquid inflow is assumed to occur uniformly through an annular band. This assumption corresponds to the passage of the entering liquid below the skirt of the laboratory device into the inner region described by the mathematical model. The axisymmetric assumption is more valid in this study than the previous one[3] as a result of this inflow along all points on the circumference of the mathematical representation of the chamber.

The equations used in the mathematical model written in cylindrical coordinates are as follows:

1. The Continuity Equation

$$\frac{\partial u}{\partial r} + \frac{u}{r} + \frac{\partial w}{\partial z} = 0 \qquad (1)$$

2. The Momentum Equations

$$u\frac{\partial u}{\partial r} + w\frac{\partial u}{\partial z} - \frac{v^2}{r} = -\frac{1}{\rho}\frac{\partial p}{\partial r} + (\epsilon+\nu)\left(\frac{\partial^2 u}{\partial r^2} + \frac{1}{r}\frac{\partial u}{\partial r} - \frac{u}{r^2} + \frac{\partial^2 u}{\partial z^2}\right) + 2\frac{\partial u}{\partial r}\frac{\partial \epsilon}{\partial z} + \left(\frac{\partial w}{\partial r} + \frac{\partial u}{\partial z}\right)\frac{\partial \epsilon}{\partial z} \qquad (2)$$

$$u\frac{\partial v}{\partial r} + w\frac{\partial v}{\partial z} + \frac{uv}{r} = (\epsilon+\nu)\left(\frac{\partial^2 v}{\partial r^2} + \frac{1}{r}\frac{\partial v}{\partial r} - \frac{v}{r^2} + \frac{\partial^2 v}{\partial z^2}\right) + \frac{\partial v}{\partial z}\frac{\partial \epsilon}{\partial z} + \left(\frac{\partial v}{\partial r} - \frac{v}{r}\right)\frac{\partial \epsilon}{\partial r} \qquad (3)$$

$$u\frac{\partial w}{\partial r} + w\frac{\partial w}{\partial z} = -\frac{1}{\rho}\frac{\partial p}{\partial z} + (\epsilon+\nu)\left(\frac{\partial^2 w}{\partial r^2} + \frac{1}{r}\frac{\partial w}{\partial r} + \frac{\partial^2 w}{\partial z^2}\right) + \frac{\partial w}{\partial r} + \frac{\partial u}{\partial z}\frac{\partial \epsilon}{\partial r} + 2\frac{\partial w}{\partial z}\frac{\partial \epsilon}{\partial z} \qquad (4)$$

where

u = radial component of liquid velocity
v = tangential component of liquid velocity
w = vertical component of liquid velocity
r = radial coordinate
z = vertical coordinate
ϵ = eddy viscosity
ν = kinematic viscosity
ρ = liquid density
P = pressure

Boundary Conditions

The boundary conditions for the model are derived from the chamber geometry and flowrates. As mentioned previously, inflow to the chamber is assumed to enter uniformly around the circumference of the skirt as shown in Figure 71. Along solid boundaries the two velocity components parallel to the surface are obtained from the skin friction coefficient and dynamic pressure. The skin friction coefficient utilized was set equal to 0.0025 based on the previous study.[4]

The velocity profile for the inflow has been assumed to be uniform, with a direction parallel to the sloping floor of the tank corresponding to the flow beneath the skirt of the laboratory device. Two different overflow velocity profiles were assumed. For the cases with the flat circular overflow weir a skewed velocity profile similar to that used in the previous study was assumed. (See Figure 71) For the case where the overflow weir was replaced with radial collection gutters a uniform upflow velocity was assumed across the tank surface.

Numerical Method

The approach for solving the liquid flowfield equations closely parallels that used in the previous study.[5] The continuity equation and equations of motion were rewritten in terms of the non-dimensional functions f, Ω, and G defined by the expressions

$$f = \psi / U_{ref}\, r^2 \qquad (5)$$

$$\Omega = \frac{L^2 \eta}{r U_{ref}} = \frac{L^2}{r U_{ref}}\left(\frac{\partial u}{\partial z} - \frac{\partial w}{\partial r}\right) \qquad (6)$$

$$G = \frac{L}{r U_{ref}}\, v \qquad (7)$$

Summary

The numerical techniques and system of equations used to define the liquid flowfield are the same as those used in the previous

study.[6] The boundary condition and flowrates have been modified to represent the configuration of the primary swirl concentrator developed by LaSalle Hydraulic Laboratory.

The mathematical representation of the device excludes the annular region between the skirt and wall. The assumption of axisymmetry is an appropriate one for this device since the flow enters the main portion of the chamber at all points along the circumference of the skirt. As a consequence, the mathematical representation of the liquid flowfield is very close to the actual laboratory device.

The eddy-viscosity mixing length constant and the skin friction coefficient have been assumed equal to the values obtained in the previous study.[7] A closer agreement between the velocity field predicted by the model and the laboratory data may be obtained by refinement of these values. However, particle removal efficiencies will remain essentially the same for reasons to be explained later. Therefore, the existing values are satisfactory for the purposes of this study.

PARTICLE SETTLING VELOCITY

Settling Data Analysis

a. Experimental Approach: In order to make an accurate prediction of the prototype removal efficiencies of the sewage solids in the laboratory model, it is necessary to precisely define the settling properties of actual sewage and the simulated sewage used in the laboratory model. Towards this end, extensive column settling tests were performed by Beak Consultants, Ltd. on both actual sewage and the simulated materials. The report prepared by Beak, Physical and Settling Characteristics of Particulates in Combined Sewer Overflow, Sanitary Wastewater and Urban Stormwater, describes the details of the test procedures. The column test data can be used to prepare a frequency distribution of the particle settling velocities which can be utilized to compare settling properties of different materials.

where

ψ = stream function
η = vorticity
F = nondimensional stream function
M = nondimensional vorticity function
N = non-dimensional tangential velocity function
r = radial coordinate
z = vertical coordinate
U_{ref} = reference velocity
L = reference length

The stream function, ψ, is defined so that

$$u = \frac{1}{r}\frac{\partial \psi}{\partial z} \tag{8}$$

$$w = -\frac{1}{r}\frac{\partial \psi}{\partial r}, \tag{9}$$

thereby automatically satisfying the continuity equation

$$\frac{1}{r}\frac{\partial (ru)}{\partial r} + \frac{\partial w}{\partial z} = 0 \tag{10}$$

The equations of motion are then solved, using relaxation techniques to obtain a steady state solution. Once the numerical values of f, Ω, and G are obtained, the velocity components (u, v, w) in the axisymmetric coordinate system (r, θ, z) can be found from

$$\frac{u}{U_{ref}} = \xi \frac{\partial f}{\partial \xi} \tag{11}$$

$$\frac{w}{U_{ref}} = -\left(2f + \xi \frac{\partial f}{\partial \zeta}\right) \tag{12}$$

$$\frac{v}{U_{ref}} = \xi G \tag{13}$$

b. Test Results for Actual Sewage: Figures 72 through 75 depict the composite results of column settling tests performed by Beak on Philadelphia sewage. The data points occur in triplicate representing three separate test runs. The data have also been grouped by sampling port location to identify the extent to which flocculation is occurring.

The method for detecting flocculation effects from settling column tests has been described in a paper by Camp.[8] It involves the assumption that a settling column is filled with a uniformly mixed dispersion of particles at time zero. Samples are then withdrawn at several column depths at different times. Assuming no flocculation or particles interactions, each particle will move at its free fall settling velocity. At time zero, samples

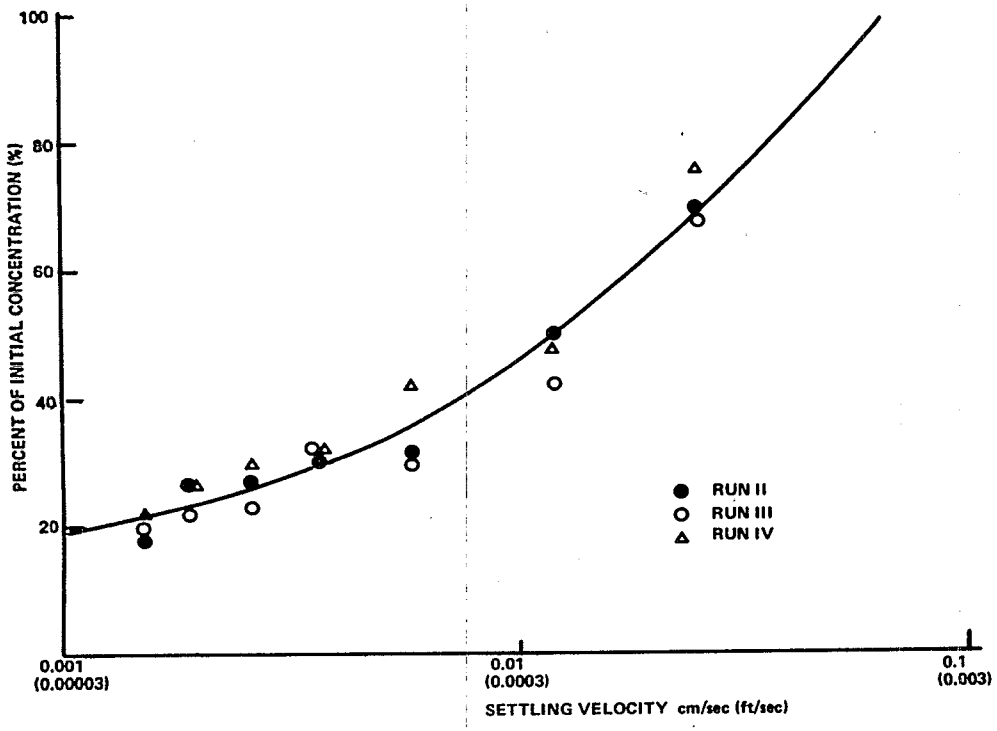

FIGURE 72 SETTLING VELOCITY DISTRIBUTION AT 30.5cm (1 ft) COLUMN SAMPLE PORT

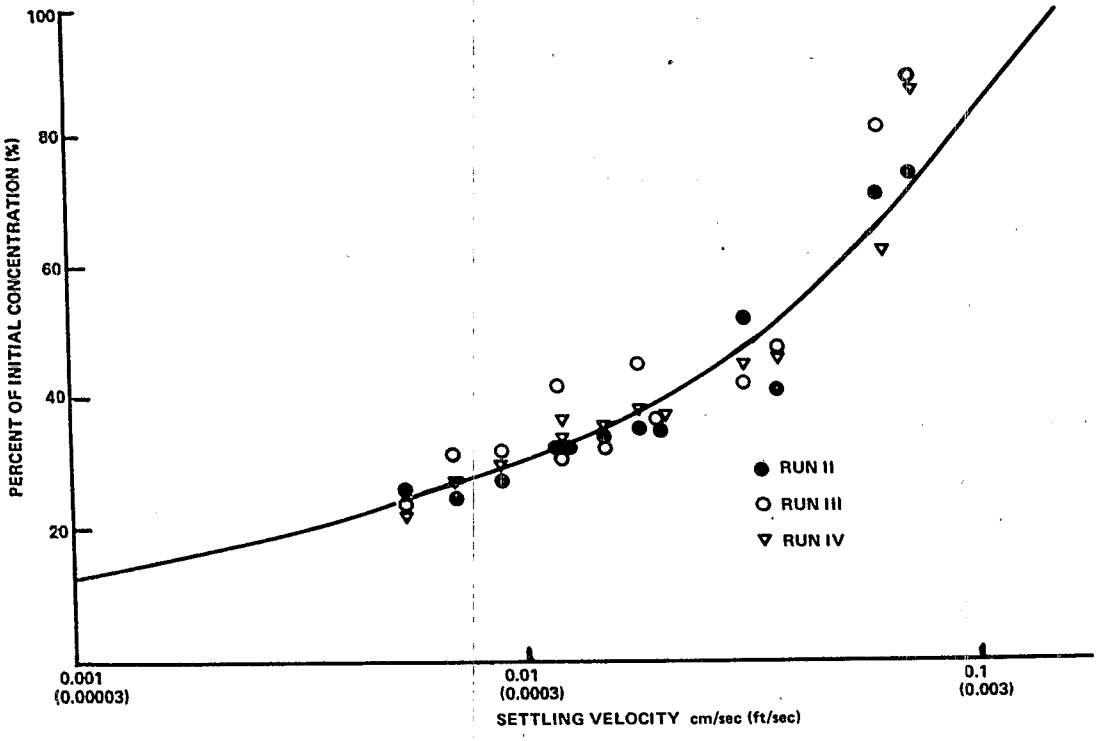

FIGURE 73 SETTLING VELOCITY DISTRIBUTION AT 61 and 91cm (2 and 3 ft) COLUMN SAMPLE PORT

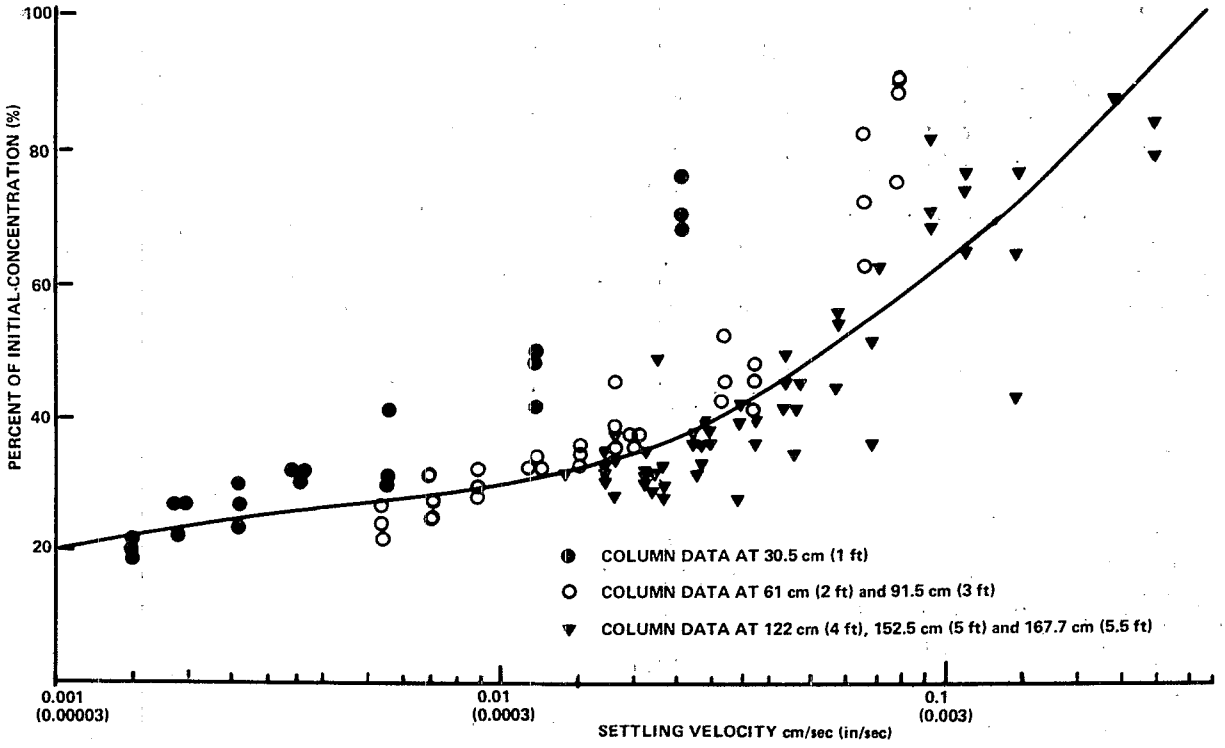

FIGURE 74 SETTLING VELOCITY DISTRIBUTION FOR ALL SAMPLE PORTS

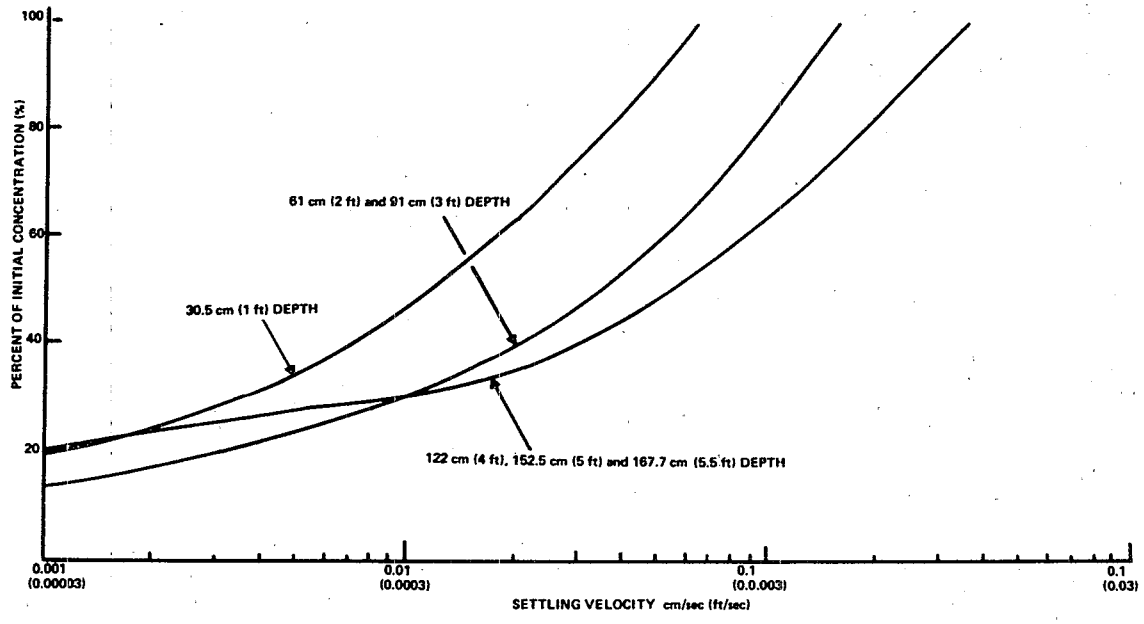

FIGURE 75 SETTLING VELOCITY DISTRIBUTION AT VARIOUS COLUMN DEPTHS

withdrawn from each sample port will thus have the same particle concentration. Inasmuch as particles passing by the sample port will be exactly replaced by particles above the sampling point, the concentration should remain uniform immediately after time zero. If it is then assumed that the particles with the highest settling velocity move at velocity V_1, the last fraction of particles with settling velocity V_1 will pass the first sample point located at depth Z_1 when $t_1 = Z_1/V_1$ as shown in Figure 76. Thus, at time t_1 the particle concentration of sample point Z_1 will change to reflect the absence of particles having a settling velocity V_1. If this principle is followed for all particles, a time versus concentration plot is obtained at each sample point. The same concentration change and distribution should be observed at the second sample located at depth Z_2 beginning at time $t_2 = Z_2/V_1$. Thus, identical curves should be obtained at subsequent sample points except for a shift in time. This time shift can be accommodated by plotting C versus Z/t for each sample port. In actuality, C has been non-dimensionalized by dividing the initial concentration C_o and plotted versus Z(sample port)$/t$ to provide a distribution of settling velocities.

If flocculation occurs in the column, particles will interact, agglomerate, and accelerate. This will result in an alteration of the time versus concentration relationship. Proceeding down the column, higher concentrations will be obtained in a relatively shorter time period, and the plot of C/C_o versus Z/t will be shifted to reflect the increased settling velocity as shown in Figure 75. Thus, instead of having one settling velocity distribution for all sampling points, separate curves can be drawn at each sampling point.

It is apparent from the data shown on Figure 75, that different settling velocity distributions are occurring at the lower depths, as a result of flocculation. Figure 75 illustrates this relative effect by overlaying curves fitted to data at different sample depths. At the 30.5 cm (1 ft) depth, 50 percent of the initial particles had a settling velocity less than 0.012 cm/sec (0.00039 ft/sec). At the 61 cm (2 ft) and 91.5 cm (3 ft) depth, 50 percent of the particles had a settling velocity less than 0.034 cm/sec (0.0011 ft/sec) and only about 33 percent had a settling velocity less than 0.012 cm/sec (0.00039 ft/sec). Finally, from 1.22 m (4 ft), 1.52 m (5 ft) and 1.67 m (5.5 ft) depth data, 50 percent of the particles had a settling velocity less than 0.055 cm/sec (0.0018 ft/sec). Thus, the median settling velocity increased from 0.012 (0.00039 ft/sec) to 0.055 cm/sec (0.0018 ft/sec) as the particles settled through the column. This indicates an increase by a factor of 4 to 5 of the median settling velocity attributable to flocculation. It can be assumed that the flocculation is more effective in increasing the settling velocity of the larger particles since the largest difference in the three curves occurs at the higher velocities.

Test Results for Simulated Sewage

Although many potentially applicable materials were examined by Beak Consultants, only three materials were found suitable for the performance testing of the laboratory hydraulic model. These materials were shredded petrothene, 100-200 mesh IRA-93 resin, and Arizona Road Dust. The settling velocity distributions for these materials appear as Figures 10 through 12 in the Beak report. No flocculation effects were reported by Beak and a single settling velocity distribution was fitted to all the data points independent of sampling depth. The discrepancies in the three runs for IRA-93 are a result of sieving techniques and will be discussed in detail in a later section.

Settling Theory

A literature search was conducted to identify the mathematical expression for describing the relationship between particle concentration and particle settling velocity. At low particle concentrations, particle interaction is minimal and each particle settles at its free fall velocity. In this region particle settling velocity can be considered independent of depth and concentrations. As the particle concentration rises the probability of particle interaction increases and two phenomena can occur.

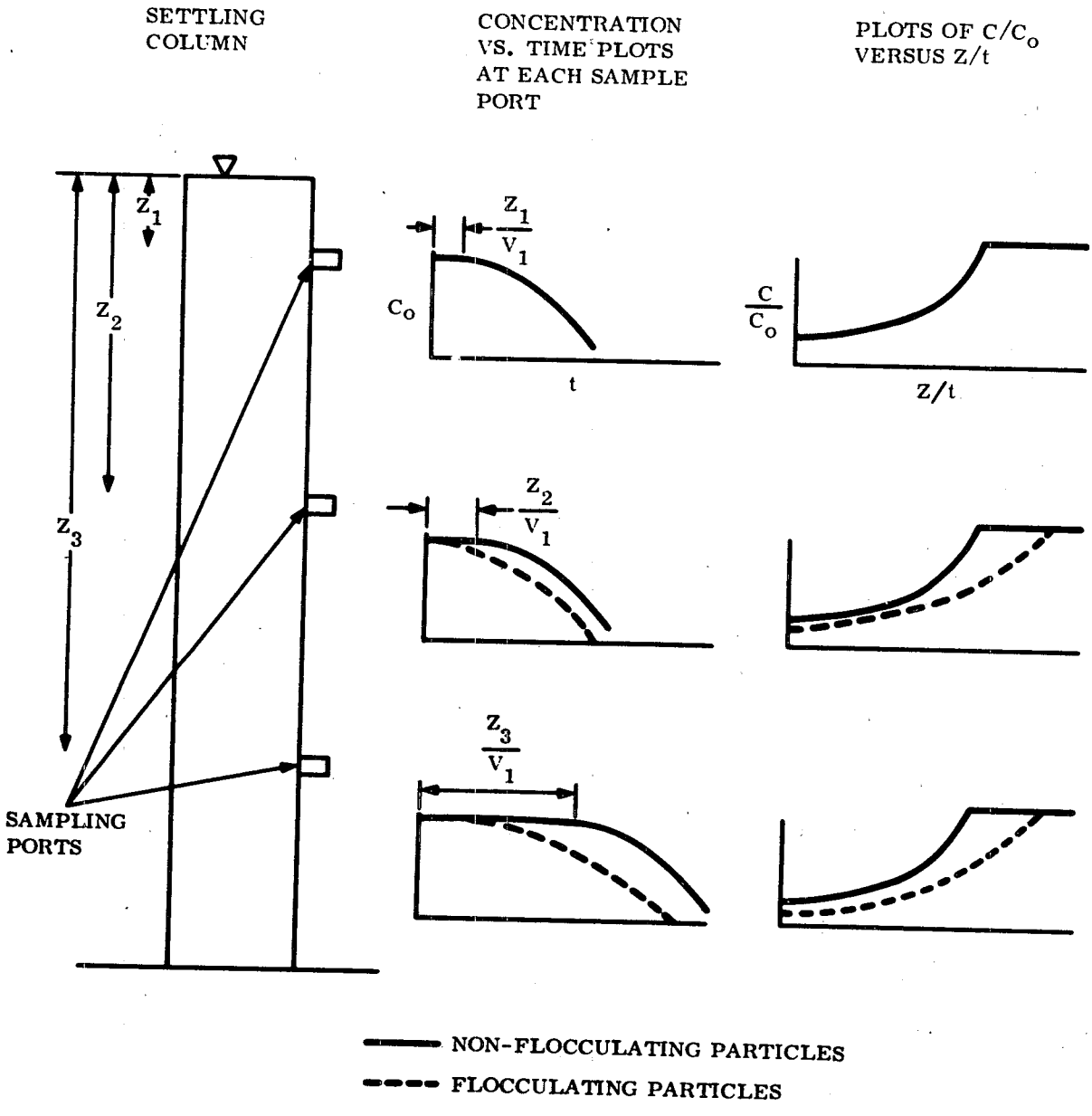

FIGURE 76 SETTLING COLUMN DATA INTERPRETATION FLOCCULATION vs NONFLOCCULATING PARTICLES

One of these phenomena is called "hindered settlement." In the regime of "hindered settlement" the particles continuously collide with one another, resulting in a decrease of the individual particle settling velocities. Camp[8] states that for raw sewage, a solids concentration of greater than 1,000 ppm must be reached before hindered settlement will be encountered. Concentrations of solids within the swirl concentrator will only approach 1,000 ppm towards the bottom of the tank. Since most of particle settling will occur in the main body of the tank, hindered settling should not be a major factor in determining removal efficiency.

The second phenomenon which can alter the particle settling velocity is flocculation. Flocculation causes an increase in settling velocity by the agglomeration, or clumping together of small particles to form larger and heavier particles. The ability of a suspension to exhibit flocculation properties depends primarily on particle chemistry and electrostatic charge. Assuming that a material has flocculating properties, agglomeration can occur at relatively low concentrations and it varies directly with particle concentration. Raw sewage can exhibit flocculation at relatively low concentrations (230 ppm) as noted by the Beak data. A detailed review of the major mechanisms responsible for flocculations and agglomeration follows.

Agglomeration Mechanisms

Agglomeration results from particle collisions induced by gravity, shear, and turbulence, as will be discussed in greater detail. The agglomeration of small particles tends to increase the average particle size, and thus improve the settling properties of the suspension.

The efficiency of the agglomeration (or flocculation) process depends on the number of particle collisions. Of course, not all particle collisions result in agglomeration. The particles may slide past each other or, in the case of a stable colloid, they may repel each other electrostatically. Nevertheless, particle collisions are a necessary condition for agglomeration, and the number of collisions per unit volume per time can be used to estimate the maximum rate at which agglomeration may occur. A review of the rather extensive literature on flocculation and coagulation processes has revealed five basic mechanisms which result in particle collisions. These mechanisms are discussed briefly below, and the appropriate collision rate equations for the case of spherical particles are summarized in Table 19.

TABLE 19
COLLISION RATES FOR VARIOUS MECHANISMS

Equation	Collision Mechanism	Collision Rate Equation	Ref.
(14)	Gravity	$N_{ij} = \frac{2\pi}{9\nu} (r_i + r_j)^2 \left\| r_i^2 - r_j^2 \right\| \left(\frac{\rho_p}{\rho_w} - 1\right)^{1/2} g\, n_i n_j$	3
(15)	Shear Flow	$N_{ij} = \frac{4}{3} (r_i + r_j)^3\, n_i\, n_j\, G'$	4
(16)	Turbulent Acceleration	$N_{ij} = \frac{2\sqrt{3}}{9\nu} (r_i + r_j)^2 \left\| r_i^2 - r_j^2 \right\| \left(\frac{p_p}{p_w} - 1\right) \left(\frac{\epsilon'^3}{\nu}\right)^{1/4} n_i\, n_j$	5
(17)	Turbulent Entrainment	$N_{ij} = \sqrt{\frac{8\pi}{15}} (r_i + r_j)^3\, n_i\, n_j \sqrt{\frac{\epsilon'}{\nu}}$	3
(18)	Brownian Motion	$N_{ij} = \frac{2kT}{3\nu} (r_i + r_j) \left(\frac{1}{r_i} + \frac{1}{r_j}\right) n_i\, n_j$	4

ν = kinematic viscosity
r_i = diameter of particle i
r_j = diameter of particle j
ρ_p = density of particle
ρ_w = density of liquid
ϵ' = energy dissipation per unit mass
n_i = number density of particle i
n_j = number density of particle j
N_{ij} = number of collision of i particles with j particles
G' = shear rate of flow

1. Gravity: Particles settling under the influence of gravity settle at different rates, depending on their size and specific gravity. Faster settling particles tend to overtake slower particles, resulting in collisions. For small particles settling in the Stokes flow regime, the collision rate is given by equation (17) of Table 19. If the particles are of the same size ($r_i = r_j$), no collision will occur. Acceleration of the ambient fluid will also cause collisions. The collision rate in an accelerated fluid can be obtained by replacing g in equation (14) with the fluid acceleration Du/Dt. For the present application, the fluid acceleration is several orders of magnitude smaller than the gravitational acceleration, and may be neglected.

2. Shear Flow: In a shear flow pattern, adjacent streamlines move with different velocities. A particle moving along one streamline may, therefore, overtake and collide with a particle on an adjacent streamline. The collision rate depends upon the collision cross section ($r_i + r_j$), and upon the shear rate of the flow G' (ft/sec/ft) as given by equation (15).

3. Turbulent Acceleration: In a turbulent flow pattern, two or more large eddies is generally small (compared with gravity), but the small eddies in the viscous dissipation range can have larger accelerations, given by[5]

$$a = \sqrt{3}\left(\frac{\epsilon'^3}{\nu}\right)^{1/4} \qquad (19)$$

in which ϵ' is the energy dissipation per unit mass, and ν is the kinematic viscosity. This mechanism is only applicable where the particles are smaller than the scale size, λ, of the energy dissipating eddies, where[4]

$$\lambda = \left(\frac{\nu^3}{\epsilon'}\right) \qquad (20)$$

As in the case of gravity, no collisions occur for particles of the same size, since both experience the same acceleration.

4. Turbulent Entrainment: If the particles are comparable in size to λ, collisions will result when a particle entrained in one turbulent eddy collides with a particle entrained in another turbulent eddy. This mechanism provides for collisions of particles of the same size, in contrast to the acceleration effect of turbulence discussed above.

5. Brownian Motion: Particles undergoing random Brownian motion due to collisions with molecules of the ambient fluid will collide. However this mechanism is only significant for very small particles (less than 1 μ).[5]

The collision rates given in Table 17 are not additive. Saffman and Turner have shown[9] that the combined effect of turbulent acceleration, turbulent entrainment, and gravity can be approximated by root-sum-squaring the individual expressions given in Table 17.

Agglomeration Kinetics

If the particles in suspension are discrete sizes, a system of equations may be derived to describe the rate of change of the number density of the i^{th} species:[5]

$$\frac{dn_i}{dt} = \sum_{j=1}^{i-1} N_{j,\,i-j} - \sum_{j=1}^{\infty} N_{ij} \qquad (21)$$

In equation (21) the number density of the i^{th} size particle is n_i, and N_{ij} are the collision rates between particles of size i and size j. It is assumed that the collision of an i particle and a j particle results in coalescence to form a particle of size $i + j$ with radius

$$r_{i+j} = (r_i^3 + r_j^3)^{1/3} . \qquad (22)$$

The first term on the right hand side of equation (21) is the sum over all collision which results in the formation of an i-size particle. For the collision rate $N_{i,k}$ between particles of size j and size k, i-size particles are produced only when $j + k = i$. The second term on the right of equation (21) is the rate of depletion of i-size particles, due to collision with all other possible particle sizes.

Equation (21) represents a system of equations; one equation for each discrete particle size. Numerical solution of these equations is possible, but very time-consuming. Such solutions have been performed by Gemmel,[10] Fair and Gemmel,[12] Ives,[13] and Hidy,[14] for various collision mechanisms.

Where the particle size distribution is continuous rather than discrete, the

coagulation process can be described with an integro-differential equation for the continuous distribution function $n(r,t)$ which is defined such that $n(r,t)\cdot dr$ is the number of particles per unit volume of size range from r to $r + dr$. The total number of particles per cubic centimeter, N_∞ is then

$$N_\infty(t) = \int_0^\infty n(r,t)\, dr. \tag{23}$$

The equation for the continuous distribution function $n(r,t)$ is analagous to equation (21) for the discrete case, and is given by

$$\frac{d}{dt} n(r,t) = \int_0^r N(\tilde{r}, (r^3 - \tilde{r}^3)^{1/3})\, d\tilde{r} - \int_0^\infty N(r,\tilde{r})\, d\tilde{r} \tag{24}$$

In equation (24), $N(r,\tilde{r})$ is the collision rate between particles size r and $\tilde{r}$. As in equation (21), the first integral on the right represents the rate of production of size r particles, and the second term represents their depletion due to collisions with all other sizes.

Friedlander, has shown that for a settling aerosol undergoing coagulation by Brownian motion, a similarity transformation for equation (24) is possible. The size distribution function, expressed in similarity variables, does not change with time. In particular, $n(v,t)$ is expressed as

$$n(v,t) = \frac{N_\infty^2}{\phi}\, \psi_1\left(\frac{vN_\infty}{\phi}\right) \tag{25}$$

where v is the particle volume, ψ, is a non-dimensional distribution function and θ, is the total volume fraction of particles.

$$\phi = \int_0^\infty v\, n(v)\, dv. \tag{26}$$

Using equation (25) in equation (24) results in an ordinary differential equation for ψ', in terms of the similarity variable $\eta = vN_\infty/\theta$.

The same similarity transformation was applied to coagulation by laminar shear flow by Swift and Friedlander. However for the case where both mechanisms (Brownian motion and laminar shear) are operative, the self-preservation hypothesis does not work.

In the present application to a nonhomogenous turbulent flowing system, none of the solution techniques described above are applicable. Equations (21) and (24) are both derived for homogenous systems. To include the spatial variations in the distribution function, $n(r,t)$, the time derivative in equation (24) must be replaced by the substantive derivative along streamlines

$$\frac{dn}{dt} \rightarrow \frac{\partial n}{\partial t} + \vec{V}\cdot \nabla n. \tag{27}$$

In addition, because of turbulence, an additional source term appears on the right hand side of equation (24) to account for dispersion of particles across streamlines, due to turbulence. The appropriate equation therefore is

$$\frac{\partial n}{\partial t} + \vec{V}\cdot \Delta n = \int_0^r N(r, (r^3 - \tilde{r}^3)^{1/3})\, d\tilde{r} - \int_0^\infty N(r,\tilde{r})\, d\tilde{r} + \nabla\cdot(\epsilon_p \nabla n) \tag{28}$$

where ϵ_p is the particulate eddy diffusivity. In equation (28), n is now a function of both space and time, i.e., $n = n(r,\tilde{x}, t)$.

The solution to equation (28) is extremely complicated. An approximate method can be developed in which the local distribution function $n(r,t)$ is approximated with a Gaussian profile

$$n(r, \vec{x}, t) \cong \frac{N_\infty}{\sigma\sqrt{2\pi}}\, exp\left(-\frac{(r-a)^2}{2\sigma^2}\right) \tag{29}$$

in which the mean radius a, standard deviation, σ, and total number density of particles N_∞, are each functions of space and time. Equations for N_∞, a, and σ can be derived by taking moments of equation (28). Using equation (29), the second of the integrals which appear in (28) can be evaluated in closed form for any of the individual collision mechanisms of Table 19. However, closed form integration is not possible with more than one mechanism

operative. Also, the first integral in equation (28) cannot be evaluated in closed form for even a single collision mechanism.

Consequently, it appears that the solution to the coagulation kinetics equation is impractical in the present application. Instead, an order of magnitude estimate has been made of the collision frequencies for each of the mechanisms in Table 19. From these numerical estimates, several important conclusions can be drawn regarding the design of the primary settler.

NUMERICAL ESTIMATES FOR COLLISION FREQUENCIES BY VARIOUS MECHANISMS

The settling column data by Beak can be used to determine the probable size range of particulates in sanitary sewage. The GE analysis of the data from the 1.22, 1.52 and 1.67 m (4, 5 and 5.5 ft) depths (Figure 74) shows that 25 percent of the particles settle slower than 0.003 cm/sec (0.00098 ft/sec), 50 percent settle slower than 0.055 cm/sec (0.0018 ft/sec) and 75 percent settle slower than about 0.13 cm/sec (0.043 ft/sec). The settling velocity of a spherical particle in the Stokes flow regime is

$$w_s = \frac{2}{9}\,\frac{g}{\nu}\,(S_g - 1)\,r^2 \,. \qquad (30)$$

Equation (30) can be used to estimate the particle size from the measured settling velocity data if the specific gravity is known. Since the specific gravity is not known, values of 1.01 and 1.05 were assumed in order to obtain the particle sizes corresponding to the 25 percent, 50 percent, and 75 percent settling velocities given above. The results of this calculation are summarized in Table 20.

For each of the particle sizes in Table 20, the number of particles per cc required to give a total concentration C, of 100 mg/l solids was calculated from

$$n = \left(100\,\frac{mg}{l}\right)\left(\frac{1l}{1000\ \text{cc}}\right)\left(\frac{3}{4\pi r^3}\ \frac{particles}{cc}\right)\left(\frac{1}{\rho_p}\ \frac{cc}{gm}\right)\left(\frac{1gm}{1000mg}\right) = \frac{3\times10^{-4}}{4\pi r^3 \rho_p} \,. \qquad (31)$$

The resulting number densities are also tabulated in Table 20.

An estimate of the collision rate from each of the mechanisms in Table 18 was next obtained under two assumptions.

a. Assume 100 mg/l of particles at the 25 percent settling rate, and 100 mg/l at the 75 percent settling rate.
b. Assume 200 mg/l of particles at the 50 percent settling rate.

Assumption (a) is a bimodal distribution, with two discrete particle sizes. Assumption (b) corresponds to a mono-disperse system of a single particle size. These calculations were performed for each of the two specific gravities 1.01 and 1.05. The calculations are outlined below for assumption (a) at 1.01 specific gravity.

(1) Gravity

$$N_{ij} = \frac{2\pi}{9\nu}\,(r_i + r_j)^2\left|r_i^2 - r_j^2\right|\left(\frac{\rho_p}{\rho_w} - 1\right)g n_i n_j$$

$$= \frac{2\pi}{9\,(0.011\ cm^2/sec)}\,(0.0246 + 0.00373)^2\left|0.0246^2 - 0.00373^2\right|\left(\frac{1.01}{1} - 1\right)(980.7\ cm/sec^2)\times(1.59\ cm^{-3})\,(4550\ cm^{-3})$$

$$= .219\ collisions/cc/sec$$

TABLE 20
PARTICLE SIZE AND NUMBER DENSITY FOR VARIOUS SETTLING VELOCITIES

Specific Gravity (gm/cc)	Settling Velocity cm/sec	Settling Velocity in/sec	Equivalent Spherical Radius cm	Equivalent Spherical Radius in	Number Density for 100 mg/l cm^{-3}
	0.13	(0.05)	0.0246	(0.009)	1.59
1.01	0.055	(0.02)	0.0160	(0.006)	5.76
	0.003	(0.001)	0.00373	(0.0015)	455.
	0.13	(0.05)	0.0112	(0.044)	16.2
1.05	0.055	(0.02)	0.00731	(0.003)	58.0
	0.003	(0.001)	0.00171	(0.0007)	4,540.

(2) Shear Flow

$$N_{ij} = \frac{4}{3} (r_i + r_j)^3 \; n_i \, n_j \, G'$$

The mean shear rate is obtained from the swirl separator. Since this function is used in the eddy viscosity formulation, it was a simple matter to average its value over the cross section. The resulting value of G' for the prototype scale separator is 0.209 sec^{-1}.

Consequently, for $sg = 1.01$ and $r_i \neq r_j$

$$N_{ij} = \frac{4}{3} (0.0246 + 0.00373)^3 \; (1.59)$$
$$(455) \; (0.209) = 0.00458 \; \textit{collisions/cc/sec}$$

(3) Turbulent Acceleration

$$N_{ij} = \frac{2\sqrt{3}\pi}{9\nu} (r_i + r_j)^2 \left| r_i^2 - r_j^2 \right| \left(\frac{\rho_p}{\rho_w} - 1 \right) \left(\frac{\epsilon'^3}{\nu} \right)^{1/4} n_i \, n_j$$

The turbulent energy dissipation is estimated, assuming that the energy inflow is entirely dissipated in the outer annulus.

The energy dissipation per unit mass is

$$\epsilon' = \frac{Q}{V} \frac{\Delta p}{p} \qquad (32)$$

The volume flowrate $Q = 0.52$ m^3/sec (17.65 cfs), prototype (1 l/sec model scale). The head loss, ΔP is

$$\Delta p = \frac{1}{2} \rho v^2 \qquad (33)$$

where the entrance velocity of the 1.22 m (4 ft) entrance sewer is

$$v = \frac{Q}{\left(\frac{\pi D^2}{4} \right)} = \frac{17.65}{\frac{\pi (4)^2}{4}} = 1.4 \, fps \; (0.43 \; m/sec)$$

so that $\Delta P = 1/2$ (10 4 kg/m^3) $(0.43)^2 = 9.6$ kg/m^3 [$\Delta P = 1/2$ (2 $slugs/ft^2 = 1.9$ lb/ft^2.] (9 x 10^{-4} atm). The volume of the outer annulus is about 60.88 m^3 (2,150 ft^3). Then from equation (32)

$$\epsilon' = \frac{(17.65)(1.9)}{(2150)(2)} = .00782 \; ft^2/sec^3$$
$$= 7.26 \; cm^2/sec^3 \; (1.13 \; in^2/sec^3)$$

This energy dissipation rate corresponds to an equivalent shear rate $G' = \sqrt{\epsilon'/\nu}$ of 26 sec^{-1}. The equivalent acceleration, a, is equation (19)

$$a = \sqrt{3} \left(\frac{\epsilon'^3}{\nu} \right)^{1/4} = \sqrt{3} \left[\frac{7.25^3}{0.011} \right]^{1/4}$$
$$= 23.7 \; cm/sec^2 \; (9.33 \; in/sec^2)$$

Since equations (14) and (15) for the collision rate due to gravity and turbulent acceleration are identical, except for the acceleration rate used, the collision rate for the former can be found as the ratio

$$(N_{ij})_{turb \; accel} = (N_{ij})_{gravity} \left(\frac{a}{g} \right)$$
$$= (.219) \; \frac{23.7}{980.7} = .00528 \; \textit{collisions/cc/sec}$$

(4) Turbulent Entrainment

$$N_{ij} = \sqrt{\frac{8\pi}{15}} (r_i + r_j)^3 \; n_i \, n_j \sqrt{\frac{\epsilon'}{\nu}}. \qquad (17)$$

(appears previously in Table 1)

Using the previous result for the energy dissipation per unit mass, ϵ',

$$N_{ij} = \sqrt{\frac{8\pi}{15}} \; (0.0246 + 0.00373)^2 \; (1.59) \; (455)$$
$$\left[\frac{7.26}{0.011} \right]^{1/2} = 8.62 \; \textit{collisions/cc/sec}$$

The results of these order of magnitude calculations are summarized in Table 21. It can be concluded from this table that turbulent entrainment and gravity are the principal mechanisms for promulgation of flocculation in the swirl concentrator.

Summary

In order to extrapolate the results of the hydraulic model testing to prototype design, it is necessary to understand the differences in settling properties between the laboratory simulated sewage and actual sewage. From column test results performed by Beak, it can be concluded that the materials in the laboratory model settle as discrete particles, while actual sewage exhibits flocculation properties even at low concentrations.

A detailed analysis of the kinetics of flocculation was performed. It was found that for flocculant materials, the degree to which flocculation and agglomeration occur depends largely on the number of particle collisions. Theoretical expressions were developed for the five basic mechanisms which can cause particle collision. These mechanisms are:

TABLE 21
ESTIMATED COLLISION RATES

Size Assumption		Collision Rates - Collisions per cc per sec Gravity	Shear	Turbulent Acceleration	Turbulent Entrainment
Sg = 1.01	$r_1 \neq r_2$	0.22	0.0046	0.0053	8.6
	$r_1 = r_2$	0.	0.00015		0.29
= 1.05	$r_1 \neq r_2$	4.8	0.044	0.12	83.
	$r_1 = r_2$	0.	0.0015		2.8

1. Gravity: Differential settling rates

2. Shear: Differential flow velocities along adjacent streamlines

3. Turbulent Accelerations: Entrainment of two or more particles in a single accelerating turbulent eddy

4. Turbulent Entrainment: Entrainment of particles in separate turbulent eddies which collide

5. Brownian Motion: Random motion caused by thermal energy of water molecules.

These expressions were used to obtain order of magnitude estimates for the number of collisions which can result from each mechanism at the flow conditions existing in the swirl concentrator. Of the five mechanisms, only gravity and turbulent entrainment appear to be significant. The turbulent entrainment mechanism is most important in the outer annulus of the concentrator where most of the inlet energy is dissipated.

It is most important to recognize that the theoretical analysis of flocculation only predicts the number of collisions or the maximum tendency toward flocculation. The actual adherence of particles to each other depends on the chemistry as well. It may well be that there is a limiting amount of flocculation which can occur as a result of other conditions. If this is the case, an increase in collisions beyond the number required to reach this threshold will not result in additional improvement in settling rates.

The column tests performed by Beak on sanitary sewage showed that a fourfold increase in the median settling velocity can be observed as a result of the gravity flocculation mechanism alone. Whether further improvement can be attained via the turbulent entrainment mechanism in the outer annulus of the swirl concentrator is unknown.

Exact mathematical modeling of the flocculation effects on the particle settling rate was deemed numerically impractical for this study. Therefore, to accommodate the flocculation of actual sewage, a settling velocity distribution indicative of the sewage after flocculation was assumed. This approach assumed after flocculation occurring in the inlet sewer and outer annulus of the swirl concentrator via gravity and turbulent entrainment mechanisms will produce a settling velocity distribution equivalent to that obtained by the gravity mechanism in the settling column test. This assumption would appear to be conservative since further improvements in settling properties might occur in the swirl concentrator.

PARTICLE FLOW CALCULATIONS

Particle Paths

Once the liquid flow has been determined the particle velocities can be determined by superimposing the particle settling rate, w_s, at each mesh point. Thus,

$$U_p = U_L \tag{34}$$

$$v_p = v_L \tag{35}$$

$$w_p = w_L + w_s \tag{36}$$

where w_s = particle settling velocity the p and L subscripts designate the particle and liquid velocity components.

The particle paths can be found by superimposing a stream function due to settling, ψ, on the liquid flow. Thus, the particle stream function ψ_p is

$$\psi_p = \psi(r,z) + \psi'(r) \tag{37}$$

where $\psi'(r)$ is defined such that

$$w_s = -\frac{1}{r}\frac{\partial \psi'}{\partial r} \tag{38}$$

or

$$\psi' = \frac{-w_s}{2} r^2. \tag{39}$$

The particle paths for a given settling velocity, w_s, are then determined by plotting lines of constant.

The particle paths obtained provide a method for visualizing the mean trajectories of the particles in the chamber. In actuality, turbulence will cause particles of a given settling path. The particle paths do not provide any information as to the concentration field. To define the concentration field, it is necessary to utilize the particle mass continuity equation as defined in the following section.

Particle Flow Equations

Particle concentrations throughout the swirl concentrator are determined by substituting the particle velocities at each mesh point, as defined by equations (34) through (36), into the particle continuity equation (40).

$$\frac{\partial c}{\partial t} + \nabla \cdot (\vec{V}_p C) = \nabla \cdot (\epsilon_p \nabla C) \tag{40}$$

where

V_p = particle velocity vector
C = particle concentration
t = time
ϵ_p = turbulent eddy diffusity

The use of Equations 34-36 for V_p assumes that inertial acceleration terms are negligible when compared to the gravity acceleration, so that particles always move at their equilibrium settling velocity with respect to the liquid flowfield.

The values of the velocities at each grid point are obtained directly from the liquid flowfield solution. The boundary conditions for the particle concentrations along the chamber wall are specified and a relaxation technique is applied to reach a steady state concentration. Removal efficiencies are then computed from mass balances utilizing the computed concentration field and specified flowrates.

Boundary Conditions

The boundary conditions for equation (40) are as follows: at the inlet, the concentration is a specified constant value, C_o. At a solid surface the total mass flux must be zero. Mathematically this can be expressed by

$$(-\vec{V}_p C + \epsilon_p \nabla C) \cdot \vec{n} = 0 \tag{41}$$

where n is the unit inward normal. The first term in equation (41) is the convective mass flux, and the second term is the mass flux due to diffusion. Equation (41) can be rewritten

$$-c(\vec{V}_p \cdot \vec{n}) + \epsilon_p \frac{\partial c}{\partial n} \tag{42}$$

velocity component normal to a solid surface the term $\vec{V}_p \cdot \vec{n}$ must equal the component of inward normal, $\vec{n}$.
where $\partial/\partial n$ denotes the directional derivative normal to the wall. Since the liquid has no velocity component normal to a solid surface, the term $\vec{V}_p \cdot \vec{n}$ must equal the component of the settling velocity normal to the wall, i.e.

$$-cw_s n_z + \epsilon_p \frac{\partial c}{\partial n} = 0 \tag{43}$$

in which n_z is the z-component of the unit inward normal, $\vec{n}$.

The derivative in equation (43) can be replaced with the first order finite difference approximation

$$\frac{\partial c}{\partial n} \cong (C_{b+1} - C_b)/\Delta n \tag{44}$$

in which C_b denotes the boundary value, C_{b+1} is the value at the interior point, and Δ_n is the distance from C_{b+1} to C_b. The result is an equation for the boundary value in terms of the interior point.

$$C_b = \frac{C_{b+1}}{1+R} \tag{45}$$

where

$$R = \frac{w_s \Delta n n_z}{\epsilon_p} \quad (46)$$

For the special case of a vertical wall, n_z = 0 so that R = 0 and the boundary condition becomes

$$C_b = C_{b+1} \quad (47)$$

Underneath the horizontal weir, n_z = 1 (z is positive downward so that w_s is positive), and equation (45) is the correct boundary condition, with $R > 0$. If the settling velocity and mesh spacing are sufficiently small that $R << 1$, equation (45) gives a wall concentration C_b, nearly equal to C_{b+1}. However if R becomes large, the concentration at the boundary becomes much smaller than at the interior point. Provided the settling velocity, w_s, is larger or at least comparable to the mean liquid upflow velocity, w_s, then C_{b+1} will itself be small (because few particles can reach the upper region of the separator), and no numerical difficulties occur. This situation corresponds to the case studied in the earlier application of the swirl concentrator to stormwater overflows.[1]

A problem arises when R is large but the settling velocity is small compared with w. In this case, a large number of particles reach the upper region of the concentrator, and C_{b+1} is nearly equal to the inlet concentration, C_o. Then equation (45) requires $C_b << C_{b+1}$, which appears as a discontinuity in the concentration field, causing numerical problems. Physically, a large R and small w_s means that the concentration is high except for a thin layer (smaller than one mesh space) immediately under the weir. This is exactly the situation for the proposed design, for which w_s is typically 0.05 cm/sec (0.00164 ft/sec) while the prototype mean upflow velocity (at 0.52 m^3/sec [17.1 cfs]) is approximately 1.3 cm/sec (0.0043 ft/sec). The R value for this case (with mesh spacing of 15 cm [0.5 ft]) is

$$R = \frac{(0.00164)(0.5)}{1.2 \times 10^{-5}} = 68$$

Thus, the large gradient in concentration under the weir occurs in a distance much smaller than the 15 cm (0.5 ft) mesh spacing. Under these circumstances, the proper boundary condition is to neglect this very small region and assign $C_b = C_{b+1}$.

A similar difficulty occurs at the bottom of the separator. In this case, the z-component of the inward normal, n_z, is negative (-1 along the horizontal portion, and - cos 60° along the sloping wall). Since R (from equation (45)) is then negative, the boundary condition calculated from equation (45) can only be used if R=1. Where this condition is satisfied (either because a very fine mesh is used, or because the settling velocity is small), the concentration gradient at the wall can be included within the computational mesh by applying equation (47).

When R is large (as in the present case), the concentration buildup at the wall due to sedimentation occurs in a region too small to be resolved with the computational mesh. The sediment layer must therefore be excluded from the computational region. Once this is done, some other criteria must be applied in order to specify the mass flux normal to the wall, Q_n, where

$$Q_n = -cw_s n_z + \epsilon_p \frac{\partial c}{\partial n} . \quad (48)$$

For example, Q_n can be positive or negative depending on whether deposition or scouring of the sediment layer is occurring.[2] If these mechanisms are in balance (no deposition or scour) then Q_n = 0.

The specification of the mass flux for the general case is quite difficult. As discussed by Chen,[11] Q_n is usually approximated by an empirical formula as a function of the local mean velocity of the main flow,[12] a function of the local velocity at the bottom,[13,14] a function of the boundary shear and critical shear stresses of the Yalin type,[15,16] or a function of the local mean velocity and depth of the main flow such as the Meyer-Peter and Muller type[17].

For a properly designed settling tank, no scouring should occur, and Q_n will always be positive along the bottom. In the present design, the inlet velocity may be high enough to scour the bottom near the inlet annulus. Where scouring does occur, the sediment deposit will eventually be removed, so that in the steady state Q_n = 0 for these regions.

The simplest hypothesis for the bottom boundary condition in the settling chamber is to assume the bottom boundary points can then be determined by treating them as interior points, except that one-sided difference approximations must be used. Particles reaching the bottom of the separator are thus assumed to pass outside the computational mesh into a thin sediment layer from which no re-suspension occurs. This procedure will tend to over-predict the efficiency of the chamber, because re-suspension of the bottom sediment is neglected.

To summarize these findings, Table 22 has been prepared to indicate under what conditions each type boundary treatment is applicable.

Numerical Methods

A numerical solution of the particle continuity equation (40) can now be obtained by applying the boundary conditions of the previous section. As noted, for large settling velocities where $w_s >> w$, a direct numerical solution of equation (40) can be obtained using equation (45) for the boundary condition under the closed top. This solution and boundary condition are essentially identical to that used in the previous study.[1] In addition, a theoretical upper limit on the removal efficiency can be readily defined for this case. When $w_s >> \overline{w}$, the mean particle flow path of all the particles will intersect the chamber floor. In the absence of turbulence, a theoretical removal efficiency of 100 percent should be obtained. In actuality, the mechanisms of particle scour, re-entrainment and turbulent diffusion will cause particles to be dispersed throughout the chamber. As a result, an actual removal efficiency less than 100 percent will occur, and concentration gradients will exist throughout the chamber. For the purpose of this study it is sufficient to state that when w_s is comparable to or greater than w, the performance of the unit will deviate from the theoretical upper limit of 100 percent removal, due to scour, re-entrainment and diffusion as noted above.

The second case, where $w_s \leqslant w$, is more representative of the conditions projected for the prototype swirl concentrator as a primary treatment device. For this case, the large concentrations of particles below the closed top cause numerical difficulties, as noted previously, which cannot be handled with a reasonable mesh spacing. To resolve this problem, the particle concentration below the weir has been assumed to be equal to the concentration at an interior point.

A second assumption was employed to define the particle boundary condition at the floor. Since the definition of particle deposition, scour and entrainment mechanism is beyond the state of the art, it was assumed that all particles which reach the floor are removed from the device and the concentration at the floor equals the concentration at the adjacent interior point. Thus, the large concentration gradients immediately adjacent to the weir and to the floor have been neglected.

The net result of these two assumptions is that, for the case where $w_s \leqslant w$, the

TABLE 22
APPLICABLE BOUNDARY CONDITIONS FOR PARTICLE CONTINUITY EQUATION

	Vertical Wall	Closed Top	Bottom
A) $\lvert R \rvert >> 1$	$c_b = c_b + 1$	$c_b = \frac{c_b + 1}{1 + R}$; $(w_s >> \overline{w})$ $c_b = c_b + 1$; $(w_s \leqslant \overline{w})$	Treat as an interior point
B) R 1	$c_b - c_b + 1$	$c_b - \frac{c_b + 1}{1 + R}$	Treat as an interior point
C) R 1	$c_b = c_b + 1$	$c_b = \frac{c_b + 1}{1 + R}$	$c_b = \frac{c_b + 1}{1 + R}$

concentration everywhere within the chamber becomes uniform and equal to the inlet concentration, C_o. To see why this is so, assume that the concentration is in fact everywhere constant. Then the turbulent diffusion term on the right side of equation (40) becomes zero, since $C = 0$, and equation (44) can be reduced to

$$\frac{\partial c}{\partial t} + \vec{V}_p \cdot \nabla C + \nabla C \cdot \vec{V}_p = 0 \qquad (49)$$

As previously noted,

$$\vec{V}_p = \vec{V}_L + w_s \vec{e}_z \qquad (50)$$

Where V_L is the liquid velocity, and $\vec{e}_z$ is a unit vector in the z-direction.

Since the divergence of the liquid velocity ($\Delta \cdot \vec{V}_L$) is zero, and since w_s is a constant

$$\nabla \cdot \vec{V}_p = 0. \qquad (51)$$

Equation (49) can therefore be written as a total derivative

$$\frac{DC}{Dt} = 0, \qquad (52)$$

where D/Dt is the total derivative along the particle streamlines.

Equation (52) states that in the absence of turbulent diffusion, the concentration remains constant along particle paths.

All regions of the chamber cross section which are connected to the inlet region by a particle path must have a concentration of C_o. The remainder of the cross section (such as the region underneath the weir) contains particle paths which originate at the weir or at the free surface. Since there is no particle flux through these surfaces in the absence of turbulent diffusion, the concentration must be zero in these regions.

The effect of turbulence is to scatter particles from regions of high concentration to regions of low concentration. Initially, therefore, turbulence will tend to decrease the concentration of regions with $C = C_o$, and to raise the concentration in the region with $C = 0$. However particles which are scattered into the closed region under the weir tend to remain there. Consequently, in the steady state, this region will fill up with particles until its concentration is also equal to C_o. This effect is readily apparent in the laboratory tests. As the particle flow is initiated, the particle cloud tends to follow the streamlines from the inlet up to the overflow, and the closed region under the weir remains clear. However, the turbidity of the closed region gradually increases, and after about 10 minutes, no concentration gradients are discernable.

Once the concentration in the chamber becomes uniform, turbulence has no further effect because the concentration gradient, ΔC, becomes negligible, and the right hand side of equation (49) can be neglected. Under these conditions equation (52) is applicable even in the presence of turbulence.

The efficiency of the concentrator can be determined as the ratio of the particle flux onto the bottom and the influent particle flux. As shown (equation 52), the concentration along the streamlines reaching the bottom will be equal to the inlet concentration, because $DC/Dt = 0$. Consequently, the particle flux reaching the bottom (from equation (48) with $DC/Dt = 0$, and $C = C_o$) *is*

$$F_B = - \int_{r_1}^{r_2} C_o \, w_s \, n_z \, (2\pi r) \, ds \qquad (53)$$

where ($2 \pi r n_z ds$) is an element of projected surface area along the bottom. Since $n_z = -dr/ds$, equation (53) gives

$$F_B = C_o \, w_s \, A_b \qquad (54)$$

where A_B is the projected area of the bottom. For the case where some fraction, η, of the liquid flow is continuously withdrawn from the underflow, an additional mass flux of $\eta Q C_o$ must be added to equation (54). The inlet mass flux is

$$F_{in} = Q C_o$$

where Q is the rate of flow of the liquid. Consequently, the separation efficiency of the chamber is

$$E = F_B / F_{in}$$

If the ratio Q / A_B is viewed as an overflow rate for the chamber (the usual overflow rate is defined by the ratio of the flowrate to the surface area), then equation (55), with $\eta = 0$, is identical to the theoretical efficiency of an ideal settling basin as derived by Camp[2] in 1945. This is a somewhat surprising result,

inasmuch as equation (55) was derived under considerably different assumptions and for an entirely different geometry than analyzed by Camp.

Summary

Particle paths in the swirl concentrator can be determined by superimposing a stream function due to the settling, ψ', on the liquid flow stream function.

Under certain conditions of particle settling rate and computational grid size, modification to the boundary conditions are required to solve the particle continuity equation. These modifications involve neglecting regions of high concentration gradients, where the gradient occurs over an interval smaller than one mesh spacing. The approximate boundary conditions are summarized in Table 21. For the laboratory model, where particle settling velocities are much smaller than the mean upflow velocity, swirl concentrator separation efficiency (ratio of gm/sec particulates reaching bottom to gm/sec particulates entering the chamber) can be approximated by equation (55).

$$E = \frac{w_s A_B}{Q} + \eta \qquad (55)$$

even for cases where the settling velocity is comparable to or greater than the overflow rate, equation (55) represents an upper limit to the performance of the swirl concentrator.

It is of interest to note that this equation is equivalent to expressions used for computing removal efficiencies for ideal settling basins.

SCALING TECHNIQUES

Scaling of the Liquid Flowfield

Scaling of the liquid flowfield can be accomplished via the same Froude scaling techniques used in the previous study.[1]

Essentially the following equations can be applied to compute dimensions, flowrates, and velocities for a prototype scale factor of S.

$$L_{\text{prototype}} = S \cdot L_{\text{model}} \qquad (56)$$

$$V_{\text{prototype}} = S \cdot V_{\text{model}} \qquad (57)$$

$$Q_{\text{prototype}} = S^{5/2} \cdot Q_{\text{model}} \qquad (58)$$

where

S = scale factor = $L_{\text{pro}}/L_{\text{pro}}$
Q_{mod} = discharge rate in model
V_{mod} = velocity in model
L_{mod} = length dimension in model
Q_{pro} = discharge rate in prototype
V_{pro} = velocity in prototype
L_{pro} = length dimension in prototype

To use equations (56) through (58) it is necessary to assume a scale factor, S. For example, assume the laboratory model constructed by the LaSalle Hydraulic Laboratory was designed to represent a prototype unit 12 times larger, i.e. $S = 12$ ($L_{\text{prototype}}/L_{\text{model}} = 12$). The corresponding velocities and flowrates for the prototype, therefore, are larger than those of the model by a factor of

$$Q_{\text{pro}} = (12)^{5/2} \cdot Q_{\text{mod}} = 500 \cdot Q_{\text{mod}}$$
$$V_{\text{pro}} = 12 \cdot V_{\text{mod}} = 3.47\, V_{\text{mod}}$$

In similar fashion, the size of a device designed to handle a specified flow of $Q = Q$ design at a removal efficiency equivalent to that of the LaSalle Hydraulic Laboratory model can be obtained from equation (58)

$$S = \left[\frac{Q\,\text{design}}{Q\,\text{model}}\right]^{2/5}$$

The corresponding S can then be used in equation (56) and (57) to compute the required dimensions and flow velocities.

Certain assumptions are implied when applying Froude scaling to the laboratory model. First the liquid flowfield boundary conditions as previously described must be maintained in the prototype unit. This can be accomplished by maintaining geometric similarity to the laboratory model.

The second assumption requires that the degree of turbulence, as defined by the eddy viscosity ϵ be maintained at the same value as the model. The nondimensional viscosity is represented by (1)

$$\hat{\epsilon} = \hat{l}^2 \cdot \sqrt{\phi} + \frac{\nu}{\omega L^2} \qquad (59)$$

where

θ = local dissipation function
l = mixing length constant
ν = kinematic viscosity
L = reference length
W = reference frequency (U_{ref}/L)

The first term on the right is the eddy viscosity arising from the Reynolds Number stresses while the second term represents the molecular viscosity. The eddy viscosity is independent of scale size and flowrate since neither W nor L appear explicitly in the first term. Thus, as the size of the chamber is increased or the discharge rate is increased, the turbulence level increases in just such a way that the same nondimensional eddy viscosity results. The second term on the right, however, depends on both the flowrate and size. This term is the reverse of a Reynolds Number based on reference length, L; reference velocity, WL; and liquid kinematic viscosity, ν.

In the previous study[1] the molecular viscosity term was very much smaller than the eddy viscosity term and could be neglected for practical purposes, permitting scaling of the liquid flow. In the present study, however, the flow regime observed in the laboratory model cannot be classified as completely turbulent. Although flows in the annular region, at and below the skirt, along the inside wall of the skirt and at the overflow region are probably turbulent, the large central region below the circular weir appears to be laminar. Thus, the laboratory model can be best characterized as transitional, containing both laminar and turbulent regions.

By contrast, the flow regime in the prototype will be fully turbulent. For example, a prototype unit represented by a 1:12 scale factor will have a Reynolds Number 41.5 times larger than that of the model, which should ensure fully turbulent flow. Consequently, some differences in the flow patterns of the laboratory model and the prototype are to be anticipated.

Scaling of the Particle Flows

Successful scaling of the particle flowfield hinges on having accurate information concerning the settling characteristics of the prototype sewage. Since both the particle path and concentration field equations can only be applied to discrete particle settling velocities, it is necessary to translate settling column data into this format. This can be accomplished by dividing frequency distribution diagrams, such as Figures 72 through 75 into several ranges of settling velocities. A first approximation of the removal efficiencies for each range can then be predicted for a chamber of a given dimension and flowrate for Equation (55).

$$E = \frac{w_s A_B}{Q} + \eta.$$

The computed removal efficiency for each settling velocity range can be multiplied by the percentage of particles represented by that settling velocity and totalled for all ranges to determine the overall predicted removal efficiency. A similar technique can be utilized to predict the mean particle paths from settling velocity data.

For particles having settling velocities much lower than the overflow rate, i.e., $w_s \ll Q/A_B$, equation (55) will closely predict observed removal efficiency. For particles having settling velocities comparable to or greater than Q/A_B, 100 percent removal efficiency should be used in lieu of equation (55). For these cases, the mathematical model will substantially overpredict the obtainable removal efficiency, since it neglects particle re-entrainment and turbulent diffusion.

Since it was not possible to incorporate flocculation effects into the mathematical model, it is necessary to include the effect of flocculation in the assumed frequency distribution of particle settling velocities. This can be accomplished by increasing the particle settling velocities based on column settling test as described previously.

Equation (55) will always place an upper limit on the attainable removal efficiencies and should only be used as a first estimate. To obtain a more realistic value for the removal efficiency, the removal efficiency curves obtained by the LaSalle Hydraulic Laboratory can be used. Scaling the laboratory results will also tend to overpredict the prototype performance because the increased turbulence in the prototype will act to resuspend some of the bottom sediments.

An outline of how the particle and liquid scaling relationships can be used for design of a prototype unit will be described later in this report.

Summary

In order to maintain similar liquid flow conditions in different size swirl concentrators it is necessary to use Froude scaling. This will insure that the ratio of the gravitational to inertial forces will be maintained constant. Froude scaling requires that liquid flow velocities be related by the square root of the scale factor and flowrates by the 5/2 power of the scale factor per equations (57) and (58).

A simplified equation (55) can be employed for obtaining a first estimate of removal efficiency for a particle having a specified settling velocity, given the size and design flowrate of the prototype unit. To obtain a more accurate estimate of the removal efficiency the prototype flowrate and particle settling velocity can be scaled back to the laboratory model via equations (57) and (58). A more accurate removal efficiency can be obtained from the laboratory data.

COMPARISON OF PREDICTED LIQUID FLOWFIELD WITH LABORATORY DATA

The mathematical model of the liquid flowfield was exercised concurrently as modifications to the original chamber configuration were implemented on the laboratory model. Since the objective of the LaSalle Laboratory was to try several different chamber configurations to achieve improved performance, no attempt was made to calibrate the mathematical model for the earlier configurations. However, certain quantitative comparisons were made which closely concurred with the flow patterns observed by the laboratory.

At the beginning of the laboratory model development, the swirl concentrator was configured as shown in Figure 70. Particular attention is called to the existence of the central standpipe and the circular overflow weir. Figures, 77, 78, and 79 show the streamlines, tangential and vertical velocity plots of this configuration as predicted by the mathematical model. A weir diameter of 46 m (15 ft) prototype scale and flowrate of 500 l/sec (17.5 cfs) prototype scale, were assumed in these calculations.

Figure 77 illustrates the cross flow streamlines within the chamber. The bottom streamline represents one percent of the flow which is withdrawn through the foul outlet at the base of the chamber. The remaining streamlines which enter beneath the skirt are in even increments of 20 percent of the flow. The circular pattern in the upper right hand portion of the cross section indicates a clockwise recirculation flow. The streamline which outlines the large empty region under the weir defines a counterclockwise recirculation region. The existence of this "dead" zone was confirmed in the laboratory dye studies. The majority of the flow in Figure 77 is seen to penetrate well into the base of the separator before turning and rising to the surface. However, during its upward passage, the flow tends to hug the outer walls, creating (undesirable) high upflow velocities. Furthermore, a significant fraction of the flow turns immediately upward after passing under the skirt, and rises directly to the surface, constituting a hydraulic "short-circuit." The existence of this short-circuit was also confirmed in the lab experiments.

The upflow velocities at various vertical elevations in the chamber are plotted in Figure 79 as a function of chamber radius. Near the top of the chamber (elevation 67 m [22 ft] prototype scale), the upflow velocity is zero underneath the weir, and then rises to a peak of about 1.5 cm/sec (0.038 ft/sec). The existence of the counterclockwise recirculation region under the weir is evidenced by the negative values of upflow velocity near the inner standpipe. At an elevation of 51 m (16.7 ft), the upflow velocity shown in Figure 79 is very high, 2.3 cm/sec (0.075 ft/sec), because the rising fluid is confirmed to a small annular region between the two recirculation zones shown in Figure 70.

This large "dead" region under the weir is undesirable on two counts. First, it represents wasted volume, since no flow enters or leaves this region, the dividing streamline could be replaced by a solid wall. Second, by reducing the effective upflow area, it results in a high upflow velocity which tends to entrain slower settling particles in the clean overflow.

The calculated tangential contours are illustrated in Figure 78. These can be

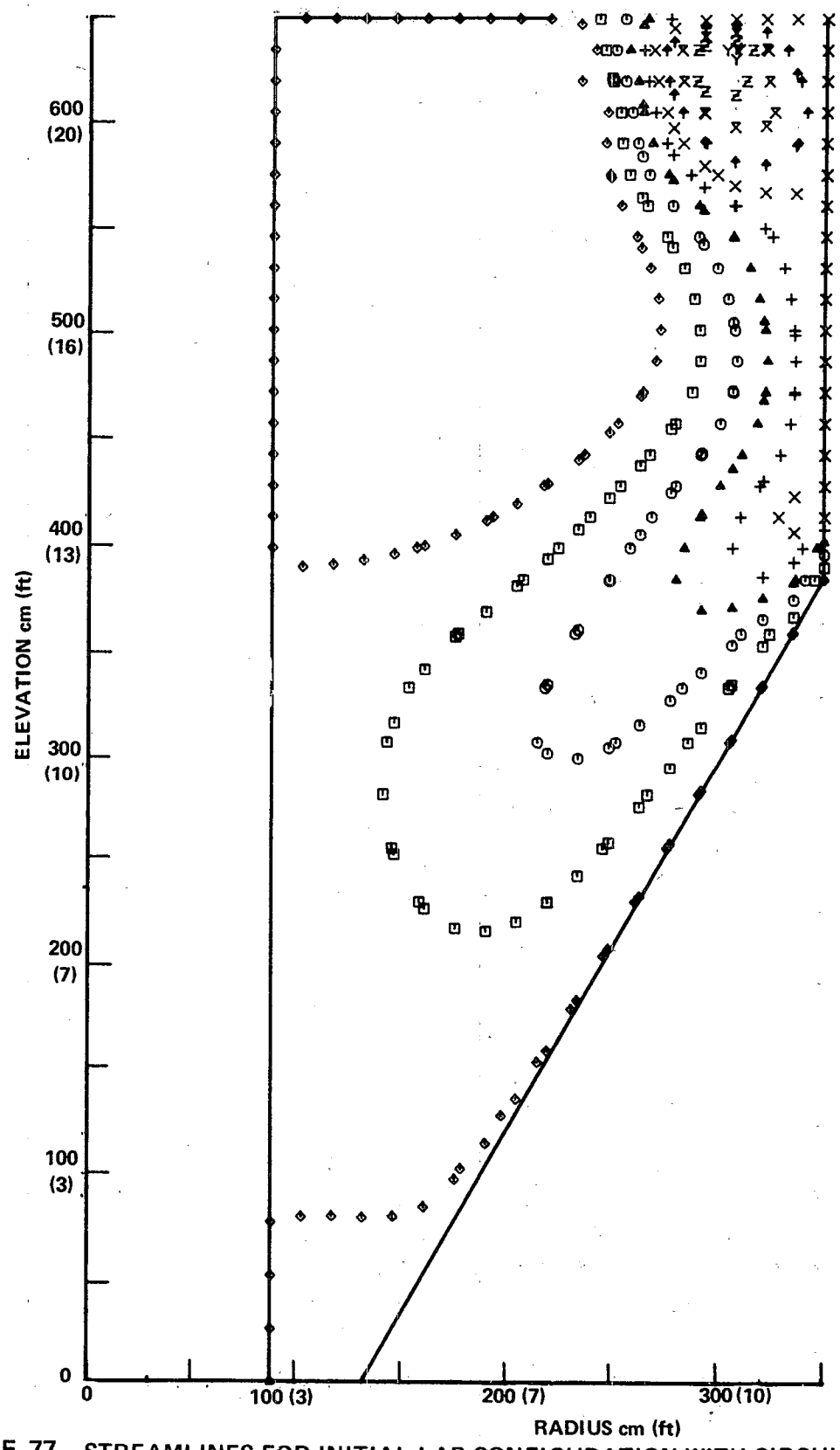

FIGURE 77 STREAMLINES FOR INITIAL LAB CONFIGURATION WITH CIRCULAR WEIR

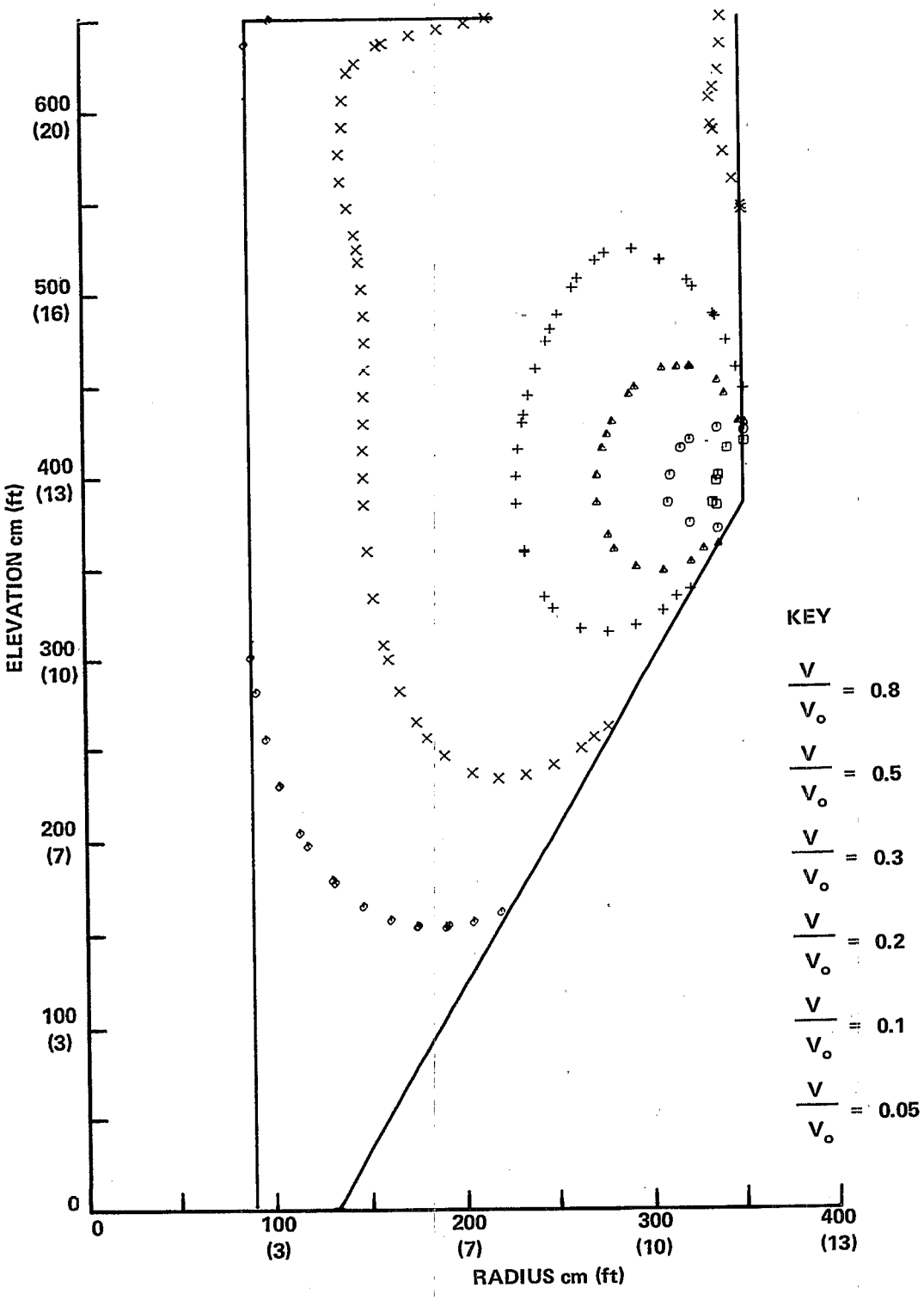

FIGURE 78 TANGENTIAL VELOCITY CONTOURS FOR INITIAL LAB CONFIGURATION WITH CIRCULAR WEIR

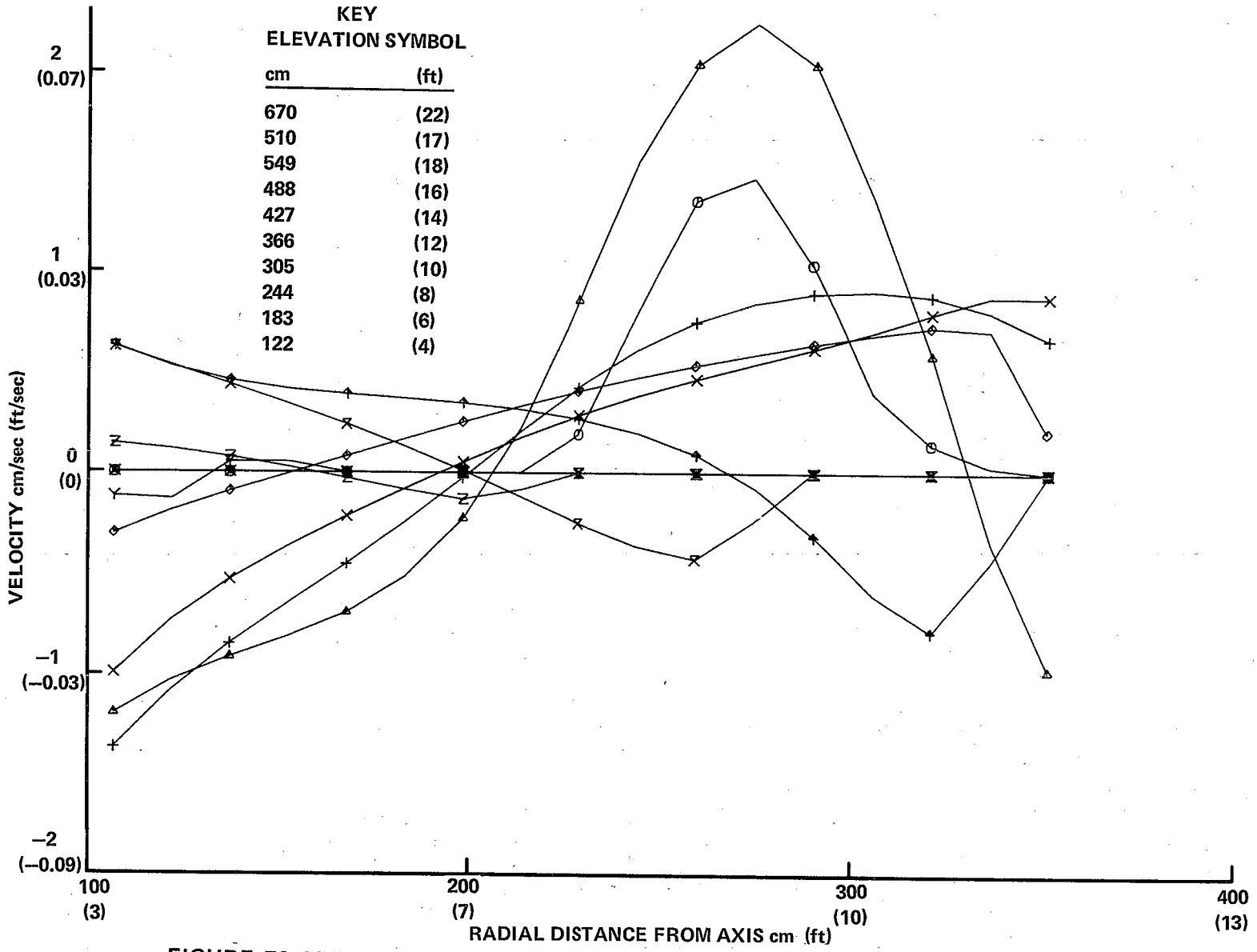

FIGURE 79 VERTICAL VELOCITY PROFILES FOR INITIAL LAB CONFIGURATION WITH CIRCULAR WEIR

compared with the velocities measured in the laboratories at various radial cross sections. The measured values are shown in Figures 49 to 56. Since the mathematical model is axisymmetric, the calculated velocity contours represent the average of the hydraulic model results over the four measurement cross sections. The calculated values are presented in terms of V/V_o, where V_o is the tangential velocity under the skirt. Since the velocity there is very nearly 30.5 cm/sec (1 ft/sec) in the LaSalle results, the specified ratios can also be interpreted directly as velocities in cm/sec.

A comparison of Figure 78 with the hydraulic laboratory results indicates that the magnitude of the velocity under the weir is correctly reproduced 0.00033 to 0.00066 cm/sec (0.1 to 0.2 ft/sec), but the velocity in the outer region near the skirt is too low. The calculated velocities decay too quickly with distance from the annular entrance under the skirt. As a consequence, the shape of the velocity profiles do not match the laboratory results very well. The reason for this mismatch is that no calibration of the model parameters was attempted. The calculations were based on the parameters used in the earlier study of the swirl concentrator as a combined sewer overflow regulator.[1] The mismatch of the calculated tangential velocities with laboratory results does not appear to affect the calculated streamline patterns, which were verified in the laboratory, or the conclusions of the study.

In order to eliminate the undesirable recirculation region under the weir, the design was modified in two ways: the circular weir was replaced with a series of eight radial gutters, and the central standpipe was removed. The removal of the standpipe increases the available cross-sectional area, thereby lowering the average upflow velocity. The radial gutter provides a more uniform withdrawal of the flow across the surface.

The mathematical model results for the revised configuration are illustrated in Figures 80, 81, and 82. The crossflow streamlines shown in Figure 80 demonstrate that the recirculation region has been eliminated by the radial gutters providing a more uniform upflow. However, contrary to expectation, a substantial fraction of the flow underneath the skirt turns sharply and rises up the inner wall of the skirt, creating a partial short-circuit. The existence of this unexpected flow pattern was also confirmed in laboratory studies.

The clustering of the streamlines near the skirt results in relatively high upflow velocities in that region, as shown in Figure 80. Note the sharp rise in velocities near the skirt at all elevations greater than 400 cm (13.1 ft). Nevertheless, the maximum upflow velocity is less than half of the values occurring in the earlier configuration, Figure 77, and over the majority of the cross section, the upflow velocity is close to the theoretical lower limit for uniform upflow.

The tangential velocity contours for the revised configuration are shown in Figure 81. Laboratory measurements for this configuration are not available, so that direct comparison is not possible. However, the vertical orientation of the velocity contours is in better qualitative agreement with the hydraulic model results for the earlier configuration.

Comparison of Math Model Particle Flow with Test Data

a. Particle Paths: The motion of particles within the swirl concentrator can be delineated by superimposing the particle settling velocity on the liquid flow streamlines. The resulting particle paths in a radial cross section of the separator are then obtained by plotting the resulting particle stream function. The results of this calculation for the initial configuration are shown in Figure 83. Only small differences between the particle paths, Figure 83, and the corresponding liquid flow streamlines, Figure 80, are apparent. The particles appear to penetrate further into the base of the separator as one would expect, and some of the particle paths terminate on the bottom, indicating settlement. The dividing streamline between the material which settles out, and that which is entrained in the overflow is marked by the symbol (→).

Figure 83 also shows the existence of a particle path (symbol ◇) within the closed recirculation region under the weir. This particle path originates at the underside of the weir, and is a consequence of assuming a

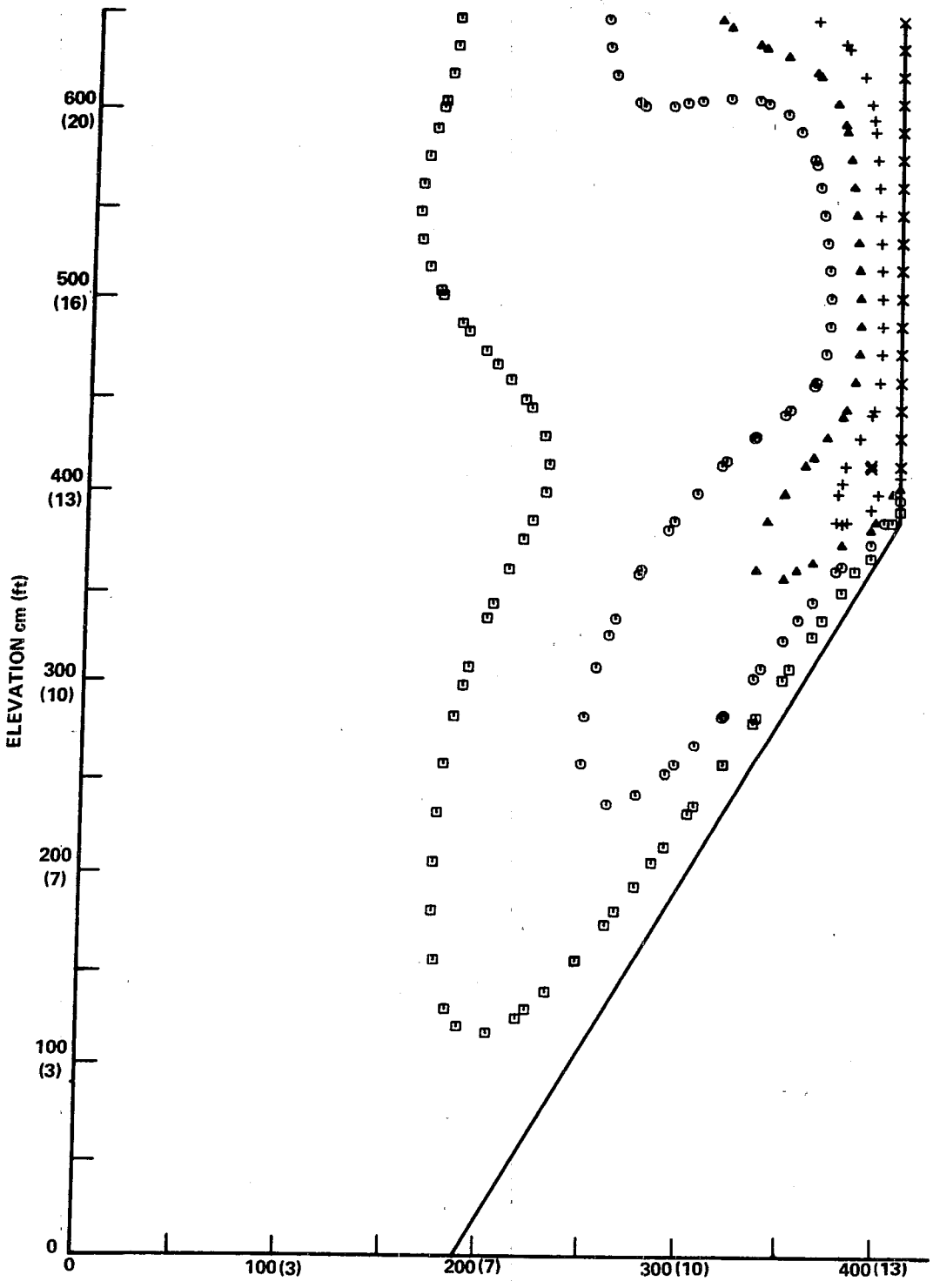

FIGURE 80 STREAMLINES FOR MODIFIED LAB CONFIGURATION WITH RADIAL GUTTERS AND STANDPIPE REMOVED

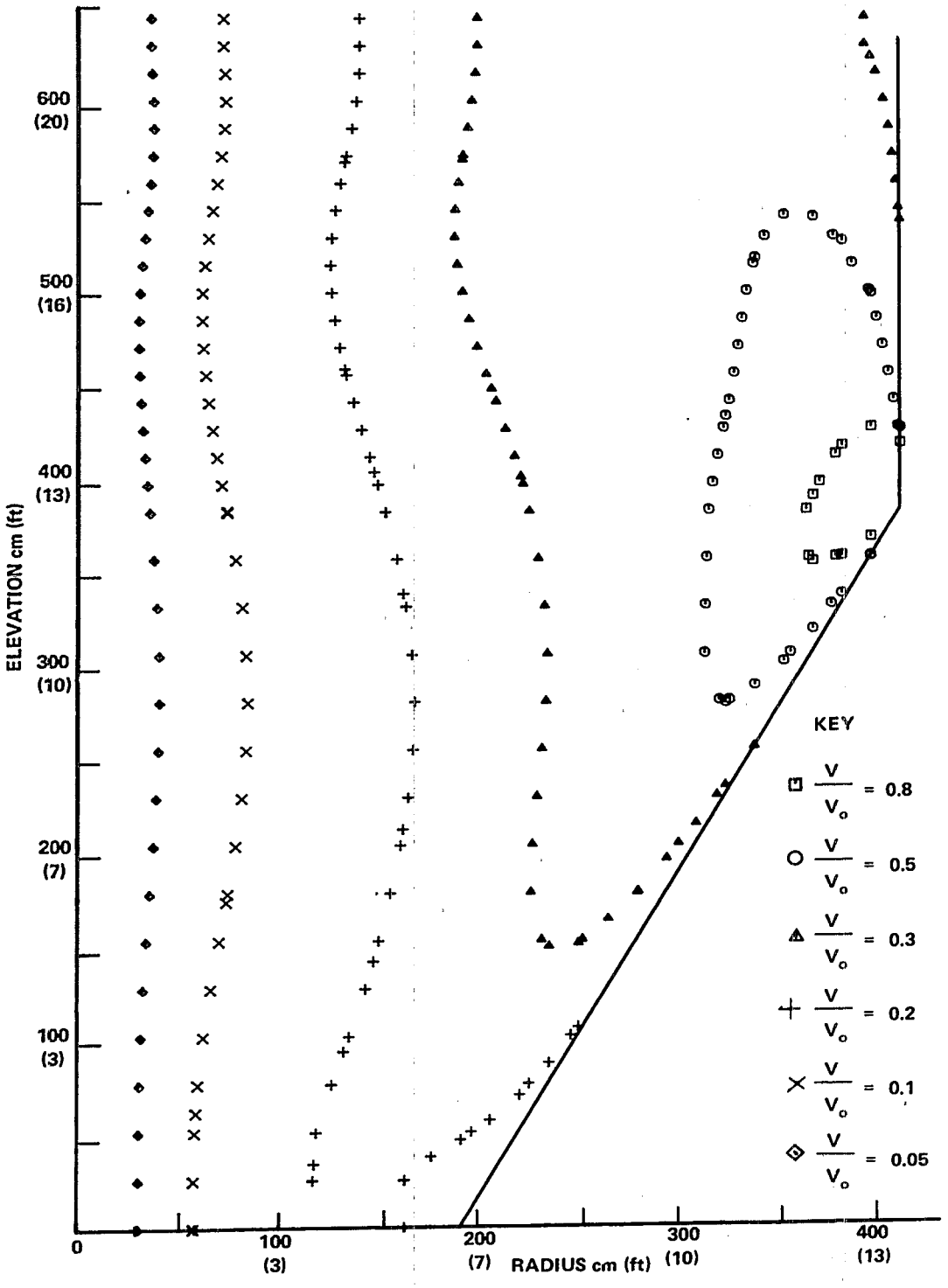

FIGURE 81 TANGENTIAL VELOCITY CONTOURS FOR MODIFIED LAB CONFIGURATION WITH RADIAL GUTTERS AND STANDPIPE REMOVED

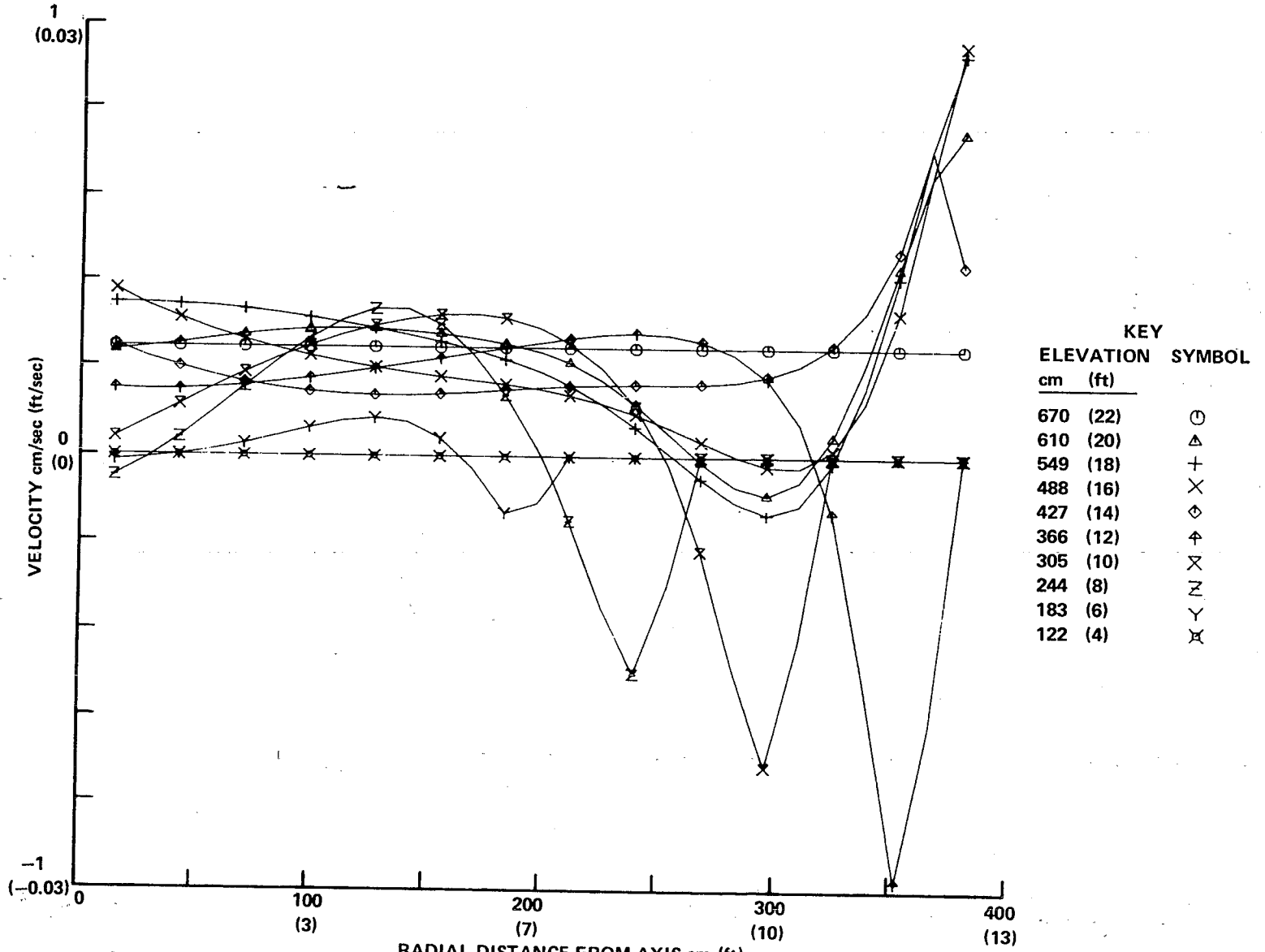

FIGURE 82 VERTICAL VELOCITY PROFILES FOR MODIFIED LAB CONFIGURATION WITH RADIAL GUTTERS AND STANDPIPE REMOVED

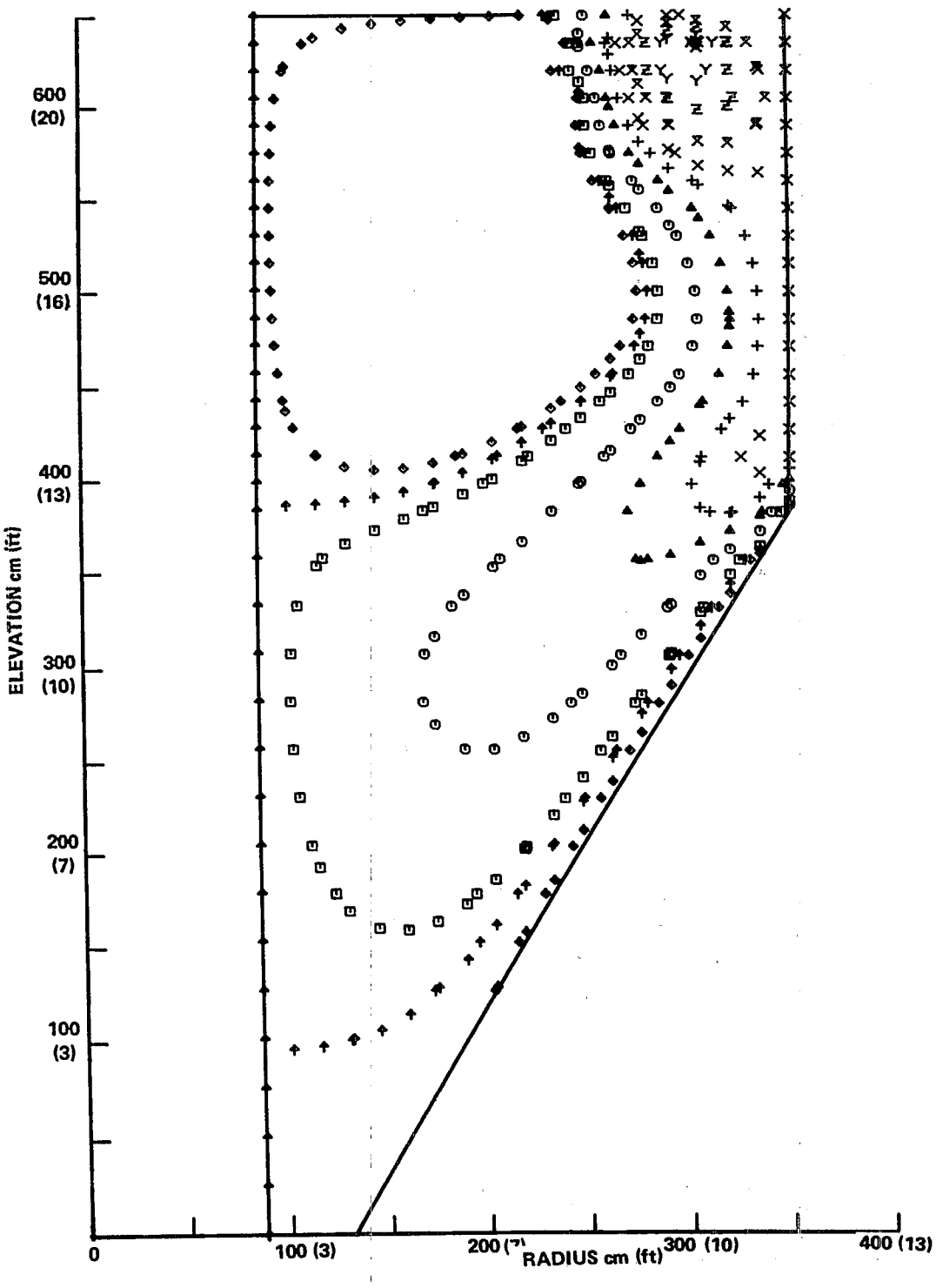

FIGURE 83 PARTICLE PATHS FOR INITIAL LAB CONFIGURATION WITH CIRCULAR WEIR AND PARTICLE SETTLING VELOCITY OF 0.05 cm/sec (0.0016 ft/sec)

settling velocity of 0.05 cm/sec (0.0016 ft/sec) everywhere so that particles appear to fall through the weir. Because the weir is actually a solid plate, the recirculation region under the weir (defined by the symbol ↑) would generally be devoid of particles, except for those scattered into this zone by turbulence. This phenomenon is observed when operating the laboratory model with IRA-93 resin. As the material enters the skirt, it initially flows down toward the base of the separator, but then tends to concentrate in the outer area near the skirt as it rises upward. For a considerable period of time, the region under the weir remains void of particles.

Particle paths for the revised chamber configuration are shown in Figures 84, 85, and 86. The total flowrate is 1 l/sec (0.034 cfs) (model scale) as before, but no flow is withdrawn from the bottom.

In Figure 84, the settling velocity is 0.05 cm/sec (0.0016 ft/sec), as in Figure 83 for the earlier configuration. Even with the more uniform upflow velocity the particles in Figure 84 still concentrate near the skirt as they rise. Figure 85 also shows an interesting effect: as the particles rising near the skirt approach the surface they are transported radially inward. They then tend to sink for a time before finally being re-entrained in the overflow, (see particle path with symbol ◊ in Figure 84). Again, the rising and falling motion of individual particles near the surface has been observed in the lab studies.

Figures 85 and 86 show the particle behavior at progressively larger settling velocities. In Figure 85, the settling velocity of 0.252 cm/sec (0.0083 ft/sec) is exactly equal to the uniform upflow velocity specified at the free surface. Consequently, none of the particles can escape through the top. In Figure 86 the settling velocity of 0.3 cm/sec (0.0098 ft/sec) exceeds the upflow velocity, and most of the particles drop like rocks to the bottom. A few, however, are entrained in the short-circuit hydraulic path up the inside of the skirt and tend to circulate within a confined region near the outer wall.

b. Removal Efficiency: Removal efficiencies were computed for the final laboratory configuration utilizing Equation (55).

Since there was no underflow for the laboratory model runs, η was set equal to zero in Equation (55). In order to identify the value of w_s to associate with the laboratory material, the settling velocity distribution curves prepared by Beak were utilized. A wide variation in the settling velocity of the resin was observed. Beak reported that these differences are attributable to different sieving techniques, and that Run 3 is representative of the materials employed by the laboratory for the model testing. The data by Beak were used to tabulate a step distribution for use with equation (55), as presented in Table 23. Table 23 was prepared by dividing the abscissa axis of Beak's Figure 10 into 10-percent segments, using the median settling velocity as representative of each particle fraction.

Using the settling velocity distributions of Table 23, an upper limit on removal efficiency can be predicted from equation (55) by computing a removal efficiency for each 10 percent fraction, totalling the results and dividing by 10. The results of this computation are shown in the second column of Table 23. If Run 3 is considered as most typical for the material used in the laboratory model tests, the mathematical model predicts 33.2 percent removal as the maximum limit on the performance at the 0.5 l/sec flowrate for 100-200 mesh resin.

The actual removal observed by LaSalle Hydraulic Laboratory was about 50 percent. Four possible explanations for this apparent discrepancy between the mathematical model predictions and laboratory data were offered,

1. Resin material may swell on contact with water, with consequent variations in settling velocities.
2. Particles may experience electrostatic attraction to the tank walls
3. Particles may not be completely dispersed as single particles.
4. Stratification may occur in the region under the skirt, giving higher concentration along particle paths which reach the bottom.

Subsequent investigations have ruled out possibilities 1-3. However, measurements at LaSalle have shown that stratification of the material does occur under the skirt. The

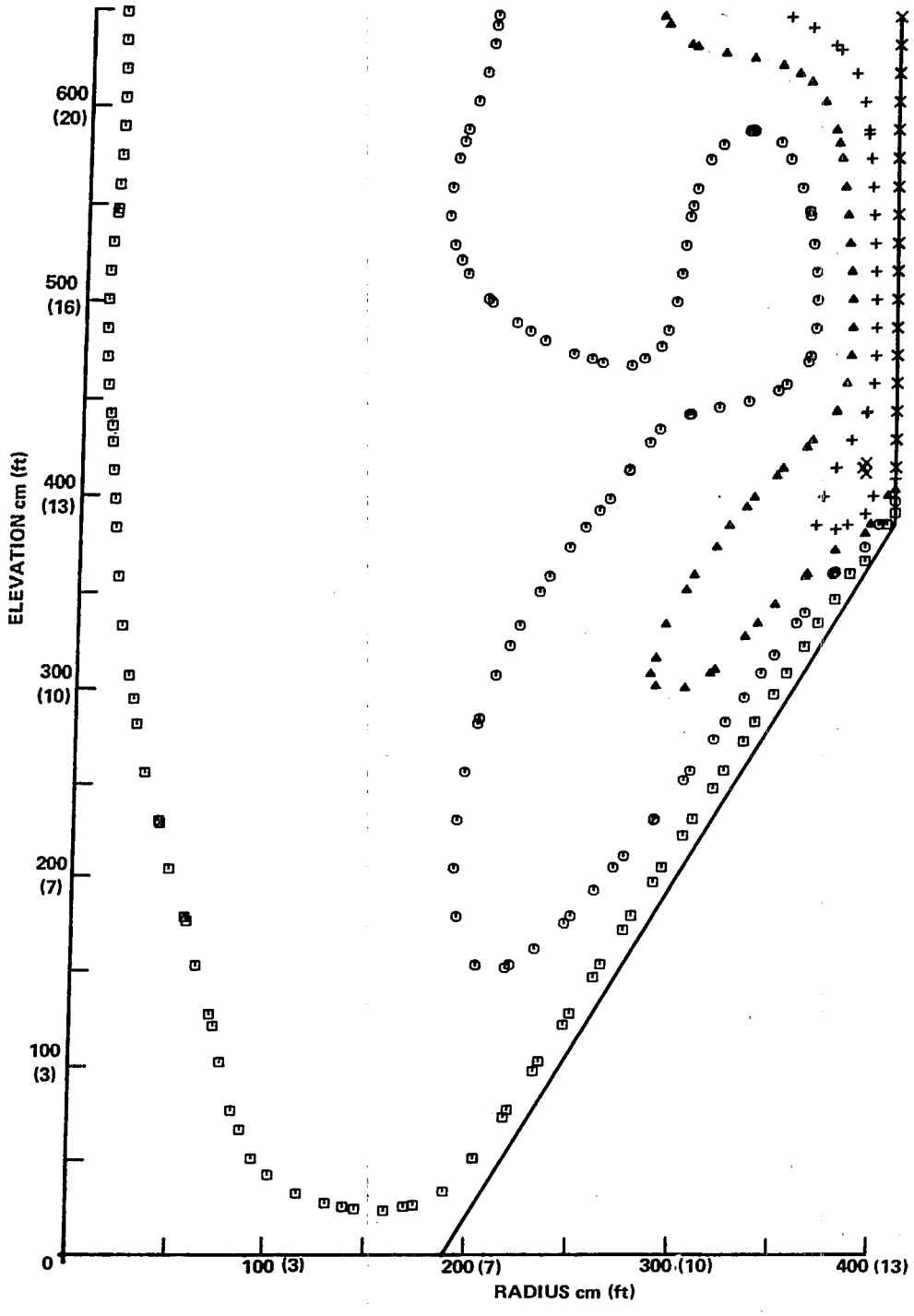

FIGURE 84 PARTICLE PATHS FOR MODIFIED LAB CONFIGURATION WITH RADIAL GUTTERS AND STANDPIPE REMOVAL AT PARTICLE SETTLING VELOCITY OF 0.05 cm/sec (0.0016 ft/sec)

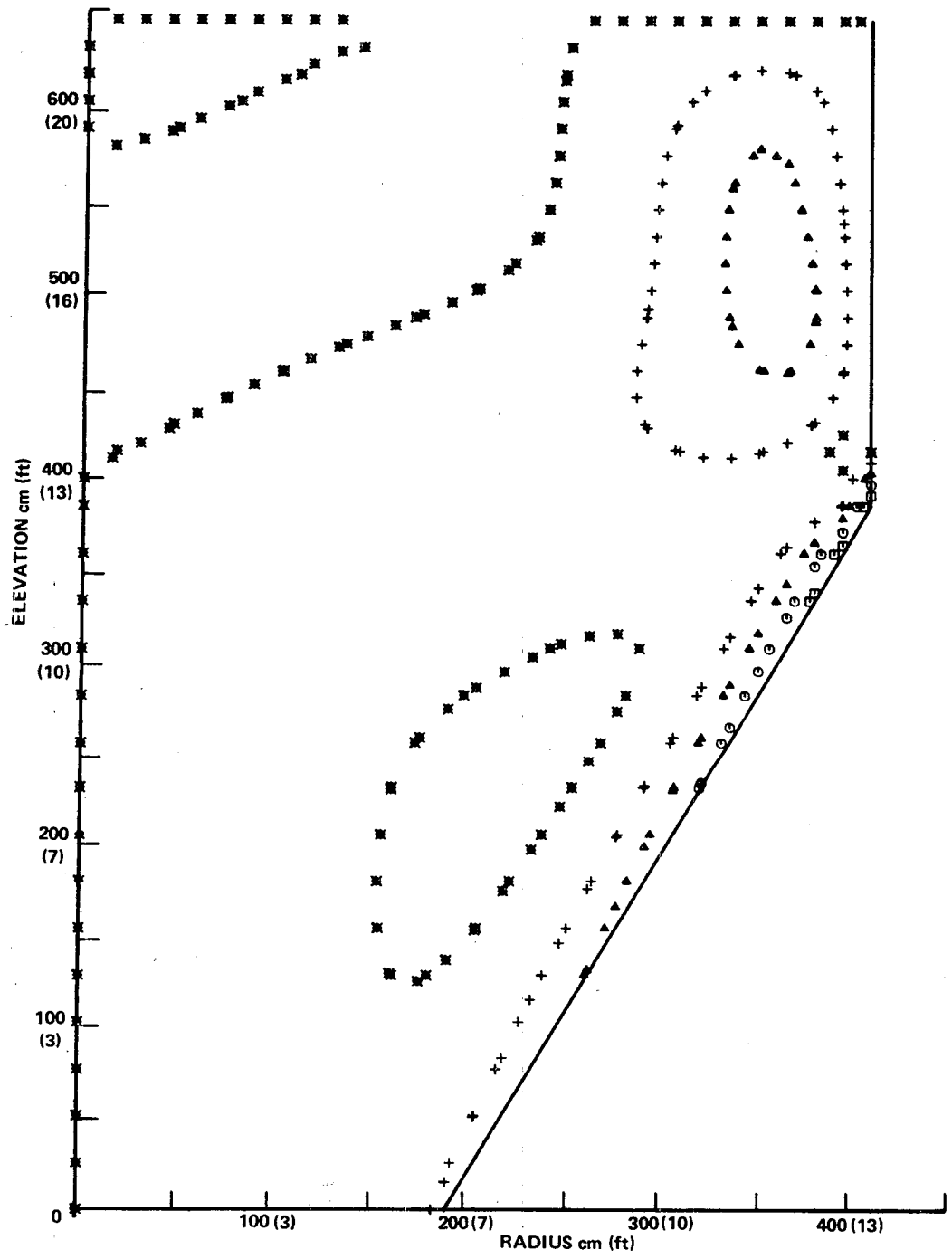

FIGURE 85 PARTICLE PATHS FOR MODIFIED LAB CONFIGURATION WITH RADIAL GUTTERS AND STANDPIPE REMOVAL AT PARTICLE SETTLING VELOCITY EQUAL TO AVERAGE UPFLOW VELOCITY OF 0.252 cm/sec (0.0083 ft/sec)

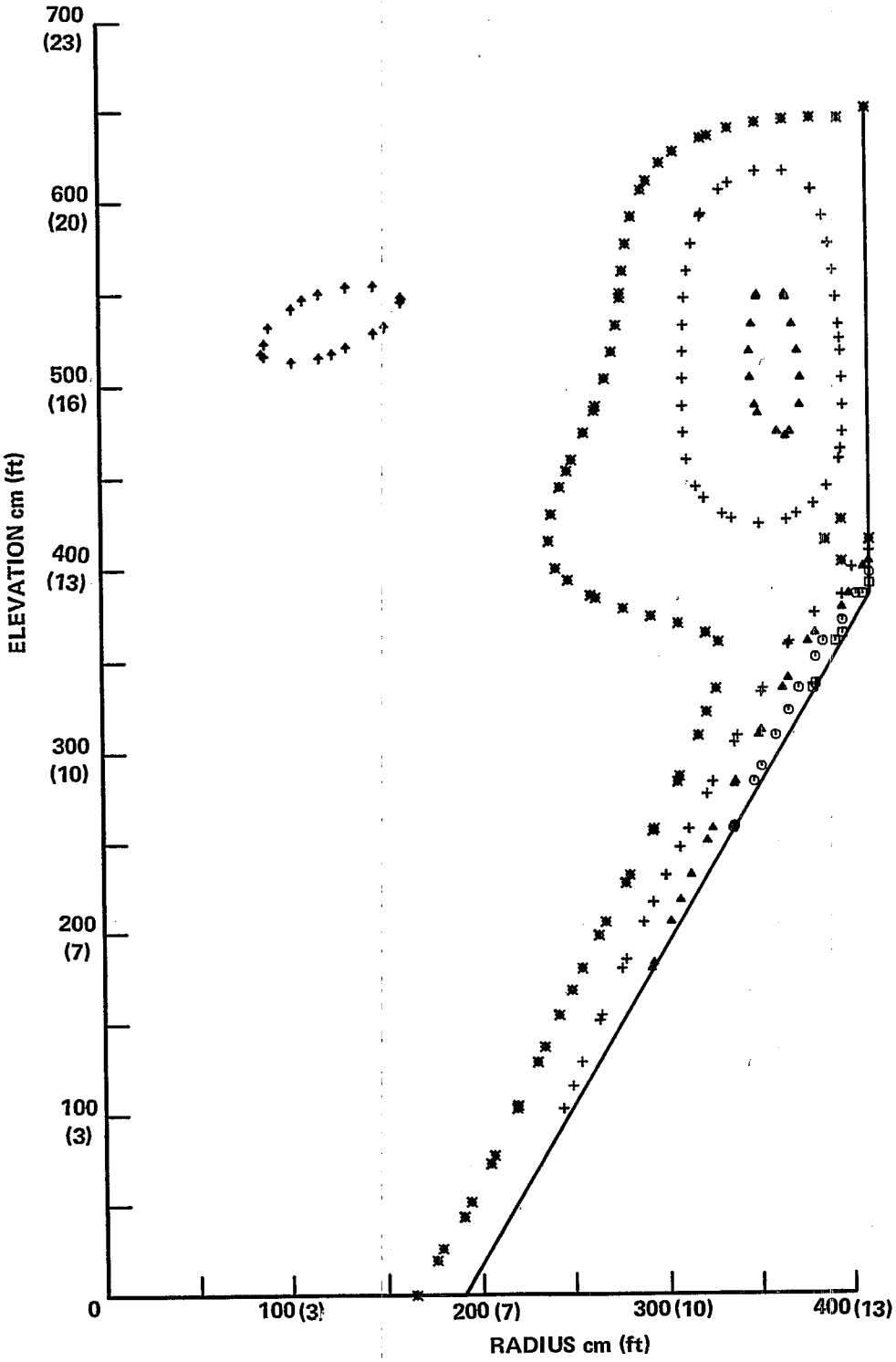

FIGURE 86 PARTICLE PATHS FOR MODIFIED LAB CONFIGURATION WITH RADIAL GUTTERS AND STANDPIPE REMOVED AT PARTICLE SETTLING VELOCITY OF 0.3 cm/sec (0.0098 ft/sec)

TABLE 23
PARTICLE SETTLING VELOCITY
DISTRIBUTION FOR 100-200 MESH IRA-93 RESIN
(From Beak Report)

Particle Class	Particle Settling Velocity cm/sec (ft/sec) Run 1 cm/sec	Run 1 ft/sec	Run 2 cm/sec	Run 2 ft/sec	Run 3 cm/sec	Run 3 ft/sec
90-100	0.051	0.002	0.130	0.004	0.102	0.003
80-90	0.037	0.0012	0.083	0.003	0.079	0.0025
70-80	0.031	0.001	0.050	0.002	0.052	0.0017
60-70	0.0262	0.0008	0.043	0.0014	0.050	0.0016
50-60	0.023	0.0007	0.032	0.001	0.042	0.0014
40-50	0.020	0.0006	0.022	0.0007	0.034	0.0011
30-40	0.0165	0.0005	0.01	0.0003	0.028	0.0009
20-30	0.011	0.0004	X	X	0.020	0.0007
10-20	X	X	X	X	0.012	0.0004
0-10	X	X	X	X	X	X
median settling velocity	0.0215	0.0007	0.026	0.0009	0.038	0.0012

TABLE 24
PREDICTED REMOVAL EFFICIENCY FOR 100-200 MESH IRA-93 RESIN
(0.5 l/sec [0.02 cfs])

Settling Velocity Distribution	Efficiency (Excluding annular area)	Revised Efficiency (Including annular area)
	Percent	Percent
Run 1	17.1	28.4
Run 2	29.4	48.4
Run 3	33.2	55.1

significance of this finding is that the outer annulus also acts as a settling chamber, so that the projected base area, A_B in equation (55), should include the area of the annulus. However, the stratification in the outer annulus will be affected by the rotational velocity in the annulus. Increasing the inlet velocity (to prevent sedimentation in the inlet sewer) may disrupt this stratification and result in poorer performance.

If the projected base area of the annulus is included in the A_B term in equation (55), substantially greater removal efficiencies result, as given in the third column in Table 24. The revised result from Run 3 is 55.1 percent which is in close agreement with the observed removal efficiency of 50 percent.

To test the validity of the mathematical model further, the mathematical model was applied to the work of Bernard Smisson at Bristol, England. Mr. Smisson pioneered the application of swirl concentration in Europe[18] and has amassed data on the use of swirl concentrators for primary sedimentation. Through correspondence with Smisson, a summary of his results using a 3.02 m (10 ft) diameter prototype chamber to settle activated sludge was obtained. A scatter diagram showing his measured efficiencies versus those calculated from equation (55) is shown in Figure 87. Although substantial numbers of his data points fall above the theoretical upper limit, it is believed that this is due to the flocculent nature of the activated

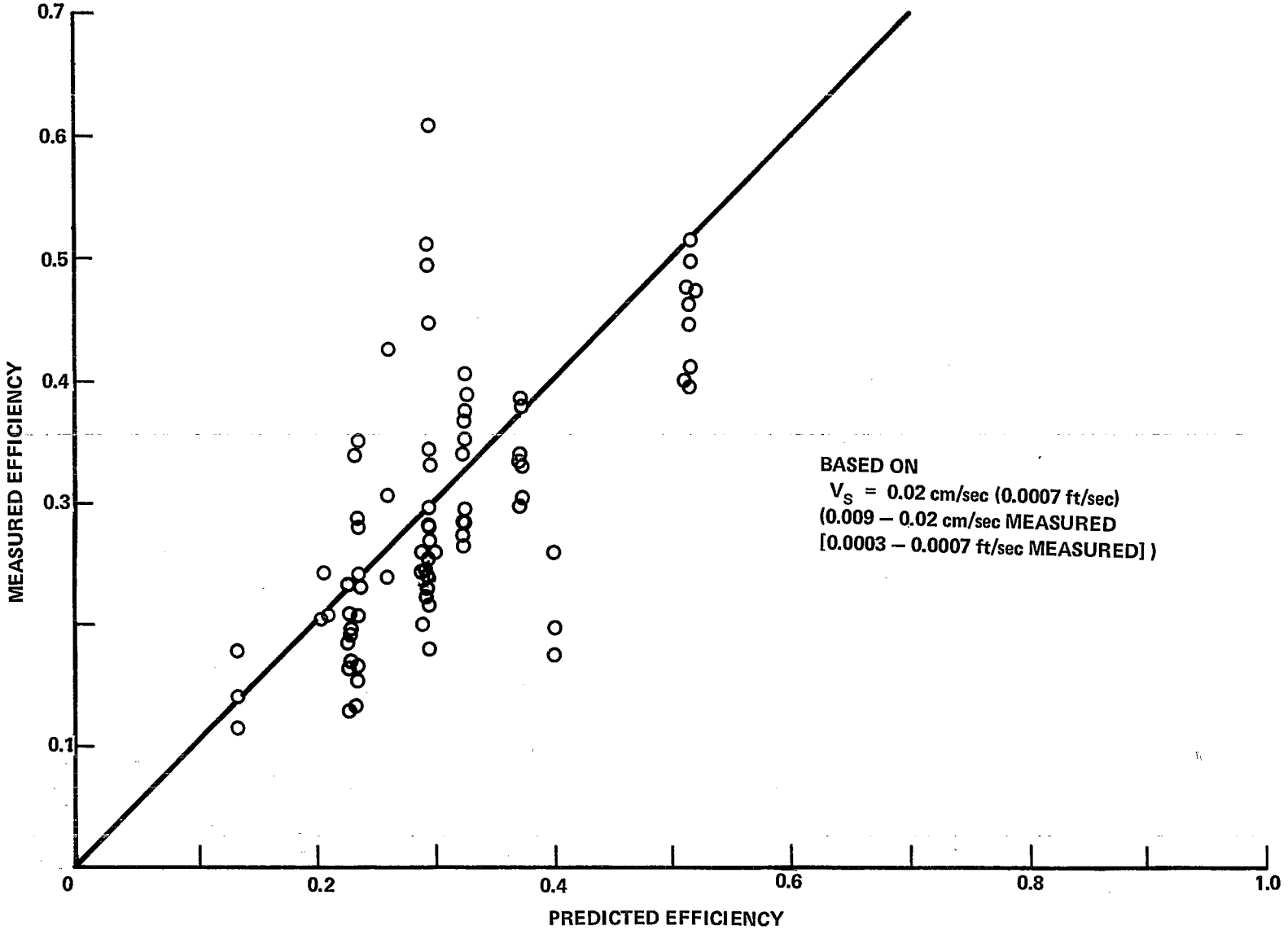

FIGURE 87 COMPARISON OF SMISSON 3 m (10 ft) PROTOTYPE DATA WITH THEORETICAL PERFORMANCE

sludge. The calculations are based on a settling velocity of 0.00182 cm/sec (0.0007 ft/sec), measured by Smisson in a dilute suspension. In the actual unit, the high inlet concentration will result in substantial increases in the settling velocity due to agglomeration of the primary particles. This possibly was noted by Smisson in his correspondence.

Additional comparisons were made with Smisson's results, using a 78 cm (30 in) diameter conical bottom tank. In this work, Smisson employed polystyrene molding beads with settling velocity of 0.038 cm/sec (0.0146 ft/sec). Measured separation efficiencies ranged from 50 to 98 percent over a range of flowrates from 0.45 to 01.25 m^3/sec (0.016 to 0.044 ft^3/sec). Equation (55) predicts a separation efficiency of 100 percent for this material over the entire flowrate range. Consequently, this model configuration appears to be less efficient than the version developed at LaSalle Hydraulic Laboratory, since the latter gives separation efficiencies which are closer to the theoretical limit.

The adjustment of A_B in equation (55) to include the annulus area was retained for all subsequent comparisons with laboratory data, and the modified equation was used to conclude these data, as shown in Figure 88, which illustrates the observed removal efficiencies as a function of the nondimensional settling parameter $(w_s A_B/Q)$ for several modifications to the chamber geometry. The theoretical efficiency as predicted by equation (55) is also shown. Data points plotted as circles in Figure 88 correspond to an early configuration using four radial gutters, with the central standpipe in place, and with the original 10 x 10 cm (4 x 4 in) inlet sewer. Subsequently, the four radial gutters were replaced with the 8-gutter configuration, with no standpipe. At the same time, the inlet dimensions were reduced to 6 x 6 cm (2.3 x 2.3 in) to raise the inlet velocity in order to prevent settling in the inlet sewer. Data points corresponding to this configuration are plotted with triangles in Figure 88. The recovery efficiency with this modification was somewhat lower, probably due to the higher velocity which tends to resuspend some of the sediment which reaches the bottom. In the final configurations, the skirt diameter was decreased from 71 to 61 cm (2.33 to 2 ft), resulting in somewhat better performance, 41 percent

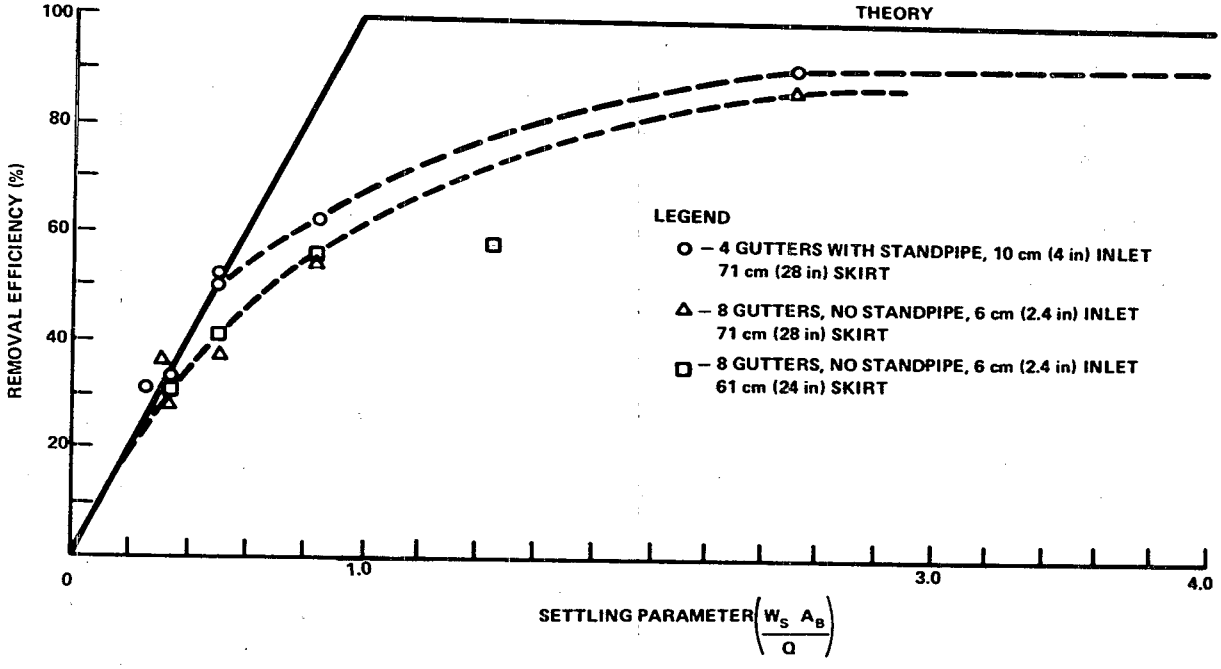

FIGURE 88 CORRELATION OF OBSERVED AND THEORETICAL MODEL PERFORMANCE

versus 37 percent, as determined with IRP resin at 0.5 l/sec (0.018 cfs). However, somewhat poorer performance with this configuration was obtained using the Arizona Road Dust, 28 percent versus 36 percent. In all cases, the laboratory data fall on or below the theoretical upper limit shown as a solid line in Figure 87. At high flowrates, where the settling velocity is less than the overflow rate, the laboratory model closely approaches the theoretical upper limit. At the lower flowrates, larger values of $w_s A_B/Q$, the laboratory results fall substantially below the upper limit due to increased turbulent diffusion and resuspension of bottom sediments.

The data shown in Figure 88 include results with IRA-93 resin with sieve sizes 100-200 (standard fraction) and 50-100 (coarser fraction). Results with the Arizona Road Dust are also included.

Since the Arizona Road Dust has a very narrow range of particle sizes, the median settling velocity can be used to arrive at an approximate overall removal efficiency for the entire distribution. For example, using the median, or 50 percent, settling velocity from Figure 10 of the Beak report, a removal efficiency of 36.6 percent is obtained as compared to the 36.3 percent calculated by dividing the distribution of settling velocities into 10 percent sections.

For the Run 3, 100-200 mesh IRA resin at a flowrate of 0.5 l/sec (0.018 cfs), the medial settling velocity of 0.037 cm/sec (0.0012 ft/sec) yields a calculated removal efficiency of 56.8 percent, as compared to the 55.1 percent calculated for the 10 percent sections. Thus, for the 100-200 mesh IRA-93 resin, which also has a relatively narrow size range of 74 u to 149u, using the median settling velocity provides a good estimate of the removal efficiency. This is an important point, since it will facilitate relating the removal efficiency observed in the laboratory to the prototype design.

Effect of Scale on Chamber Performance

The objective of the modeling work has been to provide an indication of how a prototype swirl concentrator can be expected to perform on actual sewage. To this end, it is necessary to understand the limitations and validity of the scaling laws. As has been indicated, chamber sizes, flows and particle settling velocities are scaled to represent prototype units utilizing Froude number scaling. This scaling procedure works quite well for fully turbulent flows, which tend to be independent of Reynolds Number. However, it was noted that while fully turbulent flows can be anticipated in the prototype units, the flow observed in the laboratory model at the lower flowrates was partly laminar. Thus, some can be anticipated in the flowfields of the model and prototpye, especially in those portions of the chamber where laminar flow was observed in the model.

Two approaches can be used to scale the removal efficiency. The most straightforward approach is to use equation (55) directly to predict the removal efficiency for a given overflow rate and prototype settling velocity. However, this equation neglects turbulent resuspension of bottom sediment and, therefore, will always overpredict the actual removal efficiency when the particle settling velocity is lower than the overflow rate. When the particle settling velocity is of the same magnitude or larger than the overflow rate, equation (55) will overpredict the removal by a considerable amount. Under these conditions, the second approach, using the laboratory data, should provide a more realistic estimate of removal efficiency.

The second approach is based on the condition that the prototype unit will give the same removal efficiency as the laboratory model if dimensions, flows, and velocities are related by Froude number scaling. However, Froude number scaling also preserves the equality of $w_s A_B/Q$ in the model and prototype, so that

$$\left(\frac{w_s A_B}{Q}\right)_{\text{model}} = \left(\frac{w_s A_B}{Q}\right)_{\text{prototype}}$$

Therefore if the non-dimensional settling parameter ($w_s A_B/Q$) is calculated for the prototype, the corresponding efficiency can be determined for the correlation of lab data in Figure 26.

This approach also overpredicts the prototype removal efficiency. The higher Reynolds Number in the prototype results in

greater turbulent dispersion and particle re-entrainment, particularly at model flowrates less than 0.5 l/sec (0.018 cfs) where laminar flow occurs in the laboratory model. However, the removal efficiency as scaled from the laboratory model should be closer to the prototype performance than that obtained from equation (55).

The importance of characterizing the settling properties of the sewage should be emphasized. The data in the Beak report shows large variations in settling velocity distributions. Since the actual sewage will have a wide band of settling velocities, the settling data should be divided into percentage bands and removal efficiencies computed separately for each band.

Since particle re-entrainment causes a lower removal efficiency, excessive buildup of sludge on the bottom, if allowed, will also cause reductions in removal efficiency.

Flocculation effects are difficult to assess and can only be represented by obtaining the settling velocity distribution after flocculation has occurred, as described in earlier sections.

Influence of Geometric Variables on Chamber Performance

The use of the radial gutter configuration, in lieu of the circular weir, produced a marked improvement in the performance of the device. This can be explained from the mathematical model results by comparing the vertical velocity profiles for the two configurations (Figures 79 and 82). The radial gutters resulted in more uniform upflow velocities near the surface of the tank than with the circular weir. As a result, the average upflow velocity used in equation (55) is closer to the actual value occurring at every point at the chamber surface, and the removal efficiency more closely approaches the theoretical upper limit predicted by equation (55). It is desirable to maintain this surface velocity as uniform as possible to minimize particle entrainment and short-circuiting.

A second very important geometric variable is the size of the annular region. At the flow velocities encountered in the laboratory model, this annular region served as an additional area in which particle settling could occur. In order to insure that the flow conditions in the prototype unit will also allow the annular region to participate in particle settling it is necessary to insure that significant particle resuspension and entrainment does not occur. Since the mechanism of particle entrainment and scour can be shown to depend on the ratio of the particle settling velocity to the eddy viscosity, it is necessary to maintain similarity of this ratio between the model and the prototype. For fully turbulent flows which are independent of Reynolds Number, Froude Number scaling will preserve this ratio. However, some Reynolds Number, effects may occur in this annular region. The tangential flow velocity in the annulus depends upon a balance of the angular momentum of the entering fluid and the drag losses on the walls of the annulus. Thus, if the inlet sewer velocities in the model and prototype are related via the Froude Number, the annulus velocity may not be so related because of differences in the drag losses at the different Reynold Numbers. The fact that the model Reynolds Number is smaller is counterbalanced by its smoother walls, so that, in general, the Froude Number differences between the model and prototype should be small.

Since the tangential velocities in the annular region are higher than in the main chamber, its efficiency as a settling device is probably less than that of the inner region. Consequently, increasing the size of this region at the expense of the inner region could be expected to result in somewhat poorer performance. Enlargement of the annulus should also result in somewhat greater tangential velocities for a given inlet sewer velocity, because the smaller surface area will cause lower drag losses. The larger tangential velocity will also tend to degrade the performance because of increased resuspension of bottom sediment.

However, as shown by the data in Figure 88, somewhat better performance is actually achieved with the 61 cm (2 ft) skirt than with the 71 cm (2.3 ft) skirt. This may be the result of the complex flow patterns which develop in the annulus with the smaller skirt. The annulus tangential velocity is not constant across the width of the annulus, but

contains an outer high velocity region and an inner low velocity region. This fact tends to invalidate the heuristic arguments for poorer performance noted above.

DESIGN TECHNIQUES

An example will be given to illustrate how the results of the mathematical model can be applied to estimate the removal efficiency of an actual prototype unit. The following dimensions and design flowrate have been assumed for a hypothetical example.

The sewage settling velocity distribution will be assumed to be that shown by the curve in Figure 75. This curve has been reduced to the step distribution shown in Table 25. The theoretical upper limit of removal efficiency of 46 percent was calculated from equation (55), with A_B computed for the full 3.65 m (12 ft) diameter, thus including the annular region between the skirt and wall of the effective settling zone. For settling velocities greater than the upflow velocity a 100 percent removal efficiency was assumed. It should be emphasized that the 46 percent is a theoretical upper limit on the removal efficiency that can be obtained with the prototype unit. If median particle settling velocity of 0.055 cm/sec (0.0018 ft/sec) had been used instead of the assumed distribution function, equation (55) would predict 36.2 percent removal. This emphasizes the need to have a good definition of the settling properties of the sewage.

A second estimate of the prototype removal efficiency can be obtained from the performance curves for the laboratory model as shown in Figure 88. This figure shows the removal efficiency measured by the laboratory for different material settling velocities and flowrates. To provide a convenient mechanism for predicting prototype removals, the data have been nondimensionlized and plotted as the removal efficiency versus the settling parameter $w_s A_B/Q$, where w_s equals the particle median settling velocity A_B equals the projected cross-sectional area, and Q is the volumetric flowrate. Smooth curves (dash line) have been drawn through the data points approaching a horizontal asymptote of 92.6. The 92.6 percent removal represents the value observed by the laboratory for the 150-300 mesh IRA resin having a settling parameter value of 6.85. This point is off the scale of Figure 88, and is not shown.

TABLE 25
PREDICTED REMOVAL EFFICIENCY FOR HYPOTHETICAL PROTOTYPE UNIT USING MATHEMATICAL MODEL

Percent Particles of Settling Velosity less than v_s	Percent Particles of Settling Velocity v_s	Settling Velocity v_s cm/sec	(ft/sec)	Percent Removal as Computed from Equation (55)
95	10	0.31	(0.01)	10.0
85	10	0.22	(0.007)	10.0
75	10	0.16	(0.005)	10.0
65	10	0.11	(0.004)	7.2
55	10	0.07	(0.002)	4.6
45	10	0.04	(0.001)	2.6
35	10	0.02	(0.0007)	1.3
25	10	0.003	(0.00009)	0.1
15	10	Non-Settleable		0
5	10	Non-Settleable		0
		Total Predicted Removal		46.0%

$$\text{Prototype Overflow Rage} = \frac{0.57 \text{ cfs}}{(\pi)(6\text{ft})^2} = 0.004 \text{ fps } (0.152 \text{ cm/sec})$$

The solid line shown in Figure 88 represents the theoretical upper limit on removal efficiency, as calculated from equation (55). As noted earlier and confirmed in this figure, there is close agreement between the laboratory and mathematical model when the settling velocity is substantially less than the overflow rate, i.e. values of the settling parameter less than 0.5.

Since the settling parameter used in preparing Figure 88 is dimensionless, the curve representing the laboratory data in Figure 88 is independent of scale. Therefore, removal efficiencies as predicted by the laboratory data can be readily obtained from Figure 88 by entering the curve with the appropriate value of $w_s A_B$ and Q. Using this approach, the removal efficiencies for the hypothetical example were recalculated using the lower laboratory curve in Figure 88. The results are tabulated in Table 26, Predicted Removal Efficiency for Hypothetical Prototype Unit Using Laboratory Data. The total removal efficiency obtained from the laboratory curve is 34.7 percent, as compared to the 46 percent theoretical upper limit.

As noted earlier, both the mathematical model and the laboratory data will tend to overpredict the prototype removal efficiency. Consequantly, it may be wise to make allowance for this by increasing the assumed design flowrate by a safety factor when calculating predicted removal efficiencies.

TABLE 26
PREDICTED REMOVAL EFFICIENCY FOR HYPOTHETICAL PROTOTYPE UNIT USING LABORATORY DATA

% Particles of Settling Velocity v_s	Prototype Settling Velocity cm/sec	(ft/sec)	Settling Parameter $\frac{v_s A_B}{Q}$	Removal Weighted From Figure
10	0.31	(0.01)	2.04	8.2
10	0.22	(0.007)	1.45	7.4
10	0.16	(0.005)	1.05	6.3
10	0.11	(0.004)	0.72	5.1
10	0.07	(0.002)	0.46	3.8
10	0.04	(0.001)	0.26	2.5
10	0.02	(0.0007)	0.13	1.3
10	0.003	(0.00009)	0.01	0.1
10	Non-Settleable			0
10	Non-Settleable			0
			Total Predicted Removal	34.7

a	=	mean radius, acceleration
A	=	area
C_o	=	initial particle concentration
C	=	particle concentration
E	=	efficiency
$\hat{e}$	=	unit vector
f	=	nondimensional stream function
F	=	particle mass flux
g	=	gravitational acceleration
G	=	nondimensional tangential velocity function
G'	=	shear rate of flow
l	=	mixing length
L	=	reference length
N_∞	=	total particle concentration
N_{ij}	=	particle collision rate
n	=	particle number density; particle distribution function
$\vec{n}$	=	unit normal vector
p	=	pressure
Q	=	volume flowrate
R	=	$w_s \Delta n n_z / \epsilon_p$
Re	=	Reynolds number
r	=	radial coordinate; particle radius
S	=	scaling factor
Sg	=	specific gravity
t	=	time
u_{ref}	=	reference velocity
u	=	radial velocity component
v	=	particle volume
v	=	tangential velocity component
w	=	vertical velocity component
w_s	=	particle settling velocity
$\bar{w}$	=	average upflow velocity
Z	=	depth location of column sampling port
z	=	axial coordinate
ϵ	=	eddy viscosity
ϵ_p	=	particle eddy diffusivity
ϵ'	=	energy dissipation per unit mass
ζ	=	nondimensional axial coordinate (z/L)
η	=	vorticity; underflow/overflow ratio
μ	=	molecular viscosity
ν	=	kinematic viscosity
ξ	=	nondimensional radial coordinate (r/L)
ρ	=	liquid density
σ	=	standard deviation
θ	=	volume fraction of particles
λ	=	scale size
ψ	=	stream function
ψ_1	=	nondimensional distribution function
ω	=	reference frequency
Ω	=	nondimensional vorticity function

Subscripts

b	=	boundary value, or bottom
$b+1$	=	value at point adjacent to boundary
$in.$	=	inflow
L	=	liquid
p	=	particle

Superscripts

$\rightarrow$	=	vector quantity

REFERENCES

1. American Public Works Association, "The Swirl Concentrator as a Combined Sewer Overflow Regulator." *EPA Report No. EPA-R 2-72-008, NTIS No. PB214134,* Sept. 1972
2. Camp, Thomas R., "Sedimentation and the Design of Settling Tanks," *Trans ASCE;* Vol III, 1946 (pp 895-958)
3. Saffman, P.G., and Turner, J.S., "On the Collision of Drops in Turbulent Clouds," *J. Fluid Mechanics,* Vol. 1, 1956 (pp 16-30)
4. Swift, D.L., and Friedlander, S.K., "The Coagulation of Hydrosols by Brownian Motion and Laminar Shear Flow," *J. Colloid Sci.,* Vol. 19, 1964 (pp 621-647)
5. Levich, V.G., *Psychochemical Hydrodynamics,* Prentice-Hall, Inc., Englewood Cliffs, N.J., 1962 (pp 175, 219)
6. Ives, K.J., and Bhole, A.G., "Theory of Flocculation for Continuous Flow System," *Proc. ASCE, J. Env. Eng. Div.,* Bol 99, No. EE1, Feb. 1973 (pp 17-34)
7. Hidy, G.M., "On the Theory of the Coagulation of Noninteracting Particles in Brownian Motion," *J. Colloid Sci.,* Vol. 20, 1965 (pp 123-144)
8. Gemmel, R.S., "Some Aspects of Orthokinetic Flocculation," thesis presented to Harvard University, at Cambridge, Mass. in 1963, in partial fulfillment of the requirement for the degree of Doctor of Philosphy.
9. Fair, G.M., and Gemmel, R.S., "A Mathematical Model of Coagulation," *J. Colloid Sci.,* Vol. 19, 1964 (p 360)
10. Friedlander, S.K., "Similarity Consideration for the Particle-Size Spectrum of a Coagulating, Sedimenting Aerosol," *J. Meteorology,* Vol. 17, No. 5, Oct. 1960 (pp 80-84)
11. Chen, Cheng-lung, "Sediment Dispersion in Flow with Moving Boundaries," *J. Hyd. Div., Proc. ASCE,* Vol. 97, No. HY8, Aug. 1971 (pp 1181-1201)
12. Reynolds, A.J., "Waves on the Erodible Bed of an Open Channel," *J. Fluid Mech.,* Vol. 22, Part 1, 1965 (pp 113-133)
13. Hyashi, T., "Formation of Dunes and Antidunes in Open Channels," *J. Hyd. Div., Proc. ASCE,* Vol. 96, No. HY2, Feb. 1970 (pp 357-366)
14. Kennedy, J.F., "The Mechanics of Dunes and Antidunes in Erodible - Bed Channels," *J. Fluid Mech.,* Vol 16, Part 4, 1963 (pp 521-544)
15. Engelund, F., "Instability of Erodible Bed," *J. Fluid Mech.,* Vol. 42, Part 2, 1970 (pp 225-244)
16. Smith, J.D., "Stability of a Sand Bed Subjected to a Shear Flow of a Low Froude Number," *J. Geophy. Res.,* Vol. 75, No. 30, Oct. 1970 (pp 5928-5940)
17. Gradowczyk, M.H., "Wave Propagation and Boundary Instability in Erodible Bed Channels," *J. Fluid Mech.,* Vol. 33, Part 1, 1968 (pp 93-112)
18. Smisson, B., "Design, Construction, and Performance of Vortex Overflow," *Symposium on Storm Sewage Overflows;* Institute of Civil Engineers, 1967.

APPENDIX C

SETTLEABILITY TESTS AND HYDRAULIC CHARACTERIZATION OF A PILOT (WITH REAL SEWAGE) SWIRL SEPARATOR AS A PRIMARY TREATMENT FACILITY

This appendix reports the results of the characterization of the settling properties of combined sewer overflow currently being used in studies designed to evaluate the efficiency of the pilot swirl as a primary separator. During two storm events in June 1975, the suspended solids concentration in the influent channel of the Humber Treatment Plant (Metropolitan Toronto) was found to increase to about 600 mg/l. A distinct improvement in the settleability was found even after peak flows had occurred. The settling characteristics of the combined overflow was very similar to the Amberlite IRA-93 anion exchange resin developed for laboratory scale studies conducted in an earlier phase of this project.[1]

Hydraulic characterization of the swirl separator and the primary clarifier used in this study were conducted using a dye tracer response technique. The hydraulics of the swirl separator was found to be more closely related to plug flow regime than the primary clarifier. Theoretically, the closer to a plug flow mixing regime, the better should be the solids removal efficiency.

The apparent decrease in active volume and the shift toward plug flow which occurs as flow to the swirl increases, suggests that the swirl separator should respond well as a solids separator for combined sewer storm flow in a sewage treatment plant.

SETTLEABILITY TESTS

A pilot swirl separator has been constructed at the Humber Treatment Plant operated by Metropolitan Toronto. Comparison studies of the removal efficiencies of suspended solids in the pilot swirl separator and primary clarifier were conducted during periods of normal flow and also during periods of storm flow. As part of these studies, Beak Consultants Ltd., conducted settleability tests of the combined storm flow and compared the hydraulic characteristics of the two settling devices.

Methods for Characterization of Settleability

The settling characteristics of the storm flow solids were measured on two separate occasions during the month of June 1975. Samples were collected in the influent channel of the primary clarifier. Samples were collected by the plant operators during periods of increased flow as a result of storm flow entering the plant. Arrangements were made to sample the influent during rising, peaking, and falling flows. The collected samples were picked up from the plant by Beak and all settling tests were conducted within 18 hours of sampling.

Both storm events in June occurred in the late evening when the plant flow was about 1,748 l/sec (40 mgd). Daily average plant flow is approximately 3,058 l/sec (70 mgd). The first event studied occurred at 2300 hours on June 4th, continued three hours until about 0200 hours on June 5th. The peak flow was 5,462 l/sec (125 mgd) during this event.

On June 16, a shorter, more intense storm increased plant flows from 2200 to 2300 hours producing a peak of 6,816 l/sec (156 mgd). In addition to the collection of rising, peaking, and falling stages in the primary influent channel, the influent to the swirl separator was tested for settleability at peak flows. The swirl influent and the primary clarifier influent differ only by the fact that the swirl influent is pumped out of the primary influent channel. This pumping step is the only difference between the waste received by each settling device.

The samples were tested for settleability using the same method used by Beak in its previous study.[1] This method is described in Exhibit 1 of this appendix.

Discussion of Settling Results

The results of the settleability tests are presented in Figures 89 and 90. The solids settling characteristic of the combined sewer flow is expressed as the percent removal of suspended solids as a function of the upflow

EXHIBIT 1

SETTLING COLUMN TEST METHODS

Procedure

The test column consists of a 2.03 m (6.66 ft) high, 20 cm (8 in) diameter, Plexiglas® cylinder with sampling ports as 1 ft increments. The bottom of the cylinder is fitted with a water-tight base, 30.5 cm (1 ft) diameter, to give a stable base during the test run.

Where possible, a 56.7 l (15 gal) sample should be collected and the settling test run immediately to prevent any changes in the sample. The most important variable is temperature and, where possible, the test should be performed before any great change occurs. In most cases, it is not practical (or meaningful) to attempt to adjust the sample temperature to that of the ambient temperature where the test is being performed. The temperatures of the sample in the column should be recorded at the start and the finish of the test run. The samples should be mixed thoroughly and dumped into the test column as quickly as possible. To make sure of thorough mixing in the column, a hand-made plunger was used to agitate the contents throughout the depth of the column. The timer is then started and the column is sampled at each port immediately. Starting from the top of the column, the ports sampled are at the 30.5, 61, 91, 122, 152.5, and 167.8 cm (1, 2, 3, 4, 5, and 5.5 ft) levels.

These "time zero" samples are averaged to provide the initial suspended solids of the sample in the column. The column is then sampled from each port at convenient time intervals. The suggested intervals are: 10, 20, 40, 60, 80, 100, and 120 minutes.

The samples withdrawn from each sample port (except the bottom one) should be collected in small containers (approximately 500 ml) to be analyzed for suspended solids. Care must be taken to flush out each sample port before the sample is taken. The filter paper used for this analysis should be Whatman GF-C or equivalent.

The depth of liquid in the column should be recorded initially and after each set of samples has been removed. It is more convenient to measure all depths from the top of the column.

The percent settleable solids should be determined on the large sample collected for the settling test. This is done by filling a graduated cylinder (1,000 ml) with the sample and allowing the sample to stand for one hour. After 60 minutes a sample is withdrawn from the center of the cylinder for suspended solids determination.

Interpretation of Results

Using the suspended solids results from the above procedure, the percent of initial suspended solids is calculated for each sample. Each sample is associated with a specific port, time, and liquid level. The quantity "z/t" is calculated where "z" is the distance down the column from the surface of the sample and "t" is the time at which the sample was taken. This quantity is converted to a settling velocity in cm/sec (ft/sec). Percent of initial suspended solids is then plotted against "z/t" resulting in a distribution of settling velocities of the suspended solids in the sample. When interpreted with a slightly different method, the percent removal of suspended solids can be evaluated as a function of overflow rate and of detention time. This is used for the design of a primary clarifier.

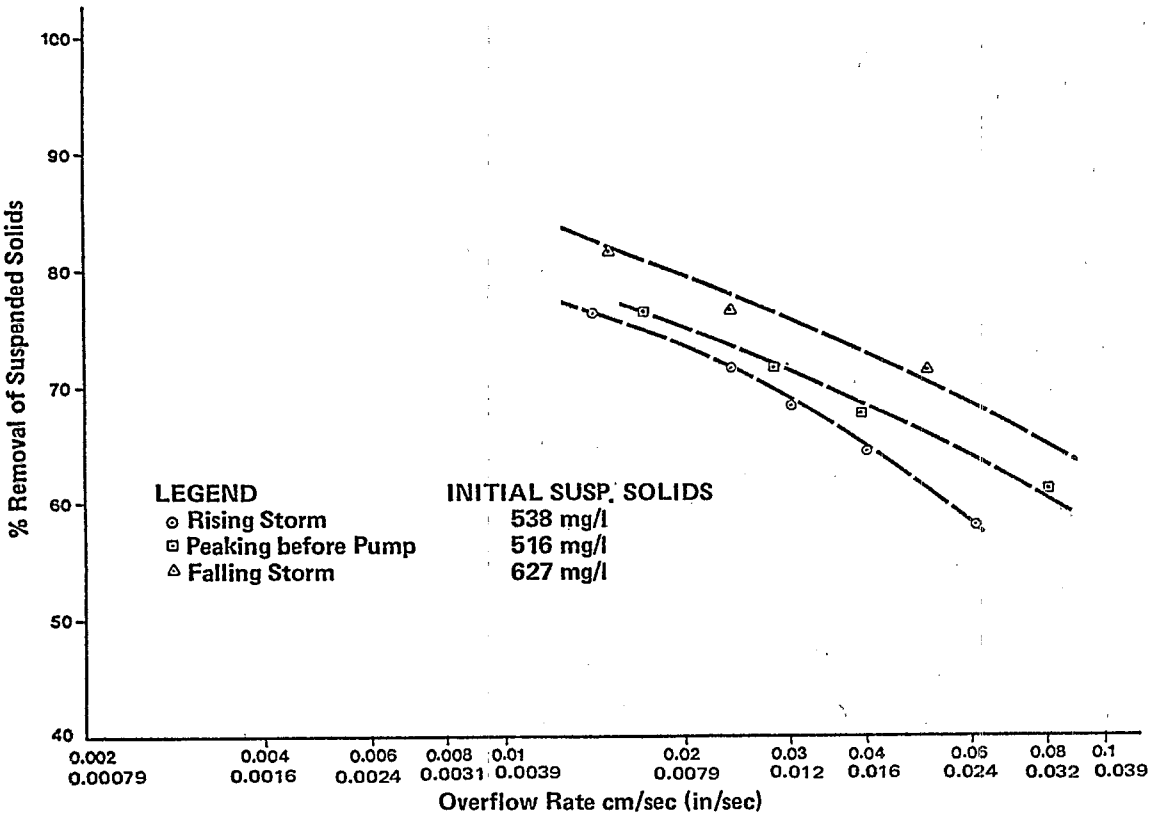

FIGURE 89 SETTLING VELOCITY CHARACTERISTICS – HUMBER TREATMENT PLANT
Storm Flow June 5, 1975

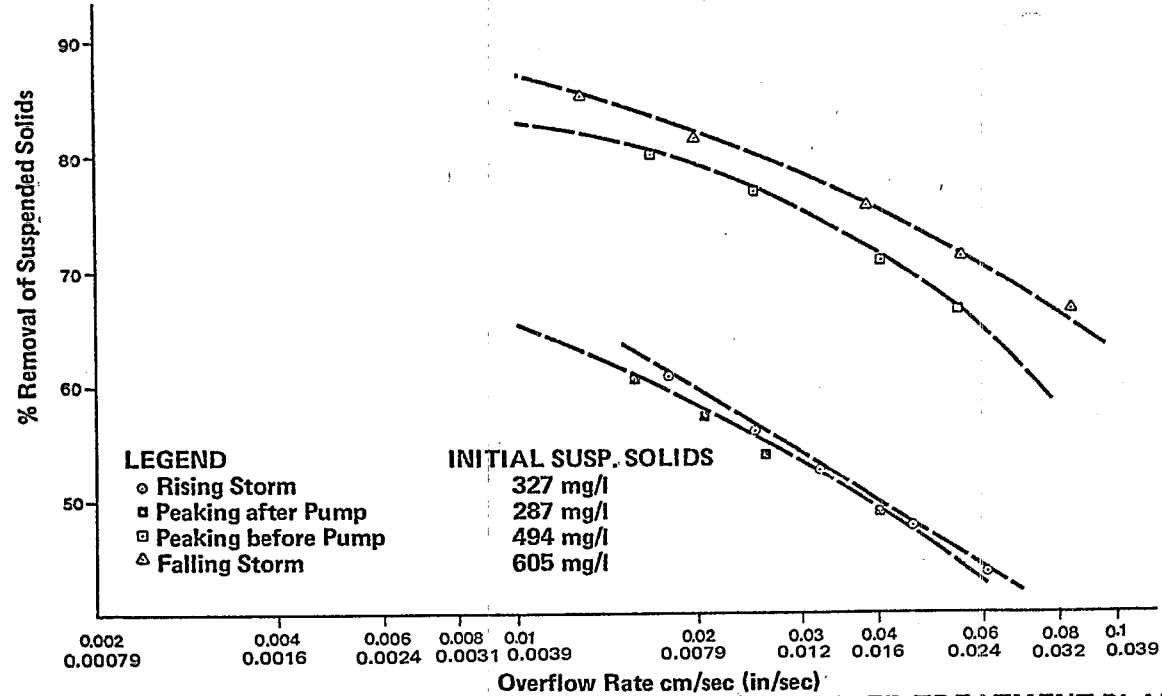

FIGURE 90 SETTLING VELOCITY CHARACTERISTICS – HUMBER TREATMENT PLANT
Storm Flow June 16, 1975

velocity or overflow rate in a settling device. During the storm of June 5, 1975, suspended solids were found to increase from 538 mg/l to 627 mg/l. The settleability of the combined sewage flow improved as the storm progressed. In fact, the predicted percent removal for a given overflow rate is greater for the combined sewage during the falling storm hydrograph compared to the peak flow condition. For a constant overflow rate of 20 l/sec (0.45 mgd) or 162 $m^3/day/m^2$ (4,000 gpd/ft^2), the predicted percent solids removals are 74, 76, and 81 percent respectively for rising, peaking, and falling storm events.

The second storm monitored was shorter; however, the storm was more intense, producing a larger peak flow. The suspended solids concentration increased from 327 mg/l to 494 mg/l to 605 mg/l as the storm progressed through the rising, peaking, and falling stages. For a constant overflow rate of 20 l/sec (0.45 mgd), the predicted percent solids removal is 60, 80, and 83 percent respectively for rising, peaking, and falling storm conditions.

A sample of the peaking flow after the lift pump to the swirl separator had lower suspended solids and poorer settling characteristics than the sample collected before the pump. In fact, the settling properties of the sample taken after the pump appears to be similar to the rising flow sample prior to the pump. Although this indicates that the pump changed the characteristics of the effluent, we do not believe that this is the correct conclusion. First, the suspended solids concentration should not change as a result of pumping. The fact that samples taken before and after the lift pump were different in suspended solids, suggests that the samples were not of the same material.

In addition, during this short, intense storm, lasting only one hour, the influent varied in quality and quantity over a brief period. The influent appeared to change in character significantly between the time the samples were collected, before and after pumping. As the solids concentration in the after pump sample is similar to the rising storm condition sample, and the settleability characteristics are identical, the pump did not appear to affect the settling properties of the solids.

Conclusions on Settleability

The combined sewer overflow events at the Humber Treatment Plant resulted in an increase in the suspended solids concentration and an improvement in the settling velocity characteristics of the waste. The solids in the influent were most settleable as the storm progressed through the rising, peaking, and falling stages. For the seven tests conducted, between 60 to 83 percent of the solids had a settling velocity of 0.2 cm/sec (0.00656 ft/sec), or more. In comparison, the IRA 93 resin simulated sewage developed by Beak for laboratory scale studies of the swirl separator, gave a range of removals from 56 to 75 percent for overflow rates of 0.2 cm/sec (0.00656 ft/sec). Thus, the simulated material used in the laboratory scale studies appears to have very closely approximated the actual solids in combined sewer overflows.

HYDRAULIC CHARACTERISTICS

Removal of "suspended" material from a water, solids mixture may be accomplished in many ways familiar to sanitary engineers. The swirl separator, like the traditional primary clarifier, accomplishes this using gravitational force to help remove the fraction of influent solids which are settleable. However, the hydrodynamic forces, due to the movement of the fluid in the vessel, are used to enhance the removal in the case of the swirl separator, whereas in the conventional clarifier, any hydrodynamic forces are "designed out" as the resulting turbulence tends to re-suspend settled material. To more fully understand the nature of the hydraulic regime governing the hydrodynamic forces present and to "characterize" the vessels into a sequence of interconnected compartments, each governed by well understood flow patterns, tracer studies using fluorescent dye were conducted on the swirl at various flowrates and on the battery of parallel primary clarifiers. The technique used is standard to chemical engineering and involves the injection of a dye into the feed stream of the vessel and the subsequent monitoring of the dye in the effluent as a function of time. Starting with an initial pulse of dye, the degree of mixing in the vessel may be deduced by matching the resultant output dye trace to the pattern that

would result from a model comprised of segments or compartments, in which the mixing is well understood and the output dye trace well known. Once the vessel has been characterized into a series of ideal tanks or reactors, it becomes possible to compare the behavior of the vessel to that expected using classical settling theory.

Methods for Hydraulic Characterization

The flow into the vessel under investigation is maintained as uniform as possible to ensure that the tank hydraulics are in steady state.

A pulse of conservative dye is injected into the inlet stream to the vessel in such a way that the dye becomes as well mixed as possible across the influent stream.

A time base is maintained throughout the investigation with zero time being the instant the dye is injected. To ensure that the effluent dye trace is measuring the hydraulics of the vessel and not the inlet/outlet channels, effects due to the latter are eliminated by injecting and monitoring the dye as close to the vessel as practical. As the pulse of dye moves through the vessel, the hydrodynamic regime alters the profile of the dye pulse and the monitoring station downstream measures the shape of the dye trace or distribution as a function of time. The alteration of the dye trace from a pulse having essentially no distribution into the final shape at the outlet monitoring point may be interpreted mathematically to yield some hypothetical network of ideal tanks. In the present study, the mathematical analysis took the form of variance analysis rather than the more involved minimization of square error. Rhodamine WT® was used as the conservative tracer and was analyzed in the form of discrete samples, each taken at a predetermined time, using fluourometric methods. To remove interferences due to the sewage, a blank sample was run through the fluorometer to establish base line calibration.

Discussion of Hydraulic Results

Details of the statistical techniques used to fit the models to the data are contained in Exhibit 2. The parameter estimates are in Table 26. Plots of the dye traces obtained and the fitted models are shown in Figures 91 through 96. Examination of the experimental residence times shows that in each case the theoretical residence time of the swirl separator, based on the calculated volume, was greater than that exhibited by the tracer and that the difference decreased with flow based on three data points as shown in Figure 97. This would indicate that as flow increases, the degree of short-circuiting increases or conversely that as flow increases, the portion of the total volume available for flow through decreases. The battery of six parallel, primary clarifiers showed 60 percent increase in the measured detention time indicating a significant amount of recirculation within the tanks, and/or an imbalance in the splitting of the flow between tanks.

The fitted parameters showed that in all cases, the swirl separator behaved more as plug flow than did the primary clarifier and that as flow increased, the swirl separator shifted more toward the plug flow regime, but even at high flow, remained less well mixed than the primary tanks. The model fitting indicated the general trend of mixing within the vessels and the fittings procedure used was not intended to provide a statistical criteria through which the best fit could be obtained. The variation in number of tanks in sewer (N) and axial dispersion coefficient (D) are indicative of the same trends in mixing and are equally useful in generalizing the hydraulics of the vessels.

Conclusions on Hydraulic Characteristics

The results of the tracer study show that the hydrodynamics of the swirl separator lie more toward the plug flow regime of mixing than do the primary clarifiers. The apparent decrease in active volume and shift toward plug flow which occurs as the flow increases in the swirl concentrator would indicate that the quiescent cone of fluid along the axis of the swirl may increase with increasing flow.

Removal efficiency decreases as the mixing regime shifts from plug flow to well mixed. The results of the tracer study would predict that the swirl, being closer to plug flow in all cases tested, would accomplish the same removal as the primary clarifiers but at a significantly higher upflow velocity or surface

TABLE 27
MODEL FITTED PARAMETER ESTIMATES

			Axial Dispersion		Tanks in Series		
Settling Device	Flow l/sec	Flow mgd	Variance τ_θ^2	Dimensionless Dispersion Number D/uL[1]	Number of Tanks in Series N[2]	Actual Mean[3] Residence Time τ_{act} (min)	Theoretical[4] Residence Time τ_{th} (min)
Swirl Primary	22.2	0.51	0.28	0.17	3.6	6.4	13.4
Swirl Primary	16.5	0.38	0.37	0.24	2.7	13.8	18.0
Swirl Primary	10.4	0.24	0.36	0.23	2.8	21	28.5
Primary Clarifier	4.785	110	0.52	0.43	1.9	75.8	47.3

[1] *the lower the dimensionless dispersion number, the lesser the mixing in the vessel. Good settling practice minimizes the axial dispersion.*

[2] *the more tanks in series, the less short-circuiting and mixing in the vessel. Good settling practice minimizes short-circuiting and mixing.*

[3] τ_{act} *less than* τ_{th} *is indicative of a dead volume zone*

[4] τ_{th} *less than* τ_{act} *is indicative of recirculation within the vessel*

EXHIBIT 2

DESCRIPTION OF HYDRAULIC MIXING MODELS

In this study, the swirl separator and the primary clarifier hydraulic characteristic have been fitted to two models. These are the axial dispersion model and the equal tank-in-series model. Tables 28 and 29 describe these models.

The degree of mixing in the axial dispersion model is described by the axial dispersion coefficient or the axial dispersion number (D/uL). Where D = the axial dispersion coefficient (m^2/sec); u = fluid velocity in the vessel; L = length of vessel. For best settling conditions in a vessel, this number should be minimized.

Mixing in tanks-in-series model is described by the number of tanks in the series (N). For best settling conditions in a vessel, N should be maximized.

Exhibit 2 (Cont'd)

TABLE 28
THE AXIAL DISPERSION MODEL

THE MODEL

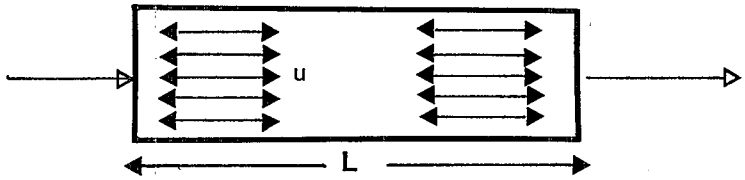

L = length of vessel (m)
u = avg. fluid velocity in vessel (m sec^{-1})
D = axial dispersion coefficient (m sec^{-1})
Pe = Peclet number = uL/D

RESIDENCE TIME DISTRIBUTION

$$E(\theta) = \tau E(t)$$

$$E(t) = \frac{Pe}{4} \exp\left[\frac{Pe}{4}(2-t)\right] \sum_{k=1}^{\infty} \left\{ \left[\frac{\lambda_k \sin(2\lambda_k)}{\lambda_k^2 + \frac{Pe^2}{4} + \frac{Pe}{4}} \right] \exp\left[\frac{-4\lambda_k^2 t}{Pe}\right] \right\}$$

$$+ \exp\left[\frac{Pe}{4}(2-t)\right] \sum_{k=1}^{\infty} \left\{ \frac{4\lambda_k^2}{Pe} \left[\frac{\lambda_k \sin(2\lambda_k)}{\lambda_k^2 + \frac{Pe^2}{4} + \frac{Pe}{4}} \right] \exp\left[\frac{-4\lambda_k^2 t}{Pe}\right] \right\}$$

where λ_k are the positive nontrivial roots of the transcendental equation:

$$\tan(2\lambda) = \frac{\lambda\, Pe}{2(\lambda^2 - \frac{Pe}{4})}$$

These may be obtained by defining $\beta_n = \lambda_{2n-1}$

and $\Upsilon_n = \lambda_{2n}$ where the β_n and Υ_n are the positive roots of the transcendental equations:

$$\tan\beta = \frac{Pe}{4\beta} \qquad \text{and} \qquad \cot\lambda = \frac{Pe}{4\lambda}$$

VARIANCE

$$\sigma_\theta^2 = 2\left(\frac{D}{uL}\right) - 2\left(\frac{D}{uL}\right)^2 \left[1 - e^{-\left(\frac{uL}{D}\right)}\right]$$

Exhibit 2 (Cont'd.)

TABLE 29
THE EQUAL TANKS-IN-SERIES MODEL

THE MODEL

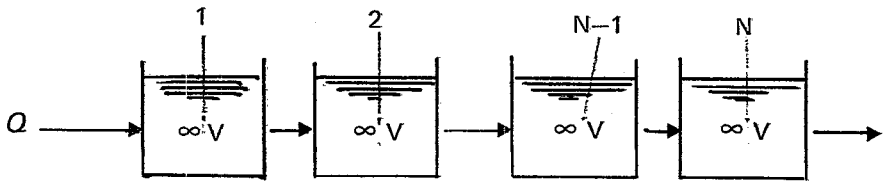

Q = flowrate (mgd)

V_T = total active volume = N V (gal)

Number of tanks = N
Volume of tanks = V

Individual vessel residence time = $\tau = V_v/Q$ min

overall mean residence time = $\tau_T = N_\tau$ min T_T

RESIDENCE TIME DISTRIBUTION

$$E(\theta) = \tau E(t)$$

$$E(t) = \frac{N^N \left[\frac{t}{\tau_T}\right]^{N-1}}{(N-1)!} \exp\left[\frac{-N\,t}{\tau_T}\right]$$

$$\Gamma(X) = (X-1)!$$

TRANSFER FUNCTION

$$G(s) = \left[\frac{1}{1+\tau s}\right]^N$$

VARIANCE

$$\sigma^2_\theta = \frac{1}{N}$$

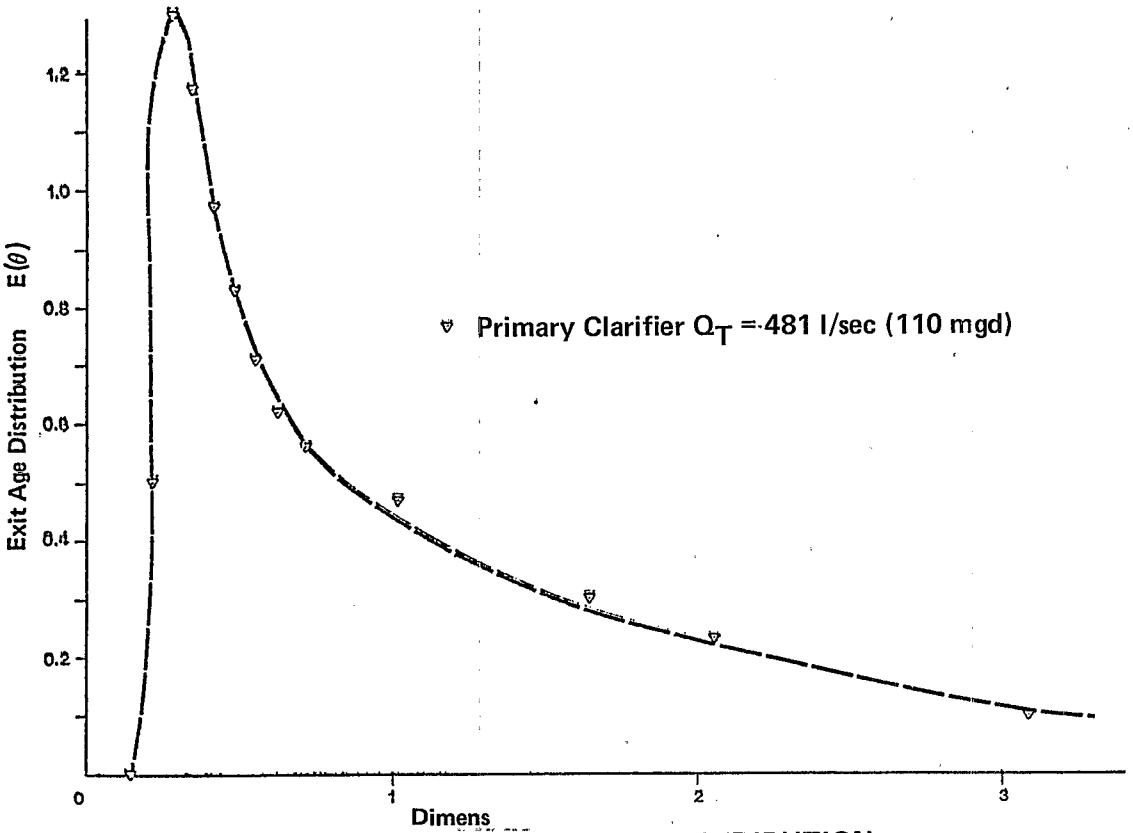

FIGURE 91 RESIDENCE TIME DISTRIBUTION

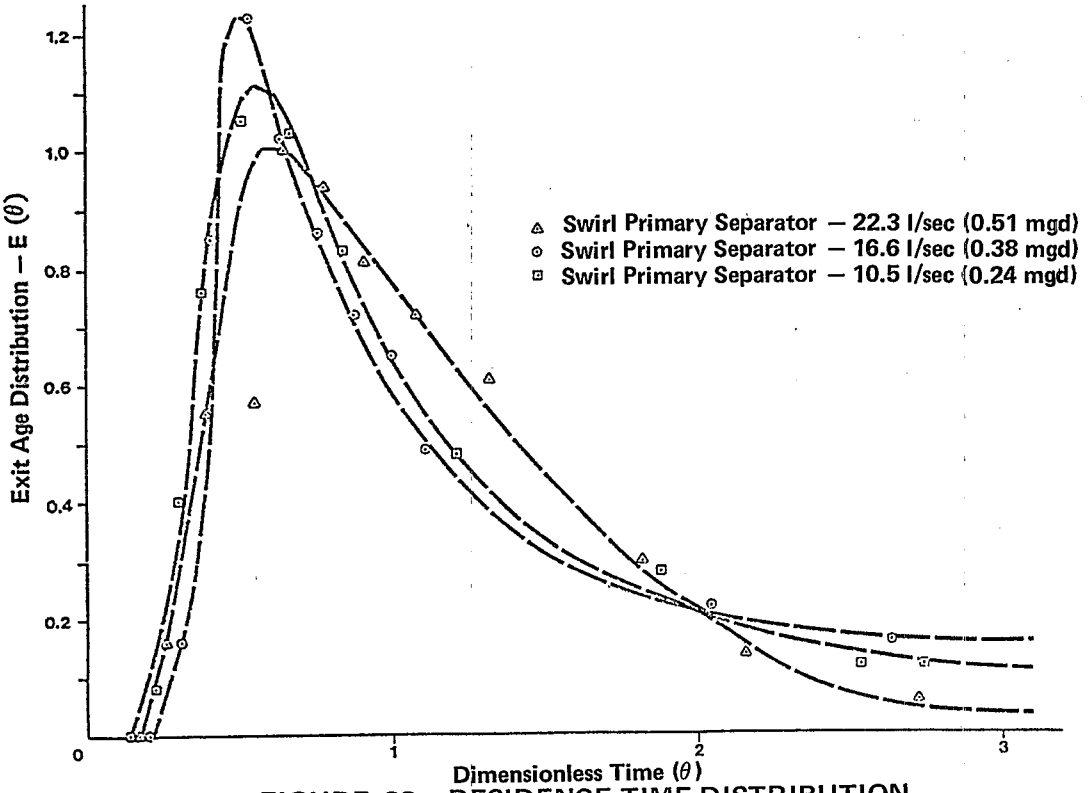

FIGURE 92 RESIDENCE TIME DISTRIBUTION

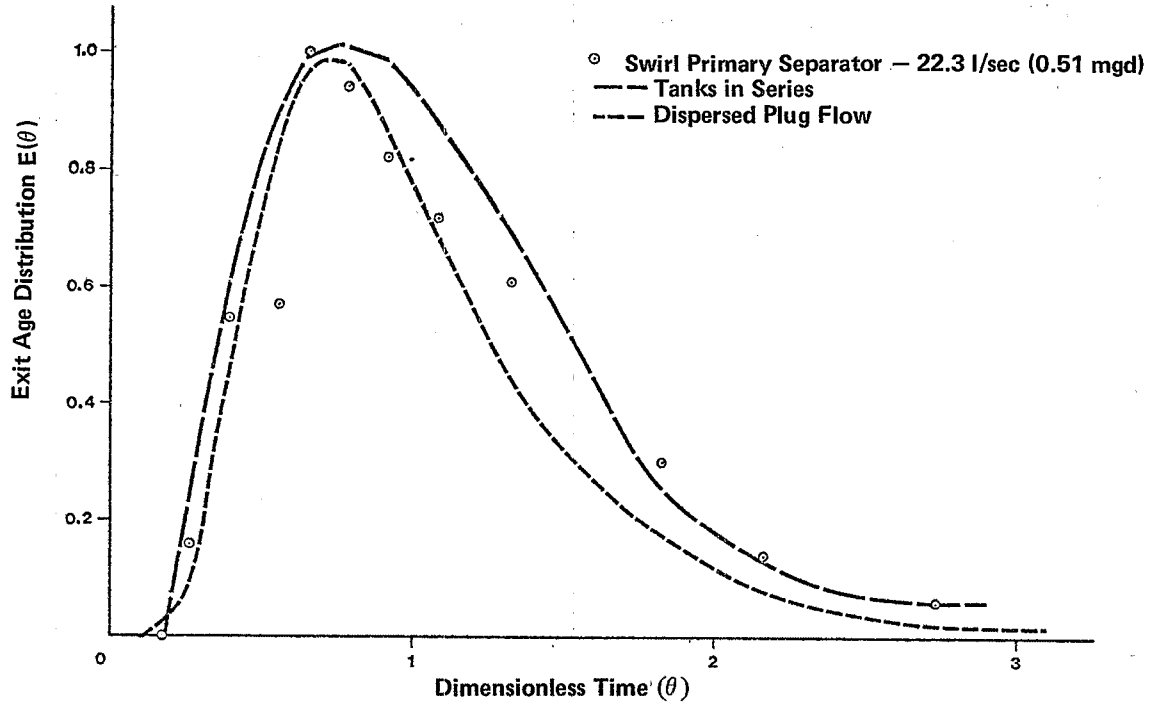

FIGURE 93 FITTED RESPONSES

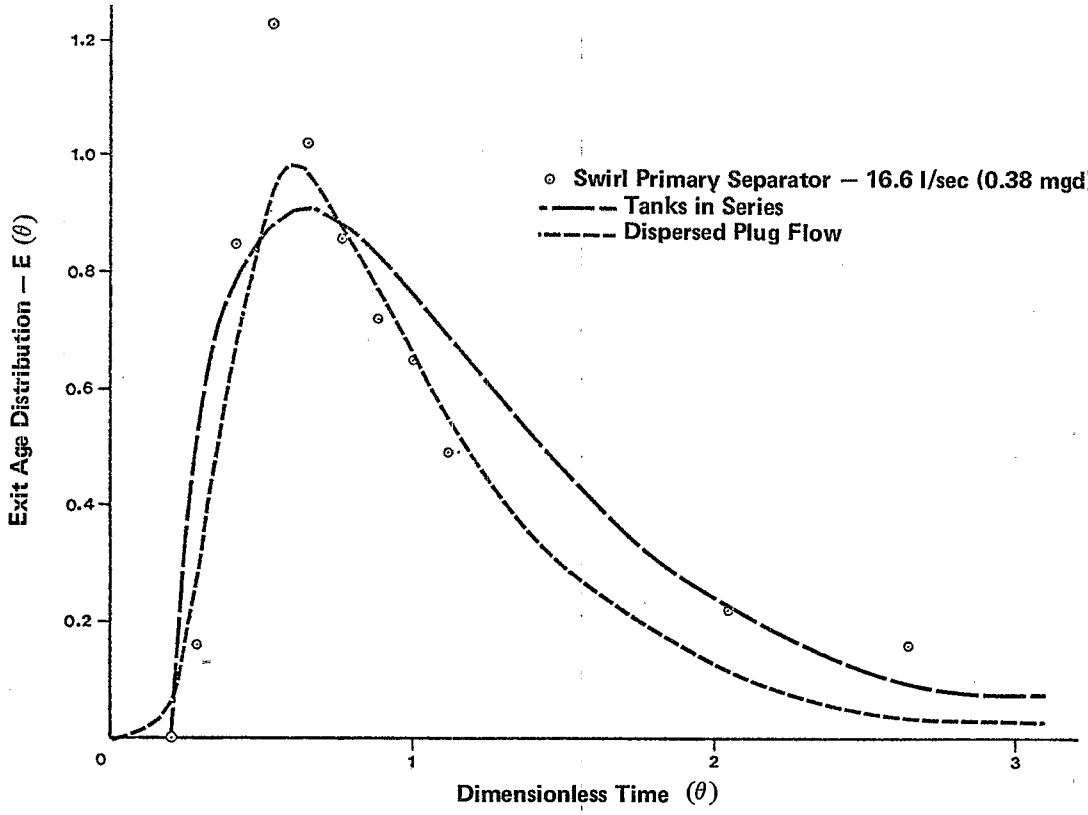

FIGURE 94 FITTED RESPONSES

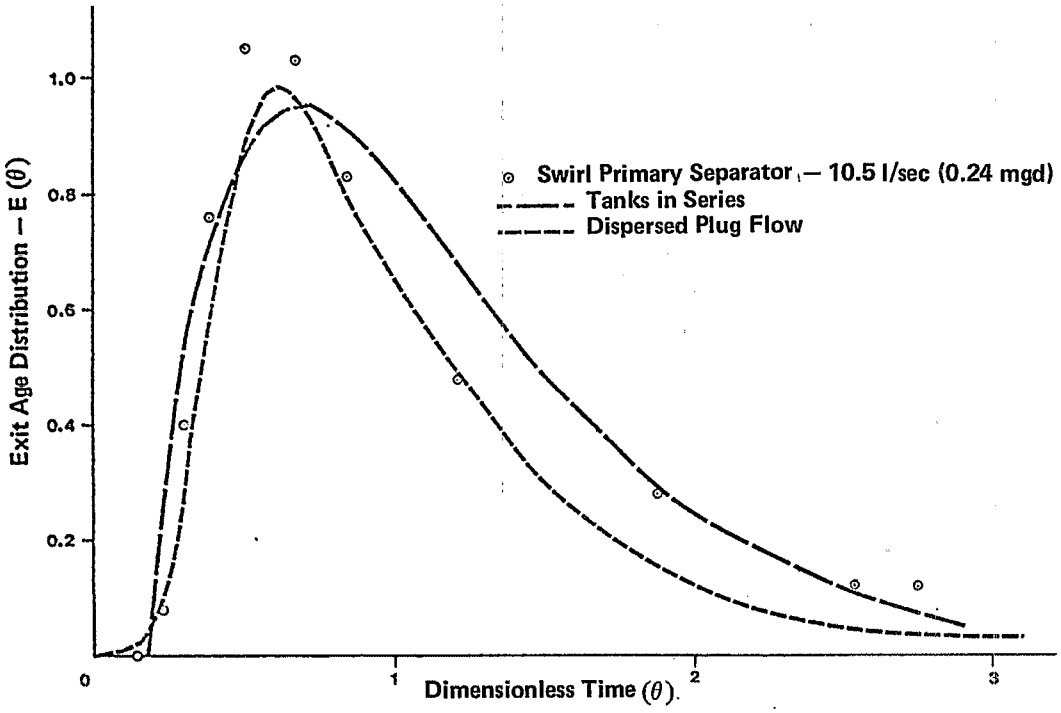

FIGURE 95 FITTED RESPONSES

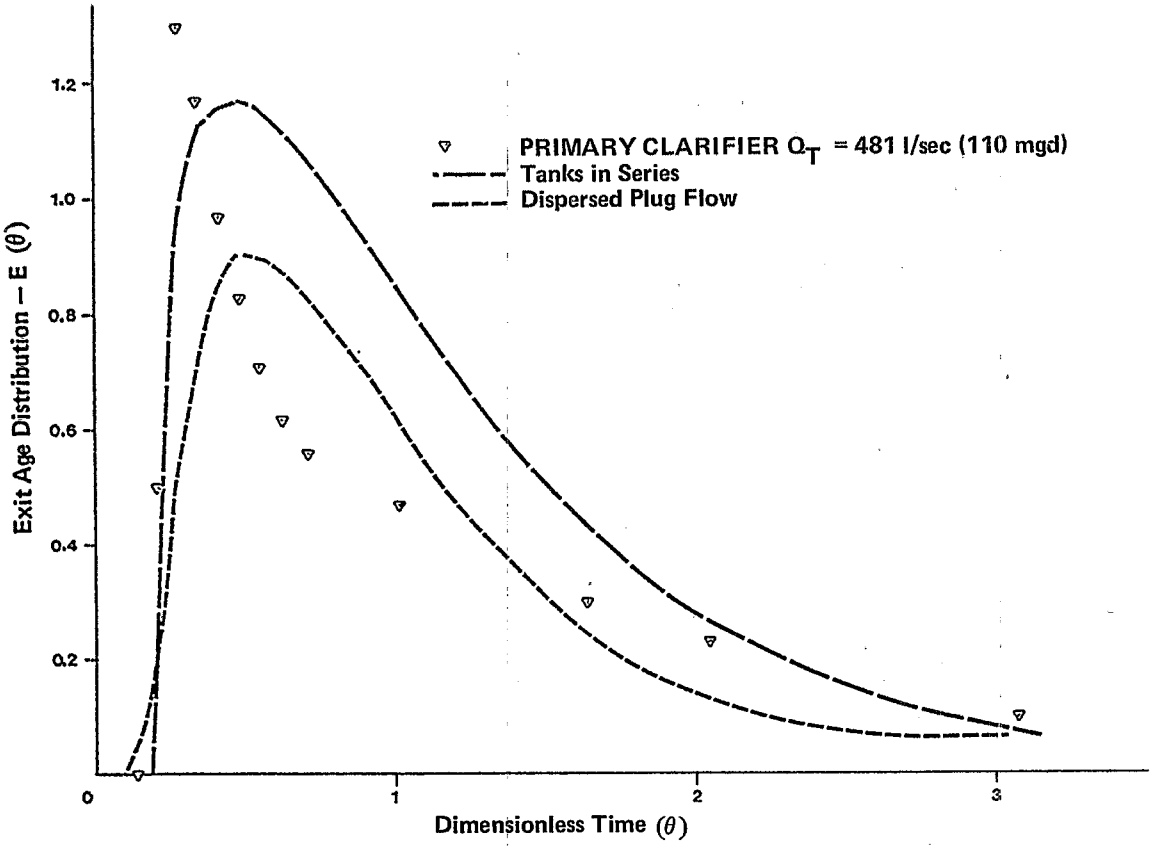

FIGURE 96 FITTED RESPONSES

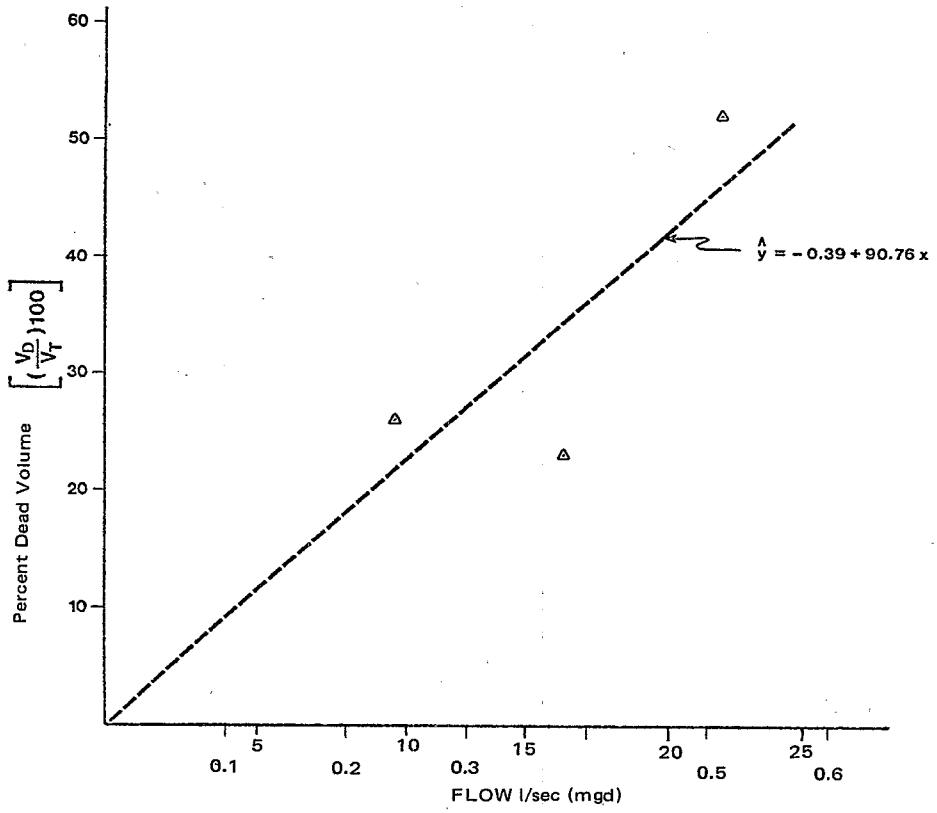

FIGURE 97 PERCENT DEAD VOLUME VERSUS FLOW, SWIRL SEPARATOR

overflow rate. Using the Froude Number in a dynamic similarity projection, there is a limit to the size of prototype swirl unit which will perform as well as the scale model tests. To compensate for the scale effects as the size is increased, it may be necessary to change the dimensions of the chamber, such as the diameter of the inner skirt baffle and the baffle clearance, and to control the weir overflow rate.

REFERENCES

1. Dalrymple, R.J., *etal.* Physical and Settling Characteristics of Particulates in Storm and Sanitary Waste Waters, *EPA Report No. EPA 670/2-75-011 , NTIS No. PB 242001*, April, 1975

APPENDIX D
PILOT TEST RESULTS

TABLE 30
DRY-WEATHER TEST SCHEDULE

Test	Test No. Swirl Conc. Inlet	Test No. Swirl Conc. Outlet	Test No. Primary Tank Inlet	Test No. Primary Tank Outlet
Settleable Solids	1	2	16	17
Total Suspended Solids	3	4	18	19
Volatile Suspended Solids	5	6	20	21
Fixed Suspended Solids	7	8	22	23
Temperature	—	—	24	—
pH	—	—	25	—
BOD_5	9	10	26	27
COD	11	12	28	29

	Sludge	Sludge
Sludge Solids Concentration	13	30
Sludge Volume	14	31

	Sewage	Sewage
Total Daily Flow	15	32

Tests 1, 2, 16, 17 — *Every four hours on grab samples.*
Tests 3 thru 8, 18 thru 23 — *Daily on composite grab samples taken every two hours proportional to flow. Run tests 16 thru 23 for one week and if little or no variation then discontinue for dry weather flow.*
Test 24 — *Every eight hours.*
Test 25 — *Every eight hours.*
Tests 9, 10, 26, 27 — *Daily on composite. Do on unfiltered sample and filtrate.*
Tests 11, 12, 28, 29 — *Daily on composite.*
Tests 13, 14, 30, 31 — *Daily on composite.*
Tests 15, 32 — *Daily.*

TABLE 31
WET-WEATHER TEST SCHEDULE

Test	Test No. Swirl Conc. Inlet	Test No. Swirl Conc. Outlet	Test No. Primary Tank Inlet	Test No. Primary Tank Outlet
Settleable Solids	50	51	52	53
Total Suspended Solids	54	55	56	57
Settling Column	—	—	60	—
Heavy Metal	—	—	61	—

	Sludge
Heavy Metal	62

Tests 50, 51, 52, 53 — *Hourly on grab samples.*
Tests 54, 55, 56, 57 — *One test for each storm event (or daily if storm exceeds one day) on composite grab samples taken hourly proportional to flow.*
Test 60 — *Three tests each during two storm events, at beginning, peak, and end of event.*
Tests 61, 62 — *One test each.*

TABLE 32
WET-WEATHER TEST DATA, SWIRL SEPARATOR
MAY 4-7, 1975

Date Flow l/sec mgd	May 4 18.8 0.43	May 5 18.8 0.43	May 6 18.8 0.43	May 7 18.8 0.43
INFLUENT				
30 Min. Settleable Solids (ml)	7.0	7.0	6.0	30.0
Total Suspended Solids (ml/l)	260	360	304	564
EFFLUENT				
30 Min. Settleable Solids (ml)	7.0	8.0	5.0	28.0
Total Suspended Solids (ml/l)	284	364	320	464
	STORM DURATION: 0900 – 2400 Hrs.	STORM DURATION: 0001 – 1000 Hrs.	STORM DURATION: 0700 – 2400 Hrs.	STORM DURATION: 0001 – 0400 Hrs.

TABLE 33
WET-WEATHER TEST DATA SWIRL SEPARATOR
MAY 15—JUNE 12, 1975

Date	May 15	May 31	June 4 & 5	June 12
Flow l/sec	18.8	18.8	18.8	18.8
mgd	0.43	0.43	0.43	0.43
INFLUENT				
30 Min. Settleable Solids ml/l	15.0	11.0	18.0	7.5
Total Suspended Solids mg/l	524	392	540	280
EFFLUENT				
30 Min. Settleable Solids ml/l	8.0	7.0	14.5	4.0
Total Suspended Solids mg/l	344	376	596	204
	STORM DURATION: 2200 – 2400 Hrs.	STORM DURATION: 0200 – 0700 Hrs.	STROM DURATION: June 4, 2300 Hr. – June 5, 0200 Hr.	STORM DURATION: 0001 – 0300 Hrs.

TABLE 34
WET-WEATHER TEST DATA PRIMARY TANKS
MAY 15–JUNE 12, 1975

Date	May 15	May 31	June 4 & 5	June 12
Flow l/sec	**6,658**	**4,456**	**7,445**	**4,823**
Flow mgd	**152.4**	**102.0**	**170.4**	**110.4**
INFLUENT				
30 Min. Settleable Solids ml/l	10.0	13.0	7.0	24.0
Total Suspended Solids mg/l	188	224	336	632
EFFLUENT				
30 Min. Settleable Solids ml/l	9.0	1.0	7.0	.5
Total Suspended Solids mg/l	324	140	272	128
Date	**May 15**	**May 31**	**June 4 & 5**	**June 12**
6 tanks – Flow l/sec	**5,828**	**4,448**	**5,243**	**6,575**
Flow mgd	**133.4**	**101.8**	**120.0**	**150.5**
INFLUENT				
30 Min. Settleable Solids ml/l	12.0	15.0	14.0	7.5
Total Suspended Solids mg/l	744	416	432	272
EFFLUENT				
30 Min. Settleable Solids ml/l	1.0	14.0	11.0	1.0
Total Suspended Solids mg/l	220	544	388	148

Note: For storm duration, see Table 31

TABLE 35
HEAVY METAL TEST DATA

(mg/l)

A. INFLUENT – PRIMARY TANKS

Date	May 4	May 5	May 6	May 7
Flow l/sec	**6,658**	**4,456**	**7,445**	**4,823**
Flow mgd	**152.4**	**102.0**	**170.4**	**110.4**
Heavy Metals mg/l (ppm)				
Cd	0.04	0.026	0.040	0.047
Cr	0.64	1.32	0.71	1.17
Cu	0.49	0.25	0.31	0.50
Fe	4.67	3.27	4.96	5.92
Pb	0.55	0.42	0.64	0.96
Hg	0.0018	0.0013	0.0009	0.31
Ni	1.12	0.10	0.26	0.31
Sn	——————Less than 0.8——————			
Zn	2.75	2.35	2.90	3.13

SLUDGE

Heavy Metals (mg/kg)				
Cd	68.2	73.5	74.7	82.1
Cr	1,827	1,861	1,626	1,675
Cu	626	660	606	651
Fe	11,420	11,450	10,575	11,640
Pb	985	998	912	1,005
Hg	3.48	3.82	4.31	4.51
Ni	193	190	213	224
Sn	55.9	91.7	70.6	39.0
Zn	6,240	6,206	5,862	6,313

B. INFLUENT – DRY WEATHER

	1975				1976
Date	**May 1**	**May 2**	**May 3**	**May 8**	**June 16, 17, 18, and 21**
Flow l/sec	4,234	4,225	3,705	4,631	**Composite Sample**
mgd	96.9	96.7	84.8	106.0	
Cd	0.062	0.089	0.072	0.049	0.04
Cr	1.43	1.60	1.24	1.03	0.95
Cu	0.48	0.43	0.44	0.38	0.47
Fe	6.95	6.60	6.70	4.96	9.78
Pb	1.65	1.33	0.98	0.92	0.32
Hg	0.0031	0.0049	0.0033	0.0029	0.0024
Ni	0.28	0.48	0.42	0.46	0.34
Sn	——————Less than 0.8——————				<0.05
Zn	2.98	3.20	2.58	2.25	3.22

Note: For storm duration see Table 30.

TABLE 36
DRY-WEATHER TEST DATA – SWIRL PRIMARY SEPARATOR
MAY 1-11, 1975

May 1 (Thurs.)	May 2 (Fri.)	May 3 (Sat.)	May 8 (Thurs.)	May 9 (Fri.)	May 10 (Sat.)	May 11 (Sun.)		DATE
1 3 0.3	1 3 0.3	1 3 0.3	1 3 0.3	1 3 0.3	1 3 0.3	1 3 0.3	l/sec mgd	Flow
17.25	20.0	21.0	11.0	11.75	15.0	18.0	30 Min. Settleable Solids ml/l	INFLUENT
576	412	432	456	460	512	472	Total Suspended Solids mg/l	
424	344	360	356	408	396	344	Volatile Suspended Solids mg/l	
152	68	72	100	52	116	128	Fixed Suspended Solids mg/l	
407	260	253	288	316	270	223	Unfiltered – BOD	
122	103	60	114	76	85	53	Filtrate – mg/l	
947	776	733	636	821	743	654	Unfiltered – COD	
							Filtrate – mg/l	
14.75	18.0	20.0	11.25	9	11.0	12.0	30 Min. Settleable Solids ml/l	EFFLUENT
388	356	380	360	360	460	512	Total Suspended Solids mg/l	
292	288	340	264	320	348	392	Volatile Suspended Solids mg/l (ppm)	
96	68	40	96	40	112	110	Fixed Suspended Solids mg/l	
386	269	243	308	264	240	262	Unfiltered – BOD	
122	105	64	117	88	83	57	Filtrate – mg/l	
815	677	683	714	706	658	670	Unfiltered – COD	
							Filtrate – mg/l	
117	358	224	311	386	225	510	Volume (gal)	SLUDGE
4.3	4.9	5.2	4.4	4.5	5.0	4.1	Solids Concentration (%)	
72.4	72.5	73.8	74.7	72.7	72.8	72.7	Total Volatile Solids (%) $\frac{TV^S}{T^S}$	
0.2	0.7	0.4	0.6	0.7	0.5	1.0	Volume to be Drawn off (%)	

TABLE 37
DRY-WEATHER TEST DATA – SWIRL PRIMARY SEPARATOR
MAY 12-18, 1975

May 12 (Mon.)	May 13 (Tues.)	May 14 (Wed.)	May 15 (Thurs.)	May 16 (Fri.)	May 17 (Sat.)	May 18 (Sun.)	DATE	
19.7 0.45	19.7 0.45	19.7 0.45	19.7 0.45	19.7 0.45	19.7 0.45	19.7 0.45	Flow	l/sec mgd
13.25	17.0	18	15	17	24	26	INFLUENT	30 Min. Settleable Solids ml/l
444	428	476	604	476	428	568		Total Suspended Solids mg/l
336	332	368	452	404	344	480		Volatile Suspended Solids mg/l
108	96	108	152	72	84	88		Fixed Suspended Solids mg/l
311	331	339	398	359	300	325		Unfiltered – BOD
102	136	132	124	119	110	88		Filtrate – mg/l
768	793	839	997	896	774	762		Unfiltered – COD
								Filtrate – mg/l
12.75	12.0	14	14.6	13.25	20.25	23.25	EFFLUENT	30 Min. Settleable Solids ml/l
408	576	440	548	436	536	472		Total Suspended Solids mg/l
308	472	348	416	364	436	392		Volatile Suspended Solids mg/l
100	104	92	132	72	100	80		Fixed Suspended Solids mg/l
313	347	358	380	347	274	307		Unfiltered – BOD
104	119	125	111	121	89	71		Filtrate – mg/l
711	895	898	911	767	759	697		Unfiltered – COD
								Filtrate – mg/l
768	803	731	379	543	514	570	SLUDGE	Volume (gal)
4.3	5.2	5.1	4.7	4.1	3.9	4.5		Solids Concentration (%)
72.8	73.1	73.7	74.3	74.3	75.5	75.2		Total Volatile Solids (%)
1.0	1.1	1.0	0.5	0.7	0.7	0.8		

TABLE 38
DRY-WEATHER TEST DATA SWIRL PRIMARY SEPARATOR
MAY 30 – JUNE 10, 1975

May 30 (Fri.)	June 2 (Mon.)	June 4 (Wed.)	June 7 (Sat.)	June 8 (Sun.)	June 9 (Mon.)	June 10 (Tues.)		
13	13	13	13	13	13	13	l/sec	Flow
0.3	0.3	0.3	0.3	0.3	0.3	0.3	mgd	
22.0	17.0	20.0[1]	[2]	[2]	17.25	16.75	30 Min. Settleable Solids ml/l	INFLUENT
660	620	668	632	572	712	472	Total Suspended Solids mg/l	
512	456	496	476	452	576	360	Volatile Suspended Solids (mg/l)	
148	164	172	156	120	136	112	Fixed Suspended Solids (mg/l)	
410	335	354	310	359	325	310	Unfiltered – BOD	
180	136	152	121	145	125	137	Filtrate – (mg/l)	
1,110	965	1,008	1,070	928	1,262	892	Unfiltered – COD	
15	12.5	16	[2]	[2]	11.75	10.75	30 Min. Settleable Solids ml/l	EFFLUENT
456	464	332	352	456	444	428	Total Suspended Solids mg/l	
368	340	252	276	372	372	320	Volatile Suspended Solids (mg/l)	
88	124	80	76	84	72	108	Fixed Suspended Solids (mg/l)	
370	290	310	350	357	320	289	Unfiltered – BOD	
170	133	134	83	144	115	122	Filtrate – mg/l	
866	788	788	818	795	894	718	Unfiltered – COD Filtrate – mg/l	
643	824	44	489	634	609	644	Volume (gal)	SLUDGE
4.9	3.8	4.3	4.3	4.3	4.3	5.2	Solids Concentration(%)	
73.3	72.6	72.2	71.1	71.3	71.9	71.7	Total Volatile Solids Concentration (%)	
1.3	1.6	–	1.0	1.3	1.2	1.3		

[1] Plant shutdown on June 3 for 3 hours so swirl was shut down and cleaned put back into service 0001 hrs. – June 4.
[2] Over 40 ml

TABLE 39
DRY-WEATHER TEST DATA SWIRL PRIMARY SEPARATOR
JUNE 16–21, 1976

Date 1975	Flow	Influent							Effluent							Sludge		
		Whole Sample				Supernatant			Whole Sample				Supernatant					
	mgd	Total Suspended Solids (ppm)	Volatile Suspended Solids (ppm)	Fixed Suspended Solids (ppm)	30-min Settleable Solids	Total Suspended Solids (ppm)	Volatile Suspended Solids (ppm)	Fixed Suspended Solids (ppm)	Total Suspended Solids (ppm)	Volatile Suspended Solids (ppm)	Fixed Suspended Solids (ppm)	30-min Settleable Solids	Total Suspended Solids (ppm)	Volatile Suspended Solids (ppm)	Fixed Suspended Solids (ppm)	Volume Gallons	Total Solids %	Total Volatile Solids %
6-16	0.2	436	351	85	20	133	111	22	166	146	20	1.0	115	105	10	408	2.54	68.0
6-17	0.2	483	386	97	19	164	155	9	249	129	120	Less than 0.1	132	117	15	629	4.28	83.5
6-18	0.2	470	387	103	16	162	140	22	173	143	30	0.1	148	132	16	646	2.40	72.5
6-21	0.2	543	453	90	22.5	175	165	10	154	148	6	0.2	143	129	14	561	2.36	72.3

Whole Sample. Sample before 30 min. settleable solids
Supernatant. Liquid portion of sample after 30 min. settleable solids

TABLE 40
DRY-WEATHER TEST DATA SWIRL PRIMARY SEPARATOR
JUNE 22-25, 1976

Date 1976	Flow	Influent							Effluent							Sludge		
		Whole Sample				Supernatant			Whole Sample				Supernatant					
	mgd	Total Suspended Solids (ppm)	Volatile Suspended Solids (ppm)	Fixed Suspended Solids (ppm)	30-min Settleable Solids	Total Suspended Solids (ppm)	Volatile Suspended Solids (ppm)	Fixed Suspended Solids (ppm)	Total Suspended Solids (ppm)	Volatile Suspended Solids (ppm)	Fixed Suspended Solids (ppm)	30-min Settleable Solids	Total Suspended Solids (ppm)	Volatile Suspended Solids (ppm)	Fixed Suspended Solids (ppm)	Volume Gallons	Total Solids %	Total Volatile Solids %
6-22	0.15	586	477	109	24	187	162	25	165	136	29	Less than 0.1	157	136	21	527	2.16	72.7
6-23	0.15	528	426	102	20	169	148	21	146	130	16	Less than 0.1	128	117	11	476	2.33	73.0
6-24	0.15	493	401	92	19	138	121	17	136	120	16	Less than 0.1	113	103	10	493	1.43	73.7
6-25	0.15	457	383	74	12	158	150	8	152	133	19	Less than 0.1	144	142	2	306	246	71.4

Whole Sample: Sample before 30 min. settleable solids
Supernatant: Liquid portion of sample after 30 min. settleable solids

TABLE 41
DRY-WEATHER TEST DATA – PRIMARY TANKS
MAY 1-11, 1975

May 1 (Thurs.)	May 2 (Fri.)	May 3 (Sat.)	May 8 (Thurs.)	May 9 (Fri.)	May 10 (Sat.)	May 11 (Sun.)		DATE
4,234	4,225	3,705	4,631	4,238	3,853	3,478	l/sec	Flow
96.9	96.7	84.8	106.0	97.0	88.2	79.6	mgd	
27.5	26.0	25.0	12.75	14.25	18.5	19.0	30 Min. Settleable Solids ml/l	INFLUENT
692	664	588	504	540	680	496	Total Suspended Solids mg/l	
520	536	488	392	484	452	380	Volatile Suspended Solids mg/l	
172	128	100	112	56	148	116	Fixed Suspended Solids mg/l	
348	286	275	352	322	295	250	Unfiltered – BOD	
118	117	82	137	88	79	66	Filtrate – mg/l	
1,021	1,010	922	796	883	875	693	Unfiltered – COD	
							Filtrate – mg/l	
65.0	65.0	64.0	64.0	65.0	64.0	63.0	Temperature (°F)	
18.3	18.3	17.7	17.7	18.3	17.7	17.2	Temperature (°C)	
7.4	7.7	–	7.5	–	–	7.6	pH	
10.5	14.25	Less than 0.5	Less than 0.5	8.0	5.0	2.0	30 Min. Settleable Solids ml/l (ppm)	EFFLUENT
232	294	86	130	224	150	160	Total Suspended Solids mg/l	
176	244	80	96	208	118	134	Volatile Suspended Solids mg/l	
56	50	6	34	16	32	26	Fixed Suspended Solids mg/l	
296	238	135	218	230	148	147	Unfiltered – BOD	
113	100	57	135	137	58	49	Filtrate – mg/l	
452	507	289	428	489	325	268	Unfiltered – COD	
1,332	1,347	1,378	1,416	1,378	1,355	1,321	Volume (m^3)	SLUDGE
352	356	364	374	364	358	349	Volume (gal x 10^3)	
4.2	4.1	4.3	4.2	4.2	4.4	4.5	Solids Concentration (%)	
2.2	2.2	2.8	2.1	2.2	2.4	2.9		

TABLE 42
DRY-WEATHER TEST DATA – PRIMARY TANKS
MAY 12 – 18, 1975

May 12 (Mon)	May 13 (Tues)	May 14 (Wed)	May 15 (Thur)	May 16 (Fri)	May 17 (Sat)	May 18 (Sun)		DATE
4,194	4,242	4,277	4,321	4,063	3,303	3,032	l/sec	FLOW
96.0	97.1	97.9	98.9	93.0	75.6	69.4	mgd	
18.25	28	27	18	16	24	26	30 Min. Settleable Solids ml/l	INFLUENT
608	440	520	700	552	668	432	Total Suspended Solids mg/l	
472	340	420	528	440	560	340	Volatile Suspended Solids mg/l	
136	100	100	172	112	108	92	Fixed Suspended Solids mg/l	
327	351	356	416	326	375	296	Unfiltered – BOD	
105	140	138	129	113	123	66	Filtrate – mg/l	
662	855	874	975	838	727	680	Unfiltered – COD	
							Filtrate mg/l	
65	66	66	66	64	65	67	Temperature (°F)	
18.3	18.8	18.8	18.8	17.7	18.3	19.4	Temperature (°C)	
7.5	7.6	7.5	7.5	7.8	-	-	pH	
17.0	7.75	11.0	14.5	2	1	1	30 Min. Settleable Solids ml/l	EFFLUENT
292	306	226	242	174	108	94	Total Suspended Solids mg/l	
224	242	180	184	134	84	84	Volatile Suspended Solids mg/l	
68	64	40	58	40	24	10	Fixed Suspended Solids mg/l	
236	255	260	277	200	163	169	Unfiltered – BOD	
103	133	128	140	128	98	81	Filtrate – mg/l –	
523	712	574	650	361	266	233	Unfiltered – COD	
1,389	1,325	1,363	1,336	1,347	1,347	1,347	Volume (m^3)	
367	350	360	353	356	356	356	Volume (gal/1,000)	SLUDGE
4.3	4.3	4.4	4.2	4.4	4.6	4.7	Solids Concentration	
2.3	2.2	2.2	2.1	2.3	2.8	3.1		

TABLE 43
DRY-WEATHER TEST DATA – PRIMARY TANKS
MAY 30 – JUNE 10, 1975

Date	May 30 (Fri.)	June 2 (Mon.)	June 4 (Wed.)	June 7 (Sat.)	June 8 (Sun.)	June 9 (Mon.)	June 10 (Tues.)
6 tanks – Flow l/sec	4,107	4,098	4,395	3,469	2,984	4,063	4,596
mgd	94.0	93.8	100.6	79.4	68.3	93.0	105.2
INFLUENT							
30 Min. Settleable Solids ml/l	24.0	21.75	20.0	[1]	[1]	17.5	16.0
Total Suspended Solids mg/l	780	648	592	610	772	884	496
Volatile Suspended Solids (mg/l)	624	476	456	464	596	732	372
Fixed Suspended Solids (mg/l)	156	172	136	146	176	152	124
Unfiltered – BOD	450	320	328	360	366	317	342
Filtrate – mg/l	170	128	142	122	132	119	132
Unfiltered – COD	1,214	995	967	991	1,210	1,090	853
Temperature (°C)	20.5	19.4	21.1	20	19.4	20.5	20.5
Temperature (°F)	69	67	70	68	67	69	69
EFFLUENT							
30 Min. Settleable Solids ml/l	11.0	9.25	11.0	[1]	[1]	7.0	6.9
Total Suspended Solids mg/l	294	332	202	72	90	346	180
Volatile Suspended Solids (mg/l)	238	258	168	60	88	298	138
Fixed Suspended Solids (mg/l)	56	74	34	12	2	48	42
Unfiltered – BOD	375	267	212	146	150	216	213
Filtrate – mg/l	210	122	121	52	131	94	115
Unfiltered – COD	605	621	497	288	253	643	537
SLUDGE							
Volume m^3		1,525	1,514	1,718	1,798	1,798	1,786
Volume (gal x 10^3)		403	400	454	454	475	472
Solids Concentration (%)	4.6	4.4	4.8	4.4	4.3	4.8	4.8
		2.6	2.4	3.4	4.0	3.1	2.7

[1] Over 40 ml/l

TABLE 44
DRY-WEATHER TEST DATA PRIMARY SETTLING TANK
JUNE 16-21, 1976

Date 1976	Flow	Influent							Effluent							Sludge		
			Whole Sample			Supernatant			Whole Sample				Supernatant					
	mgd	Total Suspended Solids (ppm)	Volatile Suspended Solids (ppm)	Fixed Suspended Solids (ppm)	30-min Settleable Solids	Total Suspended Solids (ppm)	Volatile Suspended Solids (ppm)	Fixed Suspended Solids (ppm)	Total Suspended Solids (ppm)	Volatile Suspended Solids (ppm)	Fixed Suspended Solids (ppm)	30-min Settleable Solids	Total Suspended Solids (ppm)	Volatile Suspended Solids (ppm)	Fixed Suspended Solids (ppm)	Volume Gallons	Total Solids %	Total Volatile Solids %
6-16	82.9 (99.43)								147	131	16	0.1	107	80	27		3.94	66.7
6-17	78.9 (94.68)								122	100	22	0.1	107	89	18		2.94	56.6
6-18	79.4 (95.28)								589	465	124	28	121	100	21		3.93	67.7
6-21	73.7 (88.44)								211	196	15	2.5	126	119	7		3.68	71.4

Whole Sample: Sample before 30 min. settleable solids
Supernatant: Liquid portion of sample after 30 min. settleable solids

TABLE 45
DRY-WEATHER TEST DATA PRIMARY SETTLING TANK
JUNE 22-25, 1976

Date 1976	Flow	Influent							Effluent							Sludge		
			Whole Sample			Supernatant			Whole Sample				Supernatant					
	mgd	Total Suspended Solids (ppm)	Volatile Suspended Solids (ppm)	Fixed Suspended Solids (ppm)	30-min Settleable Solids	Total Suspended Solids (ppm)	Volatile Suspended Solids (ppm)	Fixed Suspended Solids (ppm)	Total Suspended Solids (ppm)	Volatile Suspended Solids (ppm)	Fixed Suspended Solids (ppm)	30-min Settleable Solids	Total Suspended Solids (ppm)	Volatile Suspended Solids (ppm)	Fixed Suspended Solids (ppm)	Volume Gallons	Total Solids %	Total Volatile Solids %
6-22	77.2 (92.64)								570	450	120	27	150	131	19		4.23	71.3
6-23	79.3 (95.16)								447	356	91	19	124	111	13		3.68	70.4
6-24	80.0 (96.0)								462	351	111	21	98	91	7		4.06	72.2
6-25	86.4								129	121	8	Less than 0.1	83	83	-		3.52	67.8

Whole Sample: Sample before 30 min. settleable solids
Supernatant: Liquid portion of sample after 30 min. settleable solids

TABLE 46
PROPOSED TESTS SECOND SERIES

Sludge Withdrawal	Sampling (influent to swirl & primary effluent)	Sampling (swirl influent)
(hrs)	(hrs)	(hrs)
1,100	1,130	1,115 – 1,145
1,200	1,230	1,215 – 1,245
1,300	1,330	1,315 – 1,345
1,400	1,430	1,415 – 1,445

Required Analysis:

Influent to Swirl (composite of 4)	Effluent of primary clarifier (composite of 4)	Effluent of Swirl (composite of 8)
BOD_5 (total)	BOD_5 (total)	BOD_5 (total)
SS, VSS	SS, VSS	SS, VSS
COD		

Once during the 4-hour testing period, a settleable solids test should be done from each location.

TABLE 47
DRY-WEATHER TEST DATA – SWIRL PRIMARY SEPARATOR
JUNE 23 – 27, 1975

Date	June 23 (Mon)	June 24 (Tues)	June 25 (Wed)	June 26 (Thur)	June 27 (Fri)
Flow l/sec	13	13	13	13	13
Flow mgd	0.3	0.3	0.3	0.3	0.3
INFLUENT					
30 Min Settleable Solids ml/l (ppm)	11	15	11	[1]	22
Total Suspended Solids mg/l (ppm)	380	525	488	904	368
Volatile Suspended Solids mg/l (ppm)	284	380	384	692	296
Fixed Suspended Solids mg/l (ppm)	96	144	104	212	72
Unfiltered – BOD	284	301	300	382	339
Unfiltered – COD	710	785	757	1,320	830
EFFLUENT					
30 Min. Settleable Solids ml/l (ppm)	5	11	6	[1]	8
Total Suspended Solids mg/l (ppm)	192	332	252	556	332
Volatile Suspended Solids mg/l (ppm)	144	232	212	432	260
Fixed Suspended Solids mg/l (ppm)	48	100	40	124	72
Unfiltered – BOD	248	278	247	361	289
Unfiltered – COD					
SLUDGE					
Volume m^3	1.74	2.61	3.58	1.78	2.01
Volume (gal)	459	690	947	469	530
Solids Concentration	2.6	3.8	3.0	2.9	2.9
Total Volatile Solids Concentration	66.8	69.2	70.3	75.4	72.9
	0.9	1.4	1.9	0.9	1.0

[1] Over 40 ml/l

TABLE 48
DRY-WEATHER TEST DATA PRIMARY TANKS
JUNE 23 – 27, 1975

Date	June 23 (Mon)	June 24 (Tues)	June 25 (Wed)	June 26 (Thur)	June 27 (Fri)
INFLUENT					
(6 Tanks Operating) l/sec	4,264	4,238	4,142	4,142	4,382
Flow – mgd	97.6	97.0	94.8	94.8	100.3
30 Min Settleable Solids ml/l	11	15	11	[1]	22
Total Suspended Solids mg/l	380	525	488	904	368
Volatile Suspended Solids mg/l	284	380	384	692	296
Fixed Suspended Solids mg/l	96	144	104	212	72
Unfiltered – BOD	284	301	300	382	339
Unfiltered – COD	710	785	757	1,320	830
EFFLUENT					
30 Min Settleable Solids ml/l	3	3	8	11	5
Total Suspended Solids mg/l	220	224	280	336	316
Volatile Suspended Solids mg/l	164	168	244	268	256
Fixed Suspended Solids mg/l	56	56	36	68	60
Unfiltered – BOD	251	227	277	343	295
SLUDGE					
Solids Concentration (%)	3.9	4.1	4.5	4.2	4.5
Total Volatile Solids Concentration (%)	67.7	67.9	69.0	68.6	70.0

[1] Over 40 ml/l

TABLE 49
DRY-WEATHER TEST DATA SWIRL PRIMARY SEPARATOR
JULY 2 – 8, 1975

Date	July 2	July 3	July 4	July 7	July 8
Flow l/sec	19.7	19.7	19.7	19.7	19.7
Flow mgd	0.45	0.45	0.45	0.45	0.45
INFLUENT					
30 Min Settleable Solids ml/l (ppm)	10.0	10.0	10.0	12.0	8.0
Total Suspended Solids mg/l (ppm)	464	436	512	500	440
Volatile Suspended Solids mg/l (ppm)	388	340	400	380	340
Fixed Suspended Solids mg/l (ppm)	76	96	112	120	100
Unfiltered – BOD (mg/l)	332	296	361	307	347
Unfiltered – COD (mg/l)	1,250	786	806	765	783
EFFLUENT					
30 Min Settleable Solids ml/l (ppm)	8.0	5.0	9.0	10	7.0
Total Suspended Solids mg/l (ppm)	344	424	428	364	368
Volatile Suspended Solids mg/l (ppm)	272	328	316	256	268
Fixed Suspended Solids mg/l (ppm)	72	96	112	108	100
Unfiltered – BOD (mg/l)	326	295	309	307	343
SLUDGE					
Volume m^3	1.03	0.61	0.56	0.64	0.75
Volume	272	161	147	170	199
Solids Concentration (%)	2.8	2.6	2.7	3.5	2.8
Volatile Solids Concentration (%)	76.0	71.9	72.3	70.9	76.5

TABLE 50
DRY-WEATHER TEST DATA PRIMARY TANKS
JULY 2 – 8, 1975

Date	July 2	July 3	July 4	July 7	July 8
INFLUENT					
l/sec (6 tanks in service)	3,698	3,819	3,687	3,516	3,649
Flow mgd	97.7	100.9	97.4	92.9	96.4
30 Min Settleable Solids ml/l	10.0	10.0	10.0	12.0	8.0
Total Suspended Solids mg/l	464	436	512	500	440
Volatile Suspended Solids mg/l	388	340	400	380	340
Fixed Suspended Solids mg/l	76	96	112	120	100
Unfiltered –BOD (mg/l)	332	296	361	307	347
Unfiltered – COD (mg/l)	1,250	786	806	765	783
EFFLUENT					
30 Min Settleable Solids ml/l (ppm)	21.0	8.0	15.0	40.0	5.0
Total Suspended Solids mg/l (ppm)	384	436	432	672	220
Volatile Suspended Solids mg/l (ppm)	300	344	328	484	136
Fixed Suspended Solids mg/l (ppm)	84	92	104	188	84
Unfiltered – BOD (mg/l)	321	290	314	332	302
SLUDGE					
Solids Concentration (%)	3.8	3.7	3.9	3.9	4.0
Volatile Solids Concentration (%)	68.4	70.0	68.4	69.2	69.4

TABLE 51
PROPOSED TESTS FINAL SERIES

Sludge Withdrawal	Sewage Sampling			
	Influent	Swirl Effluent		Primary Effluent
(hrs)	(hrs)	[1] (hrs)	[2]	(hrs)
1100 (No sample)	1100	1130	1115	1200
1130	1130	1200	1145	1230
1200	1200	1230	1215	1300
1230	1230	1300	1245	1330
1300	1300	1330	1315	1400
1330	1330	1400	1345	1430
1400	1400	1430	1415	1500
1430	1430	1500	1445	1530
1500				

[1] Time when flow is 1.3 l/sec (0.3 mgd)

[2] Time when flow is 19.7 l/sec (0.45 mgd)

TEST	TEST No.		
Sewage	Influent	Swirl Effluent	Primary Effluent
Total Suspended Solids	1	5	9
Volatile Suspended Solids	2	6	10
Fixed Suspended Solids	3	7	11
Settleable Solids by Wt.	4	8	12
Settleable Solids by Vol.	13	14	15

1 thru 15	4 tests daily on composite of two grab samples at 0.5 hour intervals
16 thru 20	1 test daily on composite taken at 0.5 hour intervals beginning 1/2 hour after start of test

Sludge	Swirl	Primary
Volume	16	—
Solids Concentration %	17	19
Volatile Solids %	18	20

TABLE 52
DRY-WEATHER TEST DATA SEPTEMBER 2, 1975

FLOW – SWIRL: 3 l/sec (0.3 mgd) PRIMARY: 3,649 l/sec (96.4 mgd)

TIME OF DAY	INFLUENT					SWIRL SEPARATOR EFFLUENT					PRIMARY SETTLING TANKS EFFLUENT					SLUDGE				
																SWIRL			PRIMARY TANK	
	30 MINUTE SETTLEABLE SOLIDS		TOTAL SUSPENDED SOLIDS	VOLATILE SUSPENDED SOLIDS	FIXED SUSPENDED SOLIDS	30 MINUTE SETTLEABLE SOLIDS		TOTAL SUSPENDED SOLIDS	VOLATILE SUSPENDED SOLIDS	FIXED SUSPENDED SOLIDS	30 MINUTE SETTLEABLE SOLIDS		TOTAL SUSPENDED SOLIDS	VOLATILE SUSPENDED SOLIDS	FIXED SUSPENDED SOLIDS	SOLIDS CONCENTRATION	VOLATILE SOLIDS CONCENTRATION	VOLUME (TOTAL)	SOLIDS CONCENTRATION	VOLATILE SOLIDS CONCENTRATION
	ml/l	mg/l	mg/l	mg/l	mg/l	ml/l	mg/l	mg/l	mg/l	mg/l	ml/l	mg/l	mg/l	mg/l	mg/l	%	%	gal	%	%
11:30	12.5	32	396	388	8															
12:00						3.0	76	248	208	40										
12:30	9.5	192	380	312	68						10.5	124	316	248	68					
1:00						3:0	80	228	192	36										
1:30	7.5	220	348	252	96						7.0	96	220	200	20					
2:00						2.5	100	216	136	80										
2:30	8.0	64	244	236	8						6.5	200	312	232	80					
3:00						2.5	40	216	200	16										
3:30											8.0	144	328	280	48	2.5	71.0	476	3.5	71.5

TABLE 53
DRY-WEATHER TEST DATA SEPTEMBER 3, 1975

FLOW – SWIRL: 1 3 l/sec (0.3 mgd) PRIMARY: 3,581 l/sec (94.6 mgd)

TIME OF DAY	INFLUENT					SWIRL SEPARATOR EFFLUENT					PRIMARY SETTLING TANKS EFFLUENT					SLUDGE				
																SWIRL			PRIMARY TANK	
	30 MINUTE SETTLEABLE SOLIDS		TOTAL SUSPENDED SOLIDS	VOLATILE SUSPENDED SOLIDS	FIXED SUSPENDED SOLIDS	30 MINUTE SETTLEABLE SOLIDS		TOTAL SUSPENDED SOLIDS	VOLATILE SUSPENDED SOLIDS	FIXED SUSPENDED SOLIDS	30 MINUTE SETTLEABLE SOLIDS		TOTAL SUSPENDED SOLIDS	VOLATILE SUSPENDED SOLIDS	FIXED SUSPENDED SOLIDS	SOLIDS CONCENTRATION	VOLATILE SOLIDS CONCENTRATION	VOLUME (TOTAL)	SOLIDS CONCENTRATION	VOLATILE SOLIDS CONCENTRATION
	ml/l	mg/l	mg/l	mg/l	mg/l	ml/l	mg/l	mg/l	mg/l	mg/l	ml/l	mg/l	mg/l	mg/l	mg/l	%	%	gals	%	%
11:30	9.0	240	456	376	80															
12:00						3.0	12	232	196	36										
12:30	9.5	204	372	308	64						2.5	52	216	188	28					
1:00						2.0	48	200	176	24										
1:30	9.5	316	456	420	36						2.5	36	180	156	24					
2:00						1.0	56	196	176	20										
2:30	8.5	132	316	268	48						2.0	48	152	148	4					
3:00						1.0	36	188	132	56										
3:30											2.0	16	132	92	40	2.0	75.0	935	3.8	71.5

TABLE 54
DRY-WEATHER TEST DATA SEPTEMBER 4, 1975

FLOW – SWIRL: 1 3 l/sec (0.3 mgd) PRIMARY: 3,607 l/sec (95.3 mgd)

TIME OF DAY	INFLUENT					SWIRL SEPARATOR EFFLUENT					PRIMARY SETTLING TANKS EFFLUENT					SLUDGE				
	30 MINUTE SETTLEABLE SOLIDS		TOTAL SUSPENDED SOLIDS	VOLATILE SUSPENDED SOLIDS	FIXED SUSPENDED SOLIDS	30 MINUTE SETTLEABLE SOLIDS		TOTAL SUSPENDED SOLIDS	VOLATILE SUSPENDED SOLIDS	FIXED SUSPENDED SOLIDS	30 MINUTE SETTLEABLE SOLIDS		TOTAL SUSPENDED SOLIDS	VOLATILE SUSPENDED SOLIDS	FIXED SUSPENDED SOLIDS	SOLIDS CONCENTRATION	VOLATILE SOLIDS CONCENTRATION	VOLUME (TOTAL)	SOLIDS CONCENTRATION	VOLATILE SOLIDS CONCENTRATION
	ml/l	mg/l	mg/l	mg/l	mg/l	ml/l	mg/l	mg/l	mg/l	mg/l	ml/l	mg/l	mg/l	mg/l	mg/l	%	%	gal	%	%
11:30	10.5	144	424	352	72															
12:00						3.0	48	252	216	36										
12:30	10.0	80	492	408	84						5.5	112	260	172	88					
1:00						2.0	60	200	120	80										
1:30	7.5	128	396	380	16						1.0	72	200	136	64					
2:00						1.0	68	200	180	20										
2:30	7.5	216	348	316	32						4.0	104	200	192	8					
3:00						1.0	23	136	92	44										
3:30											2.0	96	200	164	36	1.8	74.1	629	4.0	73

TABLE 55
DRY-WEATHER TEST DATA SEPTEMBER 5, 1975

FLOW – SWIRL: 1 3 l/sec (0.3 mgd) **PRIMARY: 3,501 l/sec (92.5 mgd)**

TIME OF DAY	INFLUENT					SWIRL SEPARATOR EFFLUENT					PRIMARY SETTLING TANKS EFFLUENT					SLUDGE				
																SWIRL			PRIMARY TANKS	
	30 MINUTE SETTLEABLE SOLIDS		TOTAL SUSPENDED SOLIDS	VOLATILE SUSPENDED SOLIDS	FIXED SUSPENDED SOLIDS	30 MINUTE SETTLEABLE SOLIDS		TOTAL SUSPENDED SOLIDS	VOLATILE SUSPENDED SOLIDS	FIXED SUSPENDED SOLIDS	30 MINUTE SETTLEABLE SOLIDS		TOTAL SUSPENDED SOLIDS	VOLATILE SUSPENDED SOLIDS	FIXED SUSPENDED SOLIDS	SOLIDS CONCENTRATION	VOLATILE SOLIDS CONCENTRATION	VOLUME (TOTAL)	SOLIDS CONCENTRATION	VOLATILE SOLIDS CONCENTRATION
	ml/l	mg/l	mg/l	mg/l	mg/l	ml/l	mg/l	mg/l	mg/l	mg/l	ml/l	mg/l	mg/l	mg/l	mg/l	%	%	gal	%	%
11:30	11.5	164	392	344	48															
12:00						4.0	192	300	272	28										
12:30	9.0	236	388	320	68						7.0	84	264	262	52					
1:00						4.0	72	280	236	44										
1:30	8.5	128	360	332	28						4.0	48	196	176	20					
2:00						2.0	68	196	164	32										
2:30	8.5	160	332	280	52						2.0	120	212	180	32					
3:00						2.0	20	140	124	16										
3:30											2.0	40	164	128	36	2.5	74.8	731	4.1	73

TABLE 56
DRY-WEATHER TEST DATA SEPTEMBER 8, 1975

FLOW — SWIRL: 1 3 l/sec (0.3 mgd) **PRIMARY: 3, 497 l/sec (92.4 mgd)**

TIME OF DAY						SWIRL SEPARATOR EFFLUENT					PRIMARY SETTLING TANKS EFFLUENT					SLUDGE				
																SWIRL			PRIMARY TANKS	
	30 MINUTE SETTLEABLE SOLIDS		TOTAL SUSPENDED SOLIDS	VOLATILE SUSPENDED SOLIDS	FIXED SUSPENDED SOLIDS	30 MINUTE SETTLEABLE SOLIDS		TOTAL SUSPENDED SOLIDS	VOLATILE SUSPENDED SOLIDS	FIXED SUSPENDED SOLIDS	30 MINUTE SETTLEABLE SOLIDS		TOTAL SUSPENDED SOLIDS	VOLATILE SUSPENDED SOLIDS	FIXED SUSPENDED SOLIDS	SOLIDS CONCENTRATION	VOLATILE SOLIDS CONCENTRATION	VOLUME (TOTAL)	SOLIDS CONCENTRATION	VOLATILE SOLIDS CONCENTRATION
	ml/l	mg/l	mg/l	mg/l	mg/l	ml/l	mg/l	mg/l	mg/l	mg/l	ml/l	mg/l	mg/l	mg/l	mg/l	%	%	gal	%	%
11:30	13.5	224	416	348	68															
12:00						2.0	164	252	220	32										
12:30	12.0	180	356	296	60						7.0	80	208	152	56					
1:00						4.0	92	240	208	32										
1:30	11.0	220	364	272	92						10.0	84	204	164	40					
2:00						2.5	76	212	152	60										
2:30	8.0	140	280	252	28						10.0	120	228	212	16					
3:00						2.0	20	148	104	44										
3:30											2.0	68	172	132	40	2.6	73.0	441	3.5	73.3

TABLE 57

DRY-WEATHER TEST DATA SEPTEMBER 9, 1975

FLOW – SWIRL: 19.7 l/sec (0.45 mgd) PRIMARY: 3,626 l/sec (95.8 mgd)

TIME OF DAY	INFLUENT					SWIRL SEPARATOR EFFLUENT					PRIMARY SETTLING TANKS EFFLUENT					SWIRL				
																SWIRL			PRIMARY TANK	
	30 MINUTE SETTLEABLE SOLIDS		TOTAL SUSPENDED SOLIDS	VOLATILE SUSPENDED SOLIDS	FIXED SUSPENDED SOLIDS	30 MINUTE SETTLEABLE SOLIDS		TOTAL SUSPENDED SOLIDS	VOLATILE SUSPENDED SOLIDS	FIXED SUSPENDED SOLIDS	30 MINUTE SETTLEABLE SOLIDS		TOTAL SUSPENDED SOLIDS	VOLATILE SUSPENDED SOLIDS	FIXED SUSPENDED SOLIDS	SOLIDS CONCENTRATION	VOLATILE SOLIDS CONCENTRATION	VOLUME (TOTAL)	SOLIDS CONCENTRATION	VOLATILE SOLIDS CONCENTRATION
	ml/l	mg/l	mg/l	mg/l	mg/l	ml/l	mg/l	mg/l	mg/l	mg/l	ml/l	mg/l	mg/l	mg/l	mg/l	%	%	gal	%	%
11:30	13.0	136	336	276	60															
11:45						5.0	104	300	240	60										
12:30	12.0	192	376	272	104						7.0	112	304	224	80					
12:46						4.5	108	308	224	84										
1:30	8.0	128	352	276	76						3.5	84	264	192	72					
1:45						3.0	124	328	244	84										
2:30	10.0	380	528	404	124						4.0	84	252	156	96					
2:45						5.0	132	372	304	68										
3:30											4.5	156	280	260	20	2.0	71.9	510	3.6	73.6

TABLE 58
DRY-WEATHER TEST DATA SEPTEMBER 10, 1975

FLOW – SWIRL: 19.7 l/sec (0.45 mgd) **PRIMARY: 3,558 l/sec (81.2 mgd)**

TIME OF DAY	INFLUENT					SWIRL SEPARATOR EFFLUENT					PRIMARY SETTLING TANKS EFFLUENT					SLUDGE				
																SWIRL			PRIMARY TANK	
	30 MINUTE SETTLEABLE SOLIDS		TOTAL SUSPENDED SOLIDS	VOLATILE SUSPENDED SOLIDS	FIXED SUSPENDED SOLIDS	30 MINUTE SETTLEABLE SOLIDS		TOTAL SUSPENDED SOLIDS	VOLATILE SUSPENDED SOLIDS	FIXED SUSPENDED SOLIDS	30 MINUTE SETTLEABLE SOLIDS		TOTAL SUSPENDED SOLIDS	VOLATILE SUSPENDED SOLIDS	FIXED SUSPENDED SOLIDS	SOLIDS CONCENTRATION	VOLATILE SOLIDS CONCENTRATION	VOLUME (TOTAL	SOLIDS CONCENTRATION	VOLATILE SOLIDS CONCENTRATION
	ml/l	mg/l	mg/l	mg/l	mg/l	ml/l	mg/l	mg/l	mg/l	mg/l	ml/l	mg/l	mg/l	mg/l	mg/l	%	%	gal	%	%
11:30	13.0	252	528	470	56															
11:45						7.0	160	328	316	12										
12:30	12.0	248	356	316	40						13.5	164	376	336	40					
12:45						7.0	76	292	260	32										
1:30	11.0	152	348	320	28						6.5	96	260	240	20					
1:45						7.0	160	328	308	20										
2:30	10.5	128	360	304	56						8.5	124	280	280	0					
2:45						6.5	116	312	248	64										
3:30											6.0	84	204	140	64	1.8	78.6	500	3.9	74.0

TABLE 59
DRY-WEATHER TEST DATA SEPTEMBER 11, 1975

FLOW – SWIRL: 19.7 l/sec (0.45 mgd) PRIMARY: 4,114 l/sec (108.7 mgd)

TIME OF DAY	INFLUENT					SWIRL SEPARATOR EFFLUENT					PRIMARY SETTLING TANKS EFFLUENT					SLUDGE				
																SWIRL			PRIMARY TANK	
	30 MINUTE SETTLEABLE SOLIDS		TOTAL SUSPENDED SOLIDS	VOLATILE SUSPENDED SOLIDS	FIXED SUSPENDED SOLIDS	30 MINUTE SETTLEABLE SOLIDS		TOTAL SUSPENDED SOLIDS	VOLATILE SUSPENDED SOLIDS	FIXED SUSPENDED SOLIDS	30 MINUTE SETTLEABLE SOLIDS		TOTAL SUSPENDED SOLIDS	VOLATILE SUSPENDED SOLIDS	FIXED SUSPENDED SOLIDS	SOLIDS CONCENTRATION	VOLATILE SOLIDS CONCENTRATION	VOLUME (TOTAL)	SOLIDS CONCENTRATION	VOLATILE SOLIDS CONCENTRATION
	ml/l	mg/l	mg/l	mg/l	mg/l	ml/l	mg/l	mg/l	mg/l	mg/l	ml/l	mg/l	mg/l	mg/l	mg/l	%	%	gal	%	%
11:30	14.0	284	472	420	52															
11:45						8.0	172	344	304	40										
12:30	13.5	220	436	376	60						18.0	284	460	392	68					
12:45						7.0	172	384	332	52										
1:30	11.5	280	636	560	76						13.5	172	384	320	64					
1:45						6.0	180	436	364	72										
2:30	9.5	132	344	276	68						9.5	144	340	308	32					
2:45						4.0	48	252	220	32										
3:30											7.5	56	272	212	60	2.3	74.1	513	3.6	73.8

TABLE 60
DRY-WEATHER TEST DATA SEPTEMBER 12, 1975

FLOW – SWIRL: 19.7 l/sec (0.45 mgd) PRIMARY: 4,084 l/sec (107.9 mgd)

TIME OF DAY	INFLUENT					SWIRL SEPARATOR EFFLUENT					PRIMARY SETTLING TANKS EFFLUENT					SLUDGE				
																SWIRL			PRIMARY TANK	
	30 MINUTE SETTLEABLE SOLIDS		TOTAL SUSPENDED SOLIDS	VOLATILE SUSPENDED SOLIDS	FIXED SUSPENDED SOLIDS	30 MINUTE SETTLEABLE SOLIDS		TOTAL SUSPENDED SOLIDS	VOLATILE SUSPENDED SOLIDS	FIXED SUSPENDED SOLIDS	30 MINUTE SETTLEABLE SOLIDS		TOTAL SUSPENDED SOLIDS	VOLATILE SUSPENDED SOLIDS	FIXED SUSPENDED SOLIDS	SOLIDS CONCENTRATION	VOLATILE SOLIDS CONCENTRATION	VOLUME (TOTAL)	SOLIDS CONCENTRATION	VOLATILE SOLIDS CONCENTRATION
	ml/l	mg/l	mg/l	mg/l	mg/l	ml/l	mg/l	mg/l	mg/l	mg/l	ml/l	mg/l	mg/l	mg/l	mg/l	%	%	gal	%	%
11:30	12.5	228	432	356	76															
11:45						6.0	144	324	264	60										
12:30	11.0	160	364	296	68						2.0	47	208	196	12					
12:45						6.5	136	344	244	100										
1:30	9.5	256	524	392	132						3.0	88	208	160	48					
1:45						6.0	132	308	240	68										
2:30	9.0	196	400	332	68						3.0	–	280	276	4					
2:45						5.0	148	372	316	56										
3:30											2.0	52	168	136	32	2.5	61.3	465	4.7	63.8

TABLE 61
DRY-WEATHER TEST DATA SEPTEMBER 15, 1975

FLOW – SWIRL: 19.7 l/sec (0.45 mgd) PRIMARY: 3,406 l/sec (77.7 ,gd)

TIME OF DAY	INFLUENT					SWIRL SEPARATOR EFFLUENT					PRIMARY SETTLING TANKS EFFLUENT					SLUDGE				
																SWIRL			PRIMARY TANK	
	30 MINUTE SETTLEABLE SOLIDS		TOTAL SUSPENDED SOLIDS	VOLATILE SUSPENDED SOLIDS	FIXED SUSPENDED SOLIDS	30 MINUTE SETTLEABLE SOLIDS		TOTAL SUSPENDED SOLIDS	VOLATILE SUSPENDED SOLIDS	FIXED SUSPENDED SOLIDS	30 MINUTE SETTLEABLE SOLIDS		TOTAL SUSPENDED SOLIDS	VOLATILE SUSPENDED SOLIDS	FIXED SUSPENDED SOLIDS	SOLIDS CONCENTRATION	VOLATILE SOLIDS CONCENTRATION	VOLUME (TOTAL)	VOLATILE SOLIDS CONCENTRATION	
	ml/l	mg/l	mg/l	mg/l	mg/l	ml/l	mg/l	mg/l	mg/l	mg/l	ml/l	mg/l	mg/l	mg/l	mg/l	%	%	gal	%	%
11:30	12.5	608	840	742	98															
11:45						8.5	136	364	284	80										
12:30	14.0	100	416	336	80						12.0	120	340	268	72					
12:45						7.0	72	340	268	72										
1:30	12.0	148	376	332	44						10.0	144	308	300	8					
1:45						6.0	140	276	268	8										
2:30	9.0	116	296	288	8						6.0	92	220	188	32					
2:45						4.0	60	204	196	8										
3:30											5.0	80	172	132	40	1.9	60.7	323	–	–

TABLE 62
DRY-WEATHER REMOVAL OF SETTLEABLE SOLIDS BY VOLUME
SWIRL FLOW 1.3 l/sec (0.3 mgd)

Date 1975	Time	Settleable Solids ml/l			% Removal	
		Influent	Swirl Effluent	Primary Effluent	Swirl	Primary
9-2	11.30	12.5	3.0	10.5	76.0	16.0
	12:30	9.5	3.0	7.0	68.4	26.3
	1.30	7.5	2.5	6.5	66.7	13.4
	2:30	8.0	2.5	8.0	68.7	0.0
	Subtotal	37.5	11.0	32.0 avg.	70.7	14.7
9-3	11:30	9.0	3.0	2.5	66.6	72.2
	12:30	9.5	2.0	2.5	78.9	73.7
	1:30	7.5	1.0	2.0	89.4	78.9
	2:30	8.5	1.0	2.0	88.2	76.4
	Subtotal	36.5	7.0	9.0 avg.	80.8	75.3
9-4	11:30	10.5	3.0	5.5	71.4	47.6
	12:30	10.0	2.0	1.0	80.0	90.0
	1:30	7.5	1.0	2.0	86.7	46.7
	2:30	7.5	1.0	2.0	86.7	73.3
	Subtotal	35.5	7.0	12.5 avg.	80.3	64.8
9-5	11:30	11.5	4.0	7.0	65.2	39.1
	12:30	9.0	4.0	4.0	55.6	55.6
	1:30	8.5	2.0	2.0	76.5	76.6
	2:30	8.5	2.0	2.0	76.5	76.5
	Subtotal	37.5	12.0	15.0 avg.	68.0	60.0
9-8	11:30	13.5	2.0	7.0	85.2	48.1
	12:30	12.0	4.0	10.0	66.7	16.7
	1:30	11.0	2.5	10.0	77.3	9.1
	2:30	8.0	2.0	2.0	75.0	75.0
	Subtotal	44.5	10.5	29.0 avg.	76.4	34.8
	Total	191.5	47.5	97.5 avg.	75.2	49.1

TABLE 63
DRY-WEATHER REMOVAL OF SETTLEABLE SOLIDS BY WEIGHT
SWIRL FLOW 1 3 l/sec (0.3 mgd)

Date 1975	Time	Settleable Solids mg/l			% Removal	
		Influent	Swirl Effluent	Primary Effluent	Swirl	Primary
9-2	11:30	32	76	124	+137.5	+287.5
	12:30	192	80	96	58.3	50.0
	1:30	220	100	200	54.5	9.1
	2:30	64	40	144	37.5	+125.0
	Subtotal	508	296	564 avg	41.7	+ 11.0
9-3	11:30	240	12	52	95.0	78.3
	12:30	204	48	36	76.5	82.4
	1:30	316	56	48	82.3	84.8
	2:30	132	36	16	72.7	87.9
	Subtotal	892	152	152 avg.	82.9	82.9
9-4	11:30	144	48	112	66.7	22.2
	12:30	80	60	72	25.0	10.0
	1:30	128	68	104	46.9	18.8
	2:30	216	28	96	87.5	55.6
	Subtotal	568	204	384 avg	64.1	32.4
9-5	11:30	164	192	84	+ 17.1	48.8
	12:30	236	72	48	69.5	79.7
	1:30	128	68	120	46.9	6.3
	2:30	160	20	48	87.5	70.0
	Subtotal	688	352	300 avg	48.8	56.4
9-8	11:30	224	164	80	26.8	64.3
	12:30	180	92	84	48.9	53.3
	1:30	220	76	120	65.5	45.5
	2:30	140	20	68	85.7	51.4
	Subtotal	764	352	352 avg	53.9	53.9
	Total	3,420	1,356	1,752 avg	60.4	48.8
	Total (disregarding samples when erosion caused effluent to be higher than influent)					
	Swirl	3,222	1,088		67.3	
	Primary	3,324		1,484 avg		55.3

TABLE 64
DRY-WEATHER REMOVAL OF TOTAL SUSPENDED SOLIDS
SWIRL FLOW 1 3 l/sec (0.3 mgd)

Date 1975	Time	Total Suspended Solids mg/l			% Removal	
		Influent	Swirl Effluent	Primary Effluent	Swirl	Primary
9-2	11:30	396	248	316	37.4	20.2
	12:30	380	228	220	40.0	42.1
	1:30	348	216	312	37.9	10.3
	2:30	244	216	328	11.5	+ 34.4
	Subtotal	1,368	908	1,176 avg	33.6	14.0
9-3	11:30	456	232	216	49.1	52.6
	12:30	372	200	180	46.2	51.6
	1:30	456	196	152	57.0	66.7
	2:30	316	188	132	40.5	58.2
	Subtotal	1,600	816	680 avg	49.0	57.5
9-4	11:30	424	252	260	40.6	38.7
	12:30	492	200	200	59.3	59.3
	1:30	396	200	200	49.5	49.5
	2:30	348	136	200	60.9	42.6
	Subtotal	1,660	788	860 avg	52.6	48.2
9-5	11:30	392	300	264	23.5	32.6
	12:30	388	280	196	27.8	49.5
	1:30	360	196	212	45.6	41.1
	2:30	332	140	164	57.8	50.6
	Subtotal	1,472	916	836 avg	37.8	43.2
9-8	11:30	416	252	208	39.4	50.0
	12:30	356	240	204	32.6	42.7
	1:30	364	212	228	41.8	37.4
	2:30	280	148	172	47.1	38.6
	Subtotal	1,416	852	812 avg	39.8	42.7
	Total	7,516	4,280	4,364 avg	43.1	41.9
	Total (disregarding samples when erosion caused effluent to be higher than influent)					
	Primary	7,272		4,036 avg		46.3

TABLE 65
DRY-WEATHER REMOVAL OF VOLATILE SUSPENDED SOLIDS
SWIRL FLOW 1 3 l/sec (0.3 mgd)

Date 1975	Time	Volatile Suspended Solids mg/l			% Removal	
		Influent	Swirl Effluent	Primary Effluent	Swirl	Primary
9-2	11:30	388	208	248	46.4	36.1
	12:30	312	192	200	38.5	35.9
	1:30	252	136	232	46.0	7.9
	2:30	236	200	280	15.3	+ 18.6
	Subtotal	1,188	736	960 avg	38.0	19.2
9-3	11:30	376	196	188	47.9	50.0
	12:30	308	176	156	42.9	49.4
	1:30	420	176	148	58.1	64.8
	2:30	268	132	92	50.7	65.7
	Subtotal	1,372	680	584 avg	50.4	57.4
9-4	11:30	352	216	172	38.6	51.1
	12:30	408	120	136	70.6	66.7
	1:30	380	180	192	52.6	49.5
	2:30	316	92	164	70.9	48.1
	Subtotal	1,456	608	664 avg	58.2	54.4
9-5	11:30	344	272	212	20.9	38.4
	12:30	320	236	176	26.2	45.0
	1:30	332	164	180	50.6	45.8
	2:30	280	124	128	55.7	54.3
	Subtotal	1,276	796	696 avg	37.6	45.5
9-8	11:30	348	220	152	36.8	56.3
	12:30	296	208	164	29.7	44.6
	1:30	272	152	212	44.1	22.0
	2:30	252	104	132	58.7	47.6
	Subtotal	1,168	684	660 avg	41.4	43.5
	Total	6,460	3,504	3,564 avg	45.8	44.8
	Total (disregarding samples when erosion caused effluent to be higher than influent)					
	Primary	6,224		3,284 avg		47.2

TABLE 66
DRY-WEATHER REMOVAL OF FIXED SUSPENDED SOLIDS
SWIRL FLOW 1 3 l/sec (0.3 mgd)

Date 1975	Time	Fixed Suspended Solids mg/l			% Removal	
		Influent	Swirl Effluent	Primary Effluent	Swirl	Primary
9-2	11:30	8	40	68	+400.0	+750.0
	12:30	68	36	20	47.0	70.0
	1:30	96	80	80	16.7	16.7
	2:30	8	16	48	+100.0	+500.0
	Subtotal	180	172	216 avg	4.4	+ 20.0
9-3	11:30	80	36	28	55.0	65.0
	12:30	64	24	24	62.5	62.5
	1:30	36	20	4	44.4	88.9
	2:30	48	56	40	+ 16.7	16.7
	Subtotal	228	136	96 avg	40.3	57.9
9-4	11:30	72	36	88	50.0	+ 22.2
	12:30	84	80	64	4.8	23.8
	1:30	16	20	8	+ 25.0	50.0
	2:30	32	44	36	37.5	12.5
	Subtotal	204	180	196 avg	11.8	3.9
9-5	11:30	48	28	52	41.7	+ 8.3
	12:30	68	44	20	35.3	70.6
	1:30	28	32	32	+ 14.3	+ 14.3
	2:30	52	16	36	69.2	30.8
	Subtotal	196	120	140 avg	38.8	28.6
9-8	11:30	68	32	56	52.9	17.6
	12:30	60	32	40	46.7	33.3
	1:30	92	60	16	34.8	82.6
	2:30	28	44	40	+ 57.1	+ 42.9
	Subtotal	248	168	152 avg	32.3	38.7
	Total	1,056	776	800 avg	26.5	24.2
	Total (disregarding samples when erosion caused effluent to be higher than influent)					
	Swirl	920	568		38.3	
	Primary	864		472 avg		45.4

TABLE 67
DRY-WEATHER REMOVAL OF SETTLEABLE SOLIDS BY VOLUME
SWIRL FLOW 19.7 l/sec (0.45 mgd)

Date 1975	Time	Settleable Solids ml/l			% Removal	
		Influent	Swirl Effluent	Primary Effluent	Swirl	Primary
9-9	11:30	13.0	5.0	7.0	61.5	46.2
	12:30	12.0	4.5	3.5	62.5	70.8
	1:30	8.0	3.0	4.0	62.5	50.0
	2:30	10.0	5.0	4.5	50.0	55.0
	Subtotal	43.0	17.5	19.0 avg	59.3	55.8
9-10	11:30	13.0	7.0	13.5	46.2	+ 3.8
	12:30	12.0	7.0	6.5	41.7	45.8
	1:30	11.0	7.0	8.5	36.4	22.7
	2:30	10.5	6.5	6.0	38.1	42.9
	Subtotal	46.5	27.5	34.5 avg	40.9	25.8
9-11	11:30	14.0	8.0	18.0	42.9	+ 28.6
	12:30	13.5	7.0	13.5	48.1	0.0
	1:30	11.5	6.0	9.5	47.8	17.4
	2:30	9.5	4.0	7.5	57.9	21.1
	Subtotal	48.5	25.0	48.5 avg	48.5	0.0
9-12	11:30	12.5	6.0	2.0	52.0	84.0
	12:30	11.0	6.5	3.0	40.9	72.7
	1:30	9.5	6.0	3.0	36.8	68.4
	2:30	9.0	5.0	7.0	44.4	77.8
	Subtotal	42.0	23.5	10.0 avg	44.0	76.2
9-15	11:30	12.5	8.5	12.0	32.0	4.0
	12:30	14.0	7.0	10.0	50.0	28.6
	1:30	12.0	6.0	6.0	50.0	50.0
	2:30	9.0	4.0	5.0	55.6	44.4
	Subtotal	47.5	25.5	33.0 avg	46.3	30.5
	Total	227.5	119.0	145.0 avg	47.7	36.3
	Total (disregarding samples when erosion caused effluent to be higher than influent)					
	Primary	200.5		113.5 avg		43.4

TABLE 68
DRY-WEATHER REMOVAL OF SETTLEABLE SOLIDS BY WEIGHT
SWIRL FLOW 19.7 l/sec (0.45 mgd)

Date 1975	Time	Settleable Solids mg/l			% Removal	
		Influent	Swirl Effluent	Primary Effluent	Swirl	Primary
9-9	11:30	136	104	112	23.5	17.6
	12:30	192	108	84	43.8	56.3
	1:30	128	124	84	3.1	34.4
	2:30	380	132	156	65.3	58.9
	Subtotal	836	468	436 avg	44.0	47.8
9-10	11:30	252	160	164	36.5	34.9
	12:30	248	76	96	69.4	61.3
	1:30	152	160	124	+ 5.3	18.4
	2:30	128	116	84	9.4	34.4
	Subtotal	780	512	468 avg	34.4	40.0
9-11	11:30	284	172	284	39.4	0.0
	12:30	220	172	172	21.8	21.8
	1:30	280	180	144	35.7	48.6
	2:30	132	48	56	63.6	57.6
	Subtotal	916	572	656 avg	37.6	28.4
9-12	11:30	228	144	47	36.8	79.4
	12:30	160	136	88	15.0	45.0
	1:30	256	132	—	48.4	—
	2:30	196	148	52	24.5	73.5
	Subtotal	840	560	187 avg	33.3	77.7
9-15	11:30	608	136	120	77.6	80.3
	12:30	100	72	144	28.0	+ 44.0
	1:30	148	140	92	5.4	37.8
	2:30	116	60	80	48.3	31.0
	Subtotal	972	408	436 avg	58.0	55.1
	Total	4,344	2,520	2,183 avg	42.0	49.7
	Total (disregarding samples when erosion caused effluent to be higher than influent)					
	Swirl	4,192	2,360		43.7	

TABLE 69
DRY-WEATHER REMOVAL OF TOTAL SUSPENDED SOLIDS
SWIRL FLOW 19.7 l/sec (0.45 mgd)

Date 1975	Time	Total Suspended Solids mg/l			% Removal	
		Influent	Swirl Effluent	Primary Effluent	Swirl	Primary
9-9	11:30	336	300	304	10.7	9.5
	12:30	376	308	264	18.1	29.8
	1:30	352	328	252	6.8	28.4
	2:30	528	372	280	29.5	47.0
	Subtotal	1,592	1,308	1,100	17.8	30.9
9-10	11:30	528	328	376	37.9	28.8
	12:30	356	292	260	18.0	27.0
	1:30	348	328	280	5.7	19.5
	2:30	360	312	204	13.3	43.3
	Subtotal	1,592	1,260	1,120	20.8	29.6
9-11	11:30	472	344	460	27.1	2.5
	12:30	436	384	384	11.9	11.9
	1:30	636	436	340	31.4	46.5
	2:30	344	252	272	26.7	20.9
	Subtotal	1,888	1,416	1,456	25.0	22.9
9-12	11:30	432	324	208	25.0	51.8
	12:30	364	344	208	5.5	42.9
	1:30	524	308	280	41.2	46.6
	2:30	400	372	168	7.0	58.0
	Subtotal	1,720	1,348	864	21.6	49.8
9-15	11:30	840	364	340	56.7	59.5
	12:30	416	340	308	18.3	26.0
	1:30	376	276	220	26.6	41.5
	2:30	296	204	172	31.1	41.9
	Subtotal	1,928	1,184	1,040	38.6	46.0
	Total	8,720	6,516	5,580	25.3	36.0

TABLE 70
DRY-WEATHER REMOVAL OF VOLATILE SUSPENDED SOLIDS
SWIRL FLOW 19.7 l/sec (0.45 mgd)

Date 1975	Time	Volatile Suspended Solids mg/l			% Removal	
		Influent	Swirl Effluent	Primary Effluent	Swirl	Primary
9-9	11:30	276	240	224	13.0	18.8
	12:30	272	224	192	17.6	29.4
	1:30	276	244	156	11.6	43.5
	2:30	404	304	260	24.7	35.6
	Subtotal	1,228	1,012	832	17.6	32.2
9-10	11:30	470	316	336	32.8	28.5
	12:30	316	260	240	17.7	24.0
	1:30	320	308	280	3.8	12.5
	2:30	304	248	140	18.4	53.9
	Subtotal	1,410	1,132	996	19.7	29.4
9-11	11:30	420	304	392	27.6	6.7
	12:30	376	332	320	11.7	14.9
	1:30	560	364	308	35.0	45.0
	2:30	276	220	212	20.3	23.2
	Subtotal	1,632	1,220	1,232	25.2	24.5
9-12	11:30	356	264	196	25.8	44.9
	12:30	296	244	160	17.6	45.9
	1:30	392	240	276	38.8	29.6
	2:30	332	316	136	4.8	59.0
	Subtotal	1,376	1,064	768	22.7	44.2
9-15	11:30	742	284	268	61.7	63.9
	12:30	336	268	300	20.2	10.7
	1:30	332	268	188	19.3	43.4
	2:30	288	196	132	31.9	54.2
	Subtotal	1,698	1,016	888	40.2	47.7
	Total	7,344	5,444	4,716	25.9	35.8

TABLE 71
DRY-WEATHER REMOVAL OF FIXED SUSPENDED SOLIDS
SWIRL FLOW 19.7 l/sec (0.45 mgd)

Date 1975	Time	Fixed Suspended Solids ppm			% Removal	
		Influent	Swirl Effluent	Primary Effluent	Swirl	Primary
9-9	11:30	60	60	80	00.0	+33.3
	12:30	104	84	72	19.2	30.8
	1:30	76	84	96	+ 10.5	+26.3
	2:30	124	68	20	45.2	83.9
	Subtotal	364	296	268 avg	18.7	26.4
9-10	11:30	56	12	40	78.6	28.6
	12:30	40	32	20	20.0	50.0
	1:30	28	20	0	28.6	100.0
	2:30	56	64	64	+ 14.3	+14.3
	Subtotal	180	128	124 avg	28.9	31.1
9-11	11:30	52	40	68	23.0	+30.8
	12:30	60	52	64	13.3	+ 6.7
	1:30	76	72	32	5.3	57.9
	2:30	68	32	60	52.9	11.8
	Subtotal	256	196	224 avg	23.4	12.5
9-12	11:30	76	60	12	21.0	84.2
	12:30	68	100	48	+ 47.0	29.4
	1:30	132	68	4	48.5	97.0
	2:30	68	56	32	17.6	52.9
	Subtotal	344	284	96 avg	17.4	72.1
9-15	11:30	98	80	72	18.4	26.5
	12:30	80	72	8	10.0	90.0
	1:30	44	8	32	81.8	27.3
	2:30	8	8	40	0.0	+40.0
	Subtotal	230	168	152 avg	26.9	33.9
	Total	1,374	1,072	864 avg	22.0	37.1
	Total (disregarding samples when erosion caused effluent to be higher than influent)					
	Swirl	1,174	824		29.8	
	Primary	1,062		452 avg		57.4

TECHNICAL REPORT DATA
(Please read Instructions on the reverse before completing)

1. REPORT NO.	2.	3. RECIPIENT'S ACCESSION NO.
EPA-600/2-78-122		

4. TITLE AND SUBTITLE
THE SWIRL PRIMARY SEPARATOR: DEVELOPMENT AND PILOT DEMONSTRATION

5. REPORT DATE
August 1978 (Issuing Date)

6. PERFORMING ORGANIZATION CODE
APWA 73-3

7. AUTHOR(S) Richard H. Sullivan, Morris M. Cohn, James E. Ure, Fred Parkinson, G. Galiana, Ralph R. Boericke, Carl Koch, Paul Zielinski

8. PERFORMING ORGANIZATION REPORT NO.

9. PERFORMING ORGANIZATION NAME AND ADDRESS
American Public Works Association
1313 East 60th Street
Chicago, Illinois 60637

10. PROGRAM ELEMENT NO.
1BC611

11. CONTRACT/GRANT NO.
68-03-0272
S803157

12. SPONSORING AGENCY NAME AND ADDRESS
Municipal Environmental Research Laboratory--Cin.,OH
Office of Research and Development
U.S. Environmental Protection Agency
Cincinnati, Ohio 45268

13. TYPE OF REPORT AND PERIOD COVERED
Final

14. SPONSORING AGENCY CODE
EPA/600/14

15. SUPPLEMENTARY NOTES This report supplements EPA-R2-72-008, EPA-670/2-74-039, and EPA-670/2-75-011.
P.O. Richard Field (201) 321-6674 FTS 340-6674
Hugh Masters (201) 321-6678 FTS 340-6678

16. ABSTRACT A study was conducted to determine if the swirl concentrator principal could be used to provide primary treatment to combined sewer overflows and municipal wastewater. A hydraulic model with synthetic wastewater and a mathematical model were both used to arrive at an optimized configuration and a design basis. The design was then tested under actual wet- and dry-weather flow conditions using a large scale, 1,137 cu m/d (0.3 mgd) pilot constructed in Toronto, Canada. The Toronto pilot evaluations confirmed the accuracy of the design (and associated design curves) developed under the model studies.

The model and pilot studies indicated that the device could achieve 30 to 50 percent settleable solids removal efficiency for flows of less than 22 l/sec (0.5 mgd) at costs comparable to, or less than, conventional treatment units. Overflow rates of two to three times that of conventional units make possible the saving.

Testing of the model and prototype was based upon the need to treat both domestic sanitary sewage and combined sewer overflows. Extensive laboratory work was conducted to determine the settling characteristics of solids to provide laboratory control and provide a correlation between the laboratory and prototype testing programs.

The swirl's height and diameter are equal, providing a relatively deep structure which enhances sludge thickening.

The Toronto pilot evaluations of the prototype unit constructed in Toronto Ontario - 1,137 cu m/d (0.3 mgd) - to determine operating efficiencies confirmed the accuracy of design and associated curves developed under the model studies.

The report contains thorough descriptions of the hydraulic/mathematical and pilot studies, and most importantly, the detailed design methodology.

17. KEY WORDS AND DOCUMENT ANALYSIS

a. DESCRIPTORS	b. IDENTIFIERS/OPEN ENDED TERMS	c. COSATI Field/Group
Waste treatment, Design criteria, Hydraulic structures, Combined sewers, Overflows, Prototypes	Swirl primary separator, Urban stormwater runoff, Combined sewer overflow, Sanitary sewage primary treatment, Prototype tests	13B

18. DISTRIBUTION STATEMENT	19. SECURITY CLASS *(This Report)*	21. NO. OF PAGES
Release to Public	Unclassified	216
	20. SECURITY CLASS *(This page)*	22. PRICE
	Unclassified	

* U.S. GOVERNMENT PRINTING OFFICE: 1978—757-140/1380

U.S. ENVIRONMENTAL PROTECTION AGENCY
Office of Research and Development
Environmental Research Information Center
Cincinnati, Ohio 45268

OFFICIAL BUSINESS
PENALTY FOR PRIVATE USE, $300
AN EQUAL OPPORTUNITY EMPLOYER

POSTAGE AND FEES PAID
U.S. ENVIRONMENTAL PROTECTION AGENCY
EPA-335

Special Fourth-Class Rate
Book

If your address is incorrect, please change on the above label tear off; and return to the above address.
If you do not desire to continue receiving these technical reports, CHECK HERE ☐; tear off label, and return it to the above address,

EPA-600/2-78-122